Distribution, abundance and life cycle of free-living *Symbiodinium*

Risa Fujise

PhD by Research

July 2018

A thesis submitted in fulfilment of the requirements for

the degree of Doctor of Philosophy in Science

Climate Change Cluster (C3),

School of Life Sciences,

University of Technology Sydney

Supervisors: Associate Professor David Suggett and Professor Peter Ralph

Certificate of Original Authorship

I, Risa Fujise declare that this thesis, submitted in fulfilment of the requirements for the award of the degree of Doctor of Philosophy in Science, in the School of Life Sciences, Faculty of Science at the University of Technology Sydney.

This thesis is wholly my own work unless otherwise reference or acknowledged. In addition, I certify that all information sources and literature used are indicated in the thesis.

This document has not been submitted for qualifications at any other academic institution.

Signature of student:

Production Note:
Signature removed prior to publication.

Risa (Lisa) Fujise

Date: 2018.07.15

Acknowledgements

First and foremost, I would like to express my deepest gratitude to my supervisors; A/Prof. David Suggett and Prof. Peter Ralph, who consistently provided patient guidance and warm encouragement throughout the journey of my PhD. I am very fortunate to have Dave as my supervisor because he always encouraged me even when I hit those "brick walls" and he corrected the course of my PhD, keeping me positive all the time. I always looked forward to having a meeting with Peter because he always provided such a new interesting insight into my research which fuelled my energy to keep walking on the long journey of the PhD. I cannot tell how much I appreciate to my supervisors' huge help to bring me to the end of my PhD.

I would also like to thank my collaborators Dr. Michael Stat (Curtin University). It was a great opportunity for me to visit TrEnD lab and analyse the samples by myself in order to deepen my knowledge and understand the principal methodology of NGS techniques. And also to Dr. Jörg Frommlet (University of Aveiro) for valuable comments and suggestions on the cell cycle analysis of *Symbiodinium*, which was not an easy journey but finally became a big success. I also greatly appreciate Dr. Matthew Nitschke for his huge help and contribution; I could not have survived without him. To Dr. Tim Kahlke for building whole pipelines for bioinformatic analysis of *Symbiodinium* – it was simply not possible to make this research a success without his huge help. To Dr. Nahshon Siboni for helping me to build the qPCR assay and always made me laugh throughout the research. To Dr. Stephen Woodcock for checking whether I was on the right path or not for the various complex statistical analysis.

I would like to express my deepest appreciation to the staff at C3: Paul Brooks, Graeme

Poleweski, Gemma Armstrong, Susan Fenech, Kun Xiao, Lucia Bennar, John Moore, Mellisa Oey; Heron Island Research Station: Maureen Roberts, Elizabeth Perkins, Pauline Dusseau, Bec Tite; and TrEnD lab: Matthew Power, Nichole White, Megan Coghlan, for full support of the experiment, sampling and analyses required to make my PhD success. Especially to Paul who supported my long PhD journey and kept watch me as a child (or maybe a grandchild), keeping me on the straight and narrow.

I would like to offer my special thanks to all of the lab members in the Suggett Lab: David Hughes, Samantha Goyen, Steph Gardner, Caitlin Lawson, Emma Camp, Mickael Ros, Nerissa Fisher, Trent Haydon and Rachel Levin; TrEnD lab: Katrina West, Frederick Seersholm, Adam Koziol, Matt Heydenrych, Tiffany Simpson, Alicia Grealy, Miwa Takahashi, Daniel Werndly and Tina Berry, for such a wonderful time in the laboratory and warm encouragement for my entire PhD life, which has been fantastic. I really enjoyed the time in Australia and now I can say with confident that I made a great choice to come to Australia to do my PhD.

Of course, I also deeply appreciate for the fundings from the University of Technology Sydney (UTS International Research Scholarship (IRS) and UTS President's Scholarship (UTSP)), Climate Change Cluster (C3 PhD fund) and Yoshida Scholarship Foundation (Scholarship grants to Japanese students to study abroad) to be able to study, and undertake research using cutting edge technologies for contributing to the research field to advance knowledge.

Finally, special thanks to my family for the consistent and unconditional support and let me open my wings and fly towards the world.

Table of Contents

List of Figures

Chapter 1

Figure 1.4. Mechanisms for regulating *Symbiodinium* density *in hospite*. **(i)** Expulsion of either detached a whole host cell or a normal cell and/or a degraded cell by exocytosis. **(ii)** Degradation (digestion) of a cell by host phagocytosis. (i) and (ii) is termed the post-mitotic process. **(iii)** Inhibition of symbiont cell growth and division through controlling cell cycle progression which is termed the pre-mitotic process (adapted and modified from Davy et al. 2012).

Figure 1.5. Life cycle of *Symbiodinium microadriaticum*. **A.** Vegetative cell. **B.** Vegetative cell undergoing binary fission, producing two daughter cells. **C.** Vegetative cyst, differing from the vegetative cell mainly in cell wall thickness. **D.** Mature zoosporangium, containing a gymnodinioid zoospore. **E.** Gymnodinioid zoospore. **F.** Aplanospore. **G.** Cyst containing two autospores. **H.** Cyst containing developing isogametes. **I.** Liberated isogametes (taken from Freudenthal 1962).

Figure 1.6. Life cycle of *Symbiodinium* including asexual reproduction (right side) and possible sexual reproduction (left side). Solid lines denote observed transformations, while dashed lines are possible routes of sexual reproduction or meiosis. **1.** Vegetative coccoid cell. **2.** Dividing vegetative cell (doublet). **3**. Motile cells. **4.** Dividing vegetative cell (triplet). **5.** Isogametes. **6.** Diploid vegetative cell resulting from fusion of the gametes. **5.** Tetrad cell, formed from meiosis of the diploid vegetative cell (adapted and modified from Fitt and Trench 1983 and Stat et al. 2006).

Figure 1.7. *Symbiodinium* cell cycle progression. Irradiance (i.e. light period, denoted by yellow field) is required for cell growth and DNA synthesis (G_1 to S to G_2/M), while dark period (black field) is required for cytokinesis of mitotic division (G_2/M to G_1).

Motility of *Symbiodinium* are synchronized to the cell cycle, and increase at the onset of light which is correlated with the G_1 phase of gymnodinioid cells, decreasing when cells enter the S phase and the lowest at G_2/M phase with coccoid cell (adapted and modified from Wang et al. 2008).

Chapter 2

Figure 2.1. Location of sampling sites and coral species. **A-B.** Location of Heron Island in southern Great Barrier Reef in east coast of Australia. **C.** Location of sampling sites (1: *Acropora aspera* site, 2: *Montipora digitata* site, and 3: *Pocillopora damicornis* site). Collected host coral species: **D.** *A. aspera*, **E.** *M. digitata*, and **F.** *P. damicornis*. **G.** Example of coral community surrounded by reef environments including *Padina* sp. (collected macroalgae species).

Figure 2.2. Environmental data on Heron reef (2015-2016). Monthly averaged sea surface temperature (SST, °C) is shown as a black solid line (left Y axis) and monthly averaged photosynthetic active radiation (PAR, μmol photons m^{-2} s^{-1}) is shown as a red dashed line (right Y axis) from January 2015 to December 2016. Samplings were performed in October 2015 (spawning season) and March 2016 (summer season) and indicated by the grey areas.

Figure 2.3. Box plots for number of sequences, clades, ITS2 variants and OTUs in each site, habitat and season. Box plots for corals are shown as pink, water as blue, sediment as yellow and macroalgae as green.

Figure 2.4. Venn diagrams for *in hospite* (coral) and free-living *Symbiodinium* genetic types in environments. Number of **A.** ITS2 variants. **B.** OTUs, belong to clade C. Number of *Symbiodinium* ITS2 variants or OTUs *in hospite* are shown with orange circles and in environment (sum of water, sediment and macroalgae samples) with green circles for each site (coral species) and season (spawning vs. summer).

Figure 2.5. Relative abundance of *Symbiodinium* clades during the spawning and summer seasons obtained by DNA metabarcoding. 48 samples: 3 sites (coral species), 4 habitats (*in hospite*, water, sediment and macroalgae), 4 replicates (a, b, c, d) for 2 seasons (spawning vs. summer). Colour of bars for each clade are shown above the graphs.

Figure 2.6. nMDS plots of *Symbiodinium* community compositions. **A.** Clade. **B.** ITS2 variant. **C.** OTU. Non-metric multidimensional scaling (nMDS) was performed on each variable per variant using Bray-Curtis Similarity. CLUSTER analysis was performed for cladal composition (**A**); similarity is shown at the 60% (green solid lines), 70% (purple dashed lines) and 80% (pink dashed lines) levels and vectors driving the clustering are shown as blue lines. Corals are represented by pink, water by blue, sediment by yellow, and macroalgae by green with site 1 with circle, site 2 with rectangle, and site 3 with square markers. Plots for the spawning season are shown with closed markers and the summer season with open markers (all combinations of the markers are shown below the graphs).

Figure 2.7. Relative abundance of *Symbiodinium* ITS2 variants during the spawning (left panel) and summer seasons (right panel) obtained by DNA metabarcoding.

Relative abundance of ITS2 variants in each replicate (n = 4) were averaged and top three ITS2 variants in each clade are shown as bar graphs for each site, habitat and season.

Figure 2.8. Heatmap of *Symbiodinium* ITS2 variant compositions. Compositions of ITS2 variants in each replicate (n = 4) were averaged and top three ITS2 variants in each clade are displayed on the right. The colour (scale bar on the top of the graph) represents the proportion of each ITS2 variants in the sample (0-10% with blue gradient and 10-100% with red gradient), and white boxes indicate an absence of the ITS2 variant.

Figure 2.9. nMDS plot of *Symbiodinium* community compositions based on abundance of clades A, C and D obtained by qPCR. Non-metric multidimensional scaling (nMDS) and CLUSTER analysis were performed on each variable per variant using Bray-Curtis Similarity. Similarity is shown at the 50% (green solid lines) and 80% (pink dashed lines) levels. Corals are represented by pink, water by blue, sediment by yellow, and macroalgae by green with site 1 with circle, site 2 with rectangle, and site 3 with square markers. Plots for the spawning season are shown with closed markers and the summer season with open markers (all combinations of the markers are shown in the graph).

Figure 2.10. Cell density of free-living *Symbiodinium* in environmental habitats obtained by qPCR. Number of cells of free-living *Symbiodinium* belong to clades A, C and D were normalised per cm^3 for each sample type (habitat) in each site and season, and replicates (n = 2-4) were averaged. Cell densities are shown in both bubble charts

(upper panel) and bar graphs (lower panel).

Figure 2.11. nMDS plot for NGS vs. qPCR *Symbiodinium* community compositions of clades A, C and D in environmental habitats. Non-metric multidimensional scaling (nMDS) was performed on each variable per variant using Bray-Curtis Similarity. Water samples are represented by blue, sediment by yellow, and macroalgae by green markers. Plots for qPCR are shown with closed markers and NGS with open markers.

Figure 2.12. Relative abundance of *Symbiodinium* clades A, C and D during the spawning and summer seasons obtained by two techniques (NGS vs. qPCR). 36 samples per season per technique: 3 sites (coral species), 3 habitats (water, sediment and macroalgae), 4 replicates (a, b, c, d) for 2 seasons (spawning vs. summer) for 2 techniques (NGS vs. qPCR). Colour of bars for each clade are shown above the graphs.

Chapter 3

Figure 3.1. Location of sampling sites and host species. **A.** Location of sampling sites in Sydney Harbour (sites 1 and 2) and Botany Bay (site 3) together with host benthic coverage bar graphs. Benthic coverage of hard corals (*Plesiastrea versipora* and *Coscinaraea mcneilli*): pink bars, soft coral (*Capnella gaboensis*): orange bars, algae: green bars, and others (abiotic substrates): purple bars, were obtained by video transects. Mean percentage of coverages are shown above each bar and error bars indicate SD. Collected host species: **B.** *P. versipora* (hard coral) and **C.** *C. gaboensis* (soft coral). **D.** Bleached *P. versipora*. **E.** Tagged *P. versipora* during the bleaching (April 2016) and the recovery (July 2016).

Figure 3.2. Environmental data in Sydney Harbour (sites 1 and 2) and Botany Bay (site 3). Monthly averaged sea surface temperature (SST, °C) are shown as black solid lines (left Y axis) and monthly averaged photosynthetic active radiation (PAR, μmol photons m^{-2} s^{-1}) are shown as red dashed lines (right Y axis) from January 2015 to December 2016 for **A.** Sydney Harbour and **B.** Botany Bay. SST thermal anomalies from past 10-year (2007-2016) are shown as black dashed lines for **C.** Sydney Harbour and **D.** Botany Bay. Samplings were performed in December 2015 (pre-bleaching) and May 2016 (bleaching) and indicated by the grey areas.

Figure 3.3. Box plots for number of sequences, clades and OTUs based on the cp23S marker in each site, habitat and sampling time. Box plots for *P. versipora* (hard coral) are shown as pink, *C. gaboensis* (soft coral) as orange, water as blue, sediment as yellow and macroalgae as green.

Figure 3.4. Box plots for number of sequences, clades, ITS2 variants and OTUs based on the ITS2 marker in each site, habitat and season. Box plots for *P. versipora* (hard coral) are shown as pink, *C. gaboensis* (soft coral) as orange, water as blue, sediment as yellow and macroalgae as green.

Figure 3.5. Venn diagrams for *in hospite* (*P. versipora* and *C. gaboensis*) and free-living types in environment. Number of **A.** ITS2 variants. **B.** OTUs. Number of *Symbiodinium* ITS2 variants or OTUs in *P. versipora* are shown with pink circles, *C. gaboensis* with orange circles and in environment (sum of water, sediment and macroalgae samples) with green circles for each site and sampling time (pre-bleaching vs. bleaching).

Figure 3.6. Relative abundance of *Symbiodinium* clades during pre-bleaching and bleaching obtained by DNA metabarcoding based on the cp23S marker. 3 sites × 5 habitats (hard coral: *P. versipora*, soft coral: *C. gaboensis*, water, sediment and macroalgae) × 4 replicates (a, b, c, d) for 2 sampling time points (pre-bleaching vs. bleaching). Note that no *C. gaboensis* samples were collected at site 1 during bleaching, and no bars in sediment and macroalgae samples were due to no amplification/no sequences. Colour of bars for each clade are shown above the graphs.

Figure 3.7. nMDS plots of *Symbiodinium* community compositions based on the cp23S marker. **A.** Clade. **B.** OTU. Non-metric multidimensional scaling (nMDS) was performed on each variable per variant using Bray-Curtis Similarity. CLUSTER analysis was performed for cladal composition (**A**); similarity is shown at the 50% (green solid lines), 80% (pink dashed lines) levels and vectors driving the clustering are shown as blue lines. Hard corals are represented by pink, soft coral by orange, water by blue, sediment by yellow, and macroalgae by green with site 1 with circle, site 2 with rectangle, and site 3 with square markers. Plots for pre-bleaching samples are shown with closed markers and bleaching samples with open markers (all combinations of the markers are shown below the graphs).

Figure 3.8. Relative abundance of *Symbiodinium* clades during pre-bleaching and bleaching obtained by DNA metabarcoding based on the ITS2 marker. 3 sites × 5 habitats (hard coral: *P. versipora*, soft coral: *C. gaboensis*, water, sediment and macroalgae) × 4 replicates (a, b, c, d) for 2 sampling time points (pre-bleaching vs. bleaching). Note that no *C. gaboensis* samples were collected at site 1 during bleaching, and no bars in water, sediment and macroalgae samples were due to no

amplification/no sequences. Colour of bars for each clade are shown above the graphs.

Figure 3.9. nMDS plots of *Symbiodinium* community compositions based on the ITS2 marker. **A.** Clade. **B.** ITS2 variant. **C.** OTU. Non-metric multidimensional scaling (nMDS) was performed on each variable per variant using Bray-Curtis Similarity. CLUSTER analysis was performed for cladal composition (**A**); similarity is shown at the 50% (green solid lines), 80% (pink dashed lines) levels and vectors driving the clustering are shown as blue lines. Hard corals are represented by pink, soft coral by orange, water by blue, sediment by yellow, and macroalgae by green with site 1 with circle, site 2 with rectangle, and site 3 with square markers. Plots for pre-bleaching samples are shown with closed markers and bleaching samples with open markers (all combinations for the markers are shown below the graphs).

Figure 3.10. Relative abundance of *Symbiodinium* ITS2 variant during pre-bleaching (left panel) and bleaching (right panel) obtained by DNA metabarcoding based on the ITS2 marker. Relative abundance of ITS2 variants in each replicate (n = 2-4, depends on the samples) were averaged and top three ITS2 variants in each clade are shown as bar graphs for each site, habitat and sampling time point.

Figure 3.11. Heatmap of *Symbiodinium* ITS2 variant compositions. Compositions of ITS2 variants in each replicate (n = 2-4, depends on the samples) were averaged and top three ITS2 variants in each clade are displayed on the right. The colour (scale bar on the top of the graph) represents the proportion of each ITS2 variants in the sample (0-10% with blue gradient and 10-100% with red gradient), and white boxes indicate an absence of the ITS2 variant.

Figure 3.12. Box plots for number of clades, ITS2 variants and OTUs based on the ITS2 marker in each region and habitat. Box plots for hard corals are shown as pink, soft coral as orange, water as blue, sediment as yellow and macroalgae as green. Sites and seasons were pooled together.

Figure 3.13. Phylogenetic trees based on OTUs together with sequences in ITS2 reference database SymTyper. **A.** Clade A OTUs in Sydney Harbour with red letters plus clade A sequences in SymTyper with black letters. **B.** Clade B OTUs in Sydney Harbour with blue letters plus clade B sequences in SymTyper with black letters. **C.** Clade C OTUs in Heron Island reef with yellow letters plus clade C sequences in SymTyper with black letters. Phylogenetic trees were created using QIIME (*make_phylogeny.py*).

Figure 3.14. Environmental data in Sydney Harbour (temperate reef) and Heron Island (tropical reef). **A.** Monthly averaged sea surface temperature (SST, °C) from January 2015 to December 2016 including sampling periods for both Sydney Harbour (December 2015 and May 2016) and Heron Island (October 2015 and March 2016). Black solid line for Sydney Harbour SST and black dashed line for Heron Island SST. **B.** Monthly averaged photosynthetic active radiation (PAR, μmol photons m^{-2} s^{-1}) from January 2015 to December 2016. Red solid line for Sydney Harbour PAR (averaged PAR at depth 5-7 m where corals inhabit) and red dashed line for Heron PAR at sea surface.

Figure 3.15. Venn diagrams to show connectivity of *Symbiodinium* genetic types between Sydney Harbour (temperate region) and Heron Island (tropical region).

Number of **A.** ITS2 variants and **B.** OTUs. Number of *Symbiodinium* ITS2 variants or OTUs (combining across sites, habitats and seasons) in Sydney Harbour are shown with blue circles and Heron Island with pink circles.

Figure 3.16. nMDS plots of *Symbiodinium* community compositions from Sydney Harbour (temperate region) and Heron Island (tropical regions) based on the ITS2 marker. **A.** ITS2 variants. **B.** OTUs. Non-metric multidimensional scaling (nMDS) was performed on each variable per variant using Bray-Curtis Similarity. Hard corals are represented by pink, soft coral by orange, water by blue, sediment by yellow and macroalgae by green markers. Plots for Sydney Harbour samples are shown as closed markers and Heron Island samples as open markers (all combinations of the markers are shown at the right to the graph).

Chapter 4

Figure 4.1. DNA histograms of cell cycle progression through 24 h. Example cell cycle analysis of *Symbiodinium* type B1 under high light treatment. First distribution (blue) are cells in G_1 phase with 1n DNA content. Second distribution (green) is G_2/M phase, where cells have 2n DNA content (twice as much as G_1 phase cells). S phase cells (red) have intermediate DNA content between G_1 and G_2/M phase cells. White bar shows the light period (8:00-20:00) and black bar shows the dark period (20:00-8:00). All distributions were produced using ModFit LT.

Figure 4.2. Cell cycle progression of four *Symbiodinium* culture strains through 24 h under two light treatments (low light vs. high light). Y axis is percentage of G_1, S and G_2/M phase, and X axis is the sampling time points (T0-24). White and black bars on

the top of each graph show the light period (T0-12) and dark period (T12-24), respectively. G_1 phase is shown as dotted lines with black circles, S phase as dashed lines with open squares, and G_2/M phase as solid lines with black rectangles. Values represent mean ± SD (n = 3).

Figure 4.3. Multi-dimensional scaling (MDS) plots of four *Symbiodinium* culture strains with cell cycle proportions corresponding to the time of the G_2/M peak. **A.** Light treatment (low light (LL) vs. high light (HL)). **B.** Temperature treatment (control vs. heat). Cluster analysis and MDS were performed on the average of each variable per variant; similarity is shown at the 93% (solid lines) and 96% (dashed lines) levels and vectors driving the clustering are shown as blue lines. Low light and high light are represented by yellow squares and orange circles, respectively. Control temperatures and heat treatments are represented by blue squares and pink circles, respectively.

Figure 4.4. F_v/F_m of four *Symbiodinium* culture strains. Changes in photophysiology under light (low light (LL) vs. high light (HL), upper panels) and temperature (control vs. heat, lower panels) treatment. Low light and control temperatures are shown as solid lines with open circles and high light and heat treatments are shown as dashed lines with black circles. Values represent mean ± SD (n = 3). The temperature increase is shown on the top X axis of each graph for heat treatment (lower panel). The temperatures for heat treatments were; day 2: 27.7 ± 0.75°C, day 3: 29.7 ± 0.87°C, day 4: 31.9 ± 0.89°C, day 5: 32.0 ± 0.81°C, day 6: 32.1 ± 0.56°C, day 7: 32.3 ± 0.84°C (± SD for daily mean temperature measured using iButton® temperature logger).

Figure 4.5. Cell cycle progression of four *Symbiodinium* culture strains through 24 h under the temperature treatment (control vs. heat). Y axis is percentage of G_1, S and G_2/M phase, and X axis is the sampling time points (T0-24). White and black bars on the top of each graph show the light period (T0-12) and dark period (T12-24), respectively. G_1 phase is shown as dotted lines with black circles, S phase as dashed lines with open squares, and G_2/M phase as solid lines with black rectangles. Values represent mean ± SD (n = 3).

Chapter 5

Figure 5.1. Key findings from the thesis. **Chapter 2**: Transiently free-living *Symbiodinium* mainly existed in water and macroalgae habitats (seems to be a main source of symbionts for hosts), in contrast, exclusively free-living types dominated in sediment. **Chapter 3**: Unique free-living populations (temperate specific types) dominated in the high-latitude temperate coral communities and the populations would shift due to an impact of the heat wave. **Chapter 4**: Cell cycle progressions of *Symbiodinium* were conserved across species, but proportions differed by species. Heat stress arrested cells in G_1 phase and supressed the growth. Arrows indicate the linkages between the chapters: Chapter 1 → 2: **Community structure** of free-living *Symbiodinium* is shaped by reef structures and environmental conditions; Chapter 2 → 3: **Population dynamic** seems to contribute for regulating community structure of *Symbiodinium* via cell cycle; Chapter 3 → 1: **Biodiversity** of free-living *Symbiodinium* is maintained via individual population turnover.

Appendix: OTU analysis for *Symbiodinium* culture strains

Figure 6.1. Box plots for percent identity of sequences within each strain. Background colour were used to classify the clade of strains: red for clade A, blue for clade B, purple for clade D, green for clade E, and orange for clade F.

List of Tables

Chapter 1

Chapter 2

of the primer sets for qPCR assays. Number of cells per qPCR reaction (5 μL) used as the highest concentration of standard DNA are shown. DNA was diluted in 1/10, 1/100, 1/1,000, 1/10,000 for making five concentrations for the calibration curves for each strain.

Table 2.2. *Symbiodinium* culture strains used as quantification standards for the qPCR assays for assessing abundance of free-living *Symbiodinium*. One culture strain from each clade was selected for use as a quantification standard for the qPCR assay for each primer set (clades A-F, except E). Number of cells per qPCR reaction (5 μL) used for making calibration curves (five concentrations) and minimum detection limits are shown.

Table 2.3. Number of sequences, ITS2 variants and OTUs belong to clades A-I, except clade E.

Table 2.4. Cell density of free-living *Symbiodinium* obtained by qPCR. Cell densities of free-living *Symbiodinium* belong to clades A, C and D were detected within the quantification range based on the calibration curves using *Symbiodinium* culture strains as standards (list in Table 2.2); however, *Symbiodinium* belong to clades B and F were below the detection limits so not included in this table. Number of cells were normalised per mL for water and sediment samples and per wet weight (g) for macroalgae samples. In addition, number of cells in all sample types (habitats) were normalised per cm^3 for comparison between different sample types. Mean ± SD (n = 2-4) are shown for all samples. Cell density of clade which was only detected in one replicate per sample is shown with no SD.

Chapter 3

Table 3.1. *Symbiodinium* culture strains used as quantitative standards for qPCR assays for assessing abundance of free-living *Symbiodinium*. One culture strain from each clade was selected for use as a quantitative standard for qPCR assay for each primer set (clades A-F). Number of cells per qPCR reaction (5 μL) used for making calibration curves (five concentrations) and minimum detection limits are shown.

Table 3.2. Number of sequences and OTUs belong to clades A-C, E and F based on the cp23S marker.

Table 3.3. Number of sequences, ITS2 variants and OTUs belong to clades A-G based on the ITS2 marker.

Chapter 4

Table 4.1. Summary of *Symbiodinium* sp. type identifiers and source (geographic origin and host species) used for cell cycle analysis.

Table 4.2. Cell cycle and growth characteristics across four *Symbiodinium* culture strains under the light treatments (low light vs. high light). Cell cycle parameters: G_1 peak, S peak and G_2/M peak proportions (the maximum % of cells, for each phase, reached throughout a diel cycle) were obtained from analysis using cell cycle software: ModFit LT. Growth rates were calculated with equation 1 using cell densities. Mean ± SD (n = 3) are shown for all parameters except for cell volume (μm^3): median (upper–lower quartile ranges) are shown. Two-way ANOVA (strains × treatments) across

variants is also shown where superscript letters indicate *post-hoc* groupings of strain effects within each treatment.

Table 4.3. Cell cycle and growth characteristics across four *Symbiodinium* culture strains under the temperature treatments (control vs. heat). Cell cycle parameters: G_1 peak, S peak and G_2/M peak proportions (the maximum % of cells, for each phase, reached throughout a diel cycle) were obtained from analysis using cell cycle software: ModFit LT. Growth rates were calculated with equation 1 using cell densities. Mean ± SD (n = 3) are shown for all parameters except for cell volume (μm^3): median (upper–lower quartile ranges) are shown. Two-way ANOVA (strains × treatments) across variants is also shown where superscript letters indicate *post-hoc* groupings of strain effects within each treatment.

Appendix: OTU analysis for *Symbiodinium* culture strains

Table 6.1. *Symbiodinium* culture strains used for the NGS analysis. *****I included two identical strains of CCMP2548 (*S. natans*) (X and Y). ******SG_37 and SG_40 were isolated from *Plesiastrea versipora*, but the isolates were possibly surface contaminants from the environment, because *P. versipora* was dominated by B18-like types based on the NGS analysis of *in hospite* samples (see Chapter 3, section 3.4.7).

Table 6.2. OTU table (97% cut-off) for *Symbiodinium* culture strains. Top three OTUs (based on the number of sequences within each strain) are highlighted with colours and OTUs which contain ≥ 1% of the reads within each sample are shown as bold. Colour coding: red for clade A, blue for clade B, yellow for clade C, purple for clade D, green for clade E, and orange for clade F.

Table 6.3. OTU table (97% cut-off) for *Symbiodinium* culture strains after applying OTU abundance filtering. OTUs which contain < 1% of the reads within each sample were replaced by 0 and removed from the OTU table if those OTUs contain 0 sequence across all samples. OTUs contain sequences are highlighted with colours.

List of Supplementary Figures

Chapter 4

Figure S4.1. Example of manual gating for *Symbiodinium* populations in flow cytometry analysis. The gating for **A.** B1, **B.** C1, **C.** C1′, and **D.** D1a strains under high light treatment at sampling time point T0. X axis is forward scatter, and Y axis is side scatter in log scale for both.

Figure S4.2. Cell densities of four *Symbiodinium* culture strains under the light treatment (low light vs. high light). B1 was diluted into half concentration at day 3 both under low light and high light treatment to prevent the over growth. Cell cycle samples were collected through days 6-7. The days circled on the X axis and corresponding cell densities were used in calculating the growth rate (equation 1). Outliers which deviated from the exponential curve were treated as counting errors and not used for calculating the growth rate. Values represent mean ± SD (n = 3).

Figure S4.3. Correlation between cell cycle and growth parameters. Relationship between **A.** Growth rate and G_1 peak proportion, **B.** Growth rate and G_2/M peak proportion, **C.** Cell volume and G_1 peak proportion, **D.** Cell volume and growth rate. Values from low light and high light were plotted (n = 24).

Figure S4.4. Cell densities of four *Symbiodinium* culture strains under the temperature treatment (control vs. heat). Cell cycle samples were collected through days 6-7. The days circled on the X axis and corresponding cell densities were used in calculating

the growth rate (equation 1). Outliers which deviated from the exponential curve were treated as counting errors and not used for calculating the growth rate. Values represent mean ± SD (n = 3). The temperature increase is shown on the top X axis of each graph for heat treatment (lower panel). The temperatures were; day 1: 26.4 ± 0.72°C, day 2: 27.7 ± 0.75°C, day 3: 29.7 ± 0.87°C, day 4: 31.9 ± 0.89°C, day 5: 32.0 ± 0.81°C, day 6: 32.1 ± 0.56°C, day 7: 32.3 ± 0.84°C (± SD for daily mean temperature measured using iButton® temperature loggers).

List of Supplementary Tables

Chapter 2

Table S2.1. Number of sequences, clades, ITS2 variants and OTUs obtained by DNA metabarcoding. Total samples are 96 samples (2 seasons × 3 sites (coral species) × 4 habitats × 4 replicates).

Table S2.2. Summary of Kruskal-Wallis test for number of clades, ITS2 variants and OTUs. **A.** Main effects. **B.** *Post-hoc* pairwise comparison for sites × habitats × seasons. df: degrees of freedom, P value: * for $P < 0.05$, ** for $P < 0.01$.

Table S2.3. Summary of PERMANOVA main effects for *Symbiodinium* community compositions. **A.** Clades. **B.** ITS2 variants. **C.** OTUs. Relative abundance of community compositions was square-root transformed and PERMANOVA was performed with sites (coral species) (3 levels), habitats (4 levels) and seasons (2 levels) as fixed factors, using type III sum of squares and unrestricted permutation of raw data with 999 permutations. MS: mean square, df: degrees of freedom, *F*: Fisher statistic, P value: * for $P < 0.05$, ** for $P < 0.01$.

Table S2.4. Summary of SIMPER analysis for *Symbiodinium* cladal community compositions. Pairwise comparison within **A.** Spawning season and **B.** Summer season. Pairwise comparison **C.** Between spawning and summer seasons. Top two clades which contributed to dissimilarity of community compositions are shown with contribution percentages (%). Clades which were more abundant in variables in

columns are shown as bold letter and clades which were more abundant in variables in rows are shown as normal letter.

Table S2.5. List of ITS2 variants and relative abundance in each sample. **A.** Spawning season. **B.** Summer season. Compositions of ITS2 variants in each replicate (n = 4) were averaged and top three ITS2 variants in each clade are listed with relative abundance (%) in each sample.

Table S2.6. Summary of SIMPER analysis for *Symbiodinium* ITS2 variant community compositions. Pairwise comparison within **A.** Spawning season and **B.** Summer season. Pairwise comparison **C.** Between spawning and summer seasons. Top two ITS2 variants which contributed to dissimilarity of community compositions are shown with contribution percentages (%). ITS2 variants which were more abundant in variables in columns are shown as bold letter and ITS2 variants which were more abundant in variables in rows are shown as normal letter.

Table S2.7. Summary of PERMANOVA main effects for *Symbiodinium* community compositions based on the abundance of clades A, C and D obtained by qPCR. Cell densities of *Symbiodinium* belong to clades A, C and D in each environmental habitat, which were normalized by cm^3, were square-root transformed and PERMANOVA was performed with sites (coral species) (3 levels), habitats (4 levels), and seasons (2 levels) as fixed factors, using type III sum of squares and unrestricted permutation of raw data with 999 permutations. MS: mean square, df: degrees of freedom, F: Fisher statistic, P value: * for $P < 0.05$, ** for $P < 0.01$.

Chapter 3

Table S3.1. Number of sequences, clades and OTUs obtained by DNA metabarcoding using the cp23S primer set. Total samples which were successfully amplified and sequenced are 109/120 samples (4 replicates × 3 sites × 5 habitats × 2 sampling times).

Table S3.2. Summary of Kruskal-Wallis test for number of clades and OTUs based on the cp23S marker. **A.** Main effects. **B.** *Post-hoc* pairwise comparison for sites × habitats × seasons. df: degrees of freedom, P value: * for $P < 0.05$, ** for $P < 0.01$.

Table S3.3. Number of sequences, clades, ITS2 variants and OTUs obtained by DNA metabarcoding using the ITS2 primer set. Total samples which were successfully amplified and sequenced are 105/120 samples (4 replicates × 3 sites × 5 habitats × 2 sampling times).

Table S3.4. Summary of Kruskal-Wallis test for number of clades, ITS2 variants and OTUs based on the ITS2 marker. **A.** Main effects. **B.** *Post-hoc* pairwise comparison for sites × habitats × seasons. df: degrees of freedom, P value: * for $P < 0.05$, ** for $P < 0.01$.

Table S3.5. Summary of PERMANOVA main effects for *Symbiodinium* community compositions based on the cp23S marker. **A.** Clades. **B.** OTUs. Relative abundance of community compositions was square-root transformed and PERMANOVA was performed with sites (3 levels), habitats (5 levels), and seasons (2 levels) as fixed factors, using type III sum of squares and unrestricted permutation of raw data with 999 permutations. MS: mean square, df: degrees of freedom, *F*: Fisher statistic, P

value: * for $P < 0.05$, ** for $P < 0.01$.

Table S3.6. Summary of SIMPER analysis for *Symbiodinium* cladal community compositions based on the cp23S marker. Pairwise comparison within **A.** Pre-bleaching and **B.** Bleaching. Pairwise comparison **C.** Between pre-bleaching and bleaching sampling time points. Top two clades which contributed to dissimilarity of community compositions are shown with contribution percentages (%). Clades which were more abundant in variables in columns are shown as bold letter and clades which were more abundant in variables in rows are shown as normal letter.

Table S3.7. Summary of PERMANOVA main effects for *Symbiodinium* community compositions based on the ITS2 marker. **A.** Clades. **B.** ITS2 variants. **C.** OTUs. Relative abundance of community compositions was square-root transformed and PERMANOVA was performed with sites (3 levels), habitats (5 levels) and seasons (2 levels) as fixed factors, using type III sum of squares and unrestricted permutation of raw data with 999 permutations. MS: mean square, df: degrees of freedom, *F*: Fisher statistic, P value: * for $P < 0.05$, ** for $P < 0.01$.

Table S3.8. Summary of SIMPER analysis for *Symbiodinium* cladal community compositions based on the ITS2 marker. Pairwise comparison within **A.** Pre-bleaching and **B.** Bleaching. Pairwise comparison **C.** Between pre-bleaching and bleaching sampling time points. Top two clades which contributed to dissimilarity of community compositions are shown with contribution percentages (%). Clades which were more abundant in variables in columns are shown as bold letter and clades which were more abundant in variables in rows are shown as normal letter.

Table S3.9. List of ITS2 variants and relative abundance in each sample. **A.** Pre-bleaching. **B.** Bleaching. Compositions of ITS2 variants in each replicate (n = 2-4, depends on the samples) were averaged and top three ITS2 variants in each clade are listed with relative abundance (%) in each sample.

Table S3.10. Summary of SIMPER analysis for *Symbiodinium* ITS2 variants community compositions based on the ITS2 marker. Pairwise comparison within **A.** Pre-bleaching and **B.** Bleaching. Pairwise comparison **C.** Between pre-bleaching and bleaching sampling time points. Top two ITS2 variants which contributed to dissimilarity of community compositions are shown with contribution percentages (%). ITS2 variants which were more abundant in variables in columns are shown as bold letter and ITS2 variants which were more abundant in variables in rows are shown as normal letter.

Chapter 4

Table S4.1. Summary of two-way ANOVA for cell cycle and growth parameters under the light treatments. **A.** Main effects. *Post-hoc* pairwise comparison for **B.** strain effects and **C.** treatment effects. Factors: strain (B1, C1, C1′ and D1a), treatment (low light, high light). Cell cycle parameters (G_1 peak, S peak and G_2/M peak proportions) were arcsine transformed and cell volume was square root transformed. MS: mean square, df: degrees of freedom, F: Fisher statistic, P value: * for $P < 0.05$, ** for $P < 0.01$.

Table S4.2. Summary of two-way ANOVA for cell cycle and growth parameters under the temperature treatments. **A.** Main effects. *Post-hoc* pairwise comparison for **B.**

strain effects and **C.** treatment effects. Factors: strain (B1, C1, C1´ and D1a), treatment (control, heat). Cell cycle parameters (G_1 peak, S peak and G_2/M peak proportions) were arcsine transformed and cell volume was square root transformed. MS: mean square, df: degrees of freedom, *F*: Fisher statistic, P value: * for $P < 0.05$, ** for $P < 0.01$.

List of Electronic Files

Chapter 2

Appendix E2.1. Output file of PERMANOVA pairwise comparison (habitat, season) for *Symbiodinium* cladal compositions obtained by NGS analysis generated using PRIMER (version 6.1.16) and PERMANOVA+ (version 1.0.6) software. Pairwise comparison output files for habitat and season factors are included in this file which significant differences were detected for these factors from the main effects (Table S2.3A).

Appendix E2.2. Output file of PERMANOVA pairwise comparison (site, habitat, season) for *Symbiodinium* ITS2 variant compositions obtained by NGS analysis generated using PRIMER (version 6.1.16) and PERMANOVA+ (version 1.0.6) software. Pairwise comparison output files for site, habitat and season factors are included in this file which significant differences were detected for these factors from the main effects (Table S2.3B).

Appendix E2.3. Output file of PERMANOVA pairwise comparison (site, habitat, season) for *Symbiodinium* OTU compositions obtained by NGS analysis generated using PRIMER (version 6.1.16) and PERMANOVA+ (version 1.0.6) software. Pairwise comparison output files for site, habitat and season factors are included in this file which significant differences were detected for these factors from the main effects (Table S2.3C).

Appendix E2.4. Output file of PERMANOVA pairwise comparison (site, habitat) for *Symbiodinium* cladal compositions (only for clades A, C and D) obtained by qPCR analysis generated using PRIMER (version 6.1.16) and PERMANOVA+ (version 1.0.6) software. Pairwise comparison output files for site and habitat factors are included in this file which significant differences were detected for these factors from the main effects (Table S2.7).

Appendix E2.5. Output file of PERMANOVA pairwise comparison (technique) for *Symbiodinium* cladal compositions (only for clades A, C and D) obtained by both NGS and qPCR analysis generated using PRIMER (version 6.1.16) and PERMANOVA+ (version 1.0.6) software.

Chapter 3

Appendix E3.1. Output file of PERMANOVA pairwise comparison (site, habitat) for *Symbiodinium* cladal compositions obtained by NGS analysis based on the cp23S marker generated using PRIMER (version 6.1.16) and PERMANOVA+ (version 1.0.6) software. Pairwise comparison output files for site and habitat factors are included in this file which significant differences were detected for these factors from the main effects (Table S3.5A).

Appendix E3.2. Output file of PERMANOVA pairwise comparison (site, habitat) for *Symbiodinium* OTU compositions obtained by NGS analysis based on cp23S primer set generated using PRIMER (version 6.1.16) and PERMANOVA+ (version 1.0.6) software. Pairwise comparison output files for site and habitat factors are included in this file which significant differences were detected for the factors from the main

effects (Table S3.5B).

Appendix E3.3. Output file of PERMANOVA pairwise comparison (site, habitat) for *Symbiodinium* cladal compositions obtained by NGS analysis based on the ITS2 marker generated using PRIMER (version 6.1.16) and PERMANOVA+ (version 1.0.6) software. Pairwise comparison output files for site and habitat factors are included in this file which significant differences were detected for these factors from the main effects (Table S3.7A).

Appendix E3.4. Output file of PERMANOVA pairwise comparison (amplicon) for *Symbiodinium* cladal compositions obtained by NGS analysis based on both cp23S and ITS2 markers generated using PRIMER (version 6.1.16) and PERMANOVA+ (version 1.0.6) software.

Appendix E3.5. Output file of PERMANOVA pairwise comparison (site, habitat) for *Symbiodinium* ITS2 variant compositions obtained by NGS analysis based on the ITS2 marker generated using PRIMER (version 6.1.16) and PERMANOVA+ (version 1.0.6) software. Pairwise comparison output files for site and habitat factors are included in this file which significant differences were detected for these factors from the main effects (Table S3.7B).

Appendix E3.6. Output file of PERMANOVA pairwise comparison (site, habitat, season) for *Symbiodinium* OTU compositions obtained by NGS analysis based on the ITS2 marker generated using PRIMER (version 6.1.16) and PERMANOVA+ (version 1.0.6) software. Pairwise comparison output files for site, habitat, season factors are

included in this file which significant differences were detected for these factors from the main effects (Table S3.7C).

Chapter 4

Appendix E4.1. Image series of *Symbiodinium* DNA contents shifting through 24 h. Forward scatter (X axis, log scale) plotted against DNA fluorescent contents (Y axis, linear scale) of **A.** B1, **B.** C1, **C.** C1´ and **D.** D1a strain under high light treatment for one replicate.

Appendix: OTU analysis for *Symbiodinium* culture strains

Appendix E6.1. zOTU table obtained by NGS analysis based on the ITS2 marker for *Symbiodinium* culture strains. zOTU taxonomies were assigned against the *Symbiodinium* ITS2 reference database "SymTyper". OTUs observed in each sample were highlighted with colours. Colour coding: red for clade A, blue for clade B, purple for clade D, green for clade E, and orange for clade F.

Appendix E6.2. zOTU table for *Symbiodinium* culture strains after applying OTU abundance filtering. zOTUs which contain < 1% of the reads within each sample were replaced by 0 and removed from the OTU table if those zOTUs contain 0 sequence across all samples. zOTUs contain sequences were highlighted with colours. Taxonomy was assigned against SymTyper.

Abstract of Thesis

Symbiodinium are endosymbiotic microalgae of reef-building corals. Photosynthesis by these algae fuels the productivity of corals and ultimately the growth of entire reef systems. However, a critical phase of *Symbiodinium*'s life history is existence as "free-living" cells prior to acquisition by their host. Free-living populations are essential for establishing symbiosis for many corals that propagate larval generation without algal symbionts, but also for recombination of host-symbiont associations recovering from stress. Despite the importance of free-living populations, their underlying biodiversity and ecology remains a black box. For example, how they distribute spatially, temporally and regionally, and contribute to coral reef ecosystems as they currently face an era of "ecological crisis", are largely unknown.

To unlock the distribution, abundance and life cycle of free-living *Symbiodinium*, I applied novel dual NGS- (eDNA metabarcoding using next generation sequencing) and qPCR-based (using clade-specific primers) approaches to first explore the qualitative and quantitative distribution and abundance of free-living *Symbiodinium* for tropical (Heron Island) (**Chapter 2**) and temperate (Sydney Harbour) (**Chapter 3**) east coast Australian coral communities that are periodically connected by the Eastern Australian Current. To further evaluate how such diversity (which is only a snap shot of population dynamics over time) is sustained as a result of individual population turnover, I analysed the *Symbiodinium* cell cycle to establish a novel baseline for how population turnover is regulated by cell cycle dynamics across species and under alternate conditions (light and temperature) (**Chapter 4**).

This thesis highlights the importance of habitat variety in sustaining diverse free-living *Symbiodinium* communities, functional plasticity and hence resistance to disturbance (**Chapter 5**). For example, I provide new insight of macroalgae habitats as key reservoirs of symbiont availability to hosts via local supply but also wider dispersal. In the latter case, I discuss that dispersal of *Symbiodinium* is critical to support paradigms of high-latitude temperate reefs acting as refugia for tropical corals under climate change, since temperate and tropical *Symbiodinium* communities are currently geographically separated. Cell cycle dynamics differed between genetically different types (species), and results in specific types proliferating faster under certain environmental conditions thereby supporting shifts in community structure. As such, cell cycle dynamics comprises a key functional trait that is still overlooked but warrants further targeted investigation, not only amongst free-living populations, but also *in hospite* to clarify how functional equilibrium under steady-state symbioses is maintained as reef environments continue to be subjected to stressors into the future.

Declaration of the Contribution to Each Chapter

Chapters 2 and 3

The same format and approach was applied to deliver both Chapters 2 and 3: Experimental design was performed by myself (Lisa Fujise) supported by A/Prof. David Suggett (UTS) and Dr. Matthew Nitschke (University of Aveiro). I was primarily responsible for the all field sampling, laboratory work, data analysis and interpretation, and writing up of the manuscripts. Dr. Stephanie Gardner (UTS) provided assistance with sampling in Heron Island (Chapter 2) and Samantha Goyen (UTS) with sampling in both Heron Island (Chapter 2) and Sydney Harbour (Chapter 3). Dr. Michael Stat and Prof. Michael Bunce (Curtin University) provided support to analyse samples using next generation sequencing (NGS) in their ultra-clean lab facility. Dr. Tim Kahlke (UTS) provided assistance for building bioinformatic pipelines for *Symbiodinium* sequence analysis, Dr. Nahshon Siboni (UTS) for qPCR assay design, and Dr. Stephen Woodcock (UTS) for statistical analysis. A/Prof. David Suggett, Prof. Peter Ralph (UTS), Dr. Matthew Nitschke provided detailed feedback on both manuscripts at various stages.

Chapter 4

This chapter has been published in *Journal of Eukaryotic Microbiology* (in January 2018):

Fujise, L., Nitschke, M. R., Frommlet, J. C., Serôdio, J., Woodcock, S., Ralph, P. J., & Suggett, D. J. 2018. Cell Cycle Dynamics of Cultured Coral Endosymbiotic Microalgae (*Symbiodinium*) Across Different Types (Species) Under Alternate Light

and Temperature Conditions. J. Eukaryot. Microbiol. doi:10.1111/jeu.12497.

Experimental design was performed by myself (Lisa Fujise) supported by A/Prof. David Suggett. Laboratory experiment, sample analysis, data analysis and writing up of the manuscript were all performed by myself with helps. Dr. Stephen Woodcock (UTS) provided assistance for statistical analysis. A/Prof. David Suggett, Dr. Jörg C. Frommlet (University of Aveiro), Dr. João Serôdio (University of Aveiro), Dr. Matthew Nitschke (University of Aveiro), and Prof. Peter Ralph (UTS) provided comprehensive feedback on the manuscript at various stages.

Chapter 1

General Introduction and thesis outline

1.1. Coral reef ecosystems

Coral reefs support exceptional biodiversity and productivity in the tropical and subtropical coastal ocean (Odum and Odum 1955; Atkinson and Grigg 1984; Knowlton et al. 2010), having 25% of all marine species despite covering only < 1% of the ocean's surface (Reaka-Kulda 1997; 2005; Knowlton et al. 2010). Form and functioning of coral reefs provide various ecological services, ranging from supporting fisheries, providing coastal protection and generating income from tourism (Kirk and Weis 2016). As such, nearly 0.5 billion people depend on coral reefs for their livelihood (Wilkinson 2008), and reefs provide a net value of US$ 30 billion per year to the global economy (Cesar et al. 2003).

Coral reef frameworks are formed through secretion of calcium carbonate, primarily by scleractinian corals (invertebrates belonging to the phylum Cnidaria; class Anthozoan) living in association with zooxanthellae, microalgal dinoflagellates of the genus *Symbiodinium* (e.g. Davy et al. 2012). This association is fundamentally symbiotic through exchange of essential nutrients between the coral host and algal symbiont (Muscatine 1967; Muscatine et al. 1981; Yellowlees et al. 2008), but it is considered to operate along a spectrum from mutualistic to parasitic (Stat et al. 2008a; Lesser et al. 2013). Under stress conditions, this symbiosis collapses resulting in coral bleaching and potentially death of the coral (e.g. Hoegh-Guldberg 1999; Brown 1997; Lesser 2011; Suggett et al. 2017). In recent decades, heat wave-induced coral bleaching via climate change has resulted in worldwide mass mortality (Glynn 1993; Brown 1997; Douglas 2003), and most recently in 2015/2016 where > 60% of corals bleached (Hughes et al. 2017) and > 25% of all corals on the Great Barrier Reef are now known to have died (Great Barrier Reef Marine Park Authority 2017).

Coral reefs have been declining year after year and it is estimated that ca. 19% of the world's coral reefs have been lost since 1950 (Wilkinson 2008) with 50% of coral cover on the Great Barrier Reef has disappeared since 1985 (De'ath et al. 2012). Coral reefs are threatened by accelerating stressors acting both globally and locally, and have now entered an era of "ecological crisis" (Suggett et al. 2017). Consequently, global calls recognise the need to urgently understand the stability and sustainability of coral reefs under future climate projection (Freeman 2015).

1.2. What are *Symbiodinium*?

Symbiodinium are unicellular microalgae within the family Symbiodiniaceae, an order Suessiales of Dinophyta first discovered and cultured by the Japanese scientist Kawaguti (originally designated as the genus *Gymnodinium*; Kawaguti 1944). Cells are typically 10 μm in diameter (varying from 5-15 μm; LaJeunesse 2001; Suggett et al. 2015) and are golden-brown in colour. *Symbiodinium* have evolved to live in endosymbiosis with various marine organisms in coral reef ecosystems, such as hard and soft corals, sea anemones, jellyfishes, and giant clams (Trench 1993; Stat et al. 2006; Pochon et al. 2014). Here, in most cases, *Symbiodinium* reside in the endodermal tissues of their hosts, receiving inorganic nutrients (e.g. CO_2, NH_3, PO_4^{3-}) and protection from grazers, in exchange for providing photosynthetic products such as glycerol, glucose, and amino acids which support the heterotrophic growth of the host (Muscatine 1967; Muscatine and Cernichiari 1969; Yellowlees et al. 2008). It is commonly thought that 60-85% of the total hosts' nutrition is derived from the organic carbon supplied from *Symbiodinium* (Muscatine et al. 1981), thus fuelling host metabolism, growth and reproduction to sustain reef-building corals in oligotrophic tropical waters (Muscatine et al. 1984; McCloskey et al. 1994; Davy et

al. 2012). Furthermore, through photosynthesis, *Symbiodinium* indirectly enhance calcification by the coral host (typically by over 100%) and therefore drive the very formation of the reef structural framework (Goreau 1959; Al-Horani et al. 2003; Davy et al. 2012). This critical symbiosis between corals and *Symbiodinium* dates back to the late Triassic period, and hence represents a successful evolutionary strategy which has existed for ca. 200 million years (Stanley and Swart 1995); however, why *Symbiodinium* entered into this symbiosis is still unresolved (Frommlet et al. 2015).

Symbiodinium can also live externally of their hosts, referred to as "free-living" cells (e.g. Carlos et al. 1999; Coffroth et al. 2006; Yamashita and Koike 2013; Cunning et al. 2015) (detailed in section 1.4). Once *ex hospite*, i.e. within pelagic or benthic habitats or as laboratory monocultures, cells exhibit two morphological phases: (i) a motile stage which has a gymnodinioid-like morphology possessing two flagella, and (ii) a coccoid stage of spherical morphology without flagella (Fig. 1.1) (Kawaguti 1944; Freudenthal 1962; Yamashita et al. 2009; Lee et al. 2015); however, *Symbiodinium in hospite* only appears to occur as the coccoid-like morphology (Kevin et al. 1969; Trench and Blank 1987).

In addition to the diversity that *Symbiodinium* display in terms of their life history, extensive research continues to demonstrate that this genus shows exceptional taxonomic diversity, as well as physiological, behavioural and morphological plasticity (e.g. Schoenberg and Trench 1980; Trench and Blank 1987; Rowan 1998; LaJeunesse 2001; Stat et al. 2006; LaJeunesse et al. 2012a; Kirk and Weis 2016). Initial observations suggested corals' symbiotic dinoflagellates were members of a

single pandemic species (*Symbiodinium microadriaticum*; Freudenthal 1962); however, increasingly sophisticated molecular phylogenetic techniques have clarified the huge genetic diversity of *Symbiodinium* (detailed in section 1.3). Consequently, a major goal of *Symbiodinium* research has moved to new era of understanding how this immense phylogenetic diversity confers differences in functional diversity of key traits that define fitness both of the free-living and symbiotic life histories (Suggett et al. 2015; Warner and Suggett 2016; Goyen et al. 2017; Suggett et al. 2017).

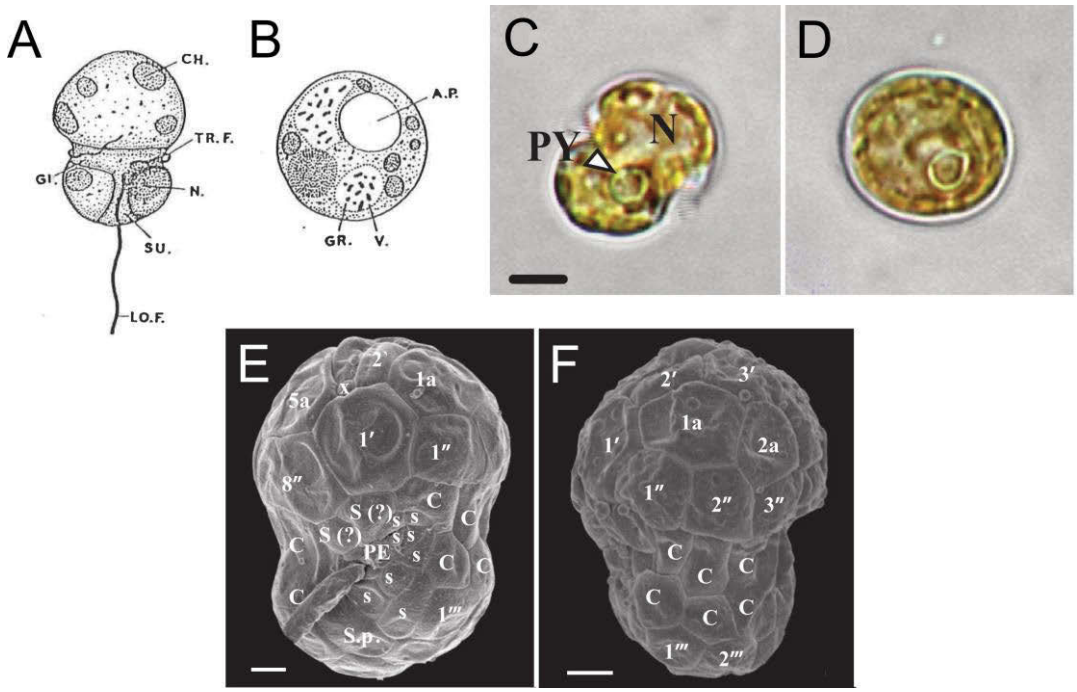

Figure 1.1. Morphologies and cellular structures of *Symbiodinium microadriaticum*. Illustrations of *Symbiodinium* cells with cellular structures (taken from Freudenthal 1962): **A.** Zoospore (motile cell), CH: chloroplast, GI: girdle, LO.F: longitudinal flagellum, N: nucleus, SU: sulcus, TR.F: transverse flagellum. **B.** Vegetative (coccoid) cell, AP: assimilation product, GR: granule, V: vacuole. Light micrographs (taken from Lee et al. 2015): **C.** Motile cell showing gymnodinioid morphology, N: nucleus, PY: pyrenoid. Scale bar = 2 μm. **D.** Coccoid cell showing non-flagellated spherical shapes. Scanning electron micrographs of motile cells (taken from Lee et al. 2015): **E.** Ventral view showing the episome, C: cingulum, PE: peduncle, s: sulcal plates. **F.** Ventral-left lateral view showing the episome. Scale bars = 1 μm.

1.3. Phylogeny and biogeography of *Symbiodinium*

Symbiodinium spp. can be divided into nine distinct monophyletic groups (clades A-I) based on nuclear ribosomal DNA (18S rDNA and 28S rDNA) and chloroplast ribosomal DNA (cp23S rDNA) (e.g. Rowan and Powers 1991; LaJeunesse 2001; 2004; Pochon and Gates 2010; Pochon et al. 2014) (Fig. 1.2, also see Fig. 1.3 for genetic markers used for identification of *Symbiodinium*); where clade A represents taxa that are the most ancestral group. However, analysis of more rapidly evolving DNA gene sequences has established the existence of hundreds of types or/and species (e.g. Sampayo et al. 2009; LaJeunesse et al. 2012a; Stat et al. 2012; LaJeunesse 2017; Thornhill et al. 2017). The most in depth and widely used

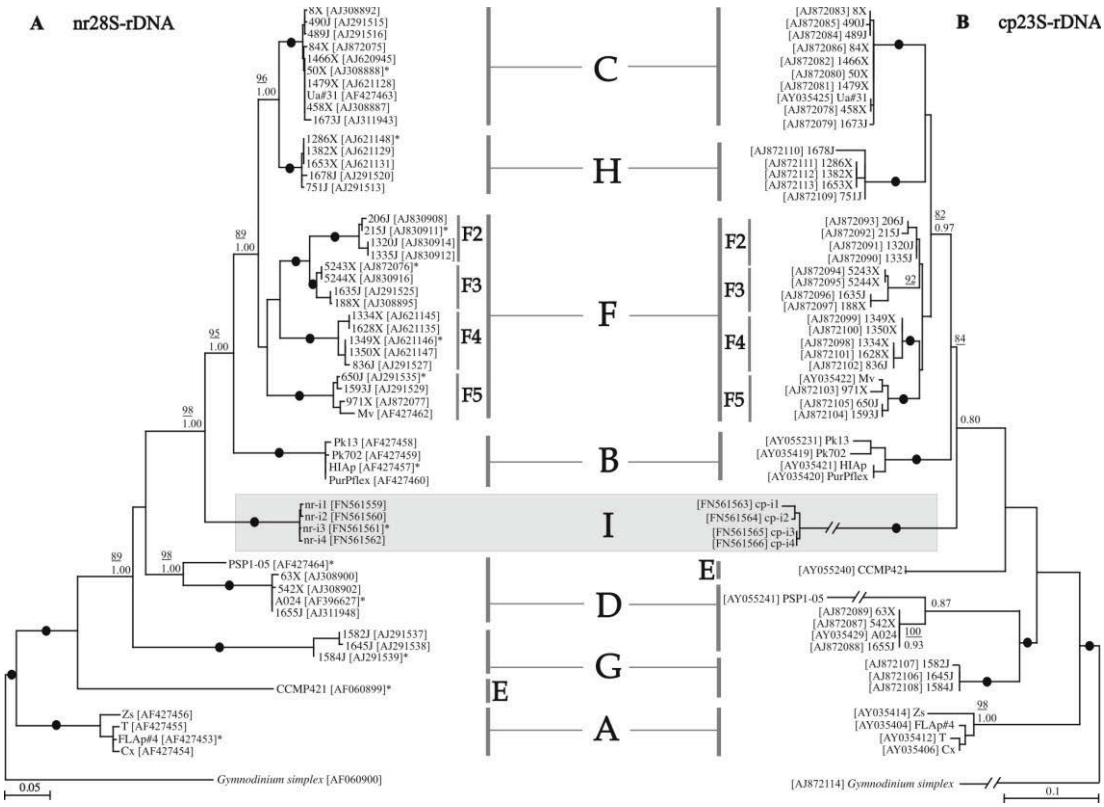

Figure 1.2. Phylogenetic tree of *Symbiodinium* according to nr28S (left) and cp23S (right) datasets (taken from Pochon and Gates 2010).

individual marker to date has been the internal transcribed spacer 2 (ITS2) region of nuclear rDNA, for which variation of ITS2-types correlate with physiological and ecological attributes (e.g. LaJeunesse 2001; 2004; Sampayo et al. 2009) and extensive databases now exist (e.g. LaJeunesse 2002; LaJeunesse et al. 2003; LaJeunesse 2004; Stat et al. 2006; Pochon et al. 2007; Lesser et al. 2013; Cunning et al. 2015; Quigley et al. 2017). For example, "SymTyper" database includes 719 ITS2 sequences (e.g. Cunning et al. 2015). Such efforts have revealed that a community of *Symbiodinium* types can exist within a single host using highly sensitive molecular

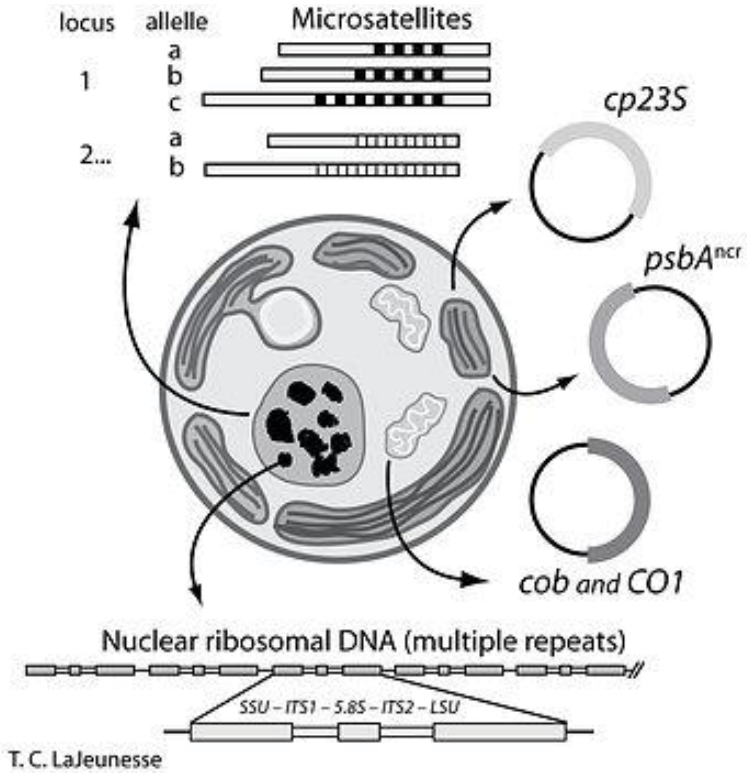

Figure 1.3. Schematic diagram of nuclear and organelle genomes used for identification of *Symbiodinium* types/species. Nuclear ribosomal genes and spacer regions, including the small subunit (SSU or 18S), large subunit (LSU or 28S), and internal spacer regions (ITS1 and ITS2), as well as the chloroplastic genes: cp23S and non-coding region of the psbA minicircle ($psbA^{ncr}$), mitochondrial cob and coI genes, and microsatellite loci (taken by Sampayo et al. 2009 and modified by LaJeunesse et al. 2012b; The Tree of Life Web Project: *Symbiodinium*).

markers (ca. ITS2) and high-resolution techniques such as denaturing-gradient gel electrophoresis (DGGE) (LaJeunesse 2001; LaJeunesse et al. 2003; 2004; 2010a; Tonk et al. 2017), cloning and sequencing (Apprill and Gates 2007; Stat et al. 2011; 2013) and recently, high throughput next generation sequencing (NGS) technique (Arif et al. 2014; Thomas et al. 2014; Boulotte et al. 2016; Quigley et al. 2017). Not only inherent diversity *in hospite*, but also massive biodiversity of free-living *Symbiodinium* have recently been confirmed to exist in coral reef environment using these techniques (e.g. Sweet 2014; Yamashita et al. 2014; Cunning et al. 2015; Quigley et al. 2017).

Whilst use of ITS2 marker has grown in popularity, it is increasingly clear that ITS2 alone cannot fully resolve *Symbiodinium* diversity. Parallel assessment of additional markers such as mitochondrial cob and coI genes, chloroplastic non-coding region of the psbA minicircle ($psbA^{ncr}$) (LaJeunesse and Thornhill 2011; Hume et al. 2015; LaJeunesse et al. 2015; Lee et al. 2015), and/or microsatellite markers (Pettay et al. 2011; LaJeunesse et al. 2012a; 2014; Thornhill et al. 2014) have recently demonstrated much greater divergence than can be achieved through ITS2 marker only; such additional markers not only enable the resolution of species identification (e.g. Hume et al. 2015; LaJeunesse et al. 2014; 2015), but also provide a means to track evolutionary paths over space and time within specific types (Thornhill et al. 2014; LaJeunesse et al. 2015). Several ITS2-types have now been confirmed to provide species level diversity based on a combination of those higher resolution genetic markers (e.g. $psbA^{ncr}$, cob and microsatellite) with defined differences in morphology, cell size, physiology (stress tolerance), and ecology (host compatibility) and increasing the number of formal descriptions of *Symbiodinium* species (e.g.

LaJeunesse et al. 2012a; 2014; 2015; LaJeunesse 2017; Wham et al. 2017). These formal species descriptions are important for reporting the ecology, physiology and genomics of coral-dinoflagellates with accuracy (Wham et al. 2017), and 20 species of *Symbiodinium* have now been described (e.g. Hume et al. 2015; LaJeunesse 2017) (Table 1.1), and this list grows annually.

Table 1.1. List of *Symbiodinium* species. 20 species are formally described, whilst 2 species (*S.* "*fitti*" and *S.* "*muscatinei*") with quotation marks are *nomina nuda* (published specific epithets without formal diagnosis). Synonyms are the species (*nomina nuda*) once thought to be a separate species, but later confirmed as identical to formally described species (adapted from LaJeunesse et al. 2012a; Stat et al. 2012; Hume et al. 2015; LaJeunesse 2017).

Clade	ITS2-type	Species	References	Synonyms
A	A1	*Symbiodinium microadriaticum*	Freudenthal (1962), Trench and Blank (1987), LaJeunesse (2017)	*Gymnodinium* "*microadriaticum*" (Taylor 1971), *Zooxnathella* "*microadriaticum*" (Loeblich and Sherley 1979)
	A2	*Symbiodinium pilosum*	Trench and Blank (1987), Trench (2000)	*Symbiodinium* "*corculorum*", *Symbiodinium* "*meandrinae*" (Banaszak et al. 1993)
	A2-relative	*Symbiodinium natans*	Hansen and Daugbjerg (2009)	
	A3	*Symbiodinium* "*fitti*"	Pinzon et al. (2011)	
	A3, A3a, A6	*Symbiodinium tridacnidorum*	Lee et al. (2015)	
	A4	*Symbiodinium linucheae*	Trench and Thinh (1995), LaJeunesse (2001)	*Gymnodinium* "*linuchaea*" (Trench and Thinh 1995)
	A13	*Symbiodinium necroappetens*	LaJeunesse et al. (2015)	*Symbiodinium microadriaticum* sub.sp "*condylactis*" (Blank and Huss 1988), *Symbiodinium* "*cariborum*" (Banaszak et al. 1993)
B	B1	*Symbiodinium antillogorgium*	Parkinson et al. (2015)	
	B1	*Symbiodinium endomadracis*	Parkinson et al. (2015)	
	B1	*Symbiodinium minutum*	LaJeunesse et al. (2012a)	
	B1	*Symbiodinium pseudominutum*	Perkinson et al. (2015)	*Symbiodinium* "*bermudense*", *Symbiodinium* "*pulchrorum*" (Banaszak et al. 1993)
	B2	*Symbiodinium psygmophilum*	LaJeunesse et al. (2012a)	
	B4	*Symbiodinium* "*muscatinei*"	LaJeunesse and Trench (2000)	
	B19	*Symbiodinium aenigmaticum*	Parkinson et al. (2015)	
C	C1	*Symbiodinium goreaui*	Trench and Blank (1987), Trench (2000)	
	C3	*Symbiodinium thermophilum*	Hume et al. (2015)	
D	D1	*Symbiodinium glynnii*	LaJeunesse et al. (2010a), Wham et al. (2017)	
	D1a, D1-4	*Symbiodinium trenchii*	LaJeunesse et al. (2005), LaJeunesse et al. (2014)	
	D8, D12, D13	*Symbiodinium eurythalpos*	LaJeunesse et al. (2014)	
	D15	*Symbiodinium boreum*	LaJeunesse et al. (2014)	
F	F1	*Symbiodinium kawagutii*	Trench and Blank (1987), Trench (2000)	
E		*Symbiodinium voratum*	Jeong et al. (2014)	*Symbiodinium* "*californium*" (Banaszak et al. 1993)

Improved resolution of *Symbiodinium* types/species diversity via molecular markers has driven the ever-growing wealth of studies examining biogeographic radiation and niche partitioning within this genus, in particular for host-symbiont associations and how these are influenced by specific environmental conditions. To date, it is generally established that (i) clades A, B, C and D are the predominant symbiont types in scleractinian corals (Pochon et al. 2014). Whilst clades C and D can also be found in foraminifera, where sequences based on cp23S rDNA have demonstrated specific sequence divergence amongst clade D for foraminifera versus corals (Santos et al. 2002); (ii) clade E is typically found free-living, and only rarely *in hospite* (and with extremely low abundance in sea anemone and scleractinian corals; Jeong et al. 2014); (iii) clades F and G are common in foraminifera and sponges, but can be found rarely in association with scleractinians (LaJeunesse 2001; Stat et al. 2006; Pochon et al. 2007); and (iv) clades H and I have been found exclusively within foraminifera to date (Pochon and Gates 2010; Kirk and Weis 2016) (Table 1.2). From this diversity, clade C is the most dominant clade associated with many marine invertebrate hosts and the most diverse in terms of types, so far divided into more than 100 ITS2-types (LaJeunesse et al. 2003; 2004; Pochon et al. 2004; Stat et al. 2006; Sampayo et al. 2007; Tonk et al. 2017). All clades include free-living life stages (e.g. Pochon et al. 2014; Cunning et al. 2015; Granados-Cifuentes et al. 2015; Quigley et al. 2017), and some types are now thought to be exclusively free-living *Symbiodinium* (e.g. Yamashita and Koike 2013) (detailed in section 1.4).

Table 1.2. Summary of *Symbiodinium* lineages and associated hosts. The nine clades (A-I) (using 28S rDNA and cp23S rDNA) which constitute the genus *Symbiodinium*, with selected literature highlighting the hosts phyla of each lineage (taken only *in hospite* information from Pochon et al. 2014).

Clade	Hosts	References
A	Cnidaria	LaJeunesse (2001), Reimer et al. (2006), Stat et al. (2008a)
	Mollusca	Baillie et al. (2000a), Ishikura et al. (2004), LaJeunesse et al. (2010b)
	Plathyelminthes	Baillie et al. (2000a)
B	Cnidaria	Coffroth et al. (2001), LaJeunesse (2001), Santos et al. (2001)
	Mollusca	LaJeunesse (2002)
	Porifera	Hunter et al. (2007)
C	Cnidaria	Coffroth and Santos (2005), LaJeunesse (2004), Sampayo et al. (2007), Wagner et al. (2011)
	Foraminifera	Pochon et al. (2001), (2004), (2006), (2007)
	Mollusca	Baillie et al. (2000a), Ishikura et al. (2004), LaJeunesse et al. (2010b)
	Plathyelminthes	Baillie et al. (2000a)
D	Cnidaria	Brown et al. (2000), Correa and Baker (2009), Jones et al. (2008)
	Foraminifera	Pochon et al. (2007), Garcia-Cuetos et al. (2005)
	Mollusca	Ishikura et al. (2004), LaJeunesse et al. (2010b)
	Porifera	Carlos et al. (1999)
E	Cnidaria	LaJeunesse and Trench (2000), LaJeunesse (2001)
F	Cnidaria	Rodriguez-Lanetty et al. (2002)
	Foraminifera	Pochon et al. (2001), (2006), (2007), Pochon and Gates (2010)
G	Cnidaria	Bo et al. (2011), van Oppen et al. (2005)
	Foraminifera	Pochon et al. (2001), (2006), (2007), Pochon and Gates (2010)
	Porifera	Schoenberg and Loh (2005), Schoenberg et al. (2008), Hill et al. (2011)
H	Foraminifera	Pochon et al. (2001), (2006), (2007), Pochon and Gates (2010)
I	Foraminifera	Pochon and Gates (2010)

Global efforts to apply molecular markers to examine *Symbiodinium* diversity are beginning to reveal broad bio-regional trends, which may ultimately prove critical to resolving adaptive radiation (Thornhill et al. 2014). Notably, the diversity of symbiont types in Caribbean reefs is higher compared to Indo-Pacific reefs (mainly the Great Barrier Reef), which harbour clades A, B and C (Baker and Rowan 1997; LaJeunesse 2002), whereas corals in Indo-Pacific mainly contain clade C symbionts (Baker and Rowan 1997; LaJeunesse et al. 2003; 2004; Tonk et al. 2017). *Symbiodinium* types A3, B1 and C1 are common in Caribbean reefs (LaJeunesse 2002), while C1, C3 and C21 types appear to dominate Indo-Pacific reefs (LaJeunesse et al. 2003, 2004; Tonk et al. 2017). However, intriguingly host diversity

is opposite where Indo-Pacific reefs have a richer diversity of hosts compared to Caribbean reefs (Baker and Rowan 1997; LaJeunesse et al. 2003). Individual host species can also associate with different symbiont types (intra-specific) over environmental gradients: (i) with depth; for example, the dominant Caribbean coral, *Orbicella faveolata* can harbour clades A and B in shallow water compared to clade C in deeper water (Rowan et al. 1997); (ii) across latitude; for example, the coral *Plesiastrea versipora* in tropical/subtropical region of Australia harbour clade C, whereas that same coral species in temperate regions harbour clade B (Rodriguez-Lanetty et al. 2001), and finally; (iii) across longitude; for example, both clades C and D *Symbiodinium* were found in zoanthid *Palythoa caesia* in the east, but only clade C in the west Indian Ocean (Burnett 2002). Reports of how host-symbiont diversity (*in hospite*) is expanding/increasing over space and time, but curiously relatively little is known about the diversity of free-living *Symbiodinium* required to understand the supply side ecology of *Symbiodinium* life history and population propagation (e.g. Yamashita and Koike 2013) (detailed in section 1.4).

One of the most important findings in recent years from the growing information on symbiont diversity is perhaps that of host-symbiont specificity. Within any given environment, many coral species appear to harbour a single clade of *Symbiodinium* (Rowan and Powers 1991; LaJeunesse 2002; Rodriguez-Lanetty et al. 2003; Pettay and LaJeunesse 2007; Thornhill et al. 2009). In spite of such specificity, many hosts appear to select *Symbiodinium* types suitable for different environmental conditions (Baillie et al. 1998; Pettay et al. 2011). For example, LaJeunesse et al. (2003) found host-specific symbiont types, such as the specialist; C17 in *Montipora* spp., C22a in *Turbinaria* spp., and C8a in *Stylophora pistillata* at 10 m depth, suggesting

specificity, but concurrently found C1, C3 and C21 *Symbiodinium* types to be generalists from a wide range of host taxa at various depths. The ability for the host to associate with different symbiont types is a particularly important trait in determining resilience to environmental stress over both space and time. Numerous reports exist that some host corals can "switch" or "shuffle" their symbiont types, especially as irradiance and temperature become anomalously high (Baker 2003; Coffroth and Santos 2005; Berkelmans and van Oppen 2006; Boulotte et al. 2016). However, whether this truly reflects acquisition of different symbionts (Kinzie et al. 2001) or natural selection from amongst the rare symbiont types already *in hospite* (Stat and Gates 2011) that may cope better under more extreme conditions remains unresolved. Even so, selection of more physiologically stress-tolerant symbionts clearly provides enhanced resilience to subsequent stressors (Silverstein et al. 2015).

Observation of different stress tolerances amongst *Symbiodinium* types has led to widespread efforts to compare the physiology of different types in an attempt to resolve common physiological traits that underpin stress resilience. LaJeunesse (2001) first discovered a positive correlation between clade and cell size, mycosporine-like amino acid production and host infectivity. Many researchers have since begun to associate different tolerances amongst specific clades; for example, clade A (the most ancestral clade) appears widely adapted to different broad environmental niches such as high irradiance (Rowan et al. 1997; Reynolds et al. 2008) and low temperature and irradiance (Savage et al. 2002; Suggett et al. 2015). Clade A types appear to exhibit significant tolerance to light and thermal stress (Reynolds et al. 2008; Suggett et al. 2008; LaJeunesse et al. 2015), whereas clade B types show more sensitivity to thermal stress (Robison and Warner 2006; Loram et al.

2007; Suggett et al. 2008) and is often more commonly associated with temperate hosts and thus a specialist of lower light and cooler conditions (Rodriguez-Lanetty et al. 2001; Silverstein et al. 2011). Clade C appears to have a higher rate of carbon fixation and translocate more carbon to promote hosts growth relative to clades A and D (Stat et al. 2008a; Cantin et al. 2009; Jones and Berkelmans 2011; Lesser et al. 2013) and this was also confirmed for the sea anemone, *Exaiptasia pallida* by inducing novel symbiosis with heterologous type D1a (*S. trenchii*) and detecting shifts of metabolic pathways from symbiont to host using a combination of transcriptomic and metabolomic analyses (Matthews et al. 2017). Corals with clade D types show significantly reduced growth rates and reproduction (Jones and Berkelmans 2010; 2011); however, the cost of hosting such a clade may prove beneficial as these corals bleach less often given their higher thermal tolerance (Stat and Gates 2011; Lesser et al. 2013; Silverstein et al. 2015). Such different physiologies of *Symbiodinium* thus potentially relate to the effectiveness of the coral-symbiosis under typical growth conditions, but also relates to the susceptibility to environmental stress and resistance to bleaching (Warner et al. 1996; Rowan et al. 1997; Warner et al. 1999; Douglas 2003). Even so, such trends generally breakdown once examining different susceptibilities at the ITS2-type level; for example, different A types can be both light-heat stress sensitive and tolerant (Robison and Warner 2006; Ragni et al. 2010), clade C was thought to be a thermally sensitive lineage, but contain *S. thermophilum* (C3) the most thermally robust symbiont (Hume et al. 2015), whilst even isolates of the same ITS2-type (C1) can show different thermal tolerance limits (Howells et al. 2012). No single study has yet broadly reconciled the ever-growing complexities of *Symbiodinium* phylogeny with a clear distribution of functional traits that indicate ecological success (Suggett et al.

2015; Warner and Suggett 2016; Goyen et al. 2017; Suggett et al. 2017). To understand this problem, research needs to be performed that separates out expression of functional traits that confer ecological success during the free-living phase (often used for culture studies) versus when *in hospite* populations. For this, studies now need to begin to compare a greater number of *Symbiodinium* genotypic variants/species for such key traits underpinning ecological fitness.

1.4. Free-living *Symbiodinium*

Symbiodinium commonly form a symbiotic relationship with many marine invertebrates (e.g. Trench 1993), but also readily exist as "free-living" cells (e.g. Carlos et al. 1999; Coffroth et al. 2006; Yamashita and Koike 2013). Despite decades of research into this organism, little is still known of *Symbiodinium*'s life cycle, in part because of its mixed life styles. For example, how cells exist as free-living in the reef environment, but subsequently switch to endosymbionts remains a mystery. Therefore, the following section summarises current knowledge of *Symbiodinium* in the free-living life stage and identifies major gaps in knowledge that still exist.

Free-living *Symbiodinium* have been found in various coral reef environments, notably water columns and sediments (e.g. Carlos et al. 1999; Hirose et al. 2008; Manning and Gates 2008; Pochon et al. 2010; Takabayashi et al. 2012; Yamashita and Koike 2013; Cunning et al. 2015; Quigley et al. 2017), and in association with macroalgae (Porto et al. 2008; Venera-Ponton et al. 2010; Yamashita and Koike 2013; Granados-Cifuentes et al. 2015) (see Table 1.3 for summary of free-living *Symbiodinium* studies). These free-living populations are a critical source for coral hosts to establish endosymbiosis within new larval generations (e.g. Coffroth et al.

2006; Nitschke et al. 2016) propagated via horizontal transmission (eggs or larvae do not contain *Symbiodinium*; Trench 1987). About 80% of spawn-gamete type corals acquire symbionts by horizontal transmission from their immediate environments (Baird et al. 2009; Harrison 2011; Hartmann et al. 2017). In addition, this free-living *Symbiodinium* source is also thought to play an important role for recovering from (or resisting) bleaching via "switching" to acquire more thermally resistant types from the environment (Baker 2003; Fautin and Buddemeier 2004; Pochon et al. 2010; Boulotte et al. 2016).

Given the growing recognition of the importance of the free-living lifestyle in maintenance of coral populations, research has intensified into attempting to understand the diversity and physiological properties of free-living cells in reef environments (as opposed to solely relying on static cultures in the laboratory) using various techniques. For example, culturing techniques (e.g. Chang 1983; Carlos et al. 1999; Hansen and Daugbjerg 2009; Hirose et al. 2008) and/or a "symbiont sampler" (= aposymbiotic hosts) (e.g. Coffroth et al. 2001; 2006; Thornhill et al. 2006) have been primarily used to collect free-living *Symbiodinium* from environment and captured *Symbiodinium* have been identified using various molecular techniques (e.g. RFLP, DGGE, sequencing). Furthermore, environmental DNA (eDNA), cloning and amplicon sequencing techniques have been subsequently applied and these various techniques provide different scales of resolution for detecting free-living *Symbiodinium* from environment (e.g. Manning and Gates 2008; Pochon et al. 2010; Takabayashi et al. 2012; Yamashita et al. 2014; Granados-Cifuentes et al. 2015). Most recently, but still rarely, high throughput DNA metabarcoding using next generation sequencing (NGS) technique has been applied to understand the

Table 1.3. Summary of free-living *Symbiodinium* studies. Literatures for free-living *Symbiodinium* diversity are listed in chronological order, with details of sampling sites (geographical location and latitude), habitats (water: colour coded as blue, sediment: yellow, macroalgae: green and others: no colour), detected clades (colour coding links to the habitats), and methodology used for collection and identification of free-living *Symbiodinium*.

Literatures		Sampling sites	Habitats				Clade									Methodology
Year	Authors	Geographic location	Water	Sediment	Macroalgae	Others	A	B	C	D	E	F	G	H	I	Identification techniques (molecular markers)
1983	Chang	New Zealand (Westland, 41°S)	W								E					microscopy observation (*Firstly classified as *Gymnodinium varians* , and now classified as *Symbiodinium vorutum*)
1999	Carlos et. al	USA (Hawai'i, Cocconut Island, 21°N)		S			A									culturing-sequencing (18S rDNA)
2001	Coffroth et al.	Panama (San Blas Island, 9°N)	W				A	B	C							symbiont sampler (octocorals: *Plexaura kuna* , *Pseudoplexaura porosa*)-RFLP (18S rDNA)
2003	Gou et al.	China (Jiazhou Bay, 36°N)	W								E					culturing-cloning-sequencing (18S rDNA)
2006	Coffroth et al.	USA (Florida Key, 25°N)	W			Benthos (Reef rubble and settlement plate)	A	B	C							symbiont sampler (octocoral: *Briareum* sp.)-RFLP (18S rDNA)
							A	B								culturing-RFLP (18S rDNA, cp23S), culturing-cloning-sequencing (ITS2 rDNA)
2006	Thornhill et al.	USA (Key Largo & Florida Bay, 25°N)	W				A	B	C	D						symbiont sampler (jelly fish: *Cassiopeya xamachana*)-DGGE (ITS2 rDNA)
2007	Koike et al.	Japan (Okinawa, Ishigaki, 24°N)	W													qPCR (18S rDNA) (cell density only)
2008	Gomez-Cabrera et al.	Australia (GBR, One Tree Island, 23°S)	W				A		C	D						symbiont sampler (scleractinian coral: *Acropora longicyanthus*)-RFLP, sequencing (28S rDNA)
2008	Hirose et al.	Japan (Okinawajima, 26°N)		S			A									culturing-cloning-sequencing (28S rDNA, ITS2 rDNA)
2008	Littman et al.	Australia (GBR, Lizard Island, 14°S)	W	S												FlowCAM/ microscopy (cell density only)
2008	Manning and Gates	USA (Hawai'i, O'ahu Island, 21°N)	W					B	C					H		eDNA-cloning-sequencing (ITS2 rDNA, cp23S)
		Mexico (Puerto Morelos, 20°N)	W					B	C	D						
2008	Porto et al.	Columbia (Cartagena, 10°N & Santa Marta, 11°N), Tobago (11°N)		S	M	Feces (stoplight parrotfish: *Sparisoma viride*)	A	B	C							eDNA-DGGE-sequencing, culturing-DGGE-sequencing
							A	B	C							
2009	Adams et al.	Japan (Okinawa, Akajima, 26°N)	W	S				B	C							symbiont sampler (scleractinial coral: *Acropora monticulosa*)-cloning-sequencing (cp23S)
							A	B	C							
2009	Hansen and Daugbjerg	Spain (Tenerife, 28°N)	W				A									culturing-sequencing (28S rDNA)
2010	Pochon et al.	USA (Hawai'i, Cocconut Island, 21°N)	W	S			A	B	C							eDNA-cloning-sequencing (cp23S)
							A		C							
2010	Reimer et al.	Japan (Ogasawara, Chichijima, 27°N)		S			A			D						culturing-cloning-sequencing (18S rDNA, 28S rDNA, cp23S)
2010	Stern et al.	Canada (Vancouver Island, 48°N)	W				E									eDNA -cloning-sequencing (COI)
2010	Venera-Ponton et al.	Australia (GBR, Heron Island & Keppel Island, 23°S)		S	M	Crustose coralline algae, algal turfs			C							eDNA-cloning-sequencing (28S rDNA) (no *Symbiodinium* was detected in sediment samples)
									C							

Table 1.3. (continued)

Literatures		Sampling sites	Habitats				Clade									Methodology
Year	Authors	Geographic location	Water	Sediment	Macroalgae	Others	A	B	C	D	E	F	G	H	I	Identification techniques (molecular markers)
2012	Castro-Sanguino and Sanchez	Colombia (Santa Marta, 11°N & Cartagena, 10°N & Isla Fuerte, 9°N)				Feces (stoplight parrotfish *Sparisoma viride*)	A	B					G			feces DNA-cloning-sequencing, culture-sequencing (cp23S)
2012	Jeong et al.	Korea (Jeju Island, 33°N)	W								E					culture-sequencing (18S rDNA, 28S rDNA)
2012	Takabayashi et al.	USA (Hawai'i, Hawai'i Island, 19°N & O'ahu Island, 21°N)	W	S			A	B	C	D						eDNA-cloning-sequencing (cp23S)
							A	B	C				G			
		USA (Florida Key, 24°N)						B					G			
			W	S			A	B	C							
2012	Zhou et al.	China (Xisha Island, 16°N)	W				A	B	C	D		F	G			eDNA-cloning-sequencing (cp23S)
2013	Cumbo et al.	Australia (GBR, Orpheus Island, 18°S & Magnetic Island, 19°S & Lizard Island, 14° S)		S			A		C	D						symbiont sampler (scleractinial coral: *Acropora millepora*, *Acropolla tenuis*)-SSCP (ITS1)
2013	Huang et al.	China (Hainan Island, 18°N)	W				A	B	C	D		F	G	H		eDNA-cloning-sequencing (cp23S)
2013	Yamashita and Koike	Japan (Kochi, 33°N & Tsushima Island, 35°N)					A		C	D						culturing/eDNA-cloning-sequencing (28S rDNA, ITS rDNA)
			W	S	M		A		C							
							A				E					
2013	Yamashita et al.	Japan (Okinawa, Ishigaki, 24°N)	W	S			A		C	D						symbiont sampler (scleractinial corals: *Acropora* spp.)-qPCR (28S rDNA)) & -cloning-sequencing (ITS rDNA), eDNA-qPCR
							A		C	D						
2014	Sweet	Australia (GBR, Heron Island, 23°S)					A		C		E					eDNA-DGGE-sequencing (ITS2) (*clade E sequences (JN406301/302) do not match with clade E *Symbiodinium* sequence in *Symbiodinium* ITS2 database "SymTyper" or
			W	S		Biofilm, mucus mats	A		C							
							A		C							
2014	Yamashita et al.	Japan (Okinawa, Ishigaki, 24°N)	W				A		C	D			G			symbiont sampler (scpleractinian corals: *Acropora* spp.)-cloning-sequencing (ITS rDNA), eDNA-cloning-sequencing (ITS rDNA)
2015	Cunning et al.	American Samoa (Ofu Island, 14°N)	W	S			A		C	D		F	G			eDNA-next generation sequencing (ITS2 rDNA)
							A		C	D		F	G			
2015	Granados-Cifuentes et al.	Netherlands Antilles (Curacao, 12°N)					A	B	C			F	G			eDNA-sequencing (cp23S)
			W	S	M	Coral rubble	A	B								
							A	B	C			F	G	H		
							A	B	C				G			
2017	Quigley et al.	Australia (GBR, Wallace Island, 11°S & Wilkie Island 13°S & Pandora Reef 18°S & Magnetic Island 19°S)		S			A	B	C	D	E	F	G	H	I	eDNA-sequencing (ITS2 rDNA)

community level biodiversity of free-living *Symbiodinium* amongst complex ecosystems (Cunning et al. 2015; Quigley et al. 2017). From these initial studies, all clades (A-I) have been found to exist in the environment as free-living. However, how this diversity in the free-living pool ultimately contributes to host-*Symbiodinium* associations remains poorly understood (Yamashita et al. 2014; Quigley et al. 2017).

Evidence now suggests that free-living *Symbiodinium* can be divided into two life history types: (i) "transiently" free-living *Symbiodinium*, which are likely to have been expelled by hosts, which occur in the surrounding environments and can form a symbiosis with new hosts (Yamashita and Koike 2013); and (ii) "exclusively" free-living *Symbiodinium*, which do not form a symbiosis with hosts and live permanently as free-living cells in the reef environment (Takabayashi et al. 2012; Yamashita and Koike 2013; Jeong et al. 2014; Nitschke et al. 2015). The transient free-living *Symbiodinium* is an important source of symbionts for many marine invertebrates (Coffroth et al. 2006; Littman et al. 2008; Nitschke et al. 2016), whereas exclusively free-living *Symbiodinium* enable understanding of evolutionary mechanisms by which *Symbiodinium* become symbiotic. In the latter case, ITS2-types A2: *S. pilosum* (Trench and Blank 1987) and A2-relative: *S. natans* (Hansen and Daugbjerg 2009) have been suggested to represent an exclusively free-living ancestor (LaJeunesse 2002; Yamashita and Koike 2013; Granados-Cifuentes et al. 2015; Nitschke et al. 2015). Also, clade E: *S. voratum* (Jeong et al. 2014), which mainly exists in temperate regions (Chang 1983; Yamashita and Koike 2013), has an ability to feed on bacteria and other small microalgae, demonstrating a possible survival strategy for *Symbiodinium* to persist in nutrient-poor coral reef habitats (Jeong et al. 2012).

Importantly, however, even the transient phase is not yet well resolved. Many existing laboratory cultures of *Symbiodinium* are originally derived from *in hospite* associations, therefore confirming that endosymbiosis for some strains is not obligatory; however, not all species appear to be culturable (Santos et al. 2001; Coffroth and Santos 2005; Yamashita and Koike 2013) suggesting that for these cell lines the transient phase may be short-lived or that we simply do not yet understand the physio-chemical environments required to sustain their specific long-term growth needs (Suggett et al. 2017). In addition, some species which are now considered as exclusively free-living types, such as *S. pilosum* (ITS2-type A2) and *S. voratum* (clade E), were once misidentified as endosymbionts found in cnidarian hosts because they grew rapidly under the culturing process which possibly out competed cells of the dominant natural population *in hospite* (LaJeunesse 2001; 2002; Jeong et al. 2014). This also supports the idea that we still do not know how to sustain transient phase of *Symbiodinium*, which primarily exists as endosymbionts of hosts, in culturing conditions.

Littman et al. (2008) revealed that free-living *Symbiodinium* were far more abundant in the sediment (1,000-4,000 cells mL^{-1}) compared to the water column (< 80 cells mL^{-1}). Indeed, corals acquire their symbiont quickly in the presence of sediment compared to seawater as the only source for symbiont (Adams et al. 2009; Cumbo et al. 2013; Nitschke et al. 2016). Thus the free-living transient phase appears to reside mainly in the benthos. In fact, recent evidence from Frommlet et al. (2015) suggests that this benthic life style might be an important survival strategy for free-living *Symbiodinium* in the environment. Frommlet et al. (2015) discovered an endolithic phase of *Symbiodinium* in culture (termed as “symbiolites”), in a wide range of

phylogenetic diversity (clades A-F; specifically, types A1, A2, A3, A12, A13, A14, B1, B2.1, B3, C2, D, E, F1, and F2), via calcifying bacterial-algal biofilms with naturally associated bacteria. This appears to be an important novel life style for benthic free-living *Symbiodinium* to provide a refuge against grazing and stressful conditions (e.g. UV light) when *ex hospite*.

1.5. *Symbiodinium in hospite*

Establishment or initiation of symbiosis between corals and *Symbiodinium* is critical to understand their transient life style from free-living to symbiotic life stage; however, this process and how it is regulated remains unclear. Two alternate acquisition modes of *Symbiodinium* initiate symbiosis: (i) vertical transmission in which corals acquire *Symbiodinium* from their parents (*Symbiodinium* are contained in eggs or larvae); (ii) horizontal transmission in which corals acquire *Symbiodinium* from the surrounding environments (eggs or larvae do not contain *Symbiodinium*) (Trench 1987) (see section 1.4). A recent study revealed that horizontal transmission (hence absence of symbiont in the early life stage) seems to provide an advantage for broadcast spawner of corals which produce eggs that tend to be positively buoyant and aggregate at the sea surface to facilitate fertilization (Hartmann et al. 2017). They possibly protect offspring from damage caused by high light and temperature experience at sea surface by harbouring photosynthetic symbionts which increase oxidative stress under such conditions. Either way, once the host acquires *Symbiodinium*, the microalgal cells exist as coccoid cells in the host's endodermal cells, dividing without transition to motile cells (Kevin et al. 1969; Trench 1979; Blank 1987; Trench and Blank 1987; Stat et al. 2006). Lectins, which is a carbohydrate-binding protein, seems to play a role in changing the morphology of

Symbiodinium from motile to coccoid stages, which are still able to divide (Koike et al. 2004), and thereby thought to have an important role in cell signalling (Wood-Charlson et al. 2006; Fransolet et al. 2012). Other reports have indicated a diel change to the life cycle stage of *Symbiodinium in hospit*e, where the presence of flagella may represent the transient production of a motile stage (Schoenberg and Trench 1980). Similarly, the presence of thecal vesicles beneath the plasma membrane could indicate an ecdysis cycle *in hospite* normally seen in free-living cells (Wakefield et al. 2000).

Functional equilibrium between hosts and *Symbiodinium* results from the continuous regulation of symbiont density *in hospite* (Trench 1987; Muscatine et al. 1989; Smith and Muscatine 1999; Baghdasarian and Muscatine 2000; Davy et al. 2012). Indeed, *Symbiodinium* densities have been shown to be relatively constant (Drew 1972; Muscatine et al. 1989; Jones and Yellowlees 1997). The growth rate of *Symbiodinium* is higher than that of the host (Muscatine et al. 1985; Hoegh-Guldberg et al. 1987; Falkowski et al. 1993). Specifically, Muscatine et al. (1985) calculated growth rates of both *Symbiodinium* and their host corals and found that growth rates of *Symbiodinium in hospite* were 3-9 folds faster than those of the corals. Therefore, it is necessary to regulate the density of the symbiont to prevent symbiont overgrowth. Three mechanisms are thought to control symbiont density: (i) expulsion of excess symbionts, (ii) degradation of excess symbionts ((i) and (ii) are termed the post-mitotic process), and (iii) inhibition of symbionts' cell growth and division (referred to as the pre-mitotic process) (Fig. 1.4) (Trench 1987; Hoegh-Guldberg and Smith 1989; Jones and Yellowlees 1997; Davy et al. 2012). Continuous expulsion of *Symbiodinium* is characteristic of many anthozoans (Jones and Yellowlees 1997;

Koike et al. 2007; Dimond and Carrington 2008; Yamashita et al. 2011), where expelled cells are both degraded and photosynthetically healthy (Jones and Yellowlees 1997; Baghdasarian and Muscatine 2000; Fujise et al. 2014). It is suggested that expulsion may provide a key mechanism for removing degraded cells or releasing excess cells to regulate the algal density *in hospite* (Falkowski et al. 1993; McCloskey et al. 1996; Jones and Yellowlees 1997; Dimond and Carrington 2008; Fujise et al. 2014).

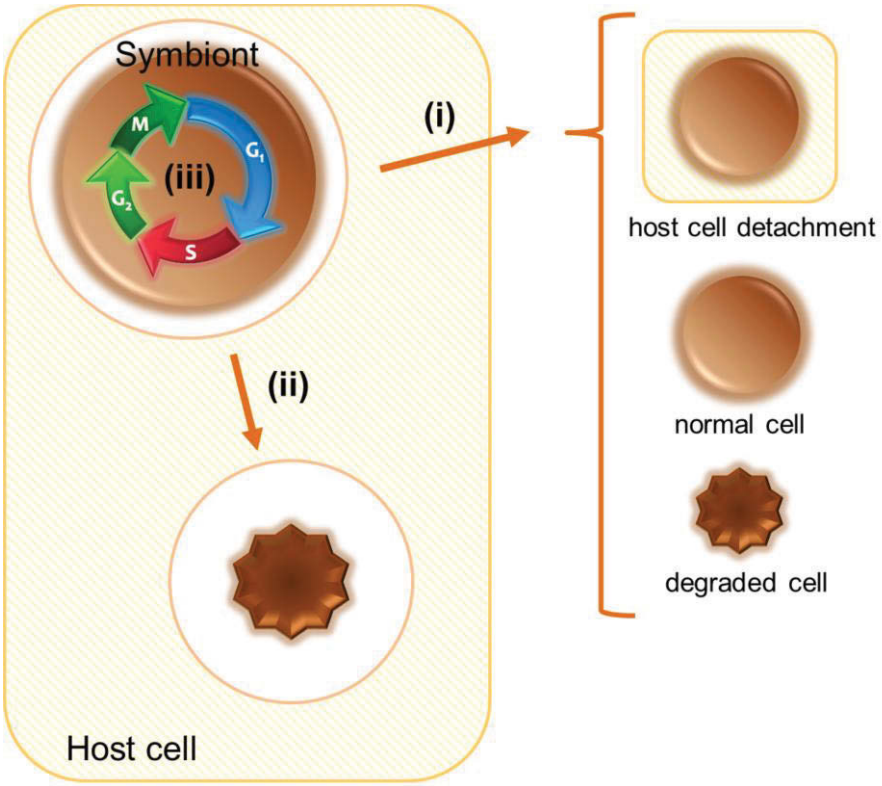

Figure 1.4. Mechanisms for regulating *Symbiodinium* density *in hospite*. **(i)** Expulsion of either detached a whole host cell or a normal cell and/or a degraded cell by exocytosis. **(ii)** Degradation (digestion) of a cell by host phagocytosis. (i) and (ii) is termed the post-mitotic process. **(iii)** Inhibition of symbiont cell growth and division through controlling cell cycle progression which is termed the pre-mitotic process (adapted and modified from Davy et al. 2012).

In addition to post-mitotic processes (above), host regulated pre-mitotic process control the cell growth of the symbionts (Falkowski et al. 1993; Smith and Muscatine 1999; Davy et al. 2012), largely since growth rates of *Symbiodinium in hospite* are lower compared to free-living cells (Chang et al. 1983; Wilkerson et al. 1988; Hoegh-Guldberg 1994; Davy et al. 1996; Smith and Muscatine 1999). Symbionts are typically nitrogen limited *in hospit*e, as evidenced by rapid symbiont population growth upon addition of nitrogen (Hoegh-Guldberg and Smith 1989; Stimson and Kinzie 1991; Muller-Parker et al. 1994), thus availability of nutrients has been well established at playing an important role in the control of *in hospite* symbiont growth. Hoegh-Guldberg and Smith (1989) reported that addition of ammonium to corals increases *Symbiodinium* cell density and cellular chlorophyll *a* content. However, Smith and Muscatine (1999) reported that the inorganic nutrient supply to starved anemone hosts did not affect the population growth of *Symbiodinium*, and the biomass of symbionts did not recover to the level observed in the fed anemone host. Smith and Muscatine (1999) applied cell cycle analysis to *Symbiodinium in hospite* and highlighted that cell cycle duration was only reduced by feeding and growth status of hosts are important for controlling cell proliferation of symbionts (detailed in section 1.6). Fitt and Cook (2001) further suggested that supply of inorganic nutrients only temporarily increases mitotic division rates and the key factor for limiting symbiont density seems to be feeding, leading to tissue accumulation and thus availability of host cell space. Indeed, mitotic division rates of *Symbiodinium* appeared the highest right after the bleaching event when the symbiont density *in hospite* was the lowest and new tissue spaces became available, and subsequently slowed down with increase of symbiont density (Jones and Yellowlees 1997). This finding also supports that one of the main factors determines algal densities reach a

steady-state is space availability. Most recently, Matthews et al. (2017) confirmed by omics (combination of transcriptomic and metabolomic analyses) that nutrient supply from host to symbiont is controlled by regulating metabolic pathways, such as nitrogen and urea cycle. Even so, the relative role of pre-mitotic control and underlying cellular mechanisms for limiting symbiont cell proliferation versus post-mitotic control to regulate symbiont density has not been identified (Davy et al. 2012) (detailed in section 1.6).

1.6. Life cycle (cell cycle) of *Symbiodinium*

Cell cycle control is closely related to the life cycle control of unicellular organisms such as *Symbiodinium*, and thus important for understanding cell proliferation and growth dynamics (Wang et al. 2013a; Dapena et al. 2015). A breakthrough in integrating and expanding upon the life cycle (cell cycle) observations first came from Freudenthal (1962) who described several phases (Fig. 1.5), but a dominant vegetative cell (coccid stage) with: (A) spherical morphology possesses thin cell walls and (B) divides to form two daughter cells by binary fission. Under some conditions, (C) these vegetative cells may form a cyst, which has a thick cell wall and is the precursor for several other cell growth forms; (D) zoosporangium containing (E) gymnodinioid zoospore that is a motile stage cell with two flagella as well as (F) aplanospore that remains non-motile and ultimately becomes vegetative cell. Zoospores are abundant in the logarithmic phase of population growth and account for up to 80-90% of the population; however, their appearance depends on the photoperiod while motile cells increase in number shortly after illumination. Cysts can produce (G) two or sometimes four daughter cells that persist for a

considerable period of time and become the vegetative cells or autospore (typically in aged cultures). Possibly, (H) the cysts can produce (I) gametes that have a spherical body, very delicate trailing flagellum but swim weakly. Observation of gamete-like cells was the first report concerning possible of sexual reproduction (meiosis) by *Symbiodinium* compared to reliance on asexual mitotic division.

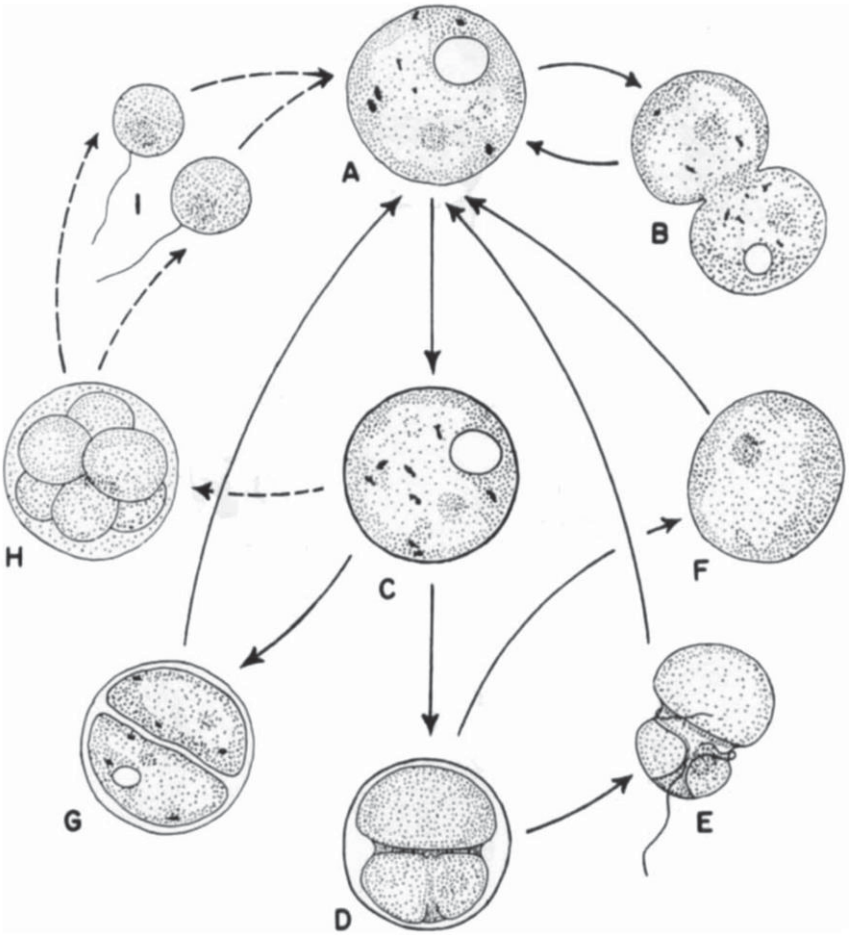

Figure 1.5. Life cycle of *Symbiodinium microadriaticum*. **A.** Vegetative cell. **B.** Vegetative cell undergoing binary fission, producing two daughter cells. **C.** Vegetative cyst, differing from the vegetative cell mainly in cell wall thickness. **D.** Mature zoosporangium, containing a gymnodinioid zoospore. **E.** Gymnodinioid zoospore. **F.** Aplanospore. **G.** Cyst containing two autospores. **H.** Cyst containing developing isogametes. **I.** Liberated isogametes (taken from Freudenthal 1962).

A major complication of Freudenthal's original pioneering description was the use of the term cyst where a cell possesses a thicker cell wall compared to the vegetative cell; however, coccoid stage cells are metabolically active and do not match the term of cyst which is an inactive resting state and thus precludes distinction of coccoid vegetative cells from true cysts (Taylor 1973; Schoenberg and Trench 1980; Fitt and Trench 1983). Consequently, Fitt and Trench (1983) modified the life cycle of *Symbiodinium* to clarify this point (Fig. 1.6, updated from Fitt and Trench 1983 and observation from Stat et al. 2006): (1) a non-motile coccoid cell arising from a motile cell, (2-3) motile cells arising from a newly divided cell, and also (4) possible production of a triplet cell (Stat et al. 2006). Importantly, from this Fitt and Trench (1983) postulated that if the vegetative cell is haploid, there is a possibility that vegetative coccid cell produces (5) isogametes and fusion to form (6) a zygote (diploid), and (7) produce a tetrad cell formed from meiosis of diploid cell. Trench (1997) later suggested that if sexual reproduction does occur it probably happens in a free-living life stage. Confirmation that the vegetative cell is haploid was not achieved until a decade later using microsatellites to examine the ploidy of *Symbiodinium* both *in hospite* and culture (Santos and Coffroth 2003). Many reports have since suggested the possibility of sexual recombination according to the molecular analysis such as using allozyme and random-amplified-polymorphic DNA (RAPD) (Baillie et al. 1998; 2000b), ITS (LaJeunesse 2001), multi-locus DNA fingerprinting (Goulet and Coffroth 2003), microsatellite (Santos et al. 2003a; Pettay et al. 2011; LaJeunesse et al. 2014), and also uncovering the existence of meiosis-specific genes and meiosis-related genes in the *Symbiodinium* genome (Chi et al. 2014). However, the definitive proof for sexual reproduction (e.g. karyogamy and meiosis) is yet to be achieved.

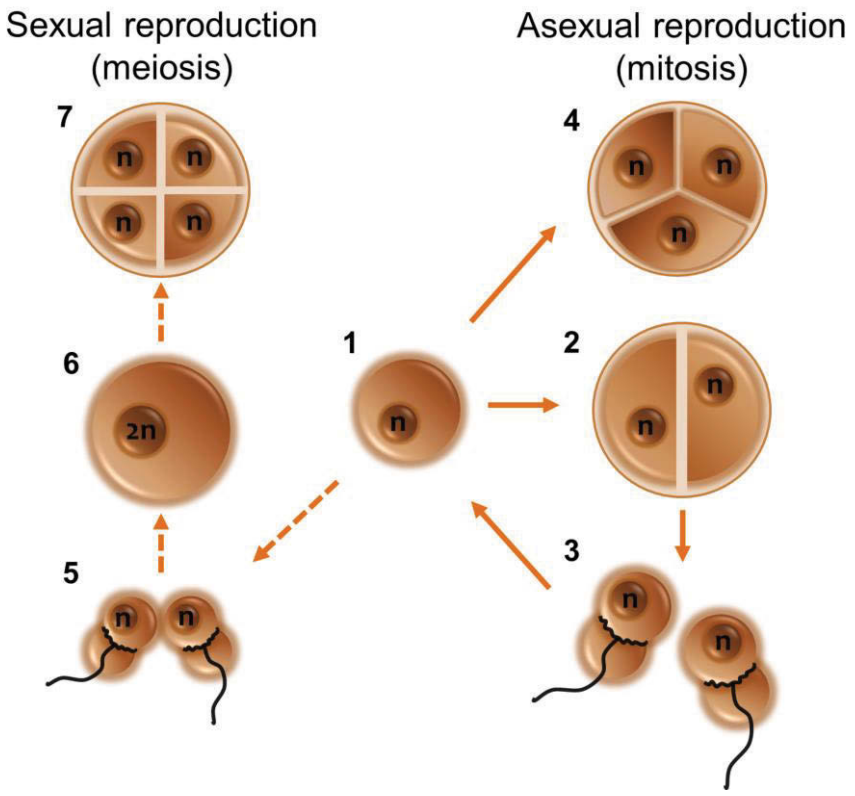

Figure 1.6. Life cycle of *Symbiodinium* including asexual reproduction (right side) and possible sexual reproduction (left side). Solid lines denote observed transformations, while dashed lines are possible routes of sexual reproduction or meiosis. **1.** Vegetative coccoid cell. **2.** Dividing vegetative cell (doublet). **3**. Motile cells. **4.** Dividing vegetative cell (triplet). **5.** Isogametes. **6.** Diploid vegetative cell resulting from fusion of the gametes. **5.** Tetrad cell, formed from meiosis of the diploid vegetative cell (adapted and modified from Fitt and Trench 1983 and Stat et al. 2006).

To identify the growth dynamics of *Symbiodinium* at the individual cell level, Wang et al. (2008) performed the cell cycle analysis upon cultured cells, and thus in free-living life stage free from host control. These authors detailed the relationship between cell cycle phasing linked to the light and dark cycle, and associated morphology, motility and photosynthetic changes of a clade B *Symbiodinium* sp.. Eukaryotic cell cycle progression is typically comprised of a sequence of events that

produce daughter cells; specifically, the progression of G_1 phase (preparation for DNA replication) to S phase (DNA synthesis), and then G_2 phase (pre-mitotic gap) to M phase (mitosis) (e.g. Griffiths 2010). Growth of *Symbiodinium* by Wang et al. (2008) showed the progression of the cell cycle from G_1 to S phase during the day and cells underwent cell division (G_2/M) and finally generated G_1 cells for the next cycle at night (Fig. 1.7). Cells were smaller in size and possessed a motile gymnodinioid morphology in G_1 phase, and the percentage of cells that were motile peaked when the percentage of G_1 cells was the highest, but decreased when cells entered to S and G_2/M phase when morphology changed to coccoid. At night, G_2/M phase cells were larger in size and maintained coccoid morphology. Intriguingly, photochemical efficiency (F_v/F_m) consistently changed with morphology and motility, peaking at the same time as motility. A second experiment in the absence of light, showed no cell cycle progression and preservation of the G_1 phase. Similarly, growth under constant light altered the cell cycle by stimulating cells to enter G_2/M and generation of 3n/4n stage cells via blockage of final cytokinesis. From these results, Wang et al. (2008) concluded that light is required for both cell growth and DNA synthesis, via progression through G_1 to S to G_2/M, whereas the dark period is necessary for cytokinesis of mitotic division to progress from G_2/M to G_1.

Cell cycle analysis has been also applied to clarify the pre-mitotic control of hosts on symbiont cell proliferation. Inorganic nutrient availability is classically considered an important factor controlling symbiont division *in hospite.* For example, rapid symbiont population growth upon addition of nitrogen has been observed (Hoegh-Guldberg and Smith 1989; Stimson and Kinzie 1991; Muller-Parker et al. 1994; Muscatine et al. 1998). Smith and Muscatine (1999) applied cell cycle analysis

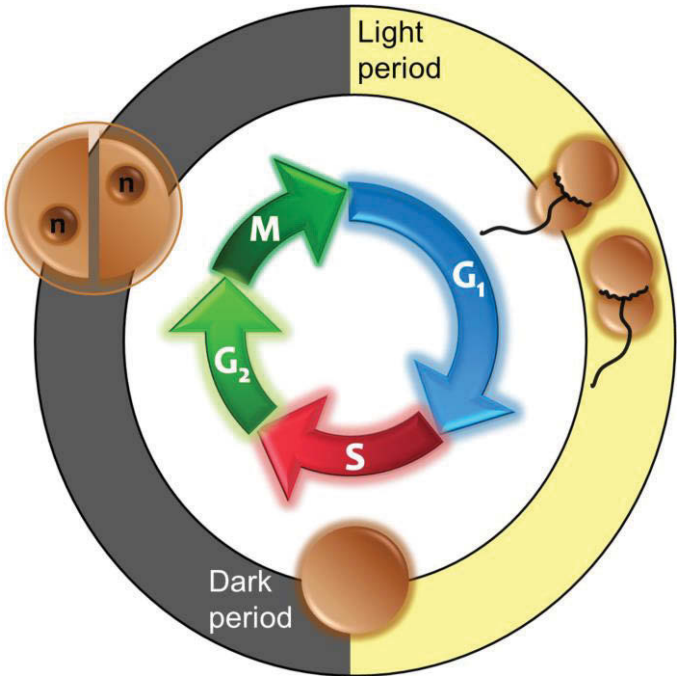

Figure 1.7. *Symbiodinium* cell cycle progression. Irradiance (i.e. light period, denoted by yellow field) is required for cell growth and DNA synthesis (G_1 to S to G_2/M), while dark period (black field) is required for cytokinesis of mitotic division (G_2/M to G_1). Motility of *Symbiodinium* are synchronized to the cell cycle, and increase at the onset of light which is correlated with the G_1 phase of gymnodinioid cells, decreasing when cells enter the S phase and the lowest at G_2/M phase with coccoid cell (adapted and modified from Wang et al. 2008).

of *Symbiodinium* (clade B, *S.* "*pulchrorum*" now described as *S. pseudominutum* (Parkinson et al. 2015), see Table 1.1 in section 1.3 for the species list) in the sea anemone (*Aiptasia pulchella*) and revealed that the G_1 phase was dramatically longer (ca. 3-4 times) in the symbiotic stage compared to the free-living cultured cells. The durations of S and G_2/M phase were significantly shorter than G_1 phase duration, but not different between the symbiotic vs. free-living life styles nor importantly the nutritional conditions. Therefore, they concluded that population growth of symbionts *in hospite* is restricted by constraints on cell cycle progression from G_1

phase through S phase via the metabolic status of the host, in particular feeding with *Artemia* sp. which stimulated the growth of the host, but not by limiting of access to nutrients that indeed resulted in accumulation of *Symbiodinium* biomass in G_1 phase. This indicates that coordination of growth (cell-division cycle) of the host with the symbiotic partners. Furthermore, Dimond et al. (2013) assessed the coordination of cellular growth of hosts (sea anemones: *Anthopleura elegantissima* and *Stichodactyla helianthus* from temperate and tropical regions, respectively) and their symbionts (*S.* "*muscatinei*" and *Symbiodinium* spp., respectively) by cell cycle analysis and found no evidence of coupled cell cycle phasing focused on G_2/M phase. Only *Symbiodinium* spp. in *S. helianthus* showed diel phasing of G_2/M phase, which peaked during night to dawn, but no diel phasing was observed for both hosts and *S.* "*muscatinei*". Dimond et al. (2013) explained that a possible reason for diel stability of *S.* "*muscatinei*" was the result of effective post-mitotic processes, such as preferential expulsion of dividing cells (Baghdasarian and Muscatine 2000). However, they found the seasonal fluctuation of proportion of G_2/M phase, whereby G_2/M proportions were higher in summer than winter for both hosts and symbionts and thus a positive relationship of cellular growth between symbiotic partners. This finding further supports that an important factor for limiting *Symbiodinium* growth *in hospite* clearly relates to host growth together with nutrition.

1.7. Research objectives and thesis outline

Many coral taxa acquire their algal symbionts (*Symbiodinium* spp.) from populations that are free-living in their immediate environment (Baird et al. 2009); even so, surprisingly little is known of the diversity and ecology of free-living *Symbiodinium*,

how they are distributed over space and time, how they interact with the environment, and how symbiotic and free-living life stages are connected. Therefore, the primary goal of this thesis is to advance our understanding of the distribution, abundance and life cycle of free-living *Symbiodinium* by unlocking the genetic diversity of *Symbiodinium* across habitats and over time (**Chapter 2**: tropical reef and **Chapter 3**: temperate reef). Both reef systems examined (Heron Island and Sydney Harbour) are located on the east coast of Australia and are periodically connected by a dynamic Eastern Australian Current (EAC; Ridgway and Dunn 2003; Booth et al. 2007; Wu et al. 2012; Oliver and Holbrook 2014). This thesis examines for the first free-living *Symbiodinium* diversity for a high-latitude temperate reef (**Chapter 3**), and therefore to understand how free-living *Symbiodinium* populations function and are structured in such a marginal environment, outcomes from **Chapters 2 and 3** were compared. Whilst such diversity is inherently connected to the health of the ecosystem (e.g. Hughes and Stachowicz 2004; Stat et al. 2006; Pauls et al. 2013), it ultimately only provides a snap shot in time and does not convey how this diversity is sustained through species-specific differences in population turnover. However, there is no information for the inherent population dynamics for *Symbiodinium* as it spans immense genetic diversity (Pochon and Gates 2010; LaJeunesse et al. 2012a; Pochon et al. 2014; LaJeunesse 2017; Thornhill et al. 2017). Therefore, to create a baseline for how *Symbiodinium* cell cycle is regulated, the fundamental mechanism for controlling population turnover, I stepped back to the laboratory to establish key patterns of cell cycle regulation across species and under different conditions known to regulate growth (light and temperature) (**Chapter 4**). This may also help to understand how specific types are optimised to specific environments (e.g. tropical and/or temperate) or conditions (e.g. thermal anomalies), and how they can

proliferate and persist. Finally, I conclude the thesis with **Chapter 5**, which considers the key findings from **Chapters 2-4** and discusses how these novel findings extend our knowledge to unlock the diversity and ecology of free-living life stage of *Symbiodinium*, which still largely remains (and hence can be considered as) a black box.

(This page is intentionally left blank)

Chapter 2

Unlocking the phylogenetic diversity and abundance of free-living *Symbiodinium* over space and time on a tropical reef (Heron Island, Australia)

This chapter is in preparation for submission, therefore the subject "we" is used here.

Lisa Fujise[1], Michael Stat[2], Michael Bunce[2], Stephanie Gardner[1], Samantha Goyen[1], Tim Kahlke[1], Matthew Nitschke[1, 3], Peter J. Ralph[1], Nahshon Siboni[1], Stephen Woodcock[1], David J. Suggett[1]

[1] Climate Change Cluster, University of Technology Sydney, Broadway, NSW 2007, Australia

[2] Trace and Environmental DNA (TrEnD) Laboratory, Curtin University, Bentley, Perth, WA 6102

[3] Center for Environmental and Marine Studies, University of Aveiro, 3810-193 Aveiro, Portugal

2.1. Abstract

Symbiodinium are tied to an endosymbiotic lifestyle with reef-forming corals, but they also live through a transient free-living life history phase. Exclusively free-living *Symbiodinium* taxa also exist that play as yet unidentified roles in reef microbial community functioning. Hence, the underlying biodiversity and ecology of free-living *Symbiodinium* communities remains a black box. We therefore coupled eDNA metabarcoding and clade-specific qPCR to resolve the complex phylogenetic diversity and abundance, respectively. This dual approach was applied for the first time to examine free-living *Symbiodinium* communities across reef habitats (water, sediment and macroalgae). Sampling was conducted of key coral hosts and over two seasons, including spawning season when recombination between host and free-living *Symbiodinium* is likely the greatest. Overall, we observed 232 Operational Taxonomic Units (OTUs) belonging to eight clades (A-I, except E) spanning 75 ITS2 variants (including both *in hospite* and free-living *Symbiodinium*). Community composition of free-living *Symbiodinium* was clearly separated by habitats, where water samples were the most closely similar to hosts, as a result of a continued population turnover of *Symbiodinium in hospite*. Sediment samples showed the most dissimilar community compositions compared to hosts due to dominance of exclusively free-living types. Macroalgae showed an intermediate diversity between water and sediment, but were identified to be the largest environmental reservoir for *Symbiodinium* according to the existence of transiently free-living types and highest cell density, suggesting a key role for macroalgae in maintaining *Symbiodinium* pools, but also in aiding distribution through herbivory.

2.2. Introduction

Dinoflagellates of the genus *Symbiodinium* are unicellular microalgae that are key primary producers in temperate and tropical reef ecosystems. *Symbiodinium* have evolved to live in endosymbiosis with various marine organisms in coral reef ecosystems, from reef-forming corals to foraminifera (Stat et al. 2006; Davy et al. 2012; Pochon et al. 2014), but possess a "free-living" lifestyle as part of ("transiently" free-living) or its entire ("exclusively" free-living) life history (e.g. Carlos et al. 1999; Pochon et al. 2010; Takabayashi et al. 2012; Yamashita and Koike 2013; Cunning et al. 2015; Granados-Cifuentes et al. 2015). The phylogenetic diversity within the *Symbiodinium* genus is extremely broad and is presently divided into nine distinct monophyletic groups (clades A-I) and hundreds of types and/or species (Pochon and Gates 2010; LaJeunesse et al. 2012a; Pochon et al. 2014; LaJeunesse 2017; Thornhill et al. 2017). To date, all of these clades have been found free-living in reef environments (e.g. Pochon et al. 2014; Cunning et al. 2015; Quigley et al. 2017). However, how this diversity within the free-living pool ultimately contributes to host-*Symbiodinium* associations is still poorly understood (Yamashita et al. 2014; Nitschke et al. 2016; Quigley et al. 2017).

Free-living *Symbiodinium* populations are an essential source for hosts that establish endosymbiosis in new generations (e.g. Coffroth et al. 2006; Nitschke et al. 2016) initiated via horizontal transmission (eggs or larvae that do not contain *Symbiodinium*; Trench 1987). Approximately 80% of corals that spawn (gamete released into the water column) acquire symbionts by horizontal transmission from their immediate environments (Baird et al. 2009; Harrison 2011). It is suggested that this process potentially confers the advantage of recombination of the host with

symbiont genotypes best adapted to their specific (local) environment (Schwarz et al. 1999; Baird et al. 2007; Howells et al. 2012; Cumbo et al. 2013). Such recombination may also occur within adult corals where "switching" to a more hardy type from the free-living *Symbiodinium* pool to resist stress (Buddemeier and Fautin 1993; Baker 2003; Boulotte et al. 2016). The inherent presence and identity of *Symbiodinium* have recently been shown to modify substrate preference (selection of crustose coralline algae: CCA) of settling coral larvae (Winkler et al. 2015). Ultimately the presence of sediment, which contains benthic *Symbiodinium* cells, appears critical in the early establishment of symbiosis with new coral recruits (Adams et al. 2009; Cumbo et al. 2013; Nitschke et al. 2016; Quigley et al. 2017). Thus, free-living *Symbiodinium* populations are important for establishing symbiosis with new generations of corals and in turn ensuring resilience and recovery following major stress impacts such as mass bleaching.

Whilst *in hospite Symbiodinium* diversity has been examined for decades, efforts to understand and explore free-living *Symbiodinium* populations within reef habitats have grown relatively recently. Culturing techniques and the use of a "symbiont sampler" (= apo-symbiotic hosts) have successfully detected free-living *Symbiodinium* in the water columns above reefs (Coffroth et al. 2001; 2006; Thornhill et al. 2006; Gómez-Cabrera et al. 2008; Hansen and Daugbjerg 2009) and within sediments (Carlos et al. 1999; Hirose et al. 2008) by integrating various molecular techniques (e.g. RFLP, DGGE, sequencing). However, not all *Symbiodinium* types (species) can be isolated and established into culture (Santos et al. 2001; Coffroth and Santos 2005; Yamashita and Koike 2013), and not all free-living *Symbiodinium* can initiate symbiosis (Coffroth et al. 2006; Yamashita et al.

2014). Thus, early efforts to assess the diversity of free-living *Symbiodinium* are likely to have vastly underestimated the true diversity as a result of these inherent methodological limitations. Molecular techniques have rapidly improved, with the most recent studies of free-living *Symbiodinium* populations employing environmental DNA (eDNA), cloning and amplicon sequencing, and hence the resolution for detecting free-living *Symbiodinium* from the environment has substantially increased (e.g. Manning and Gates 2008; Pochon et al. 2010; Venera-Ponton et al. 2010; Takabayashi et al. 2012; Zhou et al. 2012; Yamashita et al. 2014; Granados-Cifuentes et al. 2015).

Metabarcoding is a rapid method of high-throughput, DNA-based (short DNA fragment = barcode) identification of multiple species from a complex ecosystem (Cristescu 2014). Development of next generation sequencing (NGS) techniques, which enable massive parallel sequencing of bulk samples, have served as an engine of DNA metabarcoding to revolutionise community-level biodiversity analysis. Notably, it revealed extensive cryptic biodiversity of dinoflagellates in marine environments (Lin et al. 2009; Stern et al. 2010; Kohli et al. 2014a; 2014b). DNA metabarcoding has been increasingly applied to understand the finer diversity of *Symbiodinium in hospite* (e.g. Thomas et al. 2014; Boulotte et al. 2016; Ziegler et al. 2017). However, few studies are yet to apply this technique to explore free-living *Symbiodinium* populations within an ecosystem that contains a cocktail of organism diversity, including other dinoflagellates with similar DNA sequences to *Symbiodinium*. Cunning et al. (2015) found 421 *Symbiodinium* taxa across clades A, C, D, F and G with 1,186 Operational Taxonomic Units (OTUs) (*in hospite* and free-living combined) from water and sediment samples, whereas Quigley et al.

(2017) found 1,160 OTUs spanning clades A-I from sediment samples. Collectively, these efforts represent the largest biodiversity ever measured for free-living *Symbiodinium*. Some of these OTUs or types importantly overlapped with those found in host species, confirming that previously under-resolved phylogenetic diversity of free-living *Symbiodinium* pools are potentially critical for successful colonisation across broad ecological habitats or gradients of host corals.

In order to better resolve free-living *Symbiodinium* diversity over space and time, we applied eDNA metabarcoding using NGS techniques with samples from Heron Island (23°S), a well-studied reef system in the southern Great Barrier Reef. Several studies have characterised the *in hospite Symbiodinium* diversity based on denaturing-gradient gel electrophoresis (DGGE) and sequencing of 28S rDNA, ITS2 rDNA and cp23S genes (LaJeunesse et al. 2003; 2004; Stat et al. 2008b; Sampayo et al. 2009; Stat et al. 2009a) at this reef site. Two past studies have attempted to characterise free-living *Symbiodinium* on Heron Island where they detected clade C associated with macroalgae (Venera-Ponton et al. 2010) and clades A and C in water and sediment (Sweet 2014). Nonetheless, the actual free-living diversity remains entirely unresolved. Seasonality has been previously suggested to influence free-living *Symbiodinium* diversity and distribution (Sweet 2014; Granados-Cifuentes et al. 2015), and thus our sampling focused on two key seasons where host-symbiont recombination events seem to be the highest; (i) spawning when larval recruitment occurs (November, e.g. Kaniewska et al. 2015; Nitschke et al. 2016) and (ii) summer when water temperature is the highest. In the latter case, sampling coincided with the 2015/2016 El Niño heat wave event on the GBR, although Heron Island ultimately experienced only moderate thermal anomalies with

little detectable bleaching (Bainbridge 2017; Hughes et al. 2017). We also importantly supplemented our assessment with the quantification of *Symbiodinium* cells in the environment using qPCR with clade-specific primer sets (Yamashita et al. 2011; 2013). Such a step has rarely been performed (Littman et al. 2008; Yamashita et al. 2013), but provides a unique means to combine high-resolution NGS resolved phylogenetic diversity with a quantitative assessment of free-living *Symbiodinium*. We apply these two approaches in concert for the first time to bridge phylogeny, ecology and population dynamics in the study of free-living *Symbiodinium*.

2.3. Materials and Methods

2.3.1. Hosts and environmental samples collection

Sampling was conducted at three locations on the shallow reef-flat of Heron Island, southern Great Barrier Reef, Australia (23.26°S, 151.54°E). Each site (located 5-20 m from shore, Fig. 2.1) was selected to encompass a small mono-specific cluster of coral colonies; site 1: *Acropora aspera*, site 2: *Montipora digitata*, and site 3: *Pocillopora damicornis*. These coral species are common on the GBR (Madin et al. 2016) and particularly widespread on the shallow reef flat on Heron Reef (Nitschke et al. 2018). Sampling was repeated over two consecutive seasons, end of October 2015 in early summer close to spawning (5th November 2015; Gissi et al. 2017) (referred to hereafter as "spawning" season) and mid-March 2016 in late summer (referred to as "summer" season). To verify *in hospite* diversity, reference host samples were initially collected (n = 4 per species (site) and season) as small fragments (~2 cm) were rinsed with 0.2-µm filtered seawater and stored at -80°C until further molecular analysis.

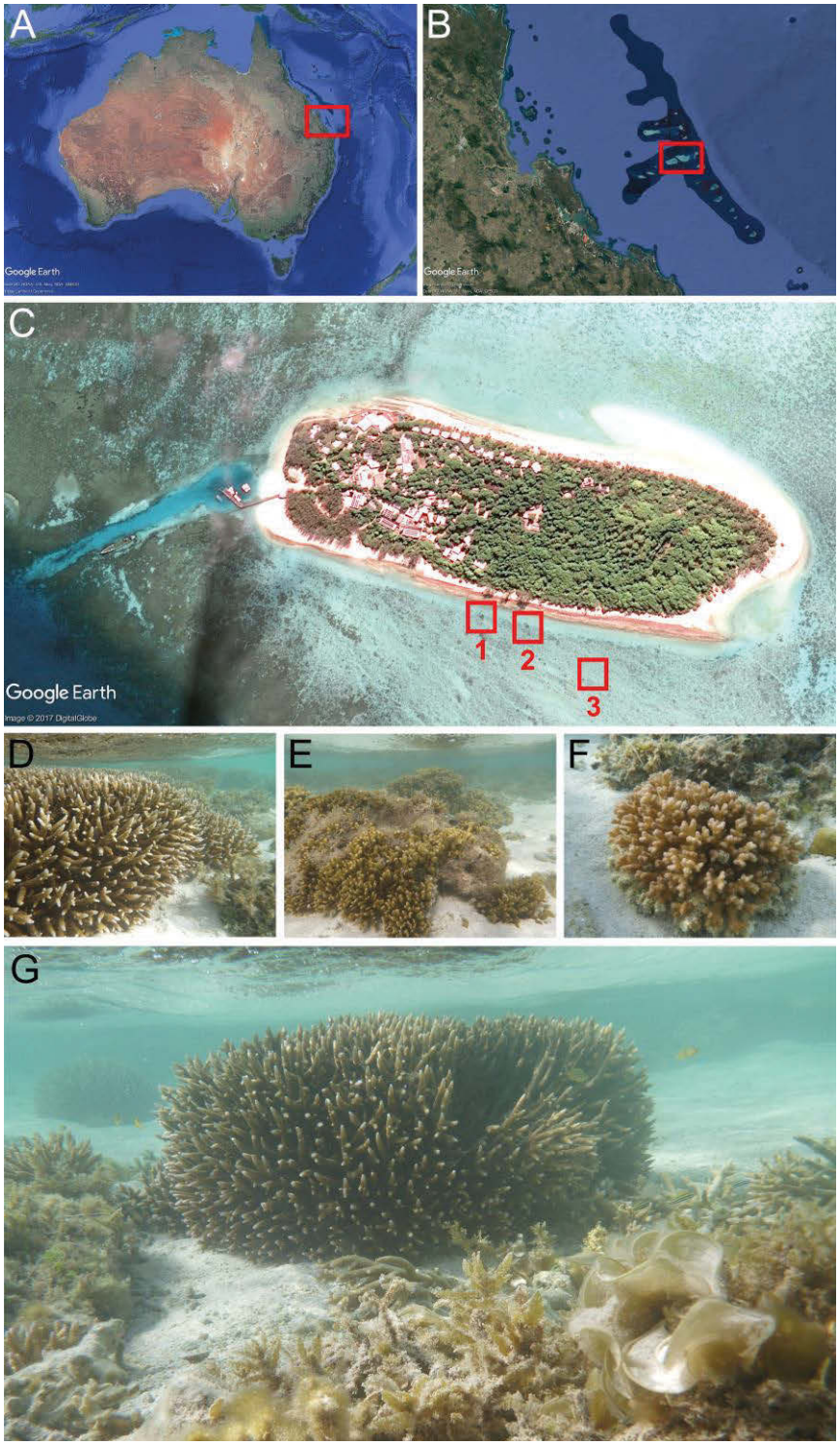

Figure 2.1. Location of sampling sites and coral species. **A-B.** Location of Heron Island in southern Great Barrier Reef in east coast of Australia. **C.** Location of sampling sites (1: *Acropora aspera* site, 2: *Montipora digitata* site, and 3: *Pocillopora damicornis* site). Collected host coral species: **D.** *A. aspera*, **E.** *M. digitata*, and **F.** *P. damicornis*. **G.** Example of coral community surrounded by reef environments including *Padina* sp. (collected macroalgae species).

Environmental samples from seawater, sediment and macroalgae (n = 4 per each sample type per site and season) were collected for free-living *Symbiodinium* assessment. Volumes of 10 L seawater were collected ca. 1 m from each host colony. Water samples were initially passed through a 20-µm nylon filter (NITEX®, SEFAR, Heiden, Switzerland) to remove large particles and filtrate was concentrated using gentle vacuum onto a 3-µm polycarbonate filter (Isopore™, EMD Millipore, MA, USA) to capture particles between 3-20 µm diameter, including *Symbiodinium*. Particles captured on the 3-µm polycarbonate filter were re-suspended with 0.2-µm filtered seawater and suspended filtrates were collected. This procedure was repeated 10 times to collect all captured particles from the filter, and microscopy was used to confirm that no microalgae-like organisms remained on the filter paper. The final suspension was concentrated by centrifuge at 2000 *g* for 5 min and stored at -80°C until further molecular analysis. The surface layer (~1 cm) of sediment near to a host colony (ca. 1 m) was collected into a sterile 50-mL centrifuge tube to a total wet volume of 25 mL. To account for disturbance/loss during sediment scooping, further interstitial sediment water was collected by inserting a custom sediment corer (3 cm diameter) capped with a modified syringe 2 cm depth into the sediment. Twenty-five mL of interstitial water was forcibly drawn through the isolated sediment core into the syringe and then combined with the sediment + interstitial water as "sediment" sample (total volume: 50 mL). Finally, ~50 g of *Padina* sp. was collected into a sterile sample bag for macroalgal-associated *Symbiodinium* analysis. *Padina* sp. has been found to be a common and dominant macroalgae across all sites (coral colony locations). Both sediment and macroalgae samples were re-suspended in 1 L of 0.2-µm filtered seawater and shaken vigorously 50 times to remove surface-attached *Symbiodinium*. Each suspension was passed in series through 250, 125, 63-µm

stacked sieves, a 20-µm nylon filter to remove large particles and then a 3-µm polycarbonate filter to capture particles containing *Symbiodinium* cells. Samples were then processed and stored as for the seawater samples.

2.3.2. Environmental data

To contrast the environmental conditions across seasons and confirm minimal impact of the 2015/2016 heat wave on Heron Island reef during sampling in mid-March (note, Bainbridge 2017 and Hughes et al. 2017 subsequently confirmed Heron Island escaped any impact of thermal-induced bleaching), environmental data were retrieved from the Heron Reef Integrated Marine Observing System (IMOS) (Bainbridge et al. 2010) via the Australian Institute of Marine Science (www.aims.gov.au) using the database provided rule-based quality control for eliminating outliers or errors (accessed 03/11/2017). Specifically, sea surface temperature (SST) at 1-2 m depth (RP2, daily temperature averages, °C) and photosynthetically active radiation (PAR, daily averages from RP8, µmol photons m^{-2} s^{-1}) above water, from January 2015 to December 2016 (including both sampling periods, October 2015 and March 2016).

2.3.3. *Symbiodinium* genetic diversity using next generation sequencing

All DNA extraction and sequencing was performed at the Trace and Environmental DNA Laboratory (Curtin University, Australia). Total genomic DNA was extracted from both host and environmental samples (half of the collected samples were used) using the DNeasy Blood & Tissue Kit (QIAGEN, Hilden, Germany) on an automated QIAcube (QIAGEN) instrument, according to the manufacturer's instructions with modifications; specifically, (i) doubling the amount of digestion reagents: 360 µL

ATL buffer + 40 µL Proteinase K, (ii) digestion at 56°C overnight for host samples and 3 hrs for environmental samples, (iii) eluted twice with 50 µL for the first elution and 50 µL for the second elution (waiting time of 5 min for both) to retrieve 100 µL eluted DNA. Extraction controls (consisting of no sample) were also processed at the same time.

A master mix for fusion tag primers, consisting of Illumina adaptor and sequencing primers, barcode indexes unique to this study, and the template-specific primers was prepared on an automated QIAgility (QIAGEN) instrument in an ultra-clean facility. The ITS2 primer set, ITSD (5′-GTGAATTGCAGAACTCCGTG-3′; Pochon et al. 2001) and ITS2rev2 (5′-CCTCCGCTTACTTATATGCTT-3′; Stat et al. 2009b) that targets the partial 5.8S, entire ITS2, and partial 28S region of nuclear ribosomal DNA of *Symbiodinium* was used for amplicon sequencing. PCR reagents used consisted of 1 × GeneAmp® PCR Gold Buffer (Life Technologies, CA, USA), 2 mM $MgCl_2$, 0.25 µM dNTPs, 10 µg BSA, 5 pmol of each primer, 0.12 × SYBR® Green (Life Technologies), 1 Unit AmpliTaq Gold® DNA polymerase (Life Technologies), 2 µL of DNA, and Ultrapure™ Distilled Water (Life Technologies) made up to 25 µL reaction. Amplification of target DNA was performed in a single round of polymerase chain reaction (PCR) on duplicates of each sample on an Applied Biosystems StepOnePlus Real-Time PCR system (Applied Biosystems, CA, USA) under the following conditions: initial denaturing at 95°C for 5 min, followed by 35-38 cycles (for endosymbiont samples) or 45 cycles (for environmental samples) of 30 sec at 95°C, 30 sec at 52°C, and 45 sec at 72°C, and a final extension at 72°C for 10 min. Duplicates originating from each sample were combined prior to amplicon pooling and library preparation.

The amplicon library for sequencing was prepared by pooling PCR products into equimolar ratios based on the qPCR Ct values and ΔRn values, and quantification using a Labchip® GX Touch HT (Perkin Elmer, MA, USA). To assess cross-contamination, PCR negative controls and amplification using the blank DNA extraction control as a template were also included in the final library for sequencing. Amplicons in the library were size-selected using a Pippin Prep (Sage Science, MA, USA) and purified using the QIAquick PCR Purification Kit (QIAGEN). The volume of purified library added for sequencing was determined using a Labchip® GX Touch HT, and sequenced using a 500 cycle MiSeq® v2 Reagent Kit and standard flow cell (2 × 250 paired end) on an Illumina MiSeq platform (Illumina, CA, USA). Low-read samples (ca. < 31,000 reads per sample after demultiplexing) were re-sequenced using the same extracted and amplified DNA and the obtained sequences were pooled together with the original run sequences for the further analysis.

2.3.4. Bioinformatic analysis

The detailed pipeline including tools used for the bioinformatic analysis for MiSeq sequences can be found in the following link: Paired end (ITS2) (Kahlke and Fujise 2017): https://doi.org/10.17605/osf.io/hcsp4.

Firstly, we re-visited to check the utility of the OTU (Operational Taxonomic Unit) approach at the 97% sequence similarity cut-off for the high-throughput NGS data analysis as per Arif et al. (2014) using more variety of culture strains (14 mono-clonal cultures across clades A, B, D, E and F) as control (included as Appendix: Culture OTU analysis), and confirmed the approach could successfully

collapse intra-genomic variations (due to multi-copy nature of rDNA and problematic for assessing diversity based on rDNA sequences) into distinct OTUs (one OTU per one strain for majority of the tested species). In addition, we also found the importance of OTU abundance filtering step for minimising the systematic errors (e.g. sequencing/PCR noise), which applying such a stricter filtering step inevitably provides more robust estimates of diversity. We used the culture analysis as a standard and applied the approach (detail is as follows) to the field samples.

Demultiplexing and removal of the primers and the paired end dual barcodes sequences from the ITS2 libraries were performed with *fastq.info* command in MOTHUR ver. 1.38.1 (Schloss et al. 2009) according to the following criteria: forward and reverse primers (0 mismatches), forward and reverse barcodes (0 mismatches). Forward and reverse sequences were joined using FLASH v.1.2.11 (Magoč and Salzberg 2011) with maximum overlap for 200 bp and *cap-mismatch-quals* option. Sequences were then filtered and discarded using *trim.seq* in MOTHUR if they did not meet the following criteria: homopolymers ≤ 5 bp, ambiguous bases = 0 bp, and average quality score ≥ 25. The quality filtering criteria were determined according to the summary of sequences obtained by *summary.seq* in MOTHUR. To remove non-*Symbiodinium* sequences (the ITS2 primer sets also amplify other dinoflagellate species), the quality filtered sequences were compared to a custom ITS2 database using BLAST and *Symbiodinium* sequences were identified using a Last Common Ancestor (LCA) algorithm as implemented in BASTA (Kahlke 2018a). Parameters used for the LCA algorithm were: -l 200, -b T, -n 0, -m 1, -i 85, and subsequently filtered with BASTA's *filter_fasta.py* script to remove non-*Symbiodinium* sequences. The resulting

Symbiodinium sequences were further dereplicated and singletons were removed using *derep_full* in vsearch ver. 2.3.2 (Rognes et al. 2016). For OTU based analysis, unique sequences were first clustered at 85% similarity cut-off (Arif et al. 2014) by *cluster_fast* in vsearch in order to split the sequences by clade. Each OTU was further inspected to identify potential inconsistencies across the clades of clustered sequences using *uc_cluster_taxa.py* in BASTA and sequences belong to each clade were extracted from the quality filtered fasta file using *extract_seqs_from_fasta.pl* (Kahlke 2018b). Subsequently, all joined fragments belonging to OTUs of the same clade were dereplicated, clustered at 97% similarity cut-off (Stat et al. 2013 2015; Cunning et al. 2015; Ziegler et al. 2017), which can be successfully collapse intra-genomic variations into distinct OTUs (Arif et al. 2014; also see Appendix: Culture OTU analysis), to identify *Symbiodinium* OTUs on a ITS2 variant level and then chimeras were removed using *uchime_ref* in vsearch. OTU taxonomies were assigned with *assign_taxonomy.py* in QIIME v.1.9.1 (Caporaso et al. 2010) using BLAST against a *Symbiodinium* ITS2 reference database "SymTyper" (Cunning et al. 2015; Boulotte et al. 2016). To create the final OTU table, clade OTU sequence files were concatenated and an OTU table was created using *usearch_global* in vsearch. Sequences in OTUs which were observed in the negative controls (1-2 sequences) were subtracted from all samples. OTU abundance filtering at 1% threshold within each sample was further applied to minimise noise (e.g. sequencing errors and PCR artifacts) and ensure relevant and robust conclusions for assessing *Symbiodinium* diversity and community composition as per Appendix: Culture OTU analysis.

2.3.5. qPCR for quantitative analysis of free-living *Symbiodinium*

We further quantified free-living *Symbiodinium* in each environmental habitat (water, sediment, macroalgae), using qPCR via 28S rDNA clade-specific primer sets (clades A-F, except clade E: Yamashita et al. 2011). Clades E, G, H and I were not considered for this process because clade E *Symbiodinium* was not detected in any samples by NGS analysis and no culture strains are currently available for clades G-I which prevents the creation of a cell number vs. DNA content standard curve for qPCR-based quantification.

Specificity and efficiency of each primer set were tested using reference *Symbiodinium* culture strains across clades A-F as per Table 2.1 (note clade E was included here to check specificity and efficiency of the clade E primer set, which was used for assessing PCR extraction efficiency). An aliquot of 10 mL from each culture strain was collected during exponential growth (ca. 5×10^5 cells) and stored at -80°C until DNA extraction. DNA was extracted from each sample ($n = 3$ per culture strain) with the same DNA extraction kits (DNeasy Blood & Tissue Kit) and protocols as for the environmental samples (described in section 2.3.3), but performed manually. Cell numbers were also calculated from each culture strain (frozen sample, $n = 3$ per strain) using a haemocytometer and light microscope (ECLIPSE Ni-E, Nikon, Tokyo, Japan) with automated capturing system (NIS-Elements Advanced Research, version 4.30, Nikon, Tokyo, Japan) (Suggett et al. 2015; Chapter 4).

To check the efficiency of each primer set, serial dilution of DNA from *Symbiodinium* culture strains was prepared at five concentrations (approx. 0.1, 1, 10, 100, and 1,000 cells/reaction: exact cell numbers in each standard are shown in

Table 2.1. *Symbiodinium* culture strains used for the efficiency and specificity check of the primer sets for qPCR assays. Number of cells per qPCR reaction (5 μL) used as the highest concentration of standard DNA are shown. DNA was diluted in 1/10, 1/100, 1/1,000, 1/10,000 for making five concentrations for the calibration curves for each strain.

Clade/ITS2 type		Species	Identity	Geographic origin	Host taxon	Standard (cells reaction^{-1})
A	A1	*S. microadriaticum*	CCMP2464, RT61	Florida (Caribbean)	*Cassiopeia xamachana* (Jellyfish)	808
	A2	*S. pilosum*	CCMP2461, RT185	Jamaica (Caribbean)	*Zoanthus sociatus* (Zoanthid)	753
	A2-relative	*S. natans*	CCMP2548, RT796	Hawai'i (Pacific)	Free-living	742
	A3	*Symbiodinium* sp.	UTS-A	Heron Island (Pacific)	Unknown	564
B	B1	*S. minutum*	CCMP2460, RT2	Florida (Caribbean)	*Aiptasia pallida* (Sea anemone)	982
	B1	*S. pseudominutum*	CCMP2463, RT12	Puerto Rico (Caribbean)	*Aiptasia tagetes* (Sea anemone)	990
C	C1	*Symbiodinium* sp.	SCF058-04	Magnetic Island (Pacific)	*Acropora millepora* (Coral)	966
	C1	*Symbiodinium* sp.	SCF055-06	Magnetic Island (Pacific)	*Acropora tenuis* (Coral)	1057
	C2	*Symbiodinium* sp.	RT203	Palau (Pacific)	*Hippopus hippopus* (Giant clam)	812
D	D1a	*S. trenchii*	CCMP3408, A001	Okinawa (Pacific)	*Acropora* sp. (Coral)	594
E	-	*S. voratum*	CCMP421	Wellington (New Zealand)	Free-living	870
	-	*S. voratum*	CCMP3420, RT383	Santa Barbara (Pacific)	Free-living	816
F	F1	*S. kawagutii*	UTS-C	Heron Island (Pacific)	*Pocillopora damicornis* (Coral)	442

Table 2.1) and master mix for each primer set and template DNA distributed to 384 well plates (HSP3805, BIO-RAD, CA, USA) on an automated epMotion® 5075 TMX (Eppendorf, Hamburg, Germany). qPCR reagents included 2.5 μL of iTaq™ Universal SYBR® Green SuperMix (BIO-RAD), 0.4 pmol of each forward and reverse primer, 2 μL of DNA, and 0.1 μL of Ultrapure™ Distilled Water (Life Technologies) to make up 5 μL reaction. All qPCR assays were performed in triplicate on a CFX384™ Real-Time System (BIO-RAD). To check the specificity of each primer set, approx. 1,000 cells per reaction derived from other clades were also subjected to qPCR. According to the specificity and efficiency tests, the following qPCR conditions were selected. For the clades A, C, D and E primer sets; initial denaturing at 95°C for 3 min, followed by two-step reactions of 40 cycles of 15 sec at 95°C and 1 min at 60°C. For the clade B primer set, initial denaturing at 95°C for 3 min, followed by four-step reactions of 40 cycles of 15 sec at 95°C, 10 sec at 63°C,

20 sec at 72°C (fluorescence data acquired), and additional 10 sec at 78°C. For the clade F primer set, initial denaturing at 95°C for 3 min, followed by three-step reactions of 40 cycles of 15 sec at 95°C, 10 sec at 63°C, and 30 sec at 72°C. All assays were followed by melting temperature curve analysis, using 0.5°C steps with a hold of 5 sec at each step from 65°C to 95°C.

For quantifying free-living *Symbiodinium* cells in environments, extracted DNA from environmental samples for sequencing (see section 2.3.3) were also used as template DNA in the qPCR assay. One culture strain from each clade was selected to use as quantification standard (Table 2.2). According to the specificity and efficiency assays, minimum quantification ranges were determined and shown in Table 2.2. Cell densities occurring below these thresholds (minimum quantification range) were excluded from further analysis. A serial dilution of the standard culture strain DNA for five concentrations was made for use as the calibration curve, and master mix for each primer set (clades A-F, except E) and template DNA (environmental DNA from each habitat per site and season) were distributed to a 384 plate in the same manner explained above. Each sample was run as a 5 μL reaction per sample in triplicate as above, and either 0.25 or 1.25 ng μL^{-1} of DNA extracted from environmental samples used as template DNA.

DNA extraction efficiency and inhibition of amplification were also tested across samples from different substrates (water, sediment and macroalgae) to ensure comparability in qPCR-retrieved cell numbers. A suspension of a known cell number of clade E *Symbiodinium* (CCMP421) (first confirming that there was no clade E *Symbiodinium* in any environmental samples by NGS) were added to samples

Table 2.2. *Symbiodinium* culture strains used as quantification standards for the qPCR assays for assessing abundance of free-living *Symbiodinium*. One culture strain from each clade was selected for use as a quantification standard for the qPCR assay for each primer set (clades A-F, except E). Number of cells per qPCR reaction (5 μL) used for making calibration curves (five concentrations) and minimum detection limits are shown.

Clade/ ITS2-type		Identity	Standard	Standard 10^{-1}	Standard 10^{-2}	Standard 10^{-3}	Standard 10^{-4}	Detection limit
			cells reaction^{-1}					
A	A1	CCMP2464, RT61	808	80.8	8.08	0.808	0.0808	0.0808
B	B1	CCMP2460, RT2	982	98.2	9.82	0.982	0.0982	0.982
C	C2	RT203	812	81.2	8.12	0.812	0.0812	0.812
D	D1a	CCMP3408	594	59.4	5.94	0.594	0.0594	0.594
F	F1	UTS-C	442	44.2	4.42	0.442	0.0442	0.442

collected from three different habitats and DNA was extracted as outlined above. DNA from the same amount of aliquot of the culture strain was extracted as for standard to check PCR inhibition and extraction efficiency for the environmental samples. qPCR assay was performed using clade E primer sets with DNA concentration: neat (no dilution), 0.25 and 1.25 ng μL^{-1} of DNA as template. The Ct values were compared with the standard and confirmed PCR inhibition was not occurred for 0.25 ng μL^{-1} of DNA concentration for all substrates and 1.25 ng μL^{-1} of DNA for water and macroalgae samples with similar DNA extraction efficiency across three substrates were obtained (efficiency range: 94-104%).

Cell number for each clade and habitat was quantified using the quantification standard obtained by culture strains and normalised to cells mL^{-1} for water and sediment samples (Littman et al. 2008) and cells g^{-1} (wet weight) for macroalgae samples (e.g. Aligizaki and Nikolaidis 2006; Kim et al. 2011). In addition, to compare cell numbers across habitats, cell numbers were normalised to cells cm^{-3} for

all samples. Sediment and water samples were calculated per unit volume; however, a unit adjustment was required for the macroalgal samples. *Symbiodinium* cell numbers in macroalgae samples were converted from per wet weight (g) to per cm^3 using the relationship between wet weight (g)/surface area (m^2): 66.4 g m^{-2} for *Padina pavonia* (Mercado et al. 1998) and boundary layer thickness: 350 μm for *Padina australis* (Hofmann et al. 2015) (note that boundary layer thickness is highly dependent on a water velocity, but the flow rate used in the experiment was ~2 cm s^{-1}). We used the thickness of boundary layer for calculating habitat volume for *Symbiodinium* on surface of macroalgae, because it is known that epiphytic organisms live within a boundary layer on the surface of thallus (Wahl et al. 2016; Noisette and Hard 2018).

Free-living *Symbiodinium* cell densities were further compared to *in hospite* cell densities (only available for spawning season). *Symbiodinium* cells were removed from the coral skeleton which were collected during the spawning season using an airbrush with known volume of 0.2-μm filtered seawater and cells counted using a haemocytometer as above. *Symbiodinium* cell density was initially normalised to coral surface area (cm^2) determined using the agarose + methylene blue coating method described in Yamashita et al. (2011), and subsequently to cm^3 by multiplying surface area by tissue thickness (mm) using values from the Coral Trait Database (https://coraltraits.org/; Madin et al. 2016): 1 mm, 0.9 mm, and 0.9 mm for *A. aspera*, *M. digitata*, *P. damicornis*, respectively.

2.3.6. Statistical analysis

Our sampling design yielded 4 replicates each for 3 sites (coral species of *A. aspera*, *M. digitata*, *P. damicornis*) × 4 habitats (host, water, sediment, macroalgae) × 2 seasons (spawning, summer). Based on the numbers of clades, ITS2 variants and OTUs in each sample, differences in richness between habitats (pooled across sites) and seasons were tested using the Kruskal-Wallis test with Bonferroni pairwise comparison *post-hoc* tests using SPSS Statistics 23 (IBM, Armonk, NY) ($P < 0.05$) ($n = 12$ for each habitat for each season). We performed subsampling with 2,000 sequences per sample to compare richness with the same sequence depth. However, richness patterns between habitats/seasons followed the pattern as for the original number of sequences (without subsampling). As such, to include as many sequences as possible especially for low-read samples, we therefore performed the statistical analysis without subsampling sequences. To visualise the overlap of taxonomic types belong to clade C (ITS2 variants and OTUs) between symbiotic (in corals) and environments (water, sediment, macroalgae), Venn diagrams were created for each site and season combination using *eulerr* package in R (http://jolars.co/). To compare the *Symbiodinium* taxonomic compositions, relative abundances of the *Symbiodinium* clades, ITS2 variants and OTUs were square-root transformed and compared between each sample using the Bray-Curtis similarity coefficient. Non-metric multi-dimensional scaling (nMDS) ordination diagrams were produced and CLUSTER analysis was performed using group averages to visualise the relationship of *Symbiodinium* community composition between sites, habitats and seasons. A permutational ANOVA (PERMANOVA) was used to test for significant differences of *Symbiodinium* taxonomic compositions (clades, ITS2 variants and OTUs) with sites (host species) (3 levels), habitats (4 levels) and seasons (2 levels) as fixed

factors, using type III sum of squares and unrestricted permutation of raw data with 999 permutations. A *post-hoc* pairwise comparison test among all pairs of levels of 'site × habitat × season' factor was used to identify where significant differences occurred. Similarity percentage (SIMPER) analysis was performed to identify which taxa were the most important to observe a pattern of similarity between samples. All multivariate analyses described above were performed using PRIMER (version 6.1.16) and PERMANOVA+ (version 1.0.6) software. To visualise the different abundance of ITS2 variants between sites, habitats and seasons, a heat map was created using *gplots* package in R (Warnes et al. 2015).

qPCR-based *Symbiodinium* cladal abundances for clades A, C and D (clades B and F were under the detection limit, thus not included into the statistical analysis) were square-root transformed and compared between each sample using the Bray-Curtis similarity coefficient, nMDS ordination diagram was produced and PERMANOVA was performed with the same factors as above. In addition, to compare *Symbiodinium* cladal compositions (clades A, C and D only) obtained using the two different techniques (NGS vs. qPCR), relative abundances of the *Symbiodinium* clades were square-root transformed and compared between each sample using the Bray-Curtis similarity coefficient. nMDS ordination diagram was produced and CLUSTER analysis was performed to visualise the relationship of *Symbiodinium* community composition between techniques, sites, habitats and seasons and PERMANOVA was performed with same setting as described above for NGS data set with the forth factor as technique (2 levels). A *post-hoc* pairwise comparison test among all pairs of levels of 'technique × site × habitat × season' factor was used to identify where significant differences occurred in the technique factor.

2.4. Results

2.4.1. SST and PAR on Heron reef (2015-2016)

Key environmental conditions known to regulate *Symbiodinium* competitive fitness; temperature and light intensity (e.g. Robison and Warner 2006), were determined for the two sampling seasons (Fig. 2.2). As expected, monthly averaged SST (°C) was higher in summer (March 2016; 26.9 ± 0.5°C, mean of daily averaged SST ± SD) compared to the spawning season (October 2015; 23.2 ± 0.9°C), by ca. 3.7°C.

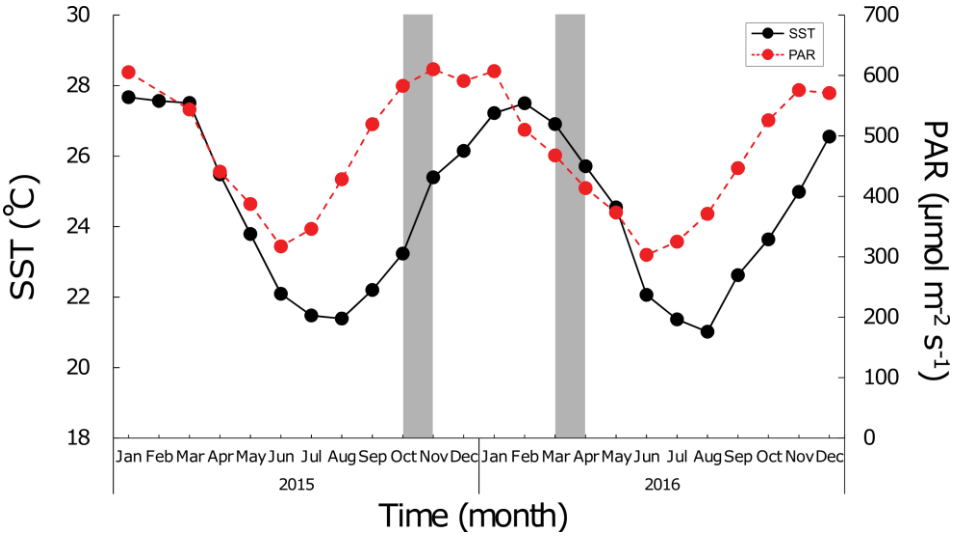

Figure 2.2. Environmental data on Heron reef (2015-2016). Monthly averaged sea surface temperature (SST, °C) is shown as a black solid line (left Y axis) and monthly averaged photosynthetic active radiation (PAR, μmol photons m^{-2} s^{-1}) is shown as a red dashed line (right Y axis) from January 2015 to December 2016. Samplings were performed in October 2015 (spawning season) and March 2016 (summer season) and indicated by the grey areas.

SSTs for summer 2016 (27.2 ± 0.9°C, 27.5 ± 0.8°C, 26.9 ± 0.5°C, monthly average for January, February, March, respectively) when mass coral bleaching events were observed in the northern and central GBR (Hughes et al. 2017) did not differ with

those for summer 2015 (27.7 ± 1.0°C, 27.6 ± 0.4°C, 27.5 ± 0.7°C, respectively), supporting that our March 2016 sampling season was not influenced by the unusually warm summer that was shown to be impacting the northern and central GBR, and thus our summer season is considered typical. In contrast to temperature, light intensity (incident PAR) was higher during the spawning season (October 2015; 583 ± 75 μmol photons m^{-2} s^{-1}, mean of daily averaged PAR ± SD) compared to the summer season (March 2016; 468 ± 115 μmol photons m^{-2} s^{-1}). Indeed, the spawning season had the highest average monthly PAR (November 2015; 610 ± 95 μmol photons m^{-2} s^{-1}) across the whole year. As such, the free-living *Symbiodinium* communities during our study period were subjected to a growth environment of lower light but warmer waters in summer compared to spawning seasons.

2.4.2. Diversity of *in hospite* and free-living *Symbiodinium* using next generation sequencing

To explore free-living *Symbiodinium* diversity, we sequentially consider the results in order from the lowest to highest resolution of genetic diversity: (i) cladal level, (ii) ITS2 variant level, and then (iii) OTU level. The OTU analysis with a 97% cut-off demonstrates species or type-level diversity that is able to minimise influences of the intra-genomic variation interfering with the diversity analysis due to the multi-copy nature of rDNA (Arif et al. 2014; also see Appendix: Culture OTU analysis). The OTU framework phylogenetically and ecologically provides the platform for examination of the taxonomic resolution and functional variability (Stat et al. 2015). For the cladal and ITS2 variant level, we combined the OTUs assigned to the same clade and same ITS2 variant, respectively. In here, we term each ITS2 sequence in the reference database SymTyper as “ITS2 variant”, because SymTyper contains

multiple sequences derived from one genome/biological entity (i.e. intra-genomic variants). Note that representative sequences of the OTUs were assigned to the closet match of taxonomy (ITS2 variant) in SymTyper. The number of OTUs were always higher than assigned ITS2 variants because of the incompleteness of the reference database, whereby novel ITS2 variants (possibly new types/species) have been increasingly detected by NGS (e.g. Cunning et al. 2015).

DNA metabarcoding using NGS for *Symbiodinium* yielded 1,808,189 sequences from 96 samples (4 replicates × 3 sites × 4 habitats × 2 seasons) after demultiplexing, quality filtering, and removing non-*Symbiodinium* sequences (26% of the total sequences belonged to *Symbiodinium*). A total of 232 OTUs were obtained and assigned to all clades (A-I) except clade E, and into 72 ITS2 variants. Numbers of sequences, clades, ITS2 variants and OTUs per site, habitat and season are shown in Fig. 2.3 as box plots and Table S2.1 as a list. Overall trends were shared at the all taxonomic levels (cladal, ITS2 variant and OTU): (i) *Symbiodinoum* richness was higher for the environmental samples compared to those in the coral hosts; however, (ii) richness did not differ between different environmental habitats (water vs. sediment vs. macroalgae) and (iii) richness did not differ between seasons (spawning vs. summer for each habitat) indicating highly stable *Symbiodinium* diversity over environmental space and time.

Total number of *Symbiodinium* clades found were significantly higher for the environmental samples (3.2 ± 0.83, 5.0 ± 1.0, 3.6 ± 0.92 clades in water, sediment, macroalgae samples, respectively, mean across all sites for both seasons ± SD) compared to the coral hosts which only harboured one clade of *Symbiodinium*

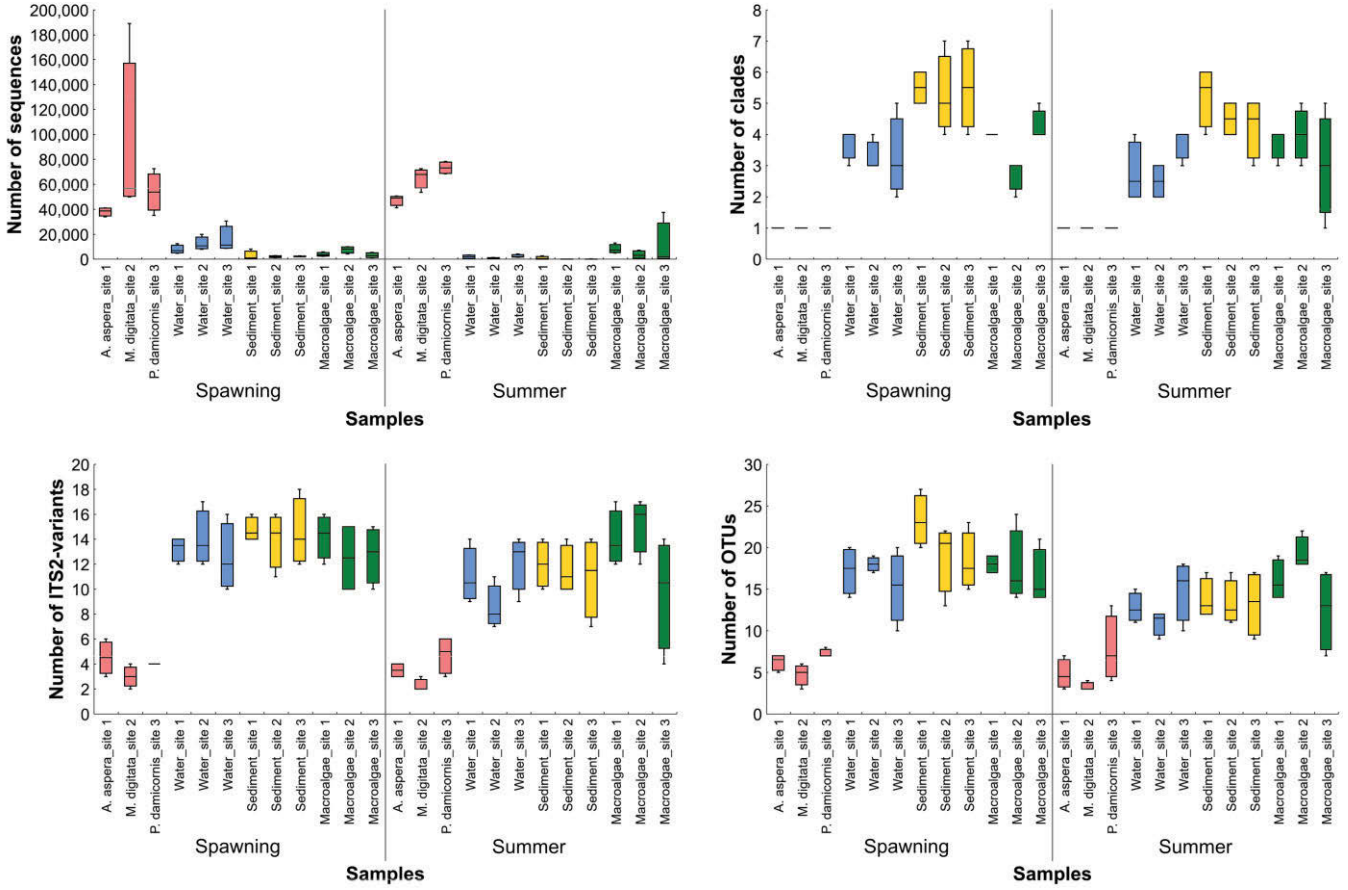

Figure 2.3. Box plots for number of sequences, clades, ITS2 variants and OTUs in each site, habitat and season. Box plots for corals are shown as pink, water as blue, sediment as yellow and macroalgae as green.

(Kruskal-Wallis test, $P < 0.05$, except for coral vs. water samples in summer season: $P = 0.15$, also see Table S2.2 for summary of Kruskal-Wallis test). No significant differences were found within environments (water vs. sediment vs. macroalgae) nor between seasons for each habitat ($P > 0.05$).

Richness of ITS2 variants of *Symbiodinium* followed the same pattern as observed in the cladal level that total number of ITS2 variants differed between environments (12 ± 2.6, 13 ± 2.5, 13 ± 3.0 ITS2 variants in water, sediment and macroalgae samples, respectively, mean across all sites for both seasons ± SD) and those in the coral hosts (4 ± 1.2 ITS2 variants) (Kruskal-Wallis test, $P < 0.05$, except coral vs. water samples in summer season: $P = 0.096$, see Table S2.2B for pairwise comparison), but not between the different environments nor between two seasons ($P > 0.05$).

Furthermore, OTU richness was significantly higher for all environmental samples (17 ± 2.9, 20 ± 3.9, 17 ± 3.0 OTUs, in water, sediment and macroalgae samples, respectively, mean across all sites for the spawning season ± SD) compared to coral samples (6.1 ± 1.4 OTUs) in the spawning seasons (Kruskal-Wallis test, $P < 0.05$). In the summer season; however, the significant difference was only detected between macroalgae (16 ± 4.1 OTUs, mean across all sites for summer season ± SD) and coral samples (5.3 ± 3.0 OTUs), but not between water (13 ± 2.8 OTUs) and corals nor between sediment (13 ± 2.7 OTUs) and corals ($P = 4.0 \times 10^{-4}$, $P = 0.18$, $P = 0.088$, respectively), since OTU richness of *Symbiodinium* for water and sediment samples in the summer season were slightly lower than those compared to the spawning season. No significant difference of *Symbiodinium* richness was found between environmental samples nor between seasons for each habitat also at the

OTU level ($P > 0.05$).

2.4.3. Connectivity of *Symbiodinium* genetic types *in hospite* and in environments

Potential connectivity of symbiotic and free-living *Symbiodinium* populations (at least at the levels measured through the genetic approaches here, see Thornhill et al. 2017), was examined for clade C, since this was the only clade found *in hospite* (Fig. 2.4). 15-28% of ITS2 variants were shared between corals and the surrounding environment (pooling all environmental habitats; water, sediment and macroalgae) for both spawning and summer seasons (Fig. 2.4A). More than 40% of ITS2 variants found *in hospite* were also found in the environmental samples during the spawning season, and for *M. digitata*, 80% of ITS2 variants found *in hospite* were also found in the environment. Slightly less overlap was observed during the summer season for *A. aspera* and *M. digitata* with 50% and 67% of ITS2 variants in corals, respectively, also found in the environment, but opposite trend was found for *P. damicornis*: increased from 43% in spawning to 56% in summer season. In contrast, 50-74% of ITS2 variants (across all sites for both seasons) were found only in the environmental samples highlighting the existence of a large number of ITS2 variants specific to environments (i.e. free-living).

Again, connectivity of OTUs between *in hospite* and the environment showed similar patterns as for ITS2 variants, but with less overlap: only 4-18% of OTUs were shared between corals and environments across all sites and seasons (Fig. 2.4B). During the spawning season, 47% and 67% of OTUs found in *A. aspera* and *M. digitata* respectively, were also found in the environment. However, only 36% of OTUs for

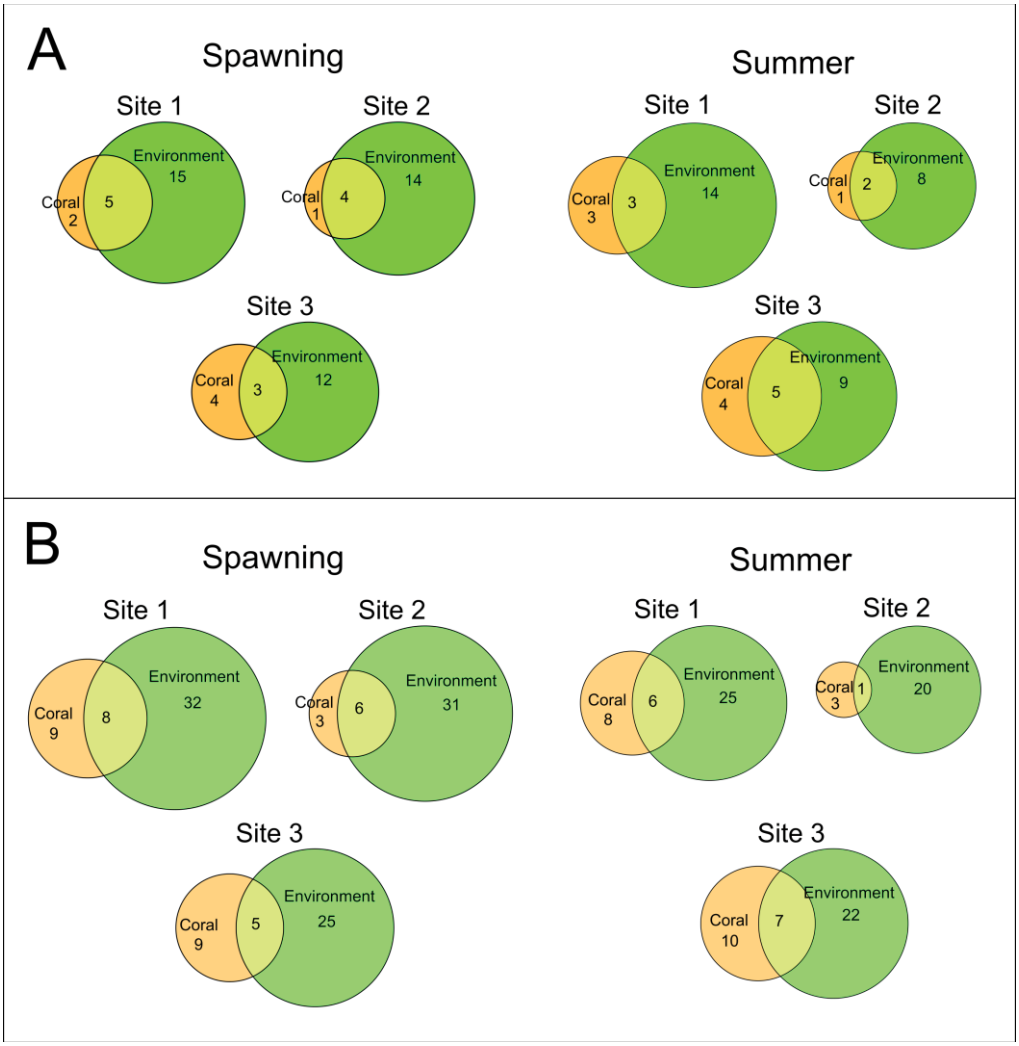

Figure 2.4. Venn diagrams for *in hospite* (coral) and free-living *Symbiodinium* genetic types in environments. Number of **A.** ITS2 variants. **B.** OTUs, belong to clade C. Number of *Symbiodinium* ITS2 variants or OTUs *in hospite* are shown with orange circles and in environment (sum of water, sediment and macroalgae samples) with green circles for each site (coral species) and season (spawning vs. summer).

P. damicornis were found in the surrounding environments. In contrast, percentages of OTUs *in hospite* which were also detected in the environmental samples decreased for the summer season to 43% and 25% for *A. aspera* and *M. digitata*, respectively, but increased to 41% for *P. damicornis*. Overall, assessing free-living *Symbiodinium*

diversity using increasing taxonomic resolution results in decreasing overlap between hosts and environments (and across different environments), likely demonstrating increasing niche specialisation of (and diversity amongst) the taxonomically rare types.

2.4.4. *Symbiodinium* community compositions between sites, habitats and seasons

Where section 2.4.2 first examines the number of taxonomic units (with increasing resolution from cladal to OTU level) across habitats (including both *in hospite* and in environments), we next focused on the community compositions of *Symbiodinium* and consider how diversity is structured across different environmental pools. We acknowledge the limitation for mapping individual biological entities (i.e. ITS2-type/species) based on ITS2 sequences. Therefore, we also supplement the information of taxa with a broader phylogenetic context together with ITS2 variants, such as C3-like type (e.g. for C1085 ITS2 variant) to aid interpretation of ecological patterns, as per Cunning et al. (2015), who also assessed free-living *Symbiodinium* diversity by high-throughput amplicon sequencing using the ITS2 marker and applied OTU based analysis with taxonomy assigned by SymTyper.

2.4.4.1. Cladal composition

Eight clades (A-I, except clade E) were found in this study, and number of sequences, ITS2 variants and OTUs in each clade are shown in Table 2.3. Consistent with previous reports for Heron Island (LaJeunesse et al. 2003; 2004; Stat et al. 2008b; 2009a), all three coral species (*A. aspera*, *M. digitata*, *P. damicornis*) harboured clade C *Symbiodinium* (Fig. 2.5), and which our analysis identified was the most abundant

(1,672,225 sequences) and taxonomically rich (35 ITS2 variants and 104 OTUs). Clade C was also the most abundant clade in the environmental samples (60% of the total environment sequences), followed by clades A (31%), D (5.5%), G (2.1%), F (1.1%), I (0.084%), B (0.084%) and H (0.020%). *Symbiodinium* sequences retrieved from the water column were predominantly clade C (69% across sites and seasons) and clades A (20%), D (10%), G (0.92%), F (0.12%), B (0.013%), with no detection of clades H and I. Macroalgal samples also exhibited a similar pattern as that for the water samples, dominated by clades C (62%) and A (35%) followed by clades G (2.1%), D (0.80%), B (0.16%), F (0.064%), and clades H and I were not detected. In contrast, sediments were dominated by clade A (67%) followed by clades F (11%), C (9.1%), G (8.4%), D (3.7%), I (0.90%), H (0.22%) and B (0.082%).

Table 2.3. Number of sequences, ITS2 variants and OTUs belong to clades A-I, except clade E.

Clade	Number of sequences	Number of ITS2 variants	Number of OTUs
A	105,224	15	75
B	287	1	2
C	1,672,225	35	104
D	19,028	7	12
F	3,777	8	25
G	7,290	3	9
H	70	1	1
I	288	2	4
Total	1,808,189	72	232

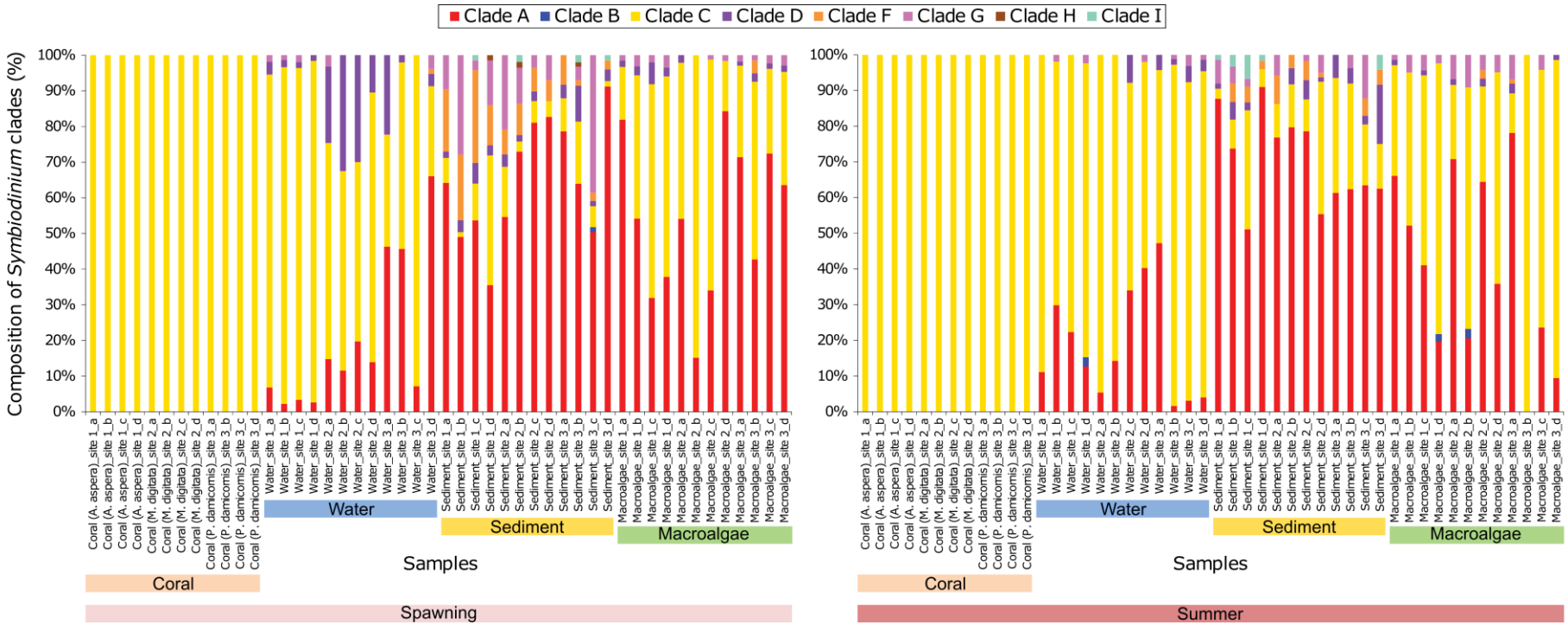

Figure 2.5. Relative abundance of *Symbiodinium* clades during the spawning and summer seasons obtained by DNA metabarcoding. 48 samples: 3 sites (coral species), 4 habitats (*in hospite*, water, sediment and macroalgae), 4 replicates (a, b, c, d) for 2 seasons (spawning vs. summer). Colour of bars for each clade are shown above the graphs.

No clear separation of community composition was observed between sites based on clade (nMDS plot; Fig. 2.6A) (PERMANOVA, $P = 0.25$, see PERMANOVA main effects in Table S2.3A). Instead, separation was clearly driven by habitats ($P = 0.001$), and particularly by *in hospite* vs. environments as far as taxonomic composition ($P < 0.05$, except coral vs. macroalgae at site 3 during the summer season: $P = 0.16$, see Appendix E2.1 for summary of PERMANOVA pairwise comparison), whereby the dissimilarity was primarily driven by clade C. Water samples showed the closest composition to corals, whereas sediments were the most dissimilar given the dominance of clade A (sediments) compared to clade C (*in hospite*). In addition, clades H and I were only detected in the sediment samples, which dissimilarity of the sediment samples was also driven by these two clades as vectors. Macroalgae samples showed an intermediate pattern between water and sediment samples. Cladal composition was significantly different between water and sediment samples in all sites and seasons ($P < 0.05$ for all combinations), water and macroalgae during the spawning season for sites 1 and 2 ($P = 0.027$, 0.028, respectively) and during the summer season for site 1 only ($P = 0.046$), and sediment and macroalgae during the spawning season for all three sites ($P = 0.031$, 0.029, 0.032, for sites 1, 2, 3, respectively), but only for site 1 during the summer season ($P = 0.032$). SIMPER analysis confirmed the major drivers separating taxonomic composition across environments; for example, for site 1 (*A. aspera* site) during the spawning season, clades A and D contributed significantly to the dissimilarity (40%, 31%, respectively) between coral and water, clades C and A (33%, 27%, respectively) between water and sediment, and clades F and C (36%, 29%, respectively) between sediment and macroalgae (see Table S2.4 for summary of SIMPER analysis).

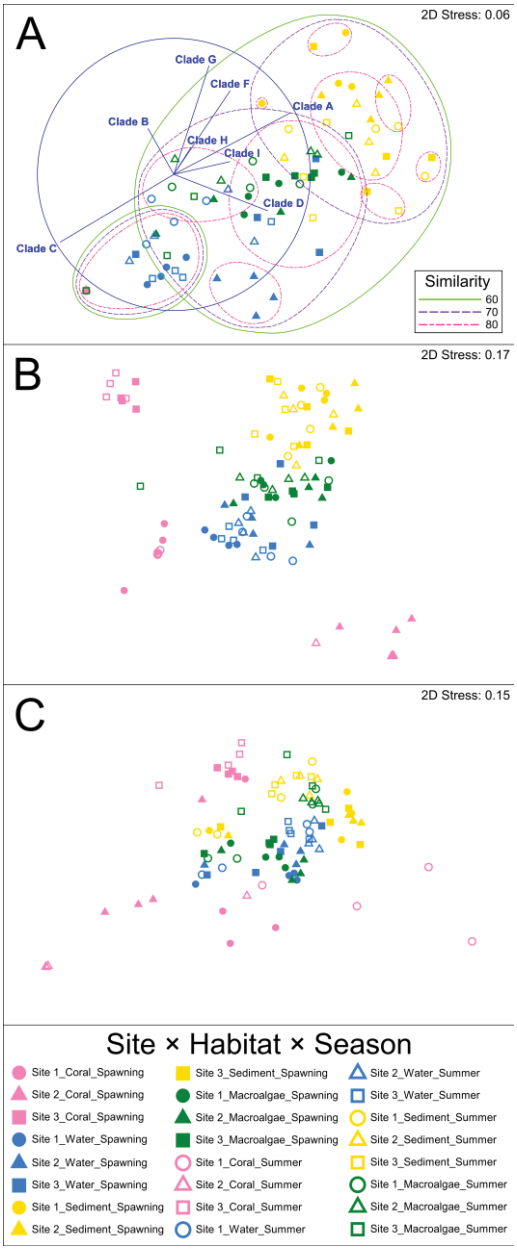

Figure 2.6. nMDS plots of *Symbiodinium* community compositions. **A.** Clade. **B.** ITS2 variant. **C.** OTU. Non-metric multidimensional scaling (nMDS) was performed on each variable per variant using Bray-Curtis Similarity. CLUSTER analysis was performed for cladal composition (**A**); similarity is shown at the 60% (green solid lines), 70% (purple dashed lines) and 80% (pink dashed lines) levels and vectors driving the clustering are shown as blue lines. Corals are represented by pink, water by blue, sediment by yellow, and macroalgae by green with site 1 with circle, site 2 with rectangle, and site 3 with square markers. Plots for the spawning season are shown with closed markers and the summer season with open markers (all combinations of the markers are shown below the graphs).

2.4.4.2. ITS2 variants composition

A total of 72 ITS2 variants were found in this study, belonging to clades A (15 ITS2 variants), B (1), C (35), D (7), F (8), G (3), H (1) and I (2). The most abundant ITS2 variants for each coral (shown as the top three ITS2 variants in each sample averaged across replicates; Table S2.5) remained constant throughout the seasons for *A. aspera*: C1085 (C3-like type: 81% and 80% during the spawning and summer season, respectively), and for *M. digitata*: C15 (62%, 76%, respectively). However, the first and second most abundant ITS2 variants changed dominance for *P. damicornis* across seasons: C42 (47%) > C1cstar (36%) and C1cstar (66%) > C42 (16%) for the spawning and summer seasons, respectively (C1cstar: C1-like type, and also C42 is thought to be a variant derived from C1 genome: C1-like type; LaJeunesse 2004). These patterns were further confirmed through nMDS and PERMANOVA (Fig. 2.6B for nMDS plot and PERMANOVA, $P < 0.05$ for all combinations, see Appendix E2.2 for pairwise comparison) showing clear separation across coral species and also seasonal differences of *in hospite* types found only in *P. damicornis* ($P = 0.031$).

Spatial differences (sites and habitats) of free-living *Symbiodinium* community composition were apparent at the ITS2 variants level (see PERMANOVA main effects in Table S2.3B and pairwise comparison in Appendix E2.2). Water samples generally followed the *in hospite* community, notably C1085 or C131 (C3-like types) (dominated in *A. aspera*), and C15-like types (C15, C15.20, C15.16) (dominated in *M. digitata*) were observed across all sites and both seasons (Fig. 2.7) and these types were also found to be abundant in macroalgae samples. A site effect was significant for the ITS2 variants composition in water samples for only between sites 1 and 2 during the spawning season ($P = 0.029$). In contrast, sediment samples were

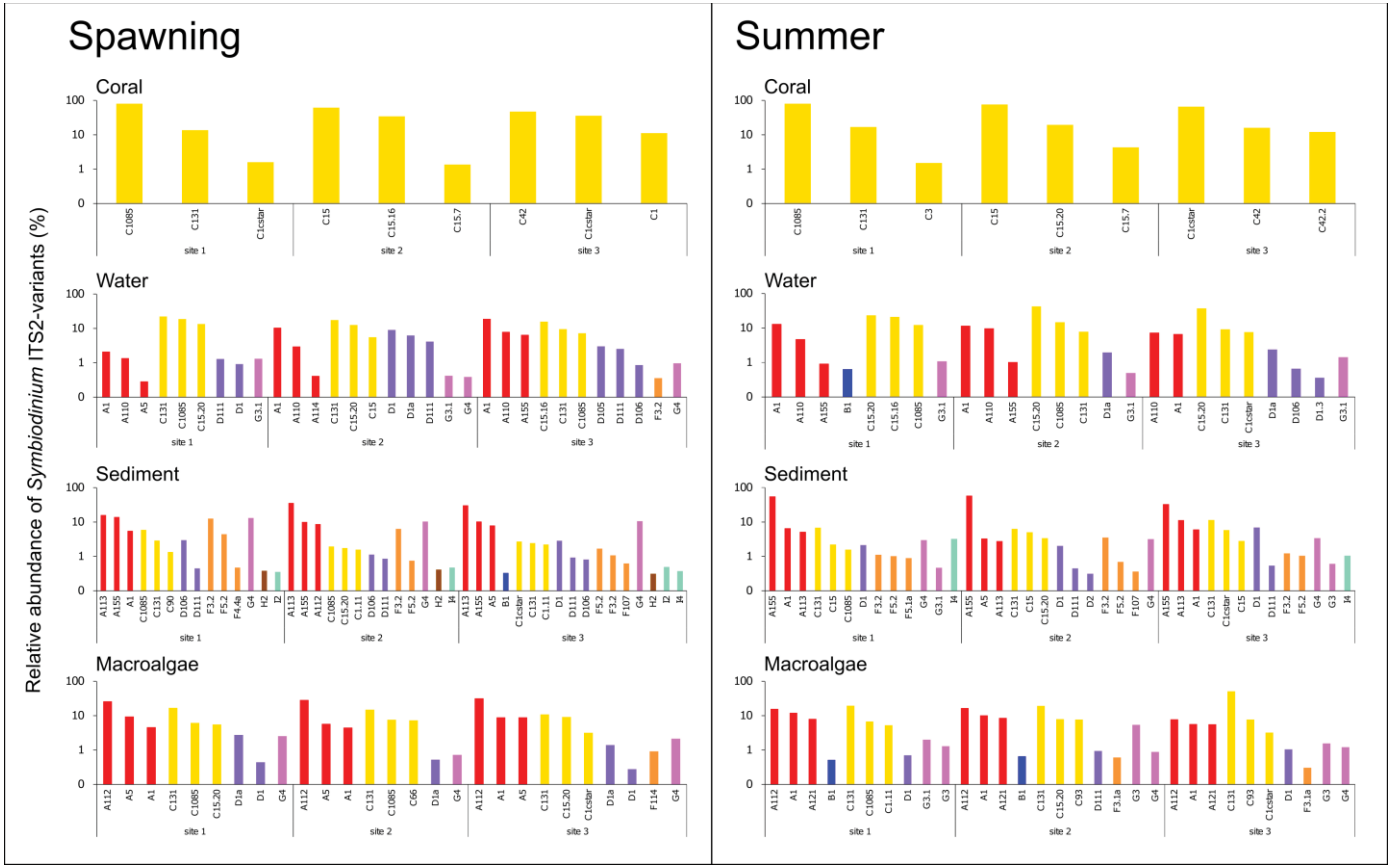

Figure 2.7. Relative abundance of *Symbiodinium* ITS2 variants during the spawning (left panel) and summer seasons (right panel) obtained by DNA metabarcoding. Relative abundance of ITS2 variants in each replicate (n = 4) were averaged and top three ITS2 variants in each clade are shown as bar graphs for each site, habitat and season.

composed by various clade A variants throughout the sites, mainly A113 (A2-relative-like type; closely related to *S. natans*) and A155 (A3-like type; closely related to *S. tridacnidrum*), whereby the former ITS2 variant is an exclusively free-living type (LaJeunesse 2002; Yamashita et al. 2014) and was also found to be abundant in macroalgae samples (A112 which is also A2-relative-like type) together with A1 and A5. SIMPER analysis also supports these types were driving the dissimilarity of community composition by habitats (Table S2.6).

Given the complexity in the differences amongst communities associated with environments and seasons, a heat map (Fig. 2.8) was used to identify the key temporal (seasonal) differences in free-living community composition. Overall, C15.20, A155 and C131 increased in abundance in summer compared to the spawning season for water, sediment and macroalgae samples, respectively, whereby these ITS2 variants contributed most to dissimilarity between seasonal communities (further confirmed by SIMPER analysis, see Table S2.6). These patterns were consistent across sites, whereas site specific increases in relative abundance of ITS2 variants were observed for the spawning season compared to summer. For example, C131, D1, A1 were more abundant in the spawning season compared to summer in water for sites 1 (*A. aspera* site), 2 (*M. digitata* site) and 3 (*P. damicornis* site), respectively, and these site-specific increases of relative abundance of ITS2 variants in the spawning season possibly reflect the important genetic types that appear in adjacent environments for establishing symbiosis with new coral generations.

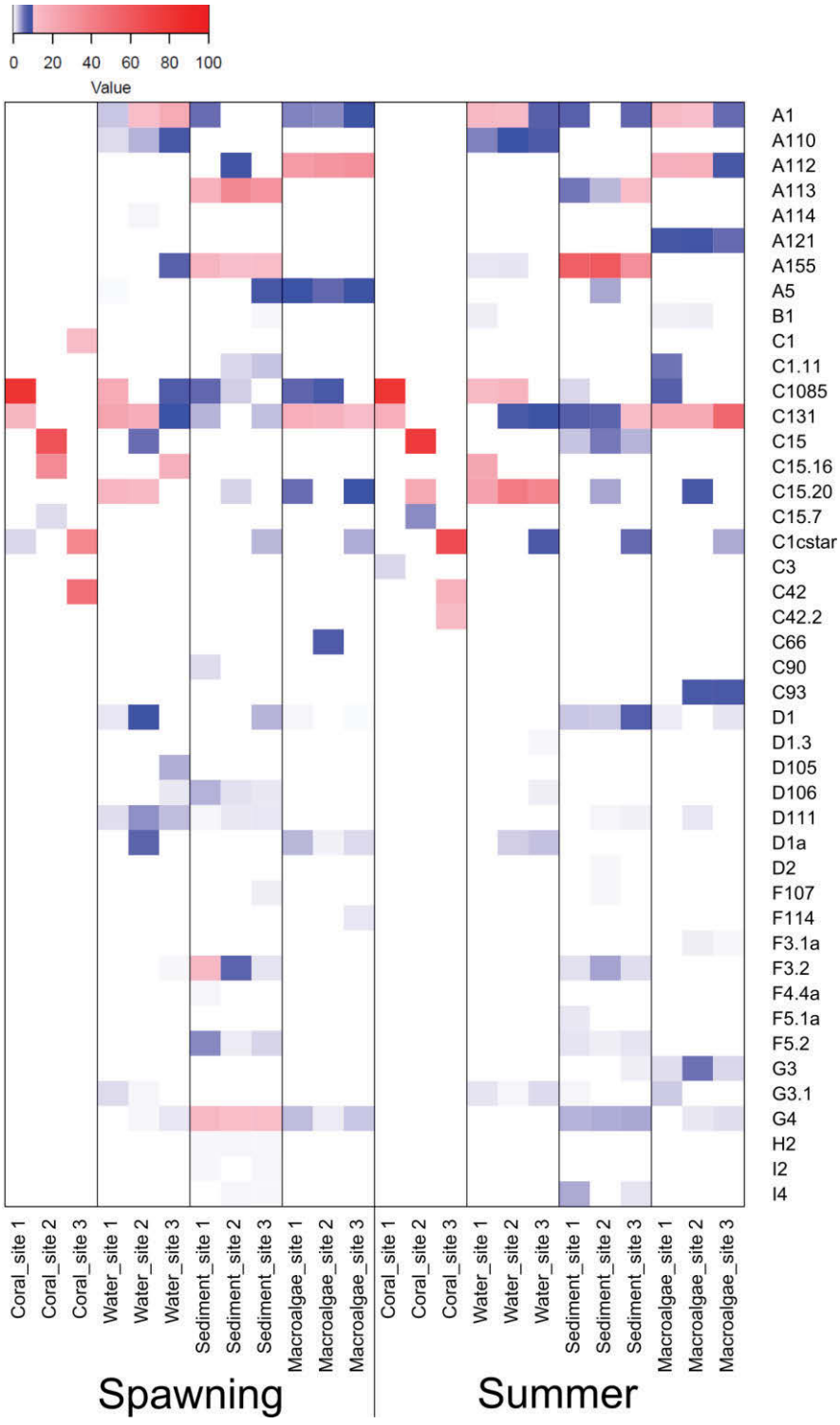

Figure 2.8. Heatmap of *Symbiodinium* ITS2 variant compositions. Compositions of ITS2 variants in each replicate (n = 4) were averaged and top three ITS2 variants in each clade are displayed on the right. The colour (scale bar on the top of the graph) represents the proportion of each ITS2 variants in the sample (0-10% with blue gradient and 10-100% with red gradient), and white boxes indicate an absence of the ITS2 variant.

2.4.4.3. OTUs composition

A total of 232 OTUs spanning clades A (75 OTUs), B (2), C (104), D (12), F (25), G (9), H (1) and I (4) was found. Unsurprisingly, compositions were more complex at the OTU level, compared to ITS2 variants due to higher resolution thus finer scale of diversity and also the incompleteness of reference databases for ITS2 variants, whereby novel types have been increasingly detected (also see 2.4.2). That said, the general trends remained consistent as for the ITS2 variant level, whereby *Symbiodinium* community compositions were significantly different across all factors (sites, habitats, seasons) (PERMANOVA main effects in Table S2.3C and pairwise comparison in Appendix E2.3). Interestingly, seasonal partitioning *in hospite* and free-living compositions became clearer at the OTU level compared to ITS2 variants level (based on nMDS; Fig. 2.6C), as confirmed by PERMANOVA that seasonal differences were significant for all environments ($P < 0.05$) except sediment at sites 1 and 2 ($P = 0.134$, $P = 0.063$, respectively), and significantly different for *in hospite* community in *M. digitata* and *P. damicornis* (PERMANOVA, $P = 0.024$, $P = 0.030$, respectively).

2.4.5. Quantification of free-living *Symbiodinium* by clade-specific qPCR

Clades A, C and D *Symbiodinium* in the environmental samples were detected within the quantification range from the culture strains (A1, C2 and D1a isolates; Table 2.2). Clades B and F *Symbiodinium* were below the threshold of detection. Thus, clades B and F were not considered further in the analysis, but clearly the lack of detection suggests that, as for the taxonomic composition within these clades, their cell numbers were extremely low/rare.

Symbiodinium cell abundances (cells cm^{-3}) differed significantly between sites and environmental habitats (nMDS plot; Fig. 2.9) (PERMANOVA main effects, P = 0.022 and P = 0.001 for sites and habitats, respectively, see Table S2.7 for main effects and Appendix E2.4 for pairwise comparison), but were stable across seasons (P = 0.48). *Symbiodinium* cell density was the highest for macroalgae (869-2,347 cells cm^{-3}: total number of cells (clades A + C + D) range of averaged replicates across sites, habitats, seasons) than sediment (72-829 cells cm^{-3}) and water samples (3-7 cells cm^{-3}) (number of cells are shown in Table 2.4, also see Fig. 2.10 for bubble charts + bar graphs). Clade C was the most numerous with 3-5 cells cm^{-3} and

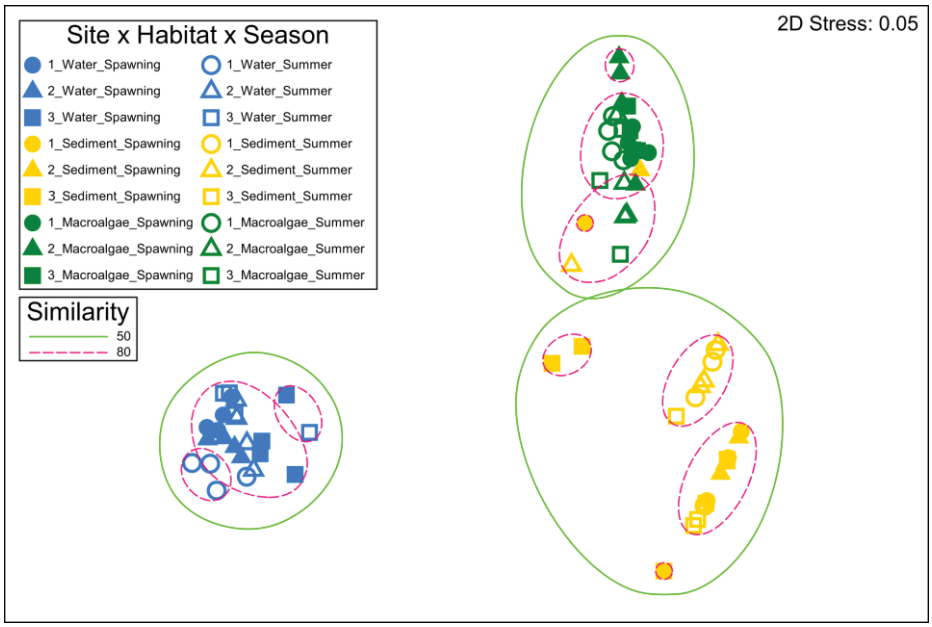

Figure 2.9. nMDS plot of *Symbiodinium* community compositions based on abundance of clades A, C and D obtained by qPCR. Non-metric multidimensional scaling (nMDS) and CLUSTER analysis were performed on each variable per variant using Bray-Curtis Similarity. Similarity is shown at the 50% (green solid lines) and 80% (pink dashed lines) levels. Corals are represented by pink, water by blue, sediment by yellow, and macroalgae by green with site 1 with circle, site 2 with rectangle, and site 3 with square markers. Plots for the spawning season are shown with closed markers and the summer season with open markers (all combinations of the markers are shown in the graph).

714-1,932 cells cm^{-3} for water and macroalgae, respectively, across all sites and seasons. However, clade C *Symbiodinium* were not detected for the majority of sediment samples (19/24), in contrast clade A was detected from all sediment samples (43-93 cells cm^{-3}). During the spawning season, *Symbiodinium* clade C cell densities in the environment were 0.000055% (water), 0.0022% (sediment), and 0.012% (macroalgae) of those recorded *in hospite* (5.8×10^6 to 1.9×10^7 cells cm^{-3} across all host taxa; Table 2.4).

Table 2.4. Cell density of free-living *Symbiodinium* obtained by qPCR. Cell densities of free-living *Symbiodinium* belong to clades A, C and D were detected within the quantification range based on the calibration curves using *Symbiodinium* culture strains as standards (list in Table 2.2); however, *Symbiodinium* belong to clades B and F were below the detection limits so not included in this table. Number of cells were normalised per mL for water and sediment samples and per wet weight (g) for macroalgae samples. In addition, number of cells in all sample types (habitats) were normalised per cm^3 for comparison between different sample types. Mean ± SD (n = 2-4) are shown for all samples. Cell density of clade which was only detected in one replicate per sample is shown with no SD.

			Clade A	Clade C	Clade D	Clade A	Clade C	Clade D
Season	Site	Habitat	cells mL^{-1} (water, sediment), cells g^{-1} (macroalgae)			cells cm^{-3} (water, sediment, and macroalgae)		
Spawning	1	*A. aspera*				1.4×10^7 (2.4×10^6)		
	2	*M. digitata*				1.9×10^7 (2.6×10^6)		
	3	*P. damicornis*				5.8×10^6 (1.6×10^6)		
	1	Water	0.2 (0.0)	4.4 (1.4)	0.4 (0.1)	0.2 (0.0)	4.4 (1.4)	0.4 (0.1)
	2	Water	0.3 (0.1)	2.6 (0.3)	0.6 (0.2)	0.3 (0.1)	2.6 (0.3)	0.6 (0.2)
	3	Water	1.0 (0.4)	4.9 (3.7)	0.6 (0.1)	1.0 (0.4)	4.9 (3.7)	0.6 (0.1)
	1	Sediment	72 (26)	373		72 (26)	373	
	2	Sediment	93 (27)	551	185	93 (27)	551	185
	3	Sediment	54 (26)	74 (2.5)		54 (26)	74 (2.5)	
	1	Macroalgae	1,050 (288)	4,405 (1,247)	693 (275)	199 (55)	836 (237)	131 (52)
	2	Macroalgae	1,558 (541)	10,184 (5,707)	627 (480)	296 (103)	1,932 (1,083)	119 (91)
	3	Macroalgae	1,374 (84)	5,234 (1,778)	527 (187)	261 (16)	993 (337)	100 (36)
Summer	1	Water	0.3 (0.2)	2.5 (0.4)	0.0 (0.0)	0.3 (0.2)	2.5 (0.4)	0.0 (0.0)
	2	Water	0.5 (0.1)	4.6 (1.6)	0.2 (0.1)	0.5 (0.1)	4.6 (1.6)	0.2 (0.1)
	3	Water	0.6 (0.8)	5.4 (0.9)	0.9 (0.1)	0.6 (0.8)	5.4 (0.9)	0.9 (0.1)
	1	Sediment	90 (33)		30 (13)	90 (33)		30 (13)
	2	Sediment	82 (37)	172	33 (6.3)	82 (37)	172	33 (6.3)
	3	Sediment	43 (4.9)		29	43 (4.9)		29
	1	Macroalgae	758 (85)	6,035 (1,870)	199 (68)	144 (16)	1,145 (355)	38 (13)
	2	Macroalgae	660 (100)	4,030 (3,456)	243 (35)	125 (19)	765 (656)	46 (6.6)
	3	Macroalgae	438 (120)	3,764 (3,042)	380 (120)	83 (23)	714 (577)	72 (23)

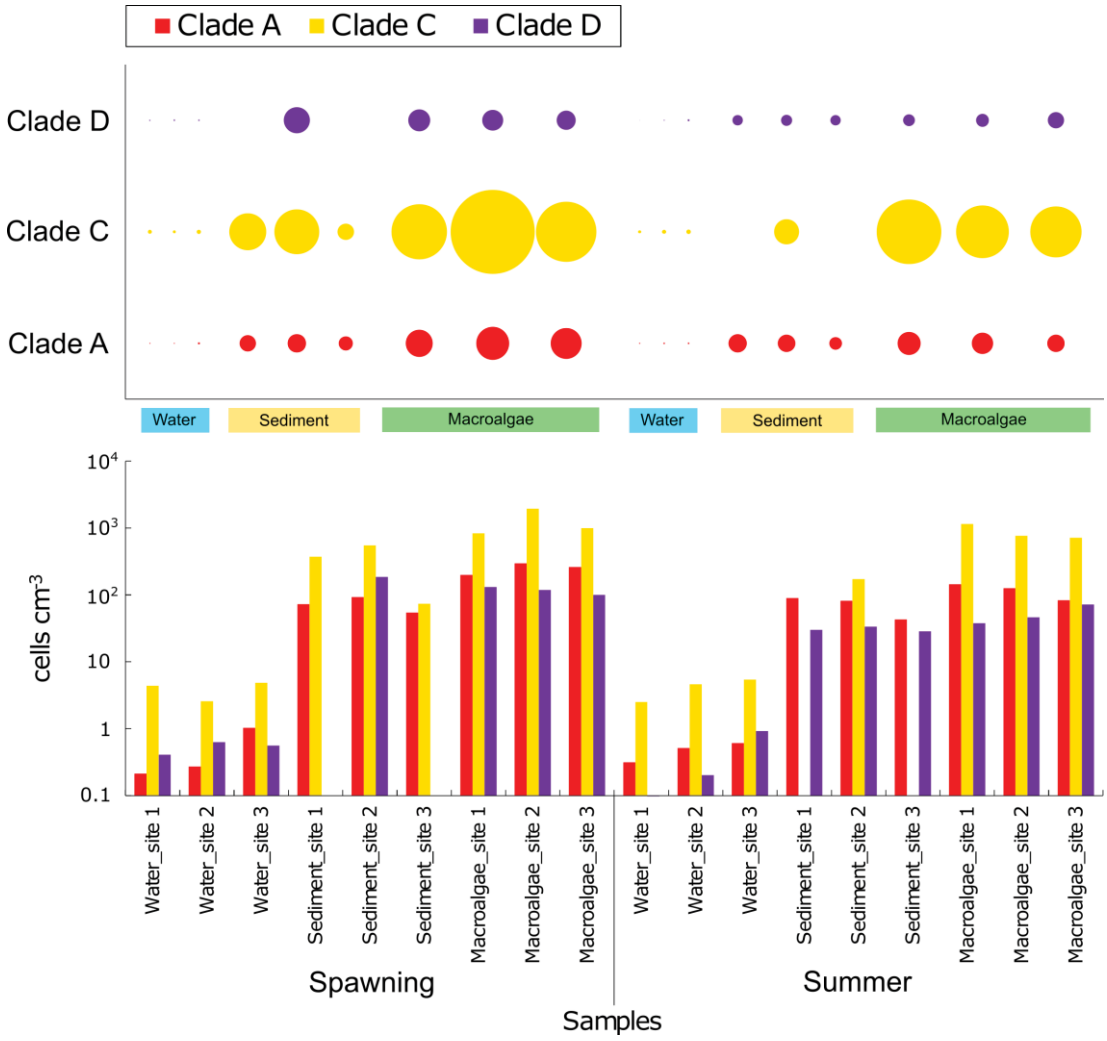

Figure 2.10. Cell density of free-living *Symbiodinium* in environmental habitats obtained by qPCR. Number of cells of free-living *Symbiodinium* belong to clades A, C and D were normalised per cm^3 for each sample type (habitat) in each site and season, and replicates (n = 2-4) were averaged. Cell densities are shown in both bubble charts (upper panel) and bar graphs (lower panel).

Finally, we examined whether cladal level community composition of *Symbiodinium* differed across sites, habitats and seasons inferred from qPCR-determined abundance of clades A, C and D compared with that from NGS-determined information. Community compositions separated by the two techniques were more evident for

macroalgae where 3/6 samples (3 sites × 2 seasons) were significantly different (PERMANOVA, $P < 0.05$, pairwise comparison for technique effects can be found in Appendix E2.5) compared to water and sediment where only 2/6 and 1/6 of the samples differed, respectively (nMDS plot; Fig. 2.11). Relative abundance of clade A in macroalgae samples was higher using NGS compared to qPCR (clade C was always dominant in qPCR) and this trend was also observed in sediment where clade C was detected by qPCR (clade C > A) (Fig. 2.12). Water samples showed a similar pattern as obtained by NGS and qPCR, whereby clade C was the most abundant clade followed by clades A or D depending on site and season.

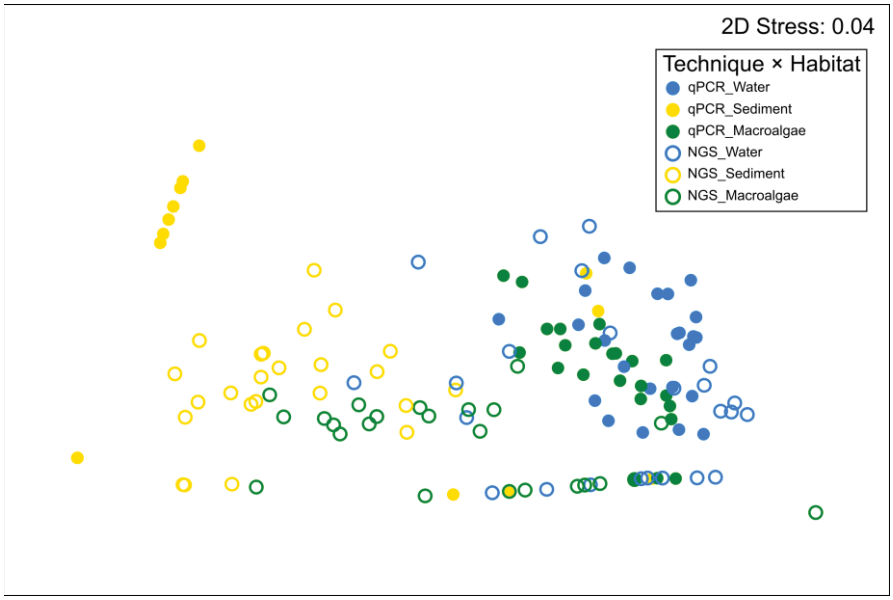

Figure 2.11. nMDS plot for NGS vs. qPCR *Symbiodinium* community compositions of clades A, C and D in environmental habitats. Non-metric multidimensional scaling (nMDS) was performed on each variable per variant using Bray-Curtis Similarity. Water samples are represented by blue, sediment by yellow, and macroalgae by green markers. Plots for qPCR are shown with closed markers and NGS with open markers.

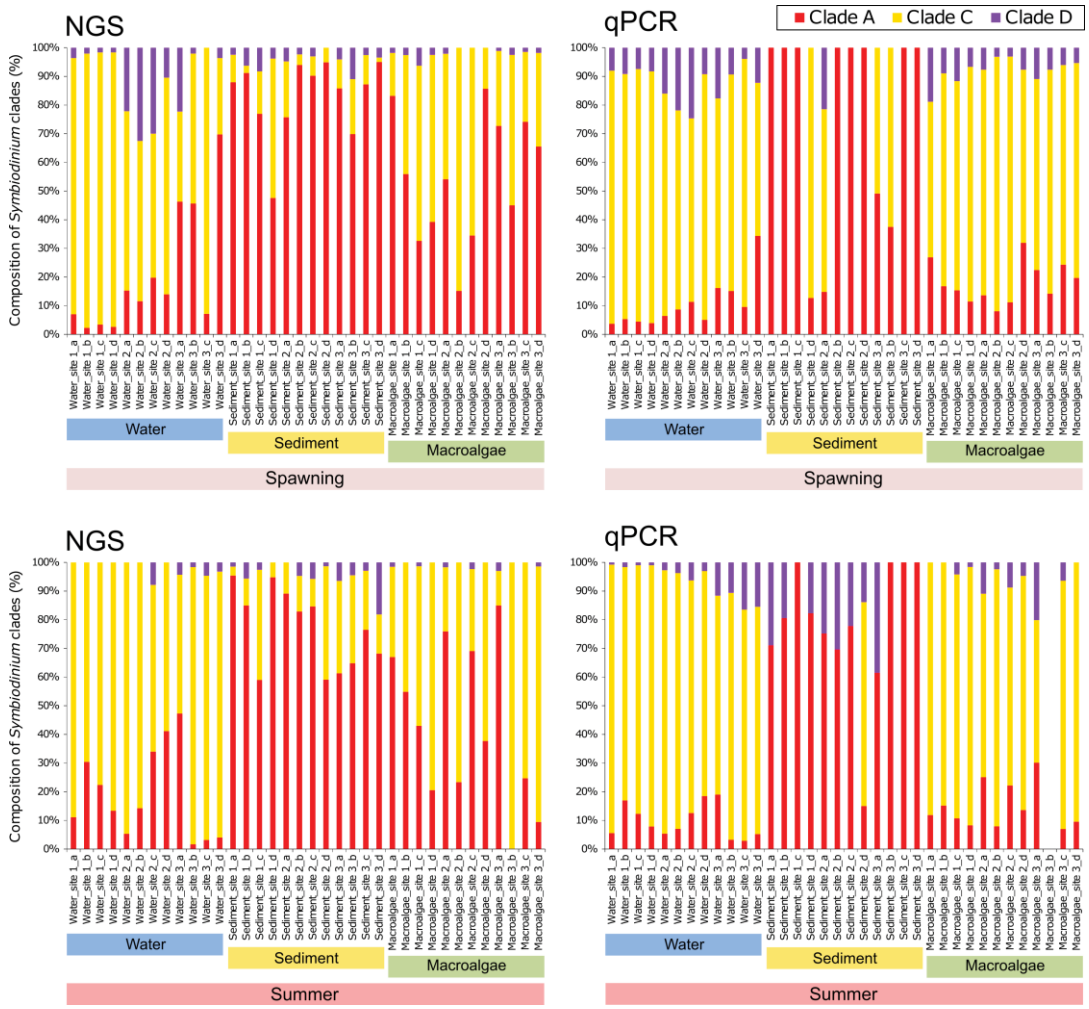

Figure 2.12. Relative abundance of *Symbiodinium* clades A, C and D during the spawning and summer seasons obtained by two techniques (NGS vs. qPCR). 36 samples per season per technique: 3 sites (coral species), 3 habitats (water, sediment and macroalgae), 4 replicates (a, b, c, d) for 2 seasons (spawning vs. summer) for 2 techniques (NGS vs. qPCR). Colour of bars for each clade are shown above the graphs.

2.5. Discussion

Free-living *Symbiodinium* are a required source of symbionts for corals (especially horizontally transmitting species) to establish new symbiotic relationships (e.g. Coffroth et al. 2006; Nitschke et al. 2016), to allow for population turnover and possibly enable corals to recover and/or resist stressors (e.g. Baker 2003; Boulotte et al. 2016). In spite of their importance to coral life history and how corals persist, the role of free-living *Symbiodinium* populations to overall life cycles remains a black box. In this study, we detailed the diversity, distribution and abundance of free-living *Symbiodinium* across environments (water, sediment and surface of macroalgae) in neighbouring sites (coral species) and seasons by integrating eDNA metabarcoding using next generation sequencing (NGS) and quantitative PCR (qPCR) for the first time.

2.5.1. High genetic diversity of free-living *Symbiodinium* are detected

Free-living *Symbiodinium* communities from Heron Island reef spanned eight clades (A-I, excluding clade E, which is primarily found in temperate waters; Chang 1983; Yamashita and Koike 2013; Jeong et al. 2014), across all environments. Such wide coverage of free-living *Symbiodinium* diversity is clearly a result of recent advances with eDNA metabarcoding using high throughput NGS to detect rare members of these communities (e.g. Arif et al. 2014, Thomas et al. 2014; Boulotte et al. 2016; Quigley et al. 2017).

We found that overall there were no significant differences of free-living *Symbiodinium* diversity between water, sediment and macroalgae habitats, or between the two key seasons (spawning vs. summer). This finding was supported at

all taxonomic levels (clade, ITS2 variant and OTU) and suggested highly stable *Symbiodinium* diversity over environmental space and time. Previous studies that explored free-living *Symbiodinium* diversity also support our finding (stable diversity across environments): Takabayashi et al. (2012) reported that four clades of *Symbiodinium* were detected in water (A-D) and sediment samples (A-C and G) from Hawai‘i using eDNA-cloning-sequencing technique; Yamashita et al. (2013) detected free-living *Symbiodinium* belonged to three clades (A, C and D) in both water and sediment samples from Okinawa, Japan using clade specific qPCR technique; and Cunning et al. (2015) detected five clades (A, C, D, F and G) of *Symbiodinium* in both water and sediment samples from American Samoa by DNA metabarcoding using NGS technique (also see Chapter 1, Table 1.3 for other studies). We postulate that environmental habitats possessing the high genetic diversity of *Symbiodinium* do so from the continuous expulsion of *Symbiodinium* from various symbiotic hosts harbouring a variety of *Symbiodinium* types (see Chapter 1, Table 1.2) (e.g. Pochon et al. 2014), as a mechanism for regulating symbiont density *in hospite* (post-mitotic process, see Chapter 1, section 1.5) (e.g. Jones and Yellowlees 1997; Dimond and Carrington 2008; Fujise et al. 2014). Indeed, sediment samples showed slightly higher cladal richness (but not significant) compared to water and macroalgae samples due to presence of clades H and I *Symbiodinium* only harboured by foraminifera (e.g. Pochon and Gates 2010; Kirk and Weis 2016). Foraminifera are mainly benthic and seem to contribute free-living *Symbiodinium* pools in the sediment (ultimately diversity of them), thus surrounding hosts diversity is an important factor for shaping the free-living pools amongst reef environments.

2.5.2. Niche separation of free-living *Symbiodinium* occurs across habitats

Community composition of *Symbiodinium* differed between sites (coral species), habitats and seasons, and the extent of dissimilarity differed with depth of taxonomic level (clade, ITS2 variant and OTU). Clade C dominated water and macroalgae habitats (as per coral hosts) whereas clade A dominated sediment, supporting previous reports that the dominant clade found in hosts reflects the abundance of those clades in surrounding waters (Manning and Gates 2008; Zhou et al. 2012; Sweet 2014; Granados-Cifuentes et al. 2015), and in neighbouring macroalgae (Porto et al. 2008; Venera-Ponton et al. 2010; Granados-Cifuentes et al. 2015). Furthermore, clade A is commonly found to be abundant in sediments (Coffroth et al. 2006; Hirose et al. 2008; Adams et al. 2009; Reimer et al. 2010; Takabayashi et al. 2012; Granados-Cifuentes et al. 2015; Quigley et al. 2017) and some types of clade A are considered exclusively free-living, i.e. not forming symbiosis over their entire life cycle (Yamashita and Koike 2013; Granados-Cifuentes et al. 2015). Yamashita and Koike (2013) reported that ITS2-type A2-relative *Symbiodinium* (closely related to *S. natans*) was the most abundant type isolated from water and sediment across Japan. In our study, A2-relative-like type (ITS2 variants A113 and A112) occurred at low levels in water samples compared to sediment and macroalgae where these ITS2 variants were most abundantly found. Therefore, we assume that sediment and macroalgae are likely more favourable habitats for exclusively free-living *Symbiodinium* compared to the water column.

2.5.3. Overlap of genetic types between *in hospite* and environments

The dominant ITS2 variants harboured in corals were C1085 (C3-like type), C15 and C42 or C1cstar (C1-like types) for *Acropora aspera*, *Montipora digitata* and

Pocillopora damicornis, respectively, and these associations are consistent with previous reports (e.g. LaJeunesse et al. 2003; Stat et al. 2009a; Fisher et al. 2012) and Coral Trait Database (https://coraltraits.org/, Madin et al. 2016) from Heron Island reef. These ITS2 variants were also abundant in environments across all habitats (water, sediment and macroalgae) for both seasons. Even though *M. digitata* and *P. damicornis* are vertically transmitting species, and thus *Symbiodinium* is maternally passed onto the next generation (Stat et al. 2008b), the fact that the dominant ITS2 variants *in hospite* were also found in relatively abundant in the environments (Fig. 2.7) is thought to be due to corals continuously expelling *Symbiodinium* into the surrounding environment to regulate the symbiont density *in hospite* (Jones and Yellowlees 1997; Dimond and Carrington 2008; Fujise et al. 2014).

A. aspera is a horizontally transmitting species (van Oppen et al. 2001; Suzuki et al. 2013) and it is known to acquire multiple types of symbionts from the surrounding environment at an early developmental stage (larvae/juvenile), notably across clades A-D (Gómez-Cabrera et al. 2008; Abrego et al. 2009; Adams et al. 2009; Cumbo et al. 2013; Yamashita et al. 2013; 2014; Quigley et al. 2017). Therefore, a broad free-living *Symbiodinium* pool of diversity is essential for selecting more beneficial types for survivorship and establishment of *Acropora* species (Gómez-Cabrera et al. 2008; Yamashita et al. 2013; 2014; Quigley et al. 2017). For example, in later developmental stages, three-dimensional shaped juveniles (approx. 2.5 years old), only harbour clade C *Symbiodinium*, with a detectable transition of dominant clade from clades A and D, which are adapted to wide range of environmental conditions (e.g. light and temperature) (Suggett et al. 2008; Stat and Gates 2011; Lesser et al. 2013; LaJeunesse et al. 2015), to clade C during developmental stages (Yamashita et

al. 2014). If indeed such a transition is essential to ensure maximum competitive fitness in establishing new adult colonies, then it is of course critical to understand the diversity of *Symbiodinium* inherently available to corals in any given environment.

Yamashita et al. (2014) reported that A1 type and D1 type were abundant in seven species of *Acropora* juveniles (two weeks after spawning) and Quigley et al. (2017) found A3 type was crucial for survivorship of juvenile *A. tenuis*. Indeed, we found A1-like types (A1, A110; closely related to *S. microadriaticum*), D1-like types (D1, D111), and A3-like type (A155; closely related to *S. tridacnidrum*) across all environmental habitats. Such overlapping of ITS2 variants was found not only in adult corals, but also in larvae/juvenile which suggests connectivity between symbiotic and free-living type (transiently free-living). There were no obvious trends in seasonality of free-living communities for A1-, A3-, C3- and D1-like types across environments (except for some combinations of ITS2 variants × habitats, see section 2.4.4.2 and Fig. 2.8) suggesting types potentially necessary for developing new symbioses with *A. aspera* larvae are always available in the environment.

It is possible to expect greater overlap between symbiotic and free-living genetic types in our study location in the south-west Pacific Ocean (Heron Island, southern GBR), where more horizontally transmitting species of corals are common (e.g. Baird 2009), as demonstrated (albeit at lower taxonomic resolution) from previous *Symbiodinium* studies (Venera-Ponton et al. 2010; Sweet 2014). Indeed, in our study, overlapping of symbiotic and free-living genetic types was observed at the OTU level, further supporting the connectivity of symbiotic versus free-living life stage of

Symbiodinium. A previous study has in fact reported limited overlap between common *Symbiodinium* types found *in hospite* relative to those found in adjacent reef water and sediment (Pochon et al. 2010); however, the authors highlighted that corals in the sampling area (Hawai‘i) were mainly composed of vertically transmitting coral species, and thus possibly explaining the limited overlap between *in hospite* and in the environment.

2.5.4. Macroalgae habitats are the main reservoir of symbionts in reefs

Abundances of free-living *Symbiodinium* belonging to clades A, C and D were obtained using qPCR with *Symbiodinium* clade-specific primer sets, and cell densities were found to be the highest for macroalgae samples compared to sediments and lowest overall in the water column. Few data exist on cell abundances of *Symbiodinium* across reef environments, and indeed those that do exist are likely to be highly variable due to the differences of (i) counting methods: Littman et al. (2008) used microscopy and FlowCAM; (ii) location: Yamashita et al. (2013) quantified free-living *Symbiodinium* cells in water in northwest Pacific (Okinawa, Japan) using the same qPCR primer sets used in this study; and (iii) source: Lin et al. (2017) evaluated the abundance of *Symbiodinium* in aquarium water using qPCR and clade-specific Taqman probes. Our results fall within the intermediate range of these observations. It is extremely difficult to distinguish *Symbiodinium* from other dinoflagellates based on morphology (Koike et al. 2007), thus it is possible that Littman et al. (2008) may have overestimated the number of *Symbiodinium* cells. Natural populations in water are likely to be less abundant compared to aquarium systems where flow (and dilution) rates (not mentioned in Lin et al. 2017) may differ. Due to the limited number of studies, the actual biomass of free-living *Symbiodinium*

which exist in reef environment remains unclear; however, the trend of *Symbiodinium* abundance between environments where more cells were found in sediment compared to water column showed agreement with Littman et al. (2008).

Symbiodinium cells tend to accumulate in the sediment because they are negatively buoyant (Howells et al. 2009), and our findings (and those of Littman et al. 2008) supports this notion that the abundance of *Symbiodinium* is higher in benthic habitats (sediment and macroalgae) compared to the water column. Indeed, we found the highest abundance of free-living *Symbiodinium* cells in macroalgae habitats (epiphytic organisms are known to live within a boundary layer on the surface of thallus; Wahl et al. 2016; Noisette and Hard 2018), in particular those belonging to clade C (based on qPCR), and also possessing the same ITS2 variants found in the host corals (based on NGS). Macroalgae are thought to be important habitats for dinoflagellates (Aligizaki and Nikolaidis 2006; Kim et al. 2011; Kohli et al. 2014b) including *Symbiodinium* (Porto et al. 2008; Venera-Ponton et al. 2010) because macroalgae provide inorganic nutrients (Khailov and Burlakova 1969; Grzebyk et al. 1994; Wada et al. 2007), a large habitat for attachment and settlement (Morton and Faust 1997; Parsons and Preskitt 2007), light attenuation and therefore offer a potential refuge (Porto et al. 2008). Therefore, macroalgae inevitably play an important role as source of symbionts, together with sediments.

No study exists to understand how the presence of macroalgae can improve the infection rate of *Symbiodinium* to prove macroalgae habitats actually play a role for providing symbiont sources for hosts. This is important to clarify because macroalgae may potentially provide an even larger reservoir of symbionts than

sediments, which has been confirmed to enhance uptake of *Symbiodinium* and considered as a key habitat of symbiont sources for corals (e.g. Adams et al. 2009; Nitschke et al. 2016). Still only few studies have included macroalgae as potential reservoirs for free-living *Symbiodinium* (Porto et al. 2008; Venera-Ponton et al. 2010; Yamashita and Koike 2013; Granados-Cifuentes et al. 2015). However, importantly, Porto et al. (2008) suggested herbivorous fishes (*Sparisoma virise*) which ingest the macroalgae, together with *Symbiodinium* living in the macroalgal bed, play an important role for a greater dispersal of *Symbiodinium*. Indeed, viable *Symbiodinium* cells have been found in their faeces. Castro-Sanguino and Sánchez (2012) further reported that 3.2-8.0 × 10^3 cells mL^{-1} of viable and culturable *Symbiodinium* cells found in the faeces of the fish. Therefore, it is also important to consider macroalgae not only as a free-living *Symbiodinium* reservoir, but also as a potential role for dispersal.

2.6. Conclusions

In conclusion, we found great diversity of free-living *Symbiodinium* across different environmental habitats (water, sediment and macroalgae) belonging to clades A-I, with the exception of clade E. Habitats surrounding corals and seasons clearly play a role in regulating free-living *Symbiodinium* diversity and community compositions, and in turn the pool of *Symbiodinium* available for uptake as transient symbionts during specific life stages. How transient these stages are may ultimately depend on how these cells can persist within the wider environment (see Suggett et al. 2017) which is examined in Chapter 3. Exclusively free-living types of *Symbiodinium* also exist and understanding their functional role and life history remains elusive. By integrating NGS-based genetic diversity and qPCR-based abundance approaches for

the first time, we highlight how important reef macroalgae habitats for harbouring free-living *Symbiodinium* communities, operating as reservoirs as well as potentially aiding broader dispersal through herbivores. Whether such patterns are consistent for other reef systems is largely unexplored, and applying such techniques to reef systems with very different benthic structure and environmental conditions will ultimately be required to unlock broader patterns of life history regulation. As such, the next focus for application of this dual NGS- and qPCR-based approaches is to examine another (but marginal) reef system within eastern Australia (Chapter 3).

2.7. Acknowledgements

The authors wish to thank all of the staff members in Heron Island Research Stations (The University of Queensland) for providing assistance for the samplings, all of the laboratory members in TrEnD Lab (Curtin University) for assistance of sample analysis, and Paul Brooks and Graeme Poleweski in Climate Change Cluster (University of Technology Sydney) for assistance of the sampling trips. LF was supported by Climate Change Cluster (University of Technology Sydney) and Yoshida Scholarship Foundation (Japan). DJS was supported through an ARC Discovery Grant (DP160100271). Corals and environmental samples (water, sediment and *Padina* sp.) were collected under the Great Barrier Reef Marine Park Authority permit G15/37538.1 issued to DS and LF and G15/37922.1 issued to MN.

Chapter 3

Diversity and distribution of free-living *Symbiodinium* in a high-latitude eastern Australian reef system during the 2015/2016 El Niño heat wave

This chapter is in preparation for submission, therefore the subject "we" is used here.

Lisa Fujise[1], Michael Stat[2], Michael Bunce[2], Stephanie Gardner[1], Samantha Goyen[1], Tim Kahlke[1], Matthew Nitschke[1, 3], Peter J. Ralph[1], Nahshon Siboni[1], Stephen Woodcock[1], David J. Suggett[1]

[1] Climate Change Cluster, University of Technology Sydney, Broadway, NSW 2007, Australia

[2] Trace and Environmental DNA (TrEnD) Laboratory, Curtin University, Bentley, Perth, WA 6102

[3] Center for Environmental and Marine Studies, University of Aveiro, 3810-193 Aveiro, Portugal

3.1. Abstract

Symbiodinium form an endosymbiosis with various marine invertebrates, but also exist as "free-living" cells. Availability of free-living *Symbiodinium* is essential for many coral species to persist over space and time through reproduction or recovery from environmental stressors. However, to date most knowledge of free-living *Symbiodinium* diversity, and how the free-living pool contributes to the establishment of symbiosis with surrounding hosts, has been largely based on studies from tropical reef and not from temperate coral communities. We therefore evaluated the diversity and distribution of free-living *Symbiodinium* in Sydney Harbour, which represents the southernmost coral community found along eastern Australia, over two seasons (summer 2015 vs. autumn 2016), the latter of which coincided with a mass heat wave induced bleaching event. Based on ITS2 DNA metabarcoding, we found 374 OTUs belonging to seven clades (A-G) spanning into 25 ITS2 variants from dominant coral hosts (hard coral: *Plesiastrea versipora* and soft coral: *Capnella gaboensis*) and surrounding environments (water, sediment and macroalgae). *Symbiodinium* community in water samples reflected the shifting abundance of coral hosts across sites. Interestingly, clade E (*Symbiodinium voratum*) considered a more temperate-specific species was found mainly in sediment and macroalgae during pre-bleaching and decreased frequency during the heat wave induced bleaching. We further compared this temperate *Symbiodinium* diversity with that found from the southern Great Barrier Reef. Intriguingly, *Symbiodinium* diversity *in hospite* was higher in temperate than tropical regions at the OTU level, but free-living *Symbiodinium* diversity was higher in tropical than temperate, presumably reflecting the decreasing diversity of symbiotic hosts from tropical to temperate reef systems. Only 1% of OTUs were shared between regions and geographical separation of

genetic types across this latitudinal gradient was apparent. We discuss these findings in light of suggestions that temperate reefs can operate as refugia for tropical corals as waters continue to warm due to climate change.

3.2. Introduction

Dinoflagellate microalgae of the genus *Symbiodinium* form symbioses with many marine invertebrates (Stat et al. 2006; Davy et al. 2012; Pochon et al. 2014), but commonly reside as "free-living" cells as part of their complex life history (e.g. Carlos et al. 1999; Pochon et al. 2010; Takabayashi et al. 2012; Yamashita and Koike 2013; Granados-Cifuentes et al. 2015; Cunning et al. 2015). Free-living *Symbiodinium* populations are an essential source for invertebrate hosts to establish a new symbiosis (e.g. Coffroth et al. 2006; Nitschke et al. 2016), in particular where these hosts propagate new generations horizontally and aposymbiotic planulae must acquire their algal symbionts from the surrounding environment (Trench 1987; Hartmann et al. 2017). Free-living *Symbiodinium* populations are thus fundamentally important to long-term stability of ecosystems (and notably coral reefs), but their underlying biodiversity and ecology, and how they contribute for shaping the flexibility and resilience of host-symbiont holobionts as reef ecosystems are still poorly understood.

Symbiodinium are genetically diverse and divided into nine distinct monophyletic groups (clades A-I) and hundreds of types and/or species (Pochon and Gates 2010; LaJeunesse et al. 2012a; Pochon et al. 2014; LaJeunesse 2017; Thornhill et al. 2017). Within this phylogenetic diversity, *Symbiodinium* are also highly functionally diverse (Suggett et al. 2015; Warner and Suggett 2016; Goyen et al. 2017; Suggett et al.

2017). For example, some *Symbiodinium* are generalists, forming symbiosis with a wide range of host species (e.g. ITS2-types C1 and C3; LaJeunesse 2004), whilst others are specialists, forming symbiosis with specific hosts (e.g. C15; LaJeunesse 2004) or existing as "exclusively" free-living cells (e.g. ITS2-type A2: *Symbiodinium pilosum* (Trench and Blank 1987) and A2-relative: *S. natans* (Hansen and Daugbjerg 2009); LaJeunesse 2002; Yamashita and Koike 2013; Nitschke et al. 2015, and clade E: *S. voratum* (Jeong et al. 2014); Chang 1983; Yamashita and Koike 2013). However, the underlying biology governing whether *Symbiodinium* types are generalists or specialists is still largely unknown. A key step towards answering this unknown is to reconcile the community composition of *Symbiodinium in hospite* with that in the surrounding environment (free-living) to begin resolving the broad-scale availability of types and connectivity between symbiotic and free-living phases of *Symbiodinium*'s life cycle.

All *Symbiodinium* clades (A-I) have been found free-living in various reef environments, notably the water column, sediment and in association with macroalgae (e.g. Pochon et al. 2014; Cunning et al. 2015; Quigley et al. 2017; Chapter 2). Not surprisingly, almost all studies of free-living *Symbiodinium* communities to date are from tropical coral reef environments where symbiotic host diversity and abundance are the highest (e.g. Veron 1993; Harriott and Banks 2002). Relatively few studies have examined high-latitude temperate waters for free-living *Symbiodinium*. Chang (1983) discovered free-living *Symbiodinium* (clade E) from water in West land, New Zealand (41°S) by establishing culture strains. Jeong et al. (2014) also isolated clade E *Symbiodinium* from water in Jeju Island, Korea (33°N). Furthermore, Yamashita and Koike (2013) detected free-living *Symbiodinium* (clades

A and E) from water and sediment in Kochi (33°N) and Tsushima Island (35°N), Japan by establishing culture strains and using molecular-based environmental DNA techniques. Beyond revealing the relatively common abundance of clade E (*S. voratum*) in temperate waters, we almost entirely lack knowledge of inherent diversity and abundance of free-living *Symbiodinium* in high-latitude temperate coral communities. Resolving this gap in knowledge is particularly relevant and timely given growing interest in high-latitude temperate reef systems as potential hot spots for coral reef studies (e.g. Schleyer and Celliers 2003; Halfar et al. 2005; Beger et al. 2014; Descombes et al. 2015).

High-latitude reef systems exist at the latitudinal margins for coral growth and consequently have become intensive areas of study to understand how reef-forming corals tolerate suboptimum/extreme environmental conditions (e.g. Guinotte et al. 2003; Perry and Larcombe 2003; Putnam and Gates 2015; Morgan et al. 2016). Cold water reef habitats are increasingly experiencing "tropicalisation" (Nakamura et al. 2013; Vergés et al. 2014; Tuckett et al. 2017) and thus are also considered potential refugia for tropical corals as waters continue to warm (Halfar et al. 2005; Beger et al. 2014; Descombes et al. 2015; Cacciapaglia and Woesik 2015; Morgan et al. 2017). Expansion of tropical coral species to high-latitude habitats due to increasing water temperature has already been observed in Florida (Precht and Aronson 2004), Japan (Yamano et al. 2011) and eastern Australia (Baird et al. 2012).

Australian coral distributions span a range from the Great Barrier Reef into the subtropical Solitary Islands (30°S) and Lord Howe Islands (31°S) that are the most southern coral reef systems in the world (Zann 2000; Harriott and Banks 2002).

Corals are further dispersed southwards towards more temperate waters such as Sydney Harbour (33°S) (Rodriguez-Lanetty et al. 2001; Madsen et al. 2014). Two species of scleractinian corals particularly dominate these most southerly temperate extremes: *Plesiastrea versipora* (Lamarck 1816), considered a cosmopolitan species found widely in Indo-Pacific and along the east Australian coastline (Veron 1986; Rodriguez-Lanetty et al. 2001; Wallace et al. 2009; Madsen et al. 2014); and *Coscinaraea mcneilli* (Wells 1962), considered a temperate-specialist species (Veron 2000; Silverstein et al. 2011). Soft coral species that associate with *Symbiodinium* are also found widely within Sydney Harbour surrounds, such as the temperate specialist, *Capnella gaboensis* (Verseveldt 1977) (Farrant 1986; 1987; Farrant et al. 1987). However, still little is known about the ecology of these corals and ecosystem functioning in what might be considered a marginal environment for scleractinian corals.

Corals within tropical and sub-tropical regions (e.g. LaJeunesse et al. 2003; 2004) as well as high-latitude temperate regions (Wicks et al. 2010; Silverstein et al. 2011; Lien et al. 2012) of the Indo-Pacific Ocean mainly harbour clade C *Symbiodinium*. However, at the ITS2-type level (e.g. distinct species), types of clade C appear temperate-specific (Wicks et al. 2010; Silverstein et al. 2011; Lien et al. 2012). In addition, clade B types (ITS2-types B18 and B40), which are thought to be cold-water specialists, have only been observed from temperate regions across the west coast of Australia (Silverstein et al. 2011), further supporting the idea that *Symbiodinium* types may be organised along a distinct latitudinal gradient. However, how such a pattern reflects the corresponding availability of environmental pool of *Symbiodinium* (free-living) is entirely unexplored.

For this study, we therefore focused on characterising the diversity and distribution of free-living *Symbiodinium* populations in Sydney Harbour (temperate region) for the first time. We specifically applied DNA metabarcoding using next generation sequencing (NGS) technique to resolve community level biodiversity within complex ecosystem matrices (Cristesu 2014), an approach still not widely applied to examine free-living *Symbiodinium* diversity (Cunning et al. 2015; Quigley et al. 2017; Chapter 2). We also applied qPCR (as per Chapter 2) to quantify free-living *Symbiodinium* cell abundance across environmental habitats (water, sediment, macroalgae) using clade-specific primer sets (Yamashita et al. 2011). In doing so, this study provides the first ever baseline for community composition of *Symbiodinium* in high-latitude temperate reefs. We further compared our NGS free-living *Symbiodinium* diversity data from temperate reefs with those from northern tropical reefs (results obtained from Chapter 2) to examine the degree of potential niche overlap for key *Symbiodinium* types and also temperate-specific types that could characterise the free-living *Symbiodinium* community composition in marginal environments. Our study period contrasted two seasons (summer 2015 vs. autumn 2016), which in the latter case coincided with a major heat wave induced coral bleaching event along the east coast of Australia (e.g. Hughes et al. 2017), but also Sydney Harbour where ca. 60% of all hard corals paled or bleached (Goyen et al. in prep). Importantly, no information exists for free-living *Symbiodinium* diversity (availability) during bleaching events, in spite of the key role this community may play in aiding coral recovering from bleaching (Coffroth et al. 2006; Baker et al. 2008; Boulotte et al. 2016).

3.3. Materials and methods

3.3.1. Transect analysis

Three sites were selected for this study (Fig. 3.1): two sites in Sydney Harbour, NSW, Australia; site 1: Cobblers beach, Middle Head (33.49°S, 151.15°E), site 2: Fairlight, Manly (33.48°S, 151.16°E), and one site outside of Sydney Harbour, site 3: Bare Island, Botany Bay (33.59°S, 151.13°E). Video transects were conducted to characterise abundances of hard corals (*Plesiastrea versipora* and *Coscinaraea mcneilli*) and soft coral (*Capnella gaboensis*). Parallel video transects were conducted at both Sydney Harbour sites: site 1 (50 m length at depths 2-6 m (n = 4)) and site 2 (30 m length at depths 3-7 m (n = 4)). Two adjacent 50 m length video transects were recorded for site 3 (at depths 5-10 m). Because of the narrow site and corals on shelves, we were only able to run two transects at site 3. Transect tapes followed the site contours and video recording was performed ~30 cm above the substrate. Hard corals at these sites typically form high density communities generally restricted to beds within each site, therefore transects were targeted to include these hard coral beds while also characterising the surrounding habitat. Video transects were analysed following a continuous line intercept method to calculate percentage cover of hard and soft corals at each site (Leujak and Ormond 2007).

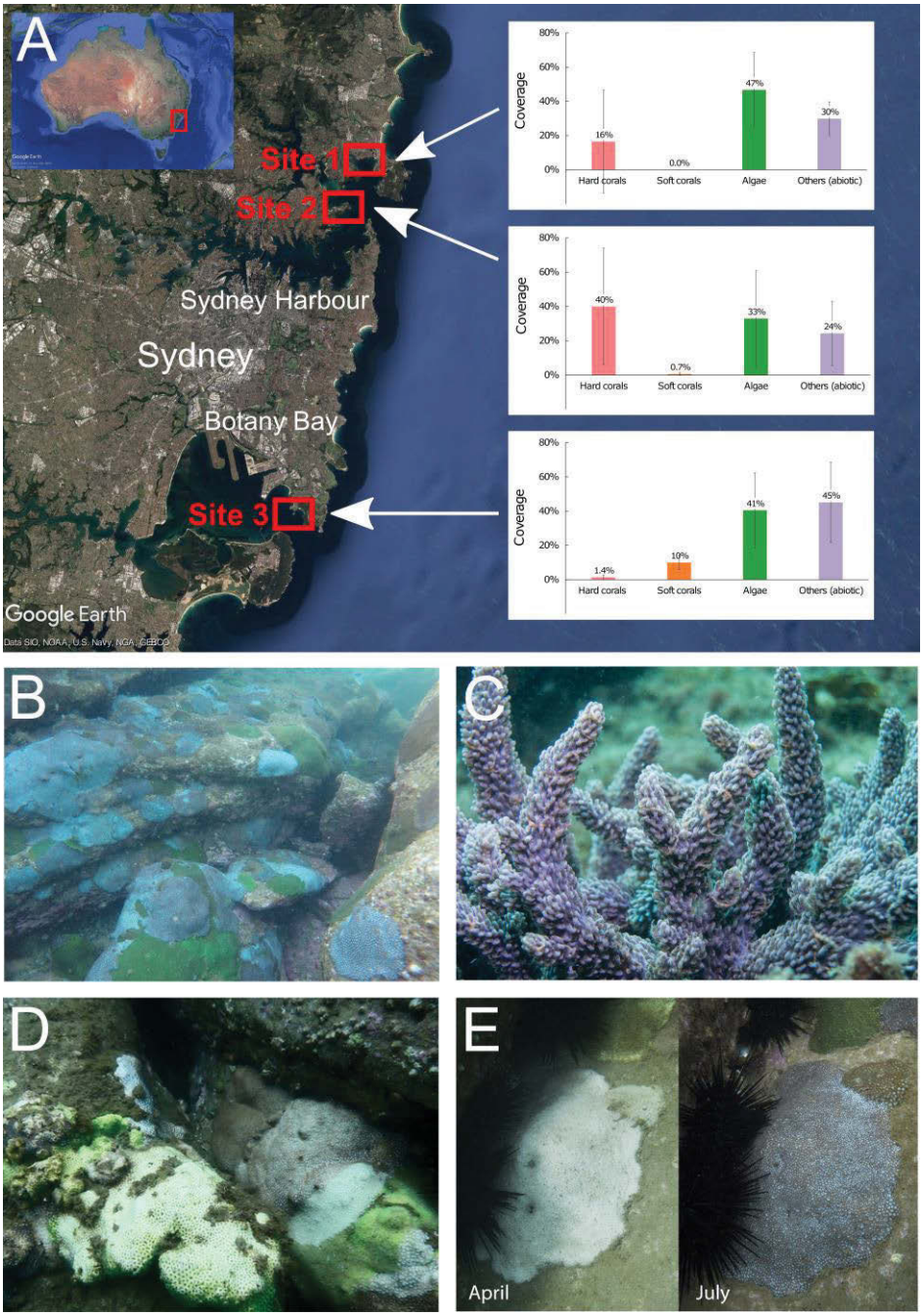

Figure 3.1. Location of sampling sites and host species. **A.** Location of sampling sites in Sydney Harbour (sites 1 and 2) and Botany Bay (site 3) together with host benthic coverage bar graphs. Benthic coverage of hard corals (*Plesiastrea versipora* and *Coscinaraea mcneilli*): pink bars, soft coral (*Capnella gaboensis*): orange bars, algae: green bars, and others (abiotic substrates): purple bars, were obtained by video transects. Mean percentage of coverages are shown above each bar and error bars indicate SD. Collected host species: **B.** *P. versipora* (hard coral) and **C.** *C. gaboensis* (soft coral). **D.** Bleached *P. versipora*. **E.** Tagged *P. versipora* during the bleaching (April 2016) and the recovery (July 2016).

3.3.2. Hosts and environmental samples collection

Sampling was conducted at three sites in summer (December) 2015, referred to hereafter as "pre-bleaching", and late autumn (May) 2016, referred to as "bleaching". Scleractinian coral *P. versipora* (n = 4 from individual colonies per site and season) and soft coral *C. gaboensis* (n = 4 from individual colonies per site and season, except for site 1 in May 2016 where samples could not be collected) were sampled as reference host samples to characterise *Symbiodinium* diversity *in hospite*. These species were selected because they represent the dominant taxa for hard corals and soft corals, respectively, for all tested sites. Small fragments (ca. 2 cm) of coral samples were rinsed with 0.2-µm filtered seawater and then stored at -80°C until further molecular analysis.

Environmental samples from seawater, sediment and macroalgae (each n = 4 per site and season) were collected to evaluate free-living *Symbiodinium* community diversity in the same manner as shown in Chapter 2 (see section 2.3.1). Briefly, 10 L of seawater were collected, passed through a 20-µm nylon filter (NITEX®, SEFAR, Heiden, Switzerland) to remove large particles, concentrated using gentle vacuum onto a 3-µm polycarbonate filter (Isopore™, EMD Millipore, MA, USA), and resuspended particles captured on the 3-µm polycarbonate filter with 0.2-µm filtered seawater. The suspension was concentrated down by centrifugation and stored at -80°C until further molecular analysis. The surface layer (~1 cm) of sediment (volume of 25 mL) was scooped into a sterile 50-mL sterile centrifuge tube from the substrate near to the host colony (ca. 1 m). Finally, ~40 g of *Ecklonia radiata* was collected into a sterile sample bag for macroalgae-associated *Symbiodinium* analysis since this species is a common and dominant macroalgae across all sites. Both

sediment and macroalgae samples were re-suspended in 1 L of 0.2-µm filtered seawater and shaken vigorously 50 times to remove surface-attached *Symbiodinium*. Each suspension was passed in series through 250, 125, 75-µm stacked sieves, a 20-µm nylon filter to remove large particles and then a 3-µm polycarbonate filter to capture particles containing *Symbiodinium* cells. Samples were then processed and stored as per the seawater samples described above.

3.3.3. Environmental data

To contrast the environmental conditions between seasons, sea surface temperature (SST, monthly averages, °C), photosynthetically active radiation (PAR, daily averages, µmol photons m^{-2} s^{-1}) and attenuation coefficient (K_d, daily averages, m^{-1}) in Sydney Harbour (including both sites 1 and 2) and Botany Bay (site 3) for 2-year data set from January 2015 to December 2016 (including both sampling periods, December 2015 and May 2016) were retrieved from satellite (in 4 km spatial resolution) (https://oceandata.sci.gsfc.nasa.gov/). Monthly averaged PAR values (µmol photons m^{-2} s^{-1}) at specific depth where corals mainly exist were calculated using equations 1-4. First, refraction of light was calculated using equation 1,

$$\frac{\text{Monthly averaged PAR}}{1.33} \quad [1]$$

where refractive index = 1.33 was used (Suggett et al. 2001). Then reflection of light was calculated and accounted for PAR penetration of water using equation 2,

$$\text{Refraction} - (\text{Refraction} \times 0.08) \quad [2]$$

where 0.08 is a ratio for scalar irradiance to the downwelling irradiance (Lee et al. 2005). Next, K_{d490}/K_{dPAR} was calculated using equation 3,

$$K_{d490} \times \left(\frac{0.36}{0.2}\right) \quad [3]$$

based on Hennige et al. (2010). Finally, PAR at each depth was calculated using equation 4 with the reflection (equation 2) and K_{d490}/K_{dPAR} (equation 3),

$$\text{Reflection} \times \text{Exp}\,(-(K_{d490}/K_{dPAR}) \times \text{depth}) \quad [4]$$

modified Suggett et al. (2001) and PAR at depths 5, 6 and 7 m were calculated according to the equations above and averaged for three depths to account for PAR at depth where corals mainly exist.

A coral bleaching event of Sydney Harbour was observed from April to June 2016 (Goyen et al. in prep), therefore SST values were also retrieved for the previous 10 years (2007-2016) to aid in the identification of thermal anomalies. Thermal anomalies (°C) for each month from January 2015 to December 2016 were calculated using equation 5,

Monthly averaged SST – Mean for 10 years (2007-2016) monthly averaged SST [5]

3.3.4. *Symbiodinium* genetic diversity using next generation sequencing

Sample preparation and processing for DNA metabarcoding of host and environmental samples were performed in the same manner described in Chapter 2 (see section 2.3.3). Briefly, total genomic DNA was extracted from both host and environmental samples (half of the collected samples were used) using the DNeasy Blood & Tissue Kit (QIAGEN, Hilden, Germany) and amplification of target DNA using qPCR (Applied Biosystems StepOnePlus Real-Time PCR, Applied Biosystems, CA, USA) was performed with the nuclear ribosomal DNA ITS2 primer set, as per Chapter 2 (section 2.3.3) for identifying *Symbiodinium* diversity, but also alongside a cp23S-HVR primer set: 23SHYPERUP (5′-TCAGTACAAATAATATGCTG-3′; Santos et al. 2003b) and 23HYPERDN (5′-TTATCGCCCCAATTAAACAGT-3′;

Manning and Gates 2008) that targets the hypervariable region of the chloroplast ribosomal DNA. Although, the cp23S-HVR provides less taxonomic resolution compared to the ITS2 or cp23S-Domain V (Pochon et al. 2010; Takabayashi et al. 2012); this primer set is highly specific for *Symbiodinium* and can discriminate *Symbiodinium* amongst a mixed community within environmental samples, whereas the ITS2 primer sets also amplify other dinoflagellates (Manning and Gates 2008; Pochon et al. 2010) (note, 26% of the total sequences obtained by ITS2 primer set belonged to *Symbiodinium* in Chapter 2). Thus, two genetic markers were used in this study to compare the diversity and community compositions at cladal level (we used the cp23S-HVR marker as a clade level marker; referred to hereafter as "cp23S") and also provide more sequence information from temperate regions where *Symbiodinium* sequence libraries are still scarce compared to those from tropical regions.

Detailed protocols for the amplification of target DNA with fusion tag primers using qPCR are described in Chapter 2 (section 2.3.3, including qPCR conditions for the ITS2 primer set). For the cp23S primer set, following qPCR conditions were used: 95°C for 5 min, followed by 37-40 cycles (for endosymbiont samples) or 45 cycles (for environmental samples) of 30 sec at 95°C, 30 sec at 50°C, and 45 sec at 72°C, and a final extension at 72°C for 10 min. The amplicon library for sequencing was prepared as per Chapter 2 (section 2.3.3) and sequenced using a 500 cycle MiSeq® v2 Reagent Kit and standard flow cell (2 × 250 paired end) for the ITS2 primer set and a 300 cycles MiSeq® v2 Reagent Kit and nano flow cell (325 single end) for the cp23S primer set on an Illumina MiSeq platform (Illumina, CA, USA). Low-read samples (ca. < 42,000 reads per sample for ITS2 and < 5000 reads per sample for

cp23S after demultiplexing) were re-sequenced using the same extracted and amplified DNA and the obtained sequences were pooled together with the original run sequences for further analysis.

3.3.5. Bioinformatic analysis

The detailed pipeline including tools used for the bioinformatic analysis for MiSeq sequences can be found in the following links:

Paired end (ITS2) (Kahlke and Fujise 2017): https://doi.org/10.17605/osf.io/hcsp4

Single end (cp23S): https://github.com/timkahlke/ampli-tools

3.3.5.1. ITS2 (paired end)

Bioinformatic analysis for ITS2 paired end sequences were performed all together with tropical (Heron Island; Chapter 2) and temperate (Sydney Harbour; this chapter) samples for comparability of genetic diversity between the two regions. The detailed protocols for these are provided in Chapter 2 (see section 2.3.4). The low read samples (< 20 reads per sample) were removed from the dataset for the further analysis.

3.3.5.2. Cp23S (single end)

Demultiplexing and removal of Illumina adaptor (P7), primers and single end dual barcodes sequences from cp23S libraries was performed with *demultiplex.py* (Kahlke 2018b) according to the following criteria: Illumina adaptor P7 (0 mismatches), forward and reverse primers (0 mismatches), forward and reverse barcodes (0 mismatches). Sequences were then filtered and discarded using *trim.seq* in MOTHUR ver. 1.38.1 (Schloss et al. 2009) if they did not meet the following

criteria: sequence length ≥ 90 bp, homopolymers ≤ 5 bp, ambiguous bases = 0 bp, and average quality score ≥ 25. The quality filtering criteria were determined according to the summary of sequences obtained by *summary.seq* in MOTHUR. All identical sequences were subsequently collapsed (unique sequence) and singletons were removed using *derep_full* in vsearch ver. 2.3.2 (Rognes et al. 2016). For Operational Taxonomic Units (OTU) based analysis, unique sequences were clustered at 97% similarity cut-off (Thomas et al. 2014) by *cluster_fast* in vsearch. Chimera sequences were removed by *uchime_ref* in vsearch. OTU taxonomies were assigned to their corresponding cp23S type (clade level) using BLAST against the custom *Symbiodinium* cp23S database by *assign_taxonomy.py* in QIIME v.1.9.1 (Caporaso et al. 2010) and OTU table was created using *usearch_global* in vsearch. Sequences in OTUs which were observed in the negative controls were subtracted from all samples. OTU abundance filtering at 1% threshold within each sample was also applied for cp23S dataset to minimise noise (e.g. sequencing errors and PCR artifacts) and ensure relevant and robust conclusions for assessing *Symbiodinium* diversity and community composition as per Appendix: Culture OTU analysis.

3.3.6. qPCR for quantitative analysis of free-living *Symbiodinium*

We further quantified free-living *Symbiodinium* in each environmental habitat (water, sediment, macroalgae), using qPCR via 28S rDNA clade-specific primer sets (clades A-F; Yamashita et al. 2011) according to the same protocol as Chapter 2 (section 2.3.5), but including clade E primer sets for qPCR assay, since clade E *Symbiodinium* was present in the temperate Sydney Harbour samples (confirmed by NGS, see results section). Briefly, extracted DNA from environmental samples for sequencing (described above, section 3.3.4) were used as template DNA in qPCR assay for six

primer sets (clades A-F) using one culture strain from each clade (Table 3.1, also see Chapter 2, Table 2.1 for the identity and origin of the culture strains) as quantification standards. 5 μL reaction per sample was made with triplicate (shown contents of qPCR reaction in Chapter 2, section 2.3.5) and 0.25 ng μL^{-1} of DNA extracted from environmental samples was used as template DNA.

Table 3.1. *Symbiodinium* culture strains used as quantitative standards for qPCR assays for assessing abundance of free-living *Symbiodinium*. One culture strain from each clade was selected for use as a quantitative standard for qPCR assay for each primer set (clades A-F). Number of cells per qPCR reaction (5 μL) used for making calibration curves (five concentrations) and minimum detection limits are shown.

Clade/ ITS2-type		Identity	Standard	Standard 10^{-1}	Standard 10^{-2}	Standard 10^{-3}	Standard 10^{-4}	Detection limit
			cells reaction^{-1}					
A	A1	CCMP2464, RT61	808	80.8	8.08	0.808	0.0808	0.0808
B	B1	CCMP2460, RT2	982	98.2	9.82	0.982	0.0982	0.982
C	C2	RT203	812	81.2	8.12	0.812	0.0812	0.812
D	D1a	CCMP3408	594	59.4	5.94	0.594	0.0594	0.594
E	-	CCMP421	816	81.6	8.16	0.816	0.0816	0.816
F	F1	UTS-C	442	44.2	4.42	0.442	0.0442	0.442

In addition, DNA extraction efficiency was tested across samples from different substrates; water, sediment and macroalgae to be able to compare the cell numbers between the habitats. Aliquots of known cell number of clade D *Symbiodinium* (CCMP3408) culture strain (ca. 72 cells per reaction) were added to samples collected from three different substrates and DNA was extracted. Note clade D *Symbiodinium* was not detected in the environment by NGS based on the cp23S marker, but detected based on the ITS2 marker with low composition (see results section: 3.4.7.1). However, no amplification was achieved for environmental samples by qPCR assay using clade D primer set within the detection range (threshold cell

density of 0.59 cells per reaction), therefore clade D was chosen as internal standard to check DNA extraction efficiency and PCR inhibition. Also, DNA from an identical volume of aliquot from culture strains was extracted for use as standard. qPCR assay was performed using clade D primer sets and Ct values were compared with the standard to calculate extraction efficiency (efficiency: 102% and 101% for water and macroalgae, respectively, but no amplification with any tested dilution for the sediment samples).

3.3.7. Statistical analysis

Our sampling design yielded 4 replicates each of 3 sites × 5 habitats (hard coral, soft coral, water, sediment, macroalgae) × 2 seasons (pre-bleaching, bleaching). Based on the number of clades, ITS2 variants and OTUs in each sample, differences in richness between habitats and seasons (for all sites pooled together) were tested using the Kruskal-Wallis test with Bonferroni pairwise comparison *post-hoc* tests using SPSS Statistics 23 (IBM, Armonk, NY) ($P < 0.05$) ($n = 12$ for each habitat and season). We performed subsampling with 2,000 sequences per samples to compare richness with the same sequence depth. However, richness patterns between habitats/seasons followed the pattern as for the original number of sequences (without subsampling). As such, to include as many sequences as possible especially for low-read samples, we therefore performed the statistical analysis without subsampling sequences. To visualise the overlap of genetic types (ITS2 variants and OTUs) belong to clades A and B between symbiotic (in hard and soft corals) and environments (water, sediment, macroalgae pooled together), Venn diagrams were created for each site and season combination using *eulerr* package in R (http://jolars.co/). To compare the *Symbiodinium* community compositions, relative

abundances of the *Symbiodinium* clades, ITS2 variants and OTUs were square-root transformed and compared between each sample using the Bray-Curtis similarity coefficient. Non-metric multi-dimensional scaling (nMDS) ordination diagrams were produced and CLUSTER analysis was performed using group averages to visualise the relationship of *Symbiodinium* community composition between sites, habitats and seasons. A permutational ANOVA (PERMANOVA) was used to test for significant differences in *Symbiodinium* taxonomic compositions (clade, ITS2 variant and OTU) with sites (3 levels), habitats (5 levels) and seasons (2 levels) as fixed factors, using type III sum of squares and the unrestricted permutation of raw data method with 999 permutations. A *post-hoc* pairwise comparison test among all pairs of factors of 'site × habitat × season' was used to identify where significant differences occurred. Similarity percentage (SIMPER) analysis was performed to identify which taxa were the most important in driving the patterns of similarity between samples.

In addition, to compare *Symbiodinium* cladal compositions obtained using the two different amplicons (cp23S vs. ITS2), relative abundances of the *Symbiodinium* clades were square-root transformed and PERMANOVA was performed with same setting as described above for each amplicon data set with the forth factor as amplicon (2 levels). A *post-hoc* pairwise comparison test among all pairs of levels of 'amplicon × site × habitat × season' factor was used to identify where significant differences occurred in the amplicon factor. All multivariate analyses described above were performed using PRIMER (version 6.1.16) and PERMANOVA+ (version 1.0.6) software. To visualise the different abundance of ITS2 variants between sites, habitats and seasons, a heat map was created using *gplots* package in R.

3.4. Results

3.4.1. Hard coral and soft coral coverage

Hard coral and soft coral coverages for each site are shown in Fig. 3.1. Hard corals (*Plesiastrea versipora* and *Coscinaraea mcneilli*) predominated at 4-6 m at site 1 and 5-7 m at sites 2 and 3, whereby benthic cover was highest at site 2 (40 ± 34%, mean coverage across all depth ± SD) followed by site 1 (16 ± 30%) and lowest at site 3 (1.4 ± 1.4%). Benthic coverage for soft corals (*Capnella gaboensis*) was higher than for hard corals for site 3 (10 ± 4.2%), but lower for site 2 (0.66 ± 0.78%) and soft corals were not found close to coral beds at site 1. Thus, relative abundance of hard corals was higher than soft corals at sites 1 and 2, and soft corals were more abundant at site 3.

3.4.2. SST and PAR in Sydney Harbour and Botany Bay (2015-2016)

To assess the environmental conditions that regulate *Symbiodinium* physiology and fitness between hosts, water temperature and light intensity from the depths where coral beds predominated (5-7 m) were compared between seasons (Fig. 3.2). Monthly averaged SST during pre-bleaching sampling period in summer season (December 2015) was 23.3°C and 22.4°C for Sydney Harbour (sites 1-2) and Botany Bay (site 3), respectively, and preceded the highest monthly SST in January (24.6°C and 23.8°C, for sites 1-2 and 3, respectively) (Fig. 3.2A, 3.2B). In contrast, SST dropped by 3.5°C and 5.0°C, respectively during bleaching in late autumn season (May 2016), to 20°C and 17°C, respectively. Monthly averaged PAR also followed the trend as seen in SST, which was highest during pre-bleaching (454 and 392 μmol photons m^{-2} s^{-1}, mean PAR at depths 5-7 m, for sites 1-2 and 3, respectively) and lowest during bleaching (63 and 48 μmol photons m^{-2} s^{-1}, respectively).

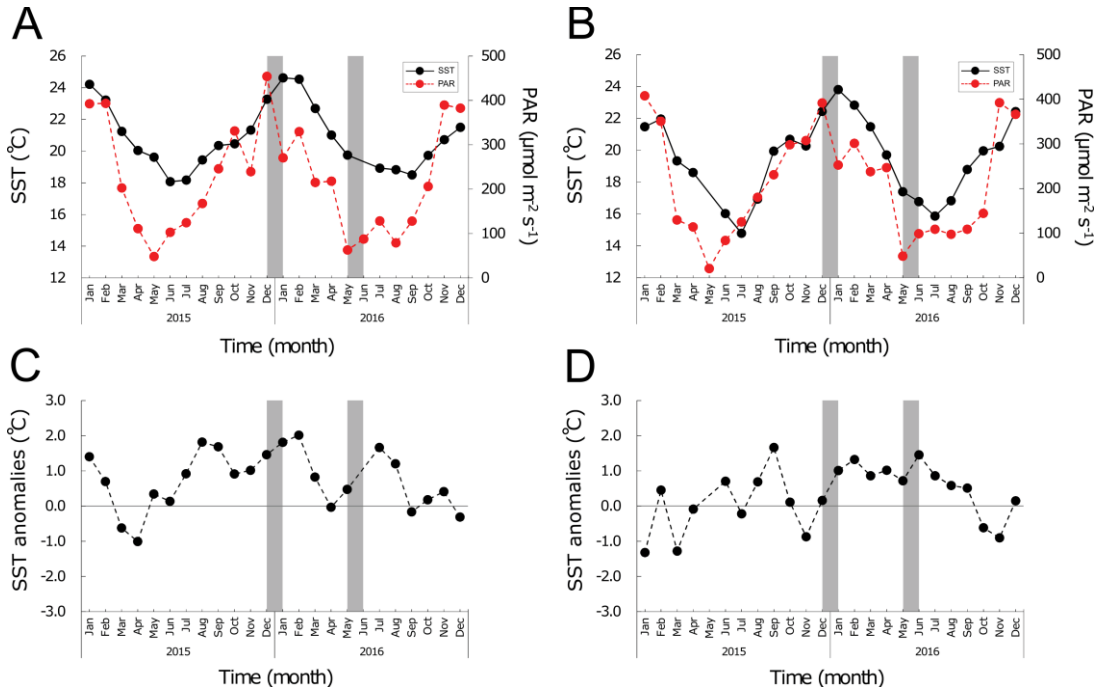

Figure 3.2. Environmental data in Sydney Harbour (sites 1 and 2) and Botany Bay (site 3). Monthly averaged sea surface temperature (SST, °C) are shown as black solid lines (left Y axis) and monthly averaged photosynthetic active radiation (PAR, µmol photons m^{-2} s^{-1}) are shown as red dashed lines (right Y axis) from January 2015 to December 2016 for **A.** Sydney Harbour and **B.** Botany Bay. SST thermal anomalies from past 10-year (2007-2016) are shown as black dashed lines for **C.** Sydney Harbour and **D.** Botany Bay. Samplings were performed in December 2015 (pre-bleaching) and May 2016 (bleaching) and indicated by the grey areas.

The mass coral bleaching event was observed during a prolonged heat wave in summer 2015/2016, which triggered severe coral bleaching in the northern and central GBR (Hughes et al. 2017). Indeed, SST thermal anomalies (how monthly averaged SST for 2015-2016 differed from monthly averaged SST of the past 10 years: 2007-2016) were positive for 18 months in Sydney Harbour throughout 2015-2016 (Fig. 3.2C) and 16 months in Botany Bay (Fig. 3.2D). In Sydney Harbour, sites 1 and 2, positive thermal anomalies were detected constantly from May 2015 to

March 2016 (0.13-2.0°C) and > 1.5°C during the summer season in 2015/2016 (1.5°C, 1.8°C, and 2.0°C higher than 10 years average SST in December 2015, January, February 2016, respectively). Botany Bay showed the similar trend with positive thermal anomalies continued from December 2015 to August 2016 (0.16-1.5°C) with slightly less anomalies during the summer season (0.16°C, 1.0°C, 1.3°C, respectively) compared to Sydney Harbour sites.

3.4.3. Diversity of *in hospite* and free-living *Symbiodinium* using next generation sequencing: cp23S

We first show the results obtained based on the cp23S primer set (clade level marker), followed by the ITS2 primer set (type/species level marker) in order to systematically evaluate genetic diversity and community composition from lower to higher taxonomic resolution (see Chapter 2 for further details, section 2.4.2).

The cp23S marker was initially used to screen clade level diversity of *Symbiodinium* both *in hospite* and free-living (as per Chapter 2, OTUs were combined for the same clade for the cladal level assessment). A total of 1,192,102 sequences were obtained from 109 samples (4 replicates × 3 sites × 5 habitats × 2 sampling time points = 120 samples, but no *C. gaboensis* samples were collected at site 1 during bleaching, no amplification or no sequences for sediment × 5, macroalgae × 2 samples) after demultiplexing and quality filtering (Table S3.1, also see Fig. 3.3 for the box plots). A total of 54 OTUs were obtained and assigned across clades A-C, E and F. All sequences recovered from the cp23S marker assigned to *Symbiodinium* (except for 97 sequences in 1 OTU which did not match anything in the *Symbiodinium* cp23S database nor GenBank: http://www.ncbi.nlm.nih.gov) demonstrating the high

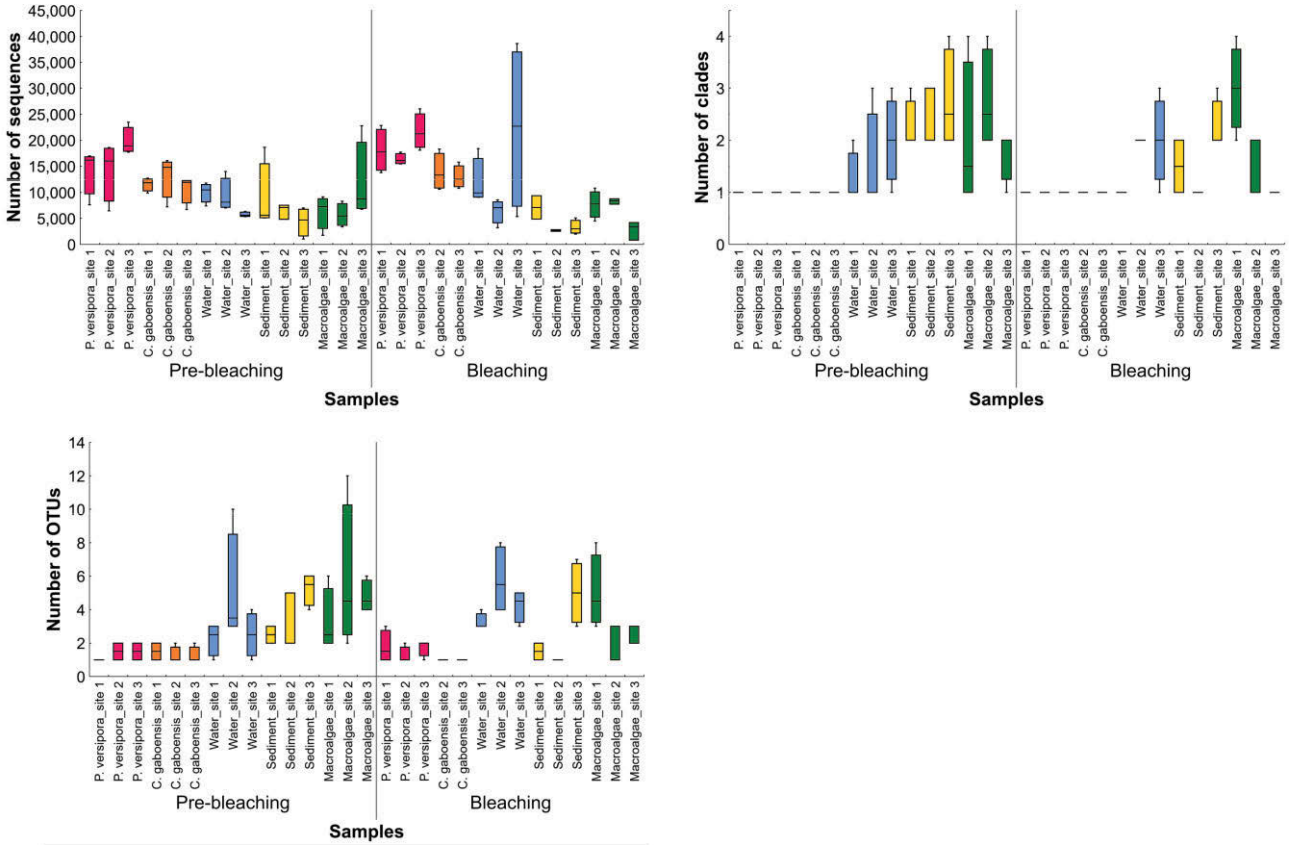

Figure 3.3. Box plots for number of sequences, clades and OTUs based on the cp23S marker in each site, habitat and sampling time. Box plots for *P. versipora* (hard coral) are shown as pink, *C. gaboensis* (soft coral) as orange, water as blue, sediment as yellow and macroalgae as green.

specificity of this primer set in detecting *Symbiodinium* from mixed dinoflagellate communities (e.g. Manning and Gates 2008; Pochon et al. 2010). Overall, cladal and OTU richness of *Symbiodinium* followed a similar pattern whereby (i) the number of clades and OTUs were higher for sediment and macroalgae samples than for hosts during the pre-bleaching period, (ii) richness did not differ between different environmental habitats (water vs. sediment vs. macroalgae) and (iii) richness did not differ between sampling time points (pre-bleaching vs. bleaching for each habitat).

Sediment and macroalgae samples contained significantly higher number (richness) of *Symbiodinium* clades (2.5 ± 0.7 and 2.2 ± 1.0 clades, respectively, mean across all sites for pre-bleaching ± SD) than hosts, *P. versipora* or *C. gaboensis* (both of the hosts harboured only one clade of *Symbiodinium* across all sites and sampling time points) for pre-bleaching (Kruskal-Wallis test, $P < 0.05$, also see Table S3.2 for summary of Kruskal-Wallis test), but not during bleaching ($P > 0.05$) due to decrease (but not significant) of the cladal richness (1.8 ± 0.7, 1.9 ± 1.1 clades in sediment and macroalgae samples, respectively). Although, water samples showed slightly less cladal richness of *Symbiodinium* (1.6 ± 0.7 clades, mean across all sites for both sampling time points ± SD) compared to sediment and macroalgae samples, there were no significant differences detected across environments (water vs. sediment vs. macroalgae) ($P > 0.05$ for all combinations, see Table S3.2B for pairwise comparison). In addition, diversity of *Symbiodinium* was stable over time ($P > 0.05$ for pre-bleaching vs. bleaching in each habitat) as well as over space (habitat).

OTU richness for *Symbiodinium* followed the same pattern as observed at the cladal level: (i) higher number of OTUs in sediment and macroalgae samples (3.6 ± 1.6,

4.6 ± 2.7 OTUs, respectively, mean across all sites for pre-bleaching ± SD) than within hosts (1.3 ± 0.49 OTUs for both *P. versipora* and *C. gaboensis*) for pre-bleaching (Kruskal-Wallis test, $P < 0.05$ for all combinations, see Table S3.2); (ii) *Symbiodinium* diversity was stable across different environments ($P > 0.05$) and for the two sampling time points in each habitat ($P > 0.05$). However, significantly higher OTUs were observed for water samples (4.4 ± 1.6 OTUs, mean across all sites for bleaching ± SD) compared to those in both hosts (1.6 ± 0.7, 1.0 ± 0.0 OTUs for *P. versipora* and *C. gaboensis*, respectively), and also associated with macroalgae (3.5 ± 1.9 OTUs) compared to *C. gaboensis* during bleaching ($P = 0.0031$, $P = 8.9 \times 10^{-5}$, $P = 0.017$ for water vs. *P. versipora*, water vs. *C. gaboensis*, macroalgae vs. *C. gaboensis*, respectively), which was not detected at the cladal level.

3.4.4. Diversity of *in hospite* and free-living *Symbiodinium* using next generation sequencing: ITS2

Based on the ITS2 marker (types/species level marker), the 105 samples (no amplification or no/low read sequences for water × 1, sediment × 7, macroalgae × 3 samples) yielded 2,923,654 sequences after demultiplexing, quality filtering and removing non-*Symbiodinium* sequences (29% of total sequences belonged to *Symbiodinium*). A total of 374 OTUs were obtained and assigned across clades A-G into 25 ITS2 variants (as per Chapter 2, OTUs were combined for the same clade and same ITS2 variant for the cladal and ITS2 variant level assessment. Each ITS2 sequence in the reference database SymTyper term as "ITS2 variant"). Clades D and G were detected using the ITS2 marker, which were not by the cp23S marker. Numbers of sequences, clades, ITS2 variants and OTUs per each site, habitats and sampling times are shown in Fig. 3.4 as box plots and Table S3.3 as a list.

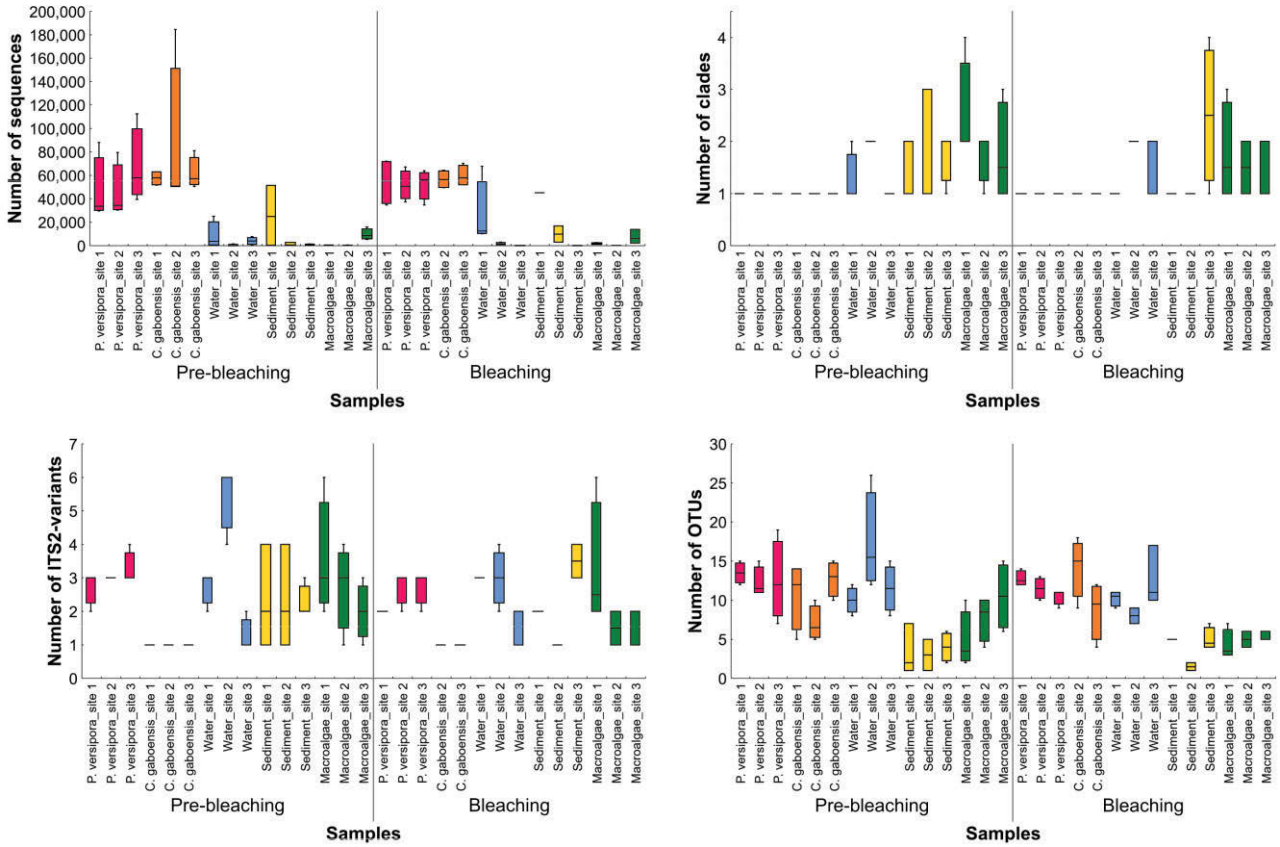

Figure 3.4. Box plots for number of sequences, clades, ITS2 variants and OTUs based on the ITS2 marker in each site, habitat and season. Box plots for *P. versipora* (hard coral) are shown as pink, *C. gaboensis* (soft coral) as orange, water as blue, sediment as yellow and macroalgae as green.

Consistent with the results obtained by the cp23S marker, number of clades (richness) observed for the various environments (water: 1.4 ± 0.51, sediment: 1.8 ± 0.90, macroalgae:1.8 ± 0.81 clades, mean across all sites for both sampling time points ± SD) was not statistically different to each other for both sampling times (Kruskal-Wallis test, $P > 0.05$, see Table S3.4 for summary of Kruskal-Wallis test). Furthermore, *Symbiodinium* diversity remained unchanged across the sampling time points in each habitat ($P > 0.05$, see Table S3.4B for pairwise comparison). Whilst cladal richness for *Symbiodinium* associated with macroalgae during the pre-bleaching period (2.0 ± 0.85 clades, mean across all sites for pre-bleaching ± SD) only showed significant difference between hosts of hard and soft corals, which both only harboured one clade of *Symbiodinium* ($P = 0.0031$ for macroalgae vs. *P. versipora* and $P = 0.0031$ for macroalgae vs. *C. gaboensis*).

As with the cladal richness, there was no significant difference in ITS2 variant richness found across any combinations of environments, nor within or between the two sampling time points (Kruskal-Wallis test, $P > 0.05$ for all combinations, see Table S3.4B). *Symbiodinium* ITS2 variant richness was not significantly different between *P. versipora* (2.8 ± 0.5 ITS2 variants, mean across all sites for both sampling times ± SD) and surrounding environments (water: 2.9 ± 1.5, sediment: 2.4 ± 1.1, macroalgae: 2.5 ± 1.4 ITS2 variants) across sampling times (Kruskal-Wallis test, $P > 0.05$). However, *C. gaboensis* only harboured one ITS2 variant across sites and sampling time points, thus the ITS2 variant richness was significantly lower compared to those in *P. versipora* for both sampling time point ($P = 6.8 \times 10^{-5}$, $P = 0.050$ for bleaching and pre-bleaching, respectively), and in water and macroalgae samples for pre-bleaching (3.2 ± 1.0 and 2.8 ± 1.4 ITS2 variants, respectively) ($P =$

0.0033 and $P = 0.0069$, respectively).

A relatively large number of OTUs were detected in water samples compared to sediment and macroalgae samples (water: 12 ± 4.2, sediment: 3.7 ± 2.0, macroalgae: 6.4 ± 3.5 OTUs, mean across all sites for both sampling times ± SD). However, differences were only significant between water and sediment during the pre-bleaching period (Kruskal-Wallis test, $P = 2.4 \times 10^{-4}$, see S3.4B for other combination) and thus free-living diversity generally remained stable across environments, as observed at the cladal and ITS2 variant level. Furthermore, no significant difference of OTU richness was observed between pre-bleaching and bleaching in each habitat ($P > 0.05$). OTU richness of *Symbiodinium* for *P. versipora* (12 ± 2.3 OTUs) was higher than for sediment at both sampling time points and macroalgae during bleaching (Kruskal-Wallis test, $P = 3.5 \times 10^{-5}$, $P = 0.0079$, $P = 0.0084$, respectively). *Symbiodinium* OTU richness for *C. gaboensis* (11 ± 4.0 OTUs) was significantly higher than for sediment samples during pre-bleaching only ($P = 0.021$).

To summarise, *Symbiodinium* richness between hosts and environmental samples was different and this was consistent based on both amplicons: cp23S (cladal level marker) and ITS2 (type/species level marker), and also with different depth of resolution for genetic diversity (i.e. resolution of taxonomy as clade, ITS2 variant or OTU level). Firstly, at the cladal level, environmental samples (sediment and macroalgae based on cp23S, and macroalgae based on ITS2) exhibited higher richness compared to *P. versipora* and *C. gaboensis* during the pre-bleaching period. OTU level for the cp23S marker and ITS2 variant level for the ITS2 marker also

followed this trend. However, the opposite relationship between *in hospite* and free-living *Symbiodinium* richness was detected at finer scales. Specifically, OTU-level based on the ITS2 marker showed similar or higher richness of *Symbiodinium in hospite* compared to within the environments (especially sediment and macroalgae). These findings suggest that inter-cladal diversity was higher in the environments, whereas intra-cladal diversity was higher in the hosts, but not resolved by ITS2 variant level (possibly due to scare reference ITS2 sequences for temperate *Symbiodinium* types). In addition, stability of *Symbiodinium* diversity across space (i.e. different environments: water vs. sediment vs. macroalgae) and two sampling time points (pre-bleaching vs. bleaching) in each habitat were consistently observed by both amplicons.

3.4.5. Connectivity of *Symbiodinium* genetic types *in hospite* and in environments based on the ITS2 marker

To next evaluate the putative connectivity of *Symbiodinium* genetic types between hosts (*P. versipora* and *C. gaboensis*) and environments (water, sediment and macroalgae), overlap of ITS2 variants and OTUs (based on the ITS2 marker) were examined for clades B and A, since these clades dominated in *P. versipora* and *C. gaboensis*, respectively (Fig. 3.5). The majority of ITS2 variants were shared between *P. versipora* and the environments at site 1 (100% and 67%, during pre-bleaching and bleaching, respectively) and site 2 (60% and 75%) whilst the shared percentage were the lowest at site 3 (40% and 40%). All ITS2 variants found in *P. versipora* were also detected in the environments for site 1 (both sampling times) and site 2 (during bleaching), but for only 50% of those were found in the environments at site 3 (both sampling times). Sites 1 and 2 had the higher relative

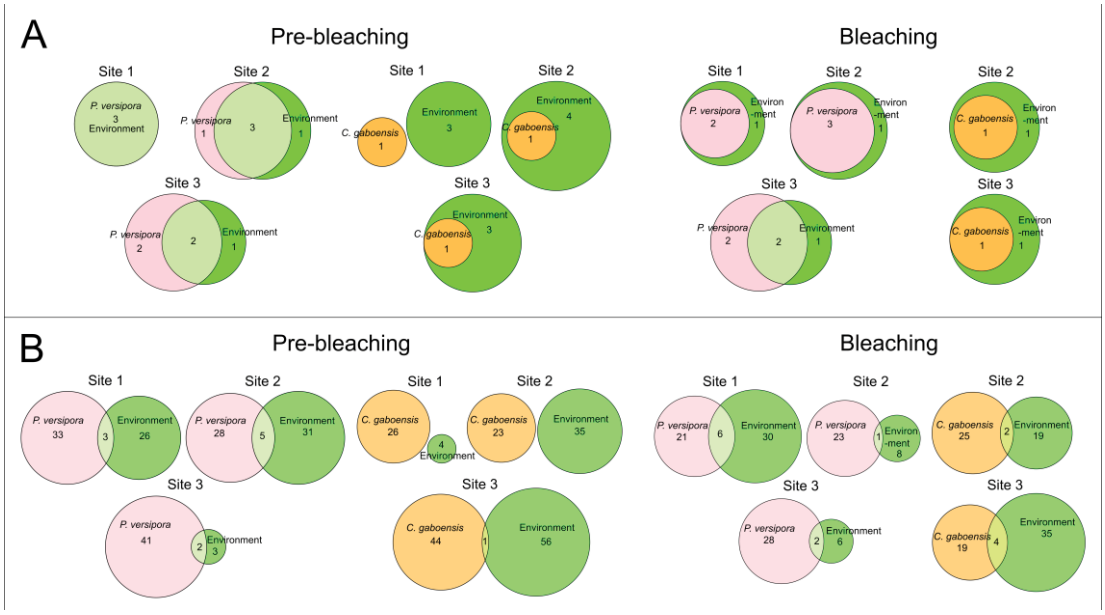

Figure 3.5. Venn diagrams for *in hospite* (*P. versipora* and *C. gaboensis*) and free-living types in environment. Number of **A.** ITS2 variants. **B.** OTUs. Number of *Symbiodinium* ITS2 variants or OTUs in *P. versipora* are shown with pink circles, *C. gaboensis* with orange circles and in environment (sum of water, sediment and macroalgae samples) with green circles for each site and sampling time (pre-bleaching vs. bleaching).

abundance of *P. versipora* compared to site 3 (see section 3.4.1 and Fig. 3.1A), which relates to the higher overlap of symbiotic and free-living genetic types at sites 1 and 2 than site 3. In addition, *P. versipora* at sites 1 and 2 were heavily impacted by the heat wave and bleached severely, whereas site 3 did not exhibit bleaching (Samantha Goyen, University of Technology Sydney, personal communication); which possibly explain why all symbiotic types were found in the environments during bleaching at sites 1 and 2, but not at site 3. Overall, 25% and 20% of all ITS2 variants were shared between *C. gaboensis* (clade A) and the surrounding environments at sites 3 and 2, respectively, compared to none of the ITS2 variant was shared at site 1 during the pre-bleaching period (Fig. 3.5A). This is consistent with

changes in relative abundance of soft corals across sites (site 3 > site 2 > site 1) (see section 3.4.1 and Fig. 3.1A) suggesting that the dominant types within abundant hosts reflect the overall richness of *Symbiodinium* genetic types within surrounding environments. In addition, all ITS2 variants found in *C. gaboensis* were also found in the environments in sites 2 and 3 for both sampling times. Thus, connectivity between ITS2 variants in hosts and environments was apparent and more overlap of genetic types were detected where the host harbouring those types were more abundant.

Less overlap was observed between *in hospite* and environments for OTUs than compared to ITS2 variants (Fig. 3.5B); 3.1-11% and 0.0-6.9% for *P. versipora* and *C. gaboensis*, respectively, across sampling time points. Even so, the trends observed for OTU overlap were generally consistent with those for ITS2 variant (above, Fig. 3.5A) for both hosts with greater overlap where relative abundance of either host was higher; *P. versipora*: site 2 (7.8%) > site 1 (4.8%) > site 3 (4.3%) and *C. gaboensis*: site 3 (0.99%) > sites 1 and 2 (0%) during pre-bleaching. 8.3%, 15% and 4.7% of OTUs found in *P. versipora* at sites 1, 2 and 3, respectively, were also found in the environments during pre-bleaching and increased during bleaching at sites 1 and 3 only (22%, 4.2% and 6.7%, respectively). In contrast, 0%, 0% and 2.2% of OTUs found in *C. gaboensis* at sites 1, 2 and 3, respectively, were detected in environments during pre-bleaching, increasing at sites 2 and 3 (7.4%, 17%, respectively) during bleaching. Again, connectivity between hosts and environment were observed in the OTU level, and abundance of host types influences the degree of connectivity.

3.4.6. *Symbiodinium* community composition between sites, habitats and sampling times: cp23S

We next examined the community composition of *Symbiodinium* found *in hospite* and in the environments following the same format as for the diversity of *Symbiodinium* in the previous section.

3.4.6.1. Cladal composition

Five clades (A-C, E and F) were found based on cp23S DNA metabarcoding, and numbers of sequences and OTUs in each clade are shown in Table 3.2. Clade B (707,977 sequences, 59% of the total sequences) was the most abundant clade followed by clade A (427,507 sequences, 36%) based on the cp23S marker, because these two clades were harboured by *P. versipora* (clade B, 100% of the total sequences in *P. versipora*) and *C. gaboensis* (clade A, 100% of the total sequences in *C. gaboensis*) (Fig. 3.6). Clade B was also the most dominant clade found in the environments (55% of the total environmental sequences) followed by clades A (34%), F (4.9%), E (3.3%) and C (2.6%). *Symbiodinium* cladal compositions were significantly different between sites (PERMANOVA, $P = 0.001$, see Table S3.5A for main effects) and habitats ($P = 0.001$), and also between hosts and environments (see Appendix E3.1 for pairwise comparison). However, the dominant clade found in water samples closely reflected the clades in the surrounding hosts at each site (Fig. 3.6); relative abundance of *P. versipora* (harboured clade B) was higher than *C. gaboensis* (clade A) at sites 1 and 2 (see Fig. 3.1A) where clade B dominated in the water samples, in contrast, *C. gaboensis* was more abundant than *P. versipora* at site 3 where clade A dominated in water. nMDS plot (Fig 3.7A) also showed this pattern visually and the dissimilarity of community compositions in the water samples was

Table 3.2. Number of sequences and OTUs belong to clades A-C, E and F based on the cp23S marker.

Clade	Number of sequences	Number of OTUs
A	427,507	19
B	707,977	18
C	13,568	2
E	17,216	2
F	25,737	12
No hit	97	1
Total	1,192,102	54

driven by clades A and B as vectors which shows MDS pattern tendencies (community composition correlation with MDS axes). Clades C, E and F were mainly found in sediment and macroalgae samples (Fig. 3.6) and these clades drove the dissimilarity of the community compositions across environments, which was also supported by SIMPER analysis (Table S3.6). Due to large variation of community compositions between replicates in the sediment and macroalgae samples, dissimilarity was not statistically significant for most of the combinations amongst environments ($P < 0.05$ for 4 out of 18 combinations, see Appendix E3.1 for pairwise comparison). That said, statistical analysis did not identify significant differences between sampling times (pre-bleaching vs. bleaching, $P = 0.15$); however, clade E (*S. voratum*, thought to be a cold water adapted temperate specialist; Jeong et al. 2014) was only detected in the pre-bleaching samples (Fig. 3.6).

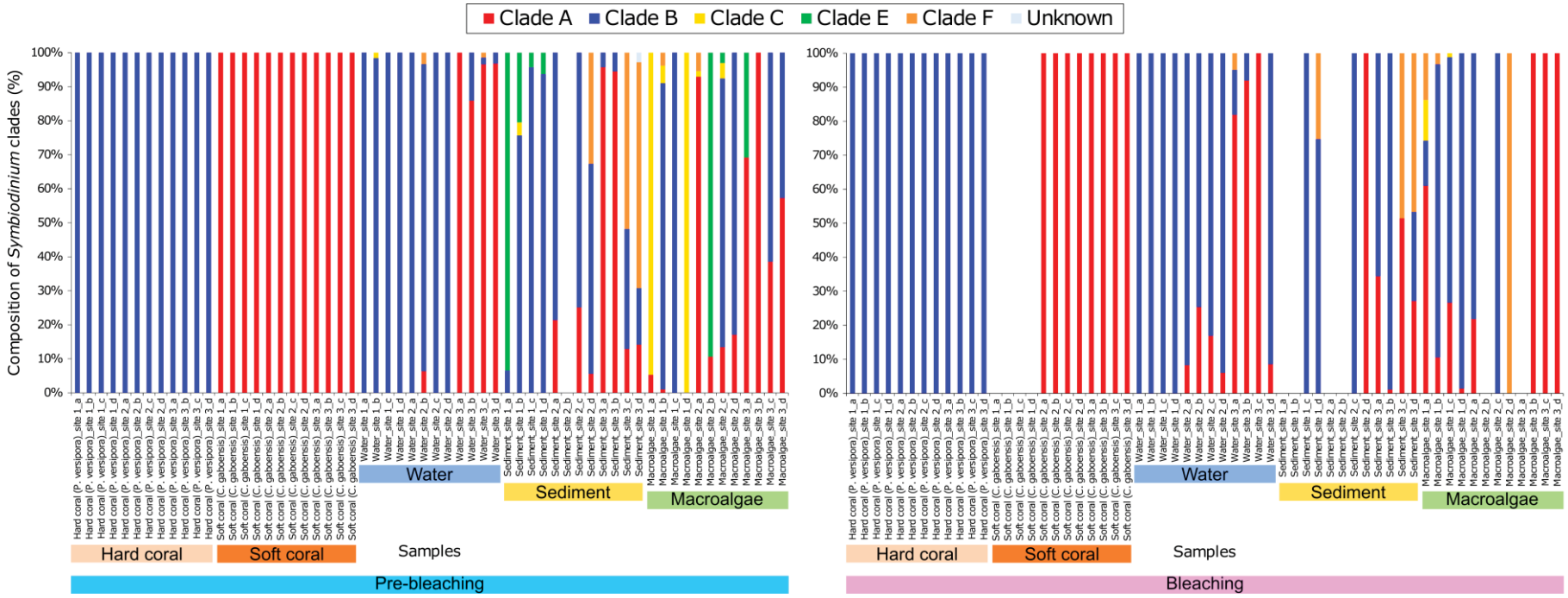

Figure 3.6. Relative abundance of *Symbiodinium* clades during pre-bleaching and bleaching obtained by DNA metabarcoding based on the cp23S marker. 3 sites × 5 habitats (hard coral: *P. versipora*, soft coral: *C. gaboensis*, water, sediment and macroalgae) × 4 replicates (a, b, c, d) for 2 sampling time points (pre-bleaching vs. bleaching). Note that no *C. gaboensis* samples were collected at site 1 during bleaching, and no bars in sediment and macroalgae samples were due to no amplification/no sequences. Colour of bars for each clade are shown above the graphs.

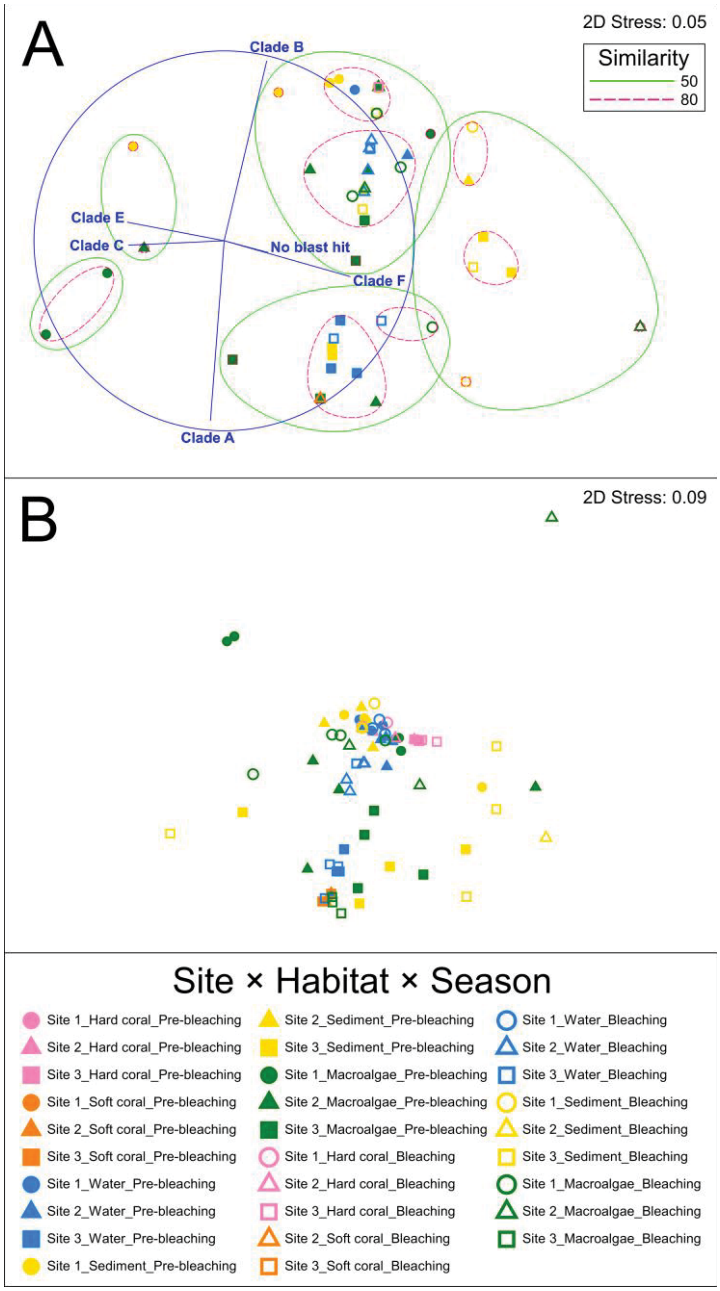

Figure 3.7. nMDS plots of *Symbiodinium* community compositions based on the cp23S marker. **A.** Clade. **B.** OTU. Non-metric multidimensional scaling (nMDS) was performed on each variable per variant using Bray-Curtis Similarity. CLUSTER analysis was performed for cladal composition (**A**); similarity is shown at the 50% (green solid lines), 80% (pink dashed lines) levels and vectors driving the clustering are shown as blue lines. Hard corals are represented by pink, soft coral by orange, water by blue, sediment by yellow, and macroalgae by green with site 1 with circle, site 2 with rectangle, and site 3 with square markers. Plots for pre-bleaching samples are shown with closed markers and bleaching samples with open markers (all combinations of the markers are shown below the graphs).

3.4.6.2. OTUs composition

A total of 54 OTUs across clades A (19 OTUs), B (18), C (2), E (2) and F (12) were obtained (Table 3.2). Patterns retrieved across sites, habitats and sampling times (Fig. 3.7B) generally reflected those retrieved from cladal compositions (Fig. 3.7A); specifically, *Symbiodinium* community compositions significantly different between sites (PERMANOVA, $P = 0.001$, see Table S3.5B for main effects) and relative abundance of hosts play an important role for differentiate OTU compositions in water samples as defined by sites. In addition, habitats partitioned the community composition ($P = 0.001$) between hosts and environments ($P < 0.05$ for 23 out of 33 combinations, see Appendix E3.2 for pairwise comparison) and significant differences across environment was detected in OTU level ($P < 0.05$ for 10 out of 18 combinations). Again, statistical analysis did not identify significant differences of community composition of *Symbiodinium* between pre-bleaching and bleaching ($P = 0.28$ for season effect).

3.4.7. *Symbiodinium* community composition between sites, habitats and sampling times: ITS2

3.4.7.1. Cladal composition

Seven clades (A-G) were found based upon ITS2 DNA metabarcoding, and numbers of sequences, ITS2 variants and OTUs in each clade are shown in Table 3.3. Clades A and B were the most abundant (1,363,958 and 1,511,630 sequences for clades A and B, respectively) and diverse (195 and 161 OTUs, respectively) found based on the ITS2 marker, because these clades were harboured by hosts; *C. gaboensis* (clade A, 100% of the total sequences in *C. gaboensis*) and *P. versipora* (clade B, 100% of the total sequences in *P. versipora*) (Fig. 3.8), and consistent with cp23S. Clade B

Table 3.3. Number of sequences, ITS2 variants and OTUs belong to clades A-G based on the ITS2 marker.

Clade	Number of sequences	Number of ITS2 variants	Number of OTUs
A	1,363,958	7	195
B	1,511,630	6	161
C	1,025	5	6
D	4,541	2	2
E	22,452	3	7
F	20,042	1	2
G	6	1	1
Total	2,923,654	25	374

was the most dominant clade found in environments (65% of all environmental sequences) followed by clades A (23%), E (5.9%), F (5.3%), D (1.2%), C (0.27%) and G (0.0016%). Trends found in *Symbiodinium* cladal community compositions between sites, habitats and sampling times by the ITS2 marker (Fig. 3.9A) agreed well with those found based on the cp23S marker (Fig. 3.7A); specifically, (i) site differentiated the community compositions significantly (PERMANOVA, $P = 0.001$, see Table S3.7A for main effects and Appendix E3.3 for pairwise comparison). Cladal composition in water samples reflected the relative abundance of host types in pre-bleaching time: sites 1 and 2: *P. versipora* > *C. gaboensis*, clades B > A in water, and sites 3: *P. versipora* < *C. gaboensis*, clades B < A in water (Fig. 3.8), and SIMPER analysis also showed the contribution of these two clades between sites (Table S3.8). Intriguingly, the relative abundance of clade A increased in the water samples during bleaching at site 2. (ii) Habitats also partitioned the community compositions (PERMANOVA, $P = 0.001$, see Table S3.7A for main effects) mainly between hosts and environments, but not across the environments ($P > 0.05$ for all combinations, except water vs. macroalgae at site 1 during pre-bleaching where this

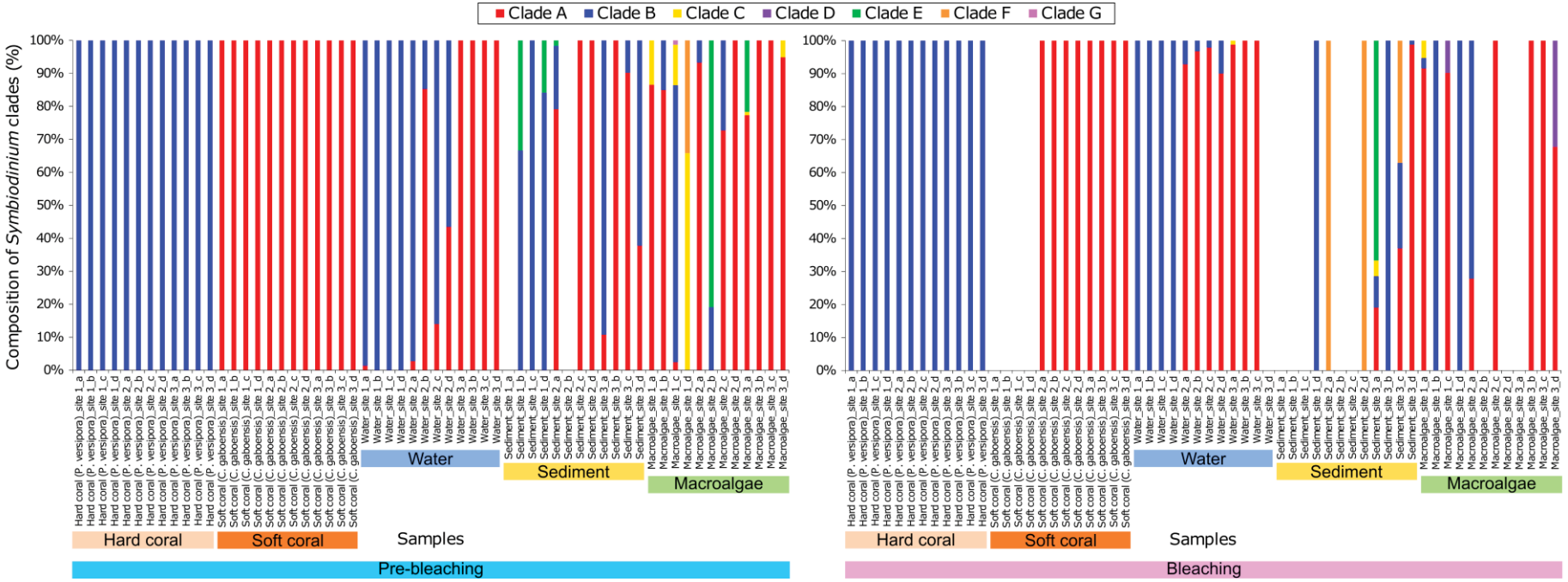

Figure 3.8. Relative abundance of *Symbiodinium* clades during pre-bleaching and bleaching obtained by DNA metabarcoding based on the ITS2 marker. 3 sites × 5 habitats (hard coral: *P. versipora*, soft coral: *C. gaboensis*, water, sediment and macroalgae) × 4 replicates (a, b, c, d) for 2 sampling time points (pre-bleaching vs. bleaching). Note that no *C. gaboensis* samples were collected at site 1 during bleaching, and no bars in water, sediment and macroalgae samples were due to no amplification/no sequences. Colour of bars for each clade are shown above the graphs.

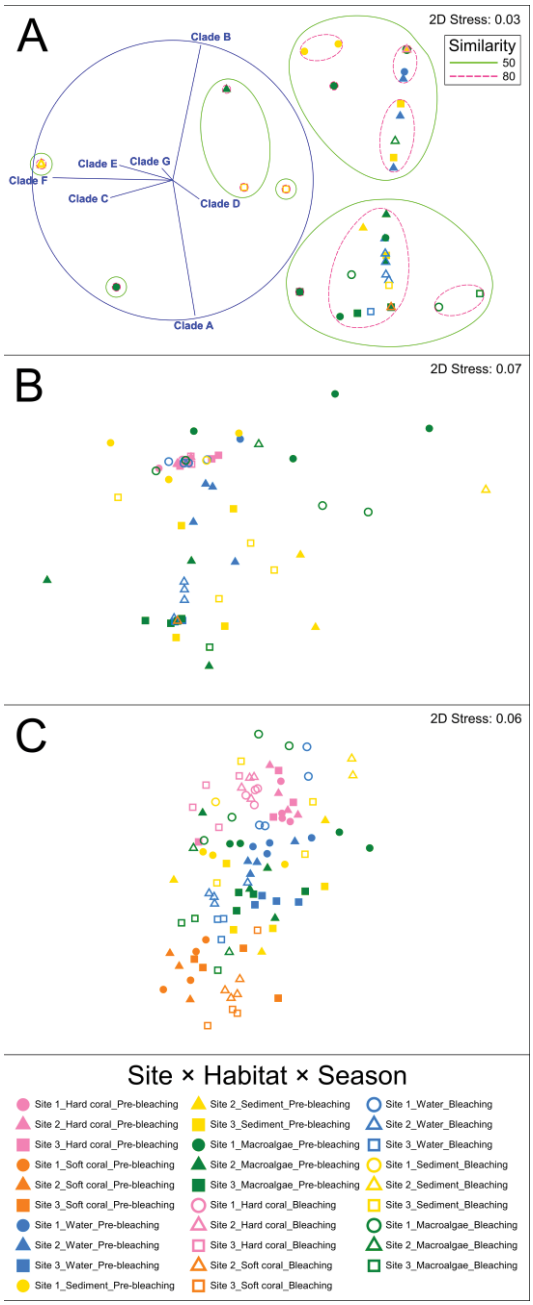

Figure 3.9. nMDS plots of *Symbiodinium* community compositions based on the ITS2 marker. **A.** Clade. **B.** ITS2 variant. **C.** OTU. Non-metric multidimensional scaling (nMDS) was performed on each variable per variant using Bray-Curtis Similarity. CLUSTER analysis was performed for cladal composition (**A**); similarity is shown at the 50% (green solid lines), 80% (pink dashed lines) levels and vectors driving the clustering are shown as blue lines. Hard corals are represented by pink, soft coral by orange, water by blue, sediment by yellow, and macroalgae by green with site 1 with circle, site 2 with rectangle, and site 3 with square markers. Plots for pre-bleaching samples are shown with closed markers and bleaching samples with open markers (all combinations for the markers are shown below the graphs).

was the only significant difference detected within environments (P = 0.035, see Appendix E3.3 for pairwise comparison). (iii) Clades C were mainly and clades E and F were exclusively found in sediment and macroalgae samples (Fig. 3.8), but where clade E was only detected during the pre-bleaching period except for one sample of sediment at site 3 during bleaching (see also SIMPER analysis in Table S3.8 for the contribution). However, clades D and G were detected by the ITS2 marker, which were not detected by the cp23S marker. Interestingly, clade D was only detected during bleaching in macroalgae samples.

Overall, cladal compositions for the two amplicons (cp23S vs. ITS2) agreed well, and significant differences of community composition between amplicons were not found in all combinations except for water at site 2 during bleaching (PERMANOVA, P = 0.026, see Appendix E3.4 for pairwise comparison in "amplicon" factor).

3.4.7.2. ITS2 variants composition

A total of 25 ITS2 variants were identified belonging to clades A (7 ITS2 variants), B (6), C (5), D (2), E (3), F (1) and G (1) (Table 3.3). As per Chapter 2, we also supplemented the information of taxa with a broader phylogenetic context (e.g. B18-like type) together with ITS2 variants to aid interpretation of ecological patterns (Cunning et al. 2015). B18-like types (B18, B18a) were the most dominant for *P. versipora* which accounting for > 95% of total sequences in *P. versipora* (Fig. 3.10, also see Table S3.9 for the list of top three ITS2 variants and compositions (%)). B40-like type (B119) was also present, but with < 4%. *Symbiodinium* harboured by *C. gaboensis* were only assigned to one ITS2 variant A136 (classified as a "temperate A type"; Hunter et al. 2007; Casado-Amezúa et al. 2014). These community

compositions for both hosts were unchanged through time (pre-bleaching vs. bleaching; PERMANOVA, $P = 0.40$ for season effect, Table S3.7B) which can also be seen in the heat map for ITS2 variants (Fig. 3.11).

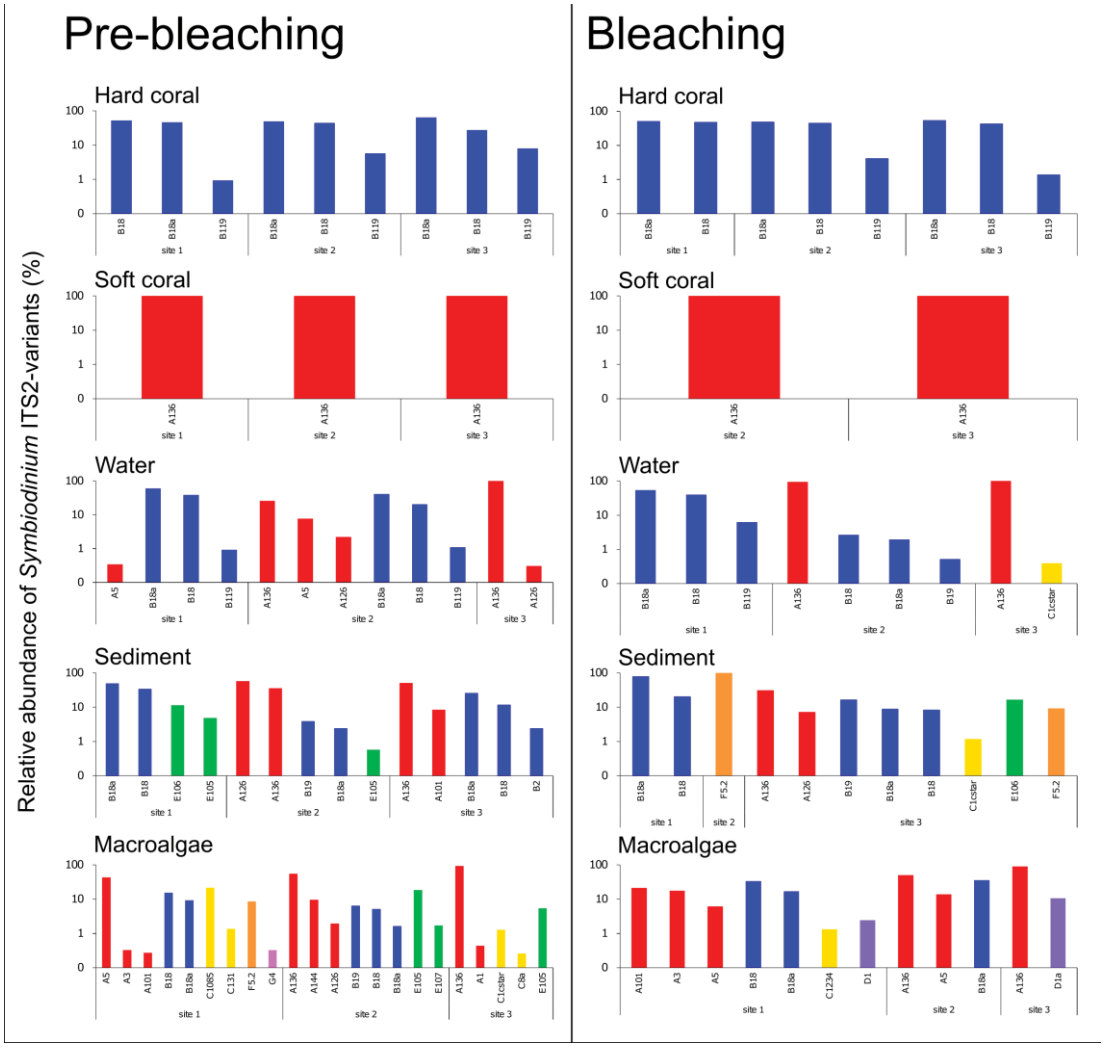

Figure 3.10. Relative abundance of *Symbiodinium* ITS2 variant during pre-bleaching (left panel) and bleaching (right panel) obtained by DNA metabarcoding based on the ITS2 marker. Relative abundance of ITS2 variants in each replicate (n = 2-4, depends on the samples) were averaged and top three ITS2 variants in each clade are shown as bar graphs for each site, habitat and sampling time point.

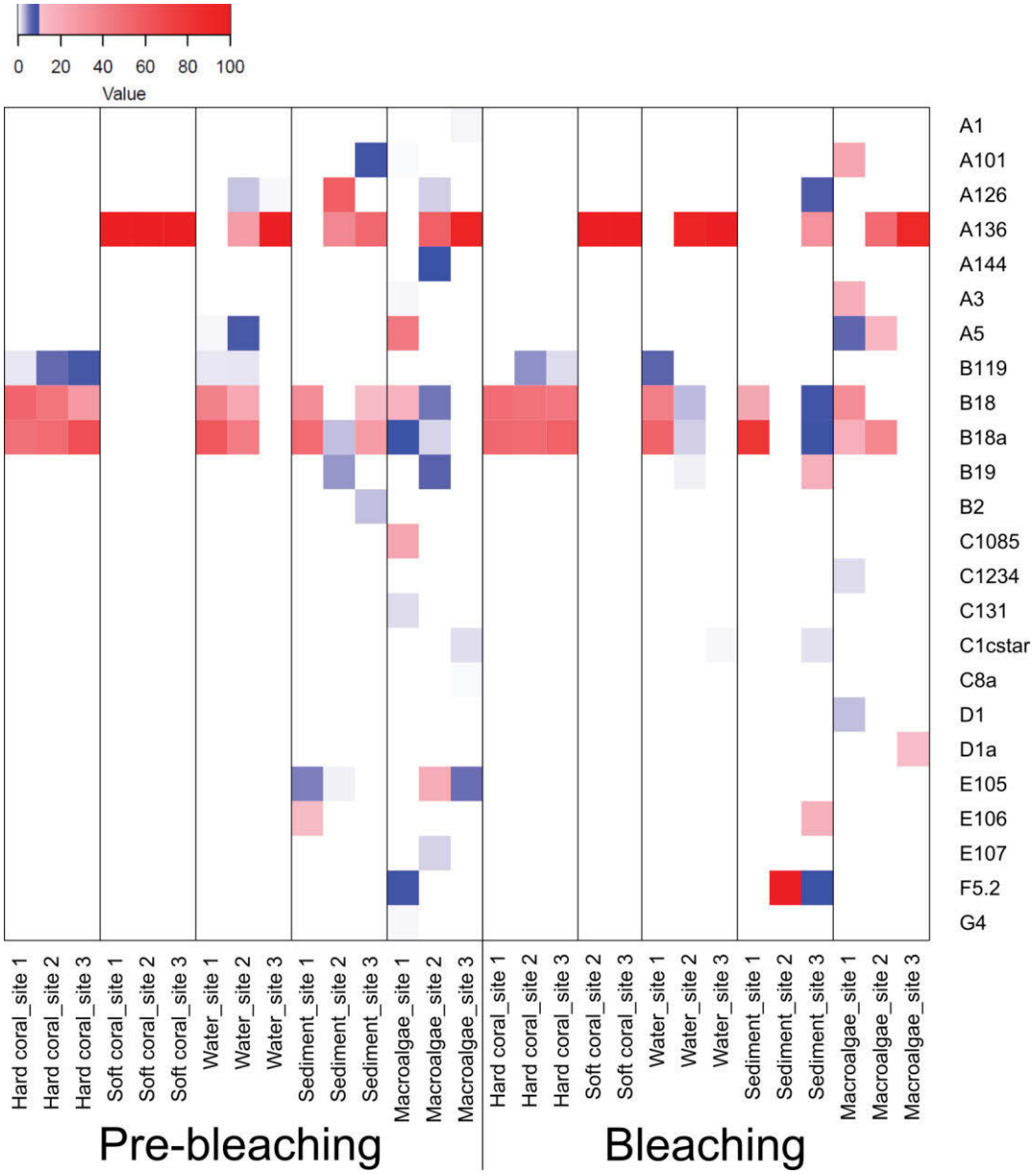

Figure 3.11. Heatmap of *Symbiodinium* ITS2 variant compositions. Compositions of ITS2 variants in each replicate (n = 2-4, depends on the samples) were averaged and top three ITS2 variants in each clade are displayed on the right. The colour (scale bar on the top of the graph) represents the proportion of each ITS2 variants in the sample (0-10% with blue gradient and 10-100% with red gradient), and white boxes indicate an absence of the ITS2 variant.

As for the cladal level community compositions (Fig. 3.9A), ITS2 variant community compositions (Fig. 3.9B) followed a similar trend, whereby community was differentiated significantly by sites and habitats, but not by sampling times (PERMANOVA, $P = 0.001$, $P = 0.001$, $P = 0.40$, respectively, see Table S3.7B for main effects). Dominant ITS2 variants found in the hosts (A136, B18, B18a) were also found abundant in the surrounding environments (water, sediment, macroalgae) suggesting close connectivity between symbiotic and free-living populations (life stages). This is particularly the case for water samples that were separated by sites ($P < 0.05$ for all combinations, except site 2 vs. site 3 during bleaching, $P = 0.15$, see Appendix E3.5 for pairwise comparisons) and corresponded to the relative abundance of *P. versipora* or *C. gaboensis* hosts dominating in each site (Fig. 3.1A) also at the ITS2 variant level.

Unique genetic types which were mainly or exclusively found in environmental samples were also discovered (Fig. 3.10). For example, various clade A variants were detected exclusively in environmental samples: A1 (closely related to *S. microadriaticum*) and A3-like types (A3, A144; closely related to *S. tridacnidrum*) were detected in macroalgae samples, A5 in water and macroalgae samples, A101 (A2-like type; closely related to *S. pilosum*) in sediment and macroalgae samples, and A126 (A10-like type) in all environments. Also, B2 was only found in sediment samples and B19 across all environments. Various C-types; C1-like types (C1cstar, C1234), C3-like types (C1085, C131), and C8-like type (C8a) were also detected in all environments but mainly in macroalgae samples. All clade E variants (E105, E106, E107) belong to one species: *S. voratum* (thought to be an exclusively free-living type) were detected only in sediment and macroalgae samples. ITS2

variant F5.2 was also found only in sediment and macroalgae samples. These ITS2 variants contributed to differentiate not only *Symbiodinium* community between *in hospite* and environments, but also across environments (Fig. 3.11, also see SIMPER analysis Table S3.10 for the contribution) where significant differences were detected between water and sediment (site 2) and water and macroalgae (sites 1 and 2) during pre-bleaching (PERMANOVA, $P = 0.026$, $P = 0.027$, $P = 0.026$, respectively, see Appendix E3.5 for pairwise comparisons). In contrast, there was no significant difference in ITS2 variant community compositions between sediment and macroalgae samples.

Although, community compositions were not statistically different between sampling times, as observed at the clade level, ITS2 variants D1 and D1a were found in macroalgae only during bleaching and clade E variants (E105, E106, E107) were detected across sediment and macroalgae but generally during the pre-bleaching period (0.57-19% of clade E variants spanning in five compartments (site × habitat) during pre-bleaching, compared to 17% in only one compartment (site 3 sediment) during bleaching) (Fig. 3.10 and also see Fig. 3.11 for the heat map), suggesting that environmental conditions during the bleaching period potentially selected against these types.

3.4.7.3. OTUs composition

Greater number of OTUs were obtained based on the ITS2 marker (374 OTUs) compared to those obtained by the cp23S marker (54 OTUs) due to the higher resolution of ITS2 marker which can detect the diversity at type/species level. Intriguingly, whilst neither cladal or ITS2 variant level analysis did not resolve any

differences in *Symbiodinium* community compositions over time, OTU compositions differed between pre-bleaching and bleaching periods (Fig. 3.9C). PERMANOVA confirmed significantly different OTU composition between pre-bleaching and bleaching times for *P. versipora* at sites 1 and 2 ($P = 0.032$, $P = 0.030$, respectively), and *C. gaboensis* at site 2 ($P = 0.028$), but not at site 3 for both hosts ($P = 0.058$ and $P = 0.182$ for *P. versipora* and *C. gaboensis*, respectively), which curiously was the only site not to undergo bleaching (Samantha Goyen, personal communication). A shift in OTU community composition between sampling time points was also observed in water samples at sites 1 and 3 ($P = 0.030$, $P = 0.057$, $P = 0.027$ at sites 1, 2 and 3, respectively), but neither in sediment nor macroalgae samples ($P > 0.05$, see Appendix E3.6 for the pairwise comparison).

3.4.8. Quantification of free-living *Symbiodinium* by clade-specific qPCR

Symbiodinium clades A and B were detected by qPCR in water samples (4 out of 24 samples and 6 out of 24 samples, respectively, were detected within the quantification range based on calibration curves created using the culture strains (see Table 3.1 for the minimum quantification ranges for each clade primer set)) and macroalgae samples (4 out of 24 samples only from the clade A assay), and thus the majority of the samples were below the detection limit suggesting that overall *Symbiodinium* communities existed as free-living cells in relatively low abundance across all sites and environmental habitats. *Symbiodinium* cells in water were mainly quantifiable at site 1 and only for one sample at site 2 (0.13 cells mL^{-1} of clade A *Symbiodinium*). At site 1, clade B *Symbiodinium* (2.7-7.5 cells mL^{-1} ($n = 4$) and 3.3-13.4 cells mL^{-1} ($n = 2$) during pre-bleaching and bleaching, respectively) was more abundant than clade A (0.019 cells mL^{-1} ($n = 1$) and 0.055-0.057 cells mL^{-1} ($n =$

2), respectively) in water samples for both sampling times. Only clade A *Symbiodinium* cells were quantifiable for macroalgae samples, one sample each from all sites during pre-bleaching (site 1: 5.8 cells g^{-1}, site 2: 2.0 cells g^{-1}, and site 3: 2.6 cells g^{-1}) and one sample from site 1 during bleaching (7.3 cells g^{-1}). *Symbiodinium* density in both water and macroalgae tended to increase during bleaching compared to those during pre-bleaching, but the sample numbers were too low to statistically determine any trends.

3.5. Discussion

Attention has been increasingly paid to high-latitude marginal reefs given their potential to operate as a refugia for tropical corals under accelerating climate change (Halfar et al. 2005; Beger et al. 2014; Cacciapaglia and Woesik 2015; Morgan et al. 2017). Diverse coral communities can thrive in high-latitude reefs (Schleyer and Celliers 2003; Halfar et al. 2005; Beger et al. 2014; Porter and Schleyer 2017), yet still little is known as to how coral communities establish and are sustained over time within such marginal conditions. This is particularly true for free-living *Symbiodinium* communities where knowledge of phylogenetic diversity is still yet to be built (Chang 1983; Yamashita and Koike 2013; Jeong et al. 2014), despite the importance of this life history phase for establishing a new symbiosis (e.g. Coffroth et al. 2006; Nitschke et al. 2016). Using eDNA metabarcoding, we have identified and evaluated the diversity of free-living *Symbiodinium* in a high-latitude temperate reef (Sydney Harbour area, 33°S) for the first time.

3.5.1. Coral hosts abundance is critical for structuring the free-living *Symbiodinium* community in temperate reef

We detected seven clades (clades A-G, combining results from the cp23S and ITS2 markers) and found community compositions differed between environmental habitats and especially between sites with different abundance of hosts, suggesting hosts may play a key role in structuring the environmental pool of *Symbiodinium*. *Symbiodinium* cladal diversity and community composition obtained from the cp23S and ITS2 primer sets corresponded well (e.g. Stat et al. 2009b; Thomas et al. 2014), thus we focus the discussion here on the more resolute ITS2-based observations.

Plesiastrea versipora harboured B18-like types (B18, B18a) in Sydney across all sampling sites. *P. versipora* is known to harbour clade C symbionts in (sub-) tropical regions (Orpheus Island (18°S) and Moreton Bay (27°S)) (Rodriguez-Lanetty et al. 2001), but switches to clade B in temperate regions including Sydney Harbour (33°S) and also in Gulf of Vincent (34°S), Batemans Bay (35°S) (Loh et al. 1998; Rodriguez-Lanetty et al. 2001). Our findings are consistent with Silverstein et al. (2011) who reported B18 for *P. versipora* at Rottnest Island (32°S) and Dunsborough (33°S) in the west coast of Australia (similar latitude to Sydney Harbour) and thus this *Symbiodinium* type is considered a more temperate specialist suited to higher latitudes (Rodriguez-Lanetty et al. 2001; Silverstein et al. 2011). *Capnella gaboensis* was dominated by A136 which was classified as “temperate A type” (Hunter et al. 2007; Casado-Amezúa et al. 2014) found within Mediterranean anthozoans, and is the first report of this *Symbiodinium* ITS2 variant from *C. gaboensis*. Other tropical *Capnella* sp. collected from the Great Barrier Reef are known to harbour a variety of clades, including those belonging to clades A, C and D (van Oppen et al. 2005), and

B1 types (Kermadec Islands, New Zealand (29°S); Wicks et al. 2010). Given the restricted nature of our sampling here, it is not possible to resolve whether this novel partnership between A136 and *C. gaboensis* is restricted to our study area, or is common across a wider geographical range.

Community composition of free-living *Symbiodinium* in the water matched closely the dominant ITS2 variants *in hospite*, an observation consistent with studies from tropical regions (Manning and Gates 2008; Zhou et al. 2012; Sweet 2014; Granados-Cifuentes et al. 2015; Chapter 2). The location of each site played a key role in driving differences in free-living *Symbiodinium* diversity, most likely because of the shift from hard to soft coral dominated benthic communities from sites 1 to 3. Therefore, it is plausible that surrounding hosts play an important role for structuring free-living *Symbiodinium* pools especially in water, where continuous expulsion of *Symbiodinium* from hosts into the water column may operate as a key mechanism regulating symbiont density *in hospite* (Jones and Yellowlees 1997; Dimond and Carrington 2008; Fujise et al. 2014). An alternative explanation could be that *P. versipora* can maintain a stable symbiosis with other symbiont types in tropical waters (ca. clade C; Rodriguez-Lanetty et al. 2001), the tight association between *in hospite* and free-living community diversity may reflect that temperate waters restrict the types of *Symbiodinium* available for association. Unfortunately, little is known of the thermal performance of different types, especially for cold water resistance, and therefore this notion clearly warrants further work.

3.5.2. Sediment and macroalgae are preferred habitats for exclusively free-living *Symbiodinium* types

Partitioning of community compositions across environments was detected in ITS2 variant levels, mainly between water and sediment/macroalgae. Clade E *Symbiodinium* (*S. voratum*), which is found mostly in temperate regions as a relatively cold-water specialist (Chang 1983; Yamashita and Koike 2013; Jeong et al. 2014), was also found in this study and predominantly in sediment and macroalgae. Clade E is rarely found *in hospite* and only in extremely low abundance (e.g. 0.03-0.06% in *Alveopora japonica*; Jeong et al. 2014), and therefore thought to be an exclusively free-living or if not opportunistic type (Yamashita and Koike 2013; Jeong et al. 2014; Thornhill et al. 2017). A2-like type (A101; closely related to *S. pilosum*) is also considered as an exclusively free-living type (LaJeunesse 2002; Yamashita and Koike 2013). Similar to clade E, this type was only found in sediment and association with macroalgae. These findings are consistent with those from tropical regions of exclusively free-living types preferentially inhabiting sediment and macroalgae habitats (Chapter 2). Thus, these types contributed to a unique community composition for sediment and macroalgae compared to water.

3.5.3. Both free-living and *in hospite Symbiodinium* community compositions were affected by the 2015/2016 heat wave

Temporal as well as spatial pattern of free-living *Symbiodinium* community compositions was observed for presence of clade E *Symbiodinium*, which became less abundant during bleaching compared to pre-bleaching. In contrast, ITS2 variants D1 and D1a which were only found during bleaching, are generally thought to increase their abundance relative to other clades during heat stress conditions (Baker

et al. 2004; Jones et al. 2008; LaJeunesse et al. 2009; Stat and Gates 2011). Environmental conditions for the two sampling time points were characterised by higher water temperature (SST) and light intensity (PAR) in pre-bleaching (summer season) compared to bleaching period (late-autumn season). Therefore, changes in *Symbiodinium* communities are arguably not consistent with changes in absolute, but rather the rate of change (or extent of anomalous) SST or PAR. Indeed, positive thermal anomalies continued for 11 months prior to bleaching (from May 2015 to March 2016 in Sydney Harbour sites 1 and 2), which act as a critical stressor to cause bleaching, and possibly explain the loss of more temperate-specific clade E and the appearance of thermally tolerant clade D types (e.g. Silverstein et al. 2015).

Although, temporal effects on the overall *Symbiodinium* community compositions in either *in hospite* and free-living communities were not statistically detected in the cladal and ITS2 variant level, a change in community composition was detected across pre-bleaching and bleaching periods at the OTU level. Interestingly, *Symbiodinium* community shifts were detected in *P. versipora* at sites 1 and 2 and *C. gaboensis* at site 2 (note there was no sample collection at site 1 during bleaching), but not at site 3 for both host species. During the summer 2015/2016 thermal anomaly, bleaching of *P. versipora* was observed only at Sydney Harbour sites 1 and 2, with ca. 60% of all colonies paled or bleached (Goyen et al. in prep). On the other hand, no bleaching was observed for *P. versipora* at site 3 (in Botany Bay). This difference in host status may explain the community shifts of *Symbiodinium* in *P. versipora* at sites 1 and 2, but not at site 3. *C. gaboensis* was not monitored for the impact of thermal stress; however, according to the symbiotic community shifts and increased of relative abundance of clade A in water during bleaching observed at site

2, *C. gaboensis* at site 2 possibly showed a sign of bleaching with the expulsion of *Symbiodinium*. Indeed, free-living *Symbiodinium* community compositions of water samples also showed significant differences between pre-bleaching and bleaching at sites 1 and 3, which possibly supports the impact of the heat wave increasing expulsion from hosts into surrounding waters via thermal stress (e.g. Fujise et al. 2013). The qPCR-based free-living *Symbiodinium* cell abundances remained relatively low across all sites and thus it is not possible to test this hypothesis.

3.5.4. Comparison of *Symbiodinium* diversity with tropical reef reveals scarce reference sequences from temperate reefs

With establishing free-living *Symbiodinium* diversity and community compositions (compared to *in hospite*) in temperate waters, we next assessed the difference/similarity compared to neighbouring tropical regions. Sydney Harbour is periodically connected to the Great Barrier Reef via the East Australian Current (EAC; Ridgway and Dunn 2003; Booth et al. 2007), and therefore we contrasted these data with corresponding data from the southern Great Barrier Reef (Heron Island) from Chapter 2 based on the ITS2 marker. In doing so, we explore how *Symbiodinium* populations could be maintained in high-latitude marginal reefs, and especially how free-living populations might contribute to resilience of coral-symbiont symbioses in marginal environments.

Tropical hard corals had higher richness of ITS2 variants (3.7 ± 1.2 ITS2 variants, mean across species and seasons ± SD) compared to temperate hard coral (2.8 ± 0.53 ITS2-types) or soft coral (1.0 ± 0.0 ITS2 variants). However, this pattern was reversed for data at the OTU level, whereby temperate hard coral (12 ± 2.3 OTUs)

and soft coral (11 ± 4.0 OTUs) had more *Symbiodinium* OTUs than for tropical hard corals (5.7 ± 2.3 OTUs) (Fig. 3.12). Uncoupling of ITS2 variant vs. OTU diversity might be explained by the limited reference data for genetic identity of *Symbiodinium* from temperate reefs at the ITS2 variant level.

To assess this hypothesis, we compared the phylogenetic positions of OTUs for clades A, B (dominant symbionts in *C. gaboensis* and *P. versipora*, respectively, collected from Sydney Harbour) and clade C (dominated in three coral species: *Acropora aspera*, *Montipora digitata* and *Pocillopora damicornis*, collected from Heron Island: Chapter 2) obtained in our studies with ITS2 sequences belonging to each clade in the reference database SymTyper by creating phylogenetic trees using QIIME (*make_phylogeny.py*) (Fig. 3.13). The majority of OTUs in clades A and B found in the temperate reef (in this Chapter) showed distinct clusters compared to SymTyper reference ITS2 sequences (Fig. 3.13A and B). On the other hand, OTUs in clade C found in Heron Island (in Chapter 2) were nested in SymTyper ITS2 sequences (Fig. 3.13C). This observation suggests that OTUs of *Symbiodinium* found in Sydney Harbour (temperate) had a distinct phylogeny compared to the reference ITS2 database, whereas OTUs from Heron Island (tropical) had close phylogeny to the reference database and thus the majority of sequences in SymTyper are presumably originating from tropical regions. Based on the analysis, the uncoupling of diversity between ITS2 variants and OTUs is clearly resulting from a lack of formal types or species designations in temperate regions where *Symbiodinium* phylogeny is distinct from tropical regions. This finding also highlights that OTU based analysis is a powerful tool to assess the diversity without taxonomic information, especially if the reference database is still under-developed.

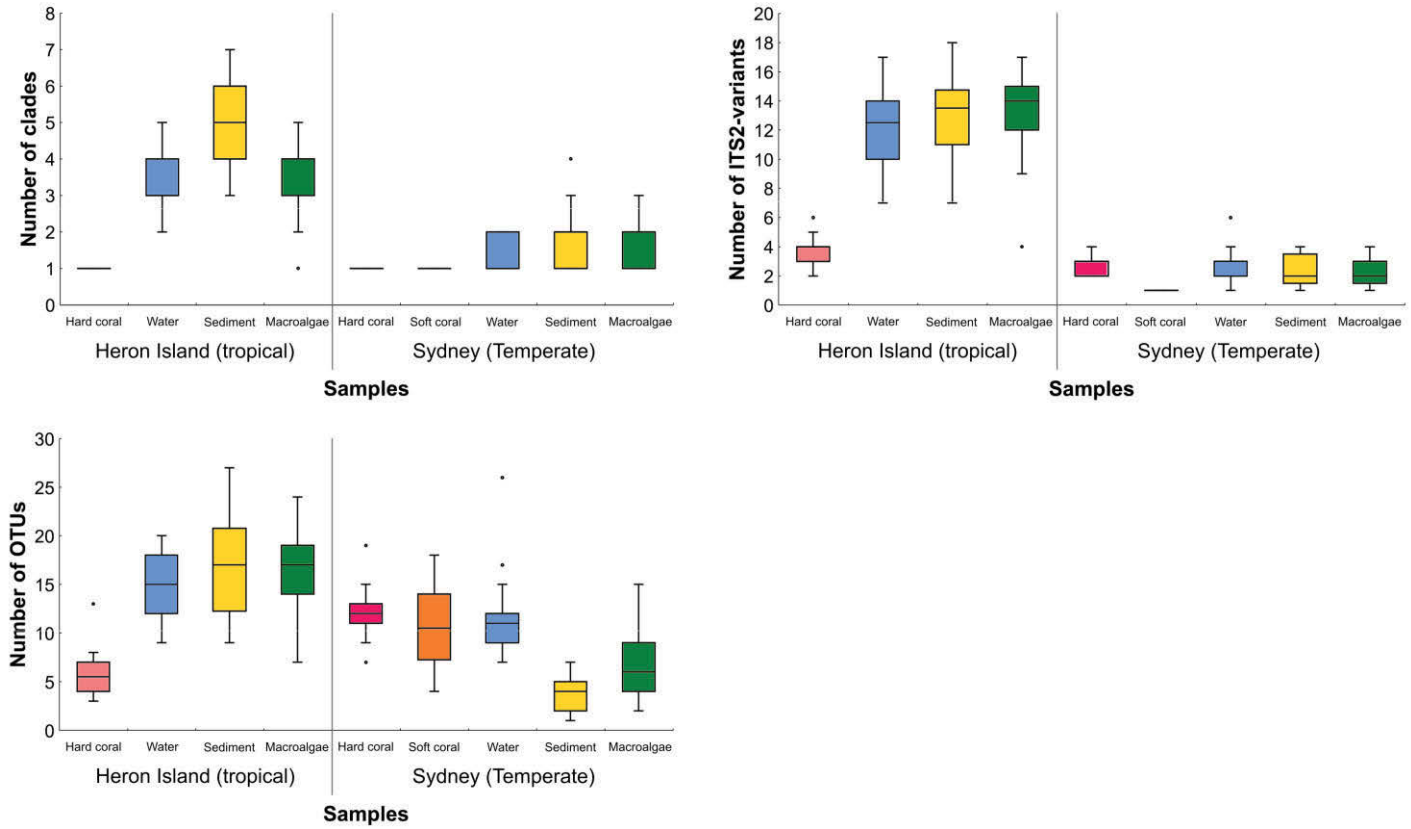

Figure 3.12. Box plots for number of clades, ITS2 variants and OTUs based on the ITS2 marker in each region and habitat. Box plots for hard corals are shown as pink, soft coral as orange, water as blue, sediment as yellow and macroalgae as green. Sites and seasons were pooled together.

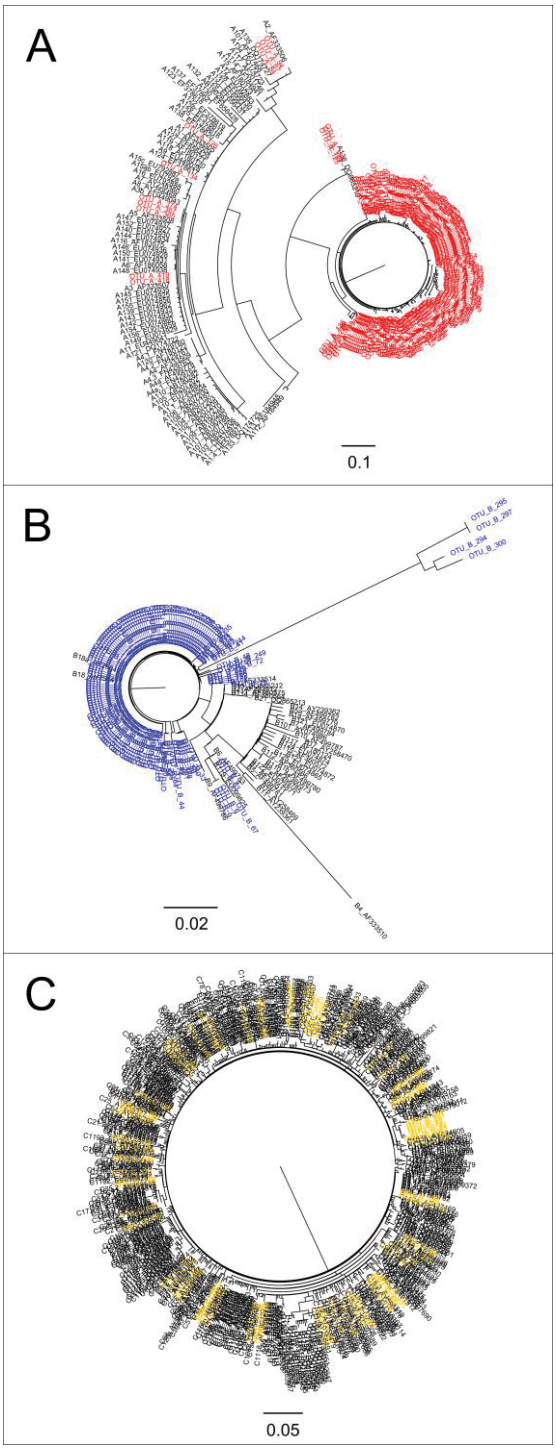

Figure 3.13. Phylogenetic trees based on OTUs together with sequences in ITS2 reference database SymTyper. **A.** Clade A OTUs in Sydney Harbour with red letters plus clade A sequences in SymTyper with black letters. **B.** Clade B OTUs in Sydney Harbour with blue letters plus clade B sequences in SymTyper with black letters. **C.** Clade C OTUs in Heron Island reef with yellow letters plus clade C sequences in SymTyper with black letters. Phylogenetic trees were created using QIIME (*make_phylogeny.py*).

The observed high-level of temperate *Symbiodinium* endemicity in Sydney Harbour may be linked to the evolution of distinct holobiont partnerships and genetic isolation of host populations at high-latitudes (Wicks et al. 2010). Rodriguez-Lanetty and Hoegh-Guldberg (2002) previously described that *P. versipora* in Sydney Harbour is indeed highly isolated due to a range expansion event. However, it is still unclear why symbiont OTU diversity was higher in temperate hosts compared to tropical hosts. Thomas et al. (2014) compared the *Symbiodinium* diversity in *Acropora* corals from tropical (Kimberley, 14°S) and temperate (Abrolhos Islands, 29°S) reefs across the western coast of Australia using DNA metabarcoding and found no differences of OTU diversity *in hospite* across latitudinal gradient, based on cp23S marker. Cp23S marker (especially for hyper variable region: HVR) has less resolution compared to the ITS2 marker (Pochon et al. 2010; Takabayashi et al. 2012), so it is unclear whether this trend would still be consistent with the higher resolution of taxonomy afforded through ITS2-based OTU analysis. Further study is required to clarify whether higher symbiont OTU diversity in temperate regions is due to differences of host species or differences of latitudinal gradients.

3.5.5. Free-living *Symbiodinium* diversity and abundance are higher for tropical than temperate reefs

In contrast to the *in hospite* diversity, free-living *Symbiodinium* diversity was higher in tropical regions compared to those in temperate region for all levels (clade, ITS2 variant and OTU) and for almost all environmental habitats (water, sediment and macroalgae) (Kruskal-Wallis test, $P < 0.05$ for 24 out of 27 combinations, pool sites and seasons) (Fig. 3.12). We suggest that free-living *Symbiodinium* diversity likely mirrors that of the total potential host diversity, which is higher in the tropics

compared to temperate region (Veron 1993; Fabricius and De'ath 2001; Harriott and Banks 2002; Butler et al. 2010). For example, diversity of scleractinian coral species declines with increasing latitude on coastal eastern Australia with the northern GBR containing nearly 400 coral taxa compared with fewer than 10 coral taxa in south-east Australia (Veron 1993; Harriott and Banks 2002). Hosts are an important factor for shaping the free-living *Symbiodinium* community, thus the lower diversity of free-living *Symbiodinium* possibly reflect the lower diversity of host species in the temperate reef. In addition, marginal environmental conditions in Sydney Harbour compared to tropical reefs, such as lower SST in winter < 20°C (Fig. 3.14), potentially further limits the niche width to types which can persist in this extreme condition and ultimately the diversity of free-living types. Specifically, only a few types were dominated in the temperate environments, such as cold water-specialised types that have an ability to tolerate low SST in winter, such as temperate A type (A136) (Hunter et al. 2007; Casado-Amezúa et al. 2014), B18-like types (Silverstein et al. 2011), B2 type (Thornhill et al. 2008), and clade E (*S. voratum*) (Jeong et al. 2014) which these characterised the temperate free-living community. More tropical *Symbiodinium* types seem well-adapted to their place of origin and typically showed declined growth rate under cold conditions (Thornhill et al. 2008), thus probably not able to persist in the temperate marginal environment which resulted in restricted diversity with the specialised types.

Within environments (water, sediment and macroalgae habitats), diversity of free-living *Symbiodinium* was stable across different habitats that was consistent across both tropical and temperate regions (Fig. 3.12). Symbiotic hosts continuously expel *Symbiodinium* into the water column to regulate symbiont density *in hospite*

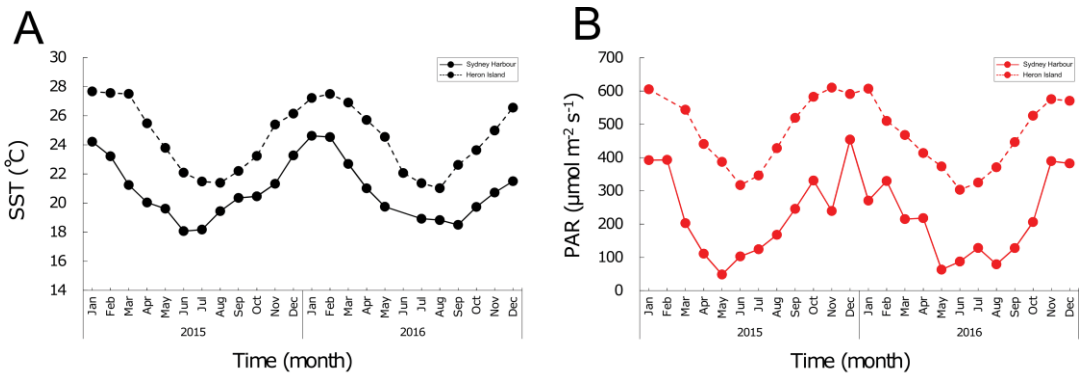

Figure 3.14. Environmental data in Sydney Harbour (temperate reef) and Heron Island (tropical reef). **A.** Monthly averaged sea surface temperature (SST, °C) from January 2015 to December 2016 including sampling periods for both Sydney Harbour (December 2015 and May 2016) and Heron Island (October 2015 and March 2016). Black solid line for Sydney Harbour SST and black dashed line for Heron Island SST. **B.** Monthly averaged photosynthetic active radiation (PAR, μmol photons m^{-2} s^{-1}) from January 2015 to December 2016. Red solid line for Sydney Harbour PAR (averaged PAR at depth 5-7 m where corals inhabit) and red dashed line for Heron PAR at sea surface.

(Jones and Yellowlees 1997; Baghdasarian and Muscatine 2000; Dimond and Carrington 2008; Fujise et al. 2014), therefore a reservoir of various types of *Symbiodinium* is likely to be found in the surrounding environment, but the community composition seems to be influenced by abundant hosts. Macroalgae provide inorganic nutrients and large surface area for attachment for associating microalgae including *Symbiodinium* (e.g. Porto et al. 2008; Venera-Ponton et al. 2010). Thus, macroalgal habitats might be more suitable compared to sediment for free-living *Symbiodinium* to persist, not only for exclusively, but also for transiently free-living types which have both symbiotic and free-living life stages.

Abundance of free-living *Symbiodinium* was also higher in tropical compared to temperate regions, where the majority of samples were below the detection limits collected from Sydney Harbour. This is also possibly explained by higher diversity and abundance of invertebrates on tropical reefs compared to temperate reefs (e.g. Veron 1993; Harriott and Banks 2002), which hosts are the source of transiently free-living types by expelling them into the environment, therefore increasing abundance of hosts, probably increasing the input of *Symbiodinium* into the environmental pool.

3.5.6. *Symbiodinium* genetic identity is separated by latitude along the east coast of Australia

Finally, we assessed connectivity of *Symbiodinium* genetic types between regions and found only 11% of ITS2 variants (10/87 ITS2 variants) and 1.3% of OTUs (8/598 OTUs) were shared between regions and the majority of ITS2 variants and OTUs were region-specific, suggesting geographical separation of *Symbiodinium* genetic identity by latitudinal gradient (Fig. 3.15). Community compositions were clearly separated by the regions for both ITS2 variant and OTU level based on nMDS plots (Fig. 3.16). Finding of limited overlap of *Symbiodinium* genetic types in tropical and temperate regions challenges the proposals that high-latitude marginal reef could act as refugia for tropical corals as waters continue to warm, since there would be few sources of symbionts available for tropical corals that require specific *Symbiodinium* type/species associations. Poleward expansion of tropical corals and "tropicalisation" of high-latitude reefs due to increased water temperature have been already reported from various locations around the world (e.g. Florida; Precht and Aronson 2004, Japan; Yamano et al. 2011, and eastern Australia; Baird et al. 2012).

These data would suggest that tropical *Symbiodinium* types will need to migrate south to sustain their tropical hosts or that temperate *Symbiodinium* adapt to warmer waters (Chakravarti et al. 2017) and so unlocking the thermal performance of different *Symbiodinium* types may prove crucial in models that attempt to track future coral migration (e.g. Cacciapaglia and Woesik 2015). In addressing such goals, it is clear that future projections must clarify free-living *Symbiodinium* diversity and community composition in reefs at the current edge of tropical host expansion where a mixture of tropical and temperate coral species exists, such as Solitary Island (e.g. Zann 2000), to understand how free-living communities are structured on such reefs.

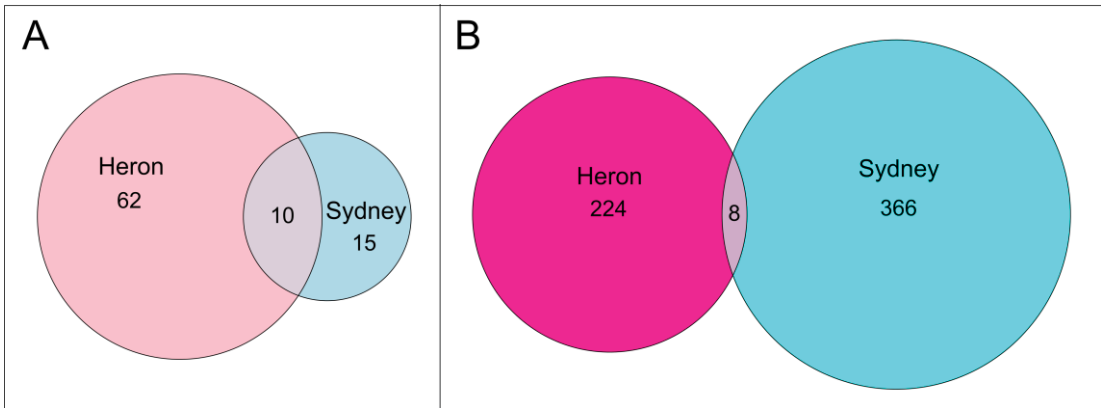

Figure 3.15. Venn diagrams to show connectivity of *Symbiodinium* genetic types between Sydney Harbour (temperate region) and Heron Island (tropical region). Number of **A.** ITS2 variants and **B.** OTUs. Number of *Symbiodinium* ITS2 variants or OTUs (combining across sites, habitats and seasons) in Sydney Harbour are shown with blue circles and Heron Island with pink circles.

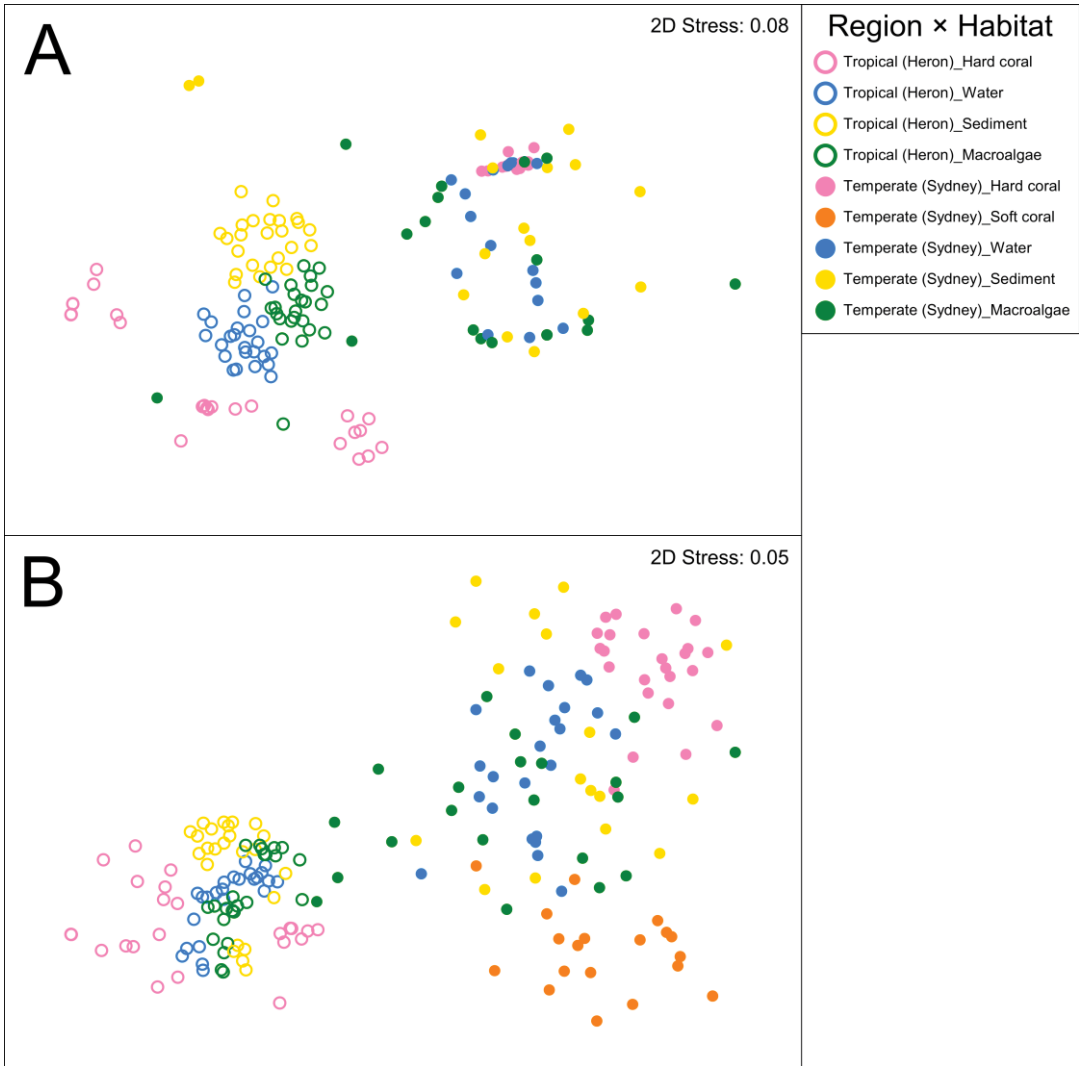

Figure 3.16. nMDS plots of *Symbiodinium* community compositions from Sydney Harbour (temperate region) and Heron Island (tropical regions) based on the ITS2 marker. **A.** ITS2 variants. **B.** OTUs. Non-metric multidimensional scaling (nMDS) was performed on each variable per variant using Bray-Curtis Similarity. Hard corals are represented by pink, soft coral by orange, water by blue, sediment by yellow and macroalgae by green markers. Plots for Sydney Harbour samples are shown as closed markers and Heron Island samples as open markers (all combinations of the markers are shown at the right to the graph).

3.6. Conclusions

In conclusion, we reported for the first time free-living *Symbiodinium* diversity and community composition in high-latitude temperate coral communities (Sydney Harbour) and examined how this contrasted with that for a tropical reef (Heron Island, southern GBR). Unique diversity and community composition of free-living *Symbiodinium* were observed in the temperate region, such as the temperate-specific clade E found in sediment and macroalgae habitats, especially pre-bleaching period. Impact of thermal anomalies upon free-living *Symbiodinium* community composition was observed in water samples (at the OTU level). In addition, *Symbiodinium* diversity within hosts was higher in the temperate than comparative tropical region, whereas free-living diversity showed the opposite trend presumably reflecting the correspondingly higher diversity of symbiotic hosts for the tropical region. Overall, genetic types of *Symbiodinium* were geographically separated. Together our novel findings highlight the importance of examining not only corals, but also free-living *Symbiodinium* populations to understand the potential of high-latitude marginal reef to act as refugia. Even so, this snap shot of community diversity, and how it changes over space and time, does not characterise the inherent dynamics underpinning this change; specifically, the processes governing individual growth and loss of any one population and hence competitive dominance. In particular, no information yet exists for a generalized model of population dynamics amongst genetically and functionally diverse *Symbiodinium*. Therefore, Chapter 4 examines the cell cycle; a core mechanism for controlling population turnover, for genetically distinct *Symbiodinium* during the free-living life stages, by using culture strains to create a novel baseline for cell proliferation.

3.7. Acknowledgements

The authors wish to thank all of the laboratory members in TrEnD Lab (Curtin University) for providing assistance of sample analysis, and Dr. Leo Hardtke (UTS) for assistance of environmental data collection from satellite. LF was supported by Climate Change Cluster (University of Technology Sydney) and Yoshida Scholarship Foundation (Japan). DJS was supported through an ARC Discovery Grant (DP160100271). Corals and environmental samples (water, sediment and *Ecklonia radiata*.) were collected under the Department of Primary Industries Scientific Collection Permit P16/0022-1.0 issued to LF and P15/0042-1.0 issued to SG.

(This page is intentionally left blank)

Chapter 4

Cell cycle dynamics of cultured coral endosymbiotic microalgae (*Symbiodinium*) across different types (species) under alternate light and temperature conditions

This chapter has been published in *Journal of Eukaryotic Microbiology* as:

Fujise, L., Nitschke, M. R., Frommlet, J. C., Serôdio, J., Woodcock, S., Ralph, P. J., & Suggett, D. J. 2018. Cell Cycle Dynamics of Cultured Coral Endosymbiotic Microalgae (*Symbiodinium*) Across Different Types (Species) Under Alternate Light and Temperature Conditions. J. Eukaryot. Microbiol. doi:10.1111/jeu.12497.

Lisa Fujise[1], Matthew R. Nitschke[1, 2], Jörg C. Frommlet[2], João Serôdio[2], Stephen Woodcock[1], Peter J. Ralph[1], David J. Suggett[1]

[1] Climate Change Cluster, University of Technology Sydney, Broadway, NSW 2007, Australia

[2] Center for Environmental and Marine Studies, University of Aveiro, 3810-193 Aveiro, Portugal

4.1. Abstract

Dinoflagellates of the genus *Symbiodinium* live in symbiosis with many invertebrates, including reef-building corals. Hosts maintain this symbiosis through continuous regulation of *Symbiodinium* cell density via expulsion and degradation (post-mitotic) and/or constraining cell growth and division through manipulation of the symbiont cell cycle (pre-mitotic). Importance of pre-mitotic regulation is unknown since little data exists on cell cycles for the immense genetic diversity of *Symbiodinium*. We therefore examined cell cycle progression for several distinct *Symbiodinium* ITS2-types (B1, C1, D1a). All types exhibited typical microalgal cell cycle progression, G_1 phase through to S phase during the light period, and S phase to G_2/M phase during the dark period. However, the proportion of cells in these phases differed between strains and reflected differences in growth rates. Undivided larger cells with 3n DNA content were observed especially in type D1a, which exhibited a distinct cell cycle pattern. We further compared cell cycle patterns under different growth light intensities and thermal regimes. Whilst light intensity did not affect cell cycle patterns, heat stress inhibited cell cycle progression and arrested all strains in G_1 phase. We discuss the importance of understanding *Symbiodinium* functional diversity and how our findings apply to clarify stability of host-*Symbiodinium* symbioses.

4.2. Introduction

Dinoflagellates of the genus *Symbiodinium* evolved an endosymbiotic lifestyle and radiated extensively within marine invertebrates, notably reef-building corals (Stat et al. 2006; Davy et al. 2012; Pochon et al. 2014). *Symbiodinium* reside in the endodermal tissues of their hosts, where they receive inorganic nutrients and protection from

grazers in exchange for their photosynthetic metabolites (e.g. Yellowlees et al. 2008). Continuous regulation of symbiont population density *in hospite* is critical to ensure a persistent functional equilibrium between *Symbiodinium* and their host (Smith and Muscatine 1999; Baghdasarian and Muscatine 2000). Maintenance of optimum *Symbiodinium* cell densities occurs via two processes: (i) post-mitotic control, including expulsion and degradation of excess symbionts; and/or (ii) pre-mitotic control, where population size is effectively regulated by limiting symbiont cell growth and division through control over their cell cycle progression (Hoegh-Guldberg and Smith 1989; Jones and Yellowlees 1997; Davy et al. 2012). In many anthozoans, post-mitotic control appears to be an important mechanism to regulate symbiont density, as they continuously expel *Symbiodinium* cells (Koike et al. 2007; Dimond and Carrington 2008; Yamashita et al. 2011) to regulate symbiont density *in hospite* (Jones and Yellowlees 1997; Dimond and Carrington 2008; Fujise et al. 2014). However, pre-mitotic control of individual cells has not been well-described and hence it is not clear whether and if so how this control mechanism contributes to the maintenance of a functional equilibrium between symbionts and host cells.

Pre-mitotic control involves the cell cycle progression of *Symbiodinium* that typically comprises a sequence of events that produce daughter cells; specifically, the progression of G_1 phase (preparation for DNA replication) to S phase (DNA synthesis), and then G_2 phase (pre-mitotic gap) to M phase (mitosis). Inorganic nutrient availability is classically considered an important factor controlling symbiont division *in hospite.* For example, rapid symbiont population growth upon addition of nitrogen has been observed (Hoegh-Guldberg and Smith 1989; Stimson and Kinzie 1991; Muller-Parker et al. 1994; Muscatine et al. 1998). Smith and Muscatine (1999) showed

that increased supply of inorganic nutrients allows *Symbiodinium* to accumulate cellular biomass (i.e. increased cell volume and chlorophyll content). However, this only translated to minor reductions in G_1 phase duration, which is the longest phase in cell cycle progression and 3-4 times longer when *in hospite* compared to free-living stage. *Symbiodinium* cell cycle phase duration (G_1 + S + G_2/M) was shortened only when the host was fed with nutrients (in the form of *Artemia* sp.). This highlights that the host-cell environment does not restrict access to nutrients or *Symbiodinium* biomass accumulation in G_1 phase, rather it restricts cell cycle progression from G_1 phase through to S phase. Fitt and Cook (2001) further suggested that supply of inorganic nutrients only temporarily increases symbiont mitotic division rates and that the actual key factor for limiting symbiont density is likely host feeding and the resulting host tissue accumulation since this regulates availability of intra-cellular space.

To further understand *Symbiodinium* cell cycle control processes, subsequent studies have turned to *Symbiodinium* populations grown in culture, and thus in a "free-living" stage outside of host control. Wang et al. (2008) detailed cell cycle phasing of a clade B *Symbiodinium* sp. strain under 12 h light:12 h dark. *Symbiodinium* cells cycled from G_1 to S phase towards the end of the light period, and towards G_2/M phase in darkness. Cytokinesis typically occurred at "dawn" (dark to light transition) while constant light temporarily inhibited cytokinesis, leading to an accumulation of G_2/M (2n), 3n, and 4n cells. Light was thus shown to be an important cue for cell growth and DNA synthesis, whereas a dark period was necessary for cytokinesis in mitotic division. Furthermore, the process of light-harvesting (photosynthetic pigment content and electron transport) which drives cell growth in the G_1 phase, has been shown to undergo circadian phasing

and rhythm-compensation during temperature fluctuations which suggests a strong endogenous algal circadian clock (Sorek and Levy et al. 2012; Sorek et al. 2013). Circadian phasing of the cell cycle is also common for other dinoflagellates (Chang and Carpenter 1988; Van Dolah and Leighfield 1999; Van Dolah et al. 2008). Such insights into cell cycle control from cultured strains have improved our general understanding of how microalgae proliferate, but how this knowledge applies to *Symbiodinium* is still largely unexplored.

Symbiodinium spp. can be divided into nine distinct monophyletic groups (clades A-I) and hundreds of "types" (species) (Pochon and Gates 2010; LaJeunesse et al. 2012a; Pochon et al. 2014; Thornhill et al. 2017), and in some instances corals can simultaneously host multiple species (Rowan and Knowlton 1995; Silverstein et al. 2015; Boulotte et al. 2016). The question of how this immense phylogenetic diversity can be mapped onto functional differences that best support competitive fitness is now beginning to drive *Symbiodinium* research in a new direction (Suggett et al. 2015; Warner and Suggett 2016; Suggett et al. 2017). The cell cycle patterns that sustain population growth described previously for a single culture strain (Wang et al. 2008) may vary across *Symbiodinium* taxa that have adapted to very different host environments (LaJeunesse et al. 2015; Leal et al. 2015); however, this is as yet untested.

In this study, we applied cell cycle analysis across strains of genetically distinct *Symbiodinium* species to examine the extent of functional diversity associated with the core process of cell cycle progression. Using high throughput flow cytometry, we examined cultured *Symbiodinium* across a range of genotypes/species (one B1: *Symbiodinium minutum*, two C1: *Symbiodinium goreaui*, and one D1a: *Symbiodinium*

trenchii) originally isolated from different Indo-Pacific coral species. Importantly, we evaluated for phylogenetic differences under alternate environmental scenarios that have previously been considered important regulators of cell cycle progression. Firstly, differences in light intensity ("low" vs. "high"). Light appears to be a critical cue for cell growth and DNA synthesis (Wang et al. 2008), and a key factor shaping the productivity, physiology, and ecology of *Symbiodinium* whether free-living (Suggett et al. 2015) or *in hospite* (Roth 2014). Thus, within physiologically utilizable limits, an increase in light intensity is expected to affect the cell cycle pattern, as the energy it provides increases the proportion of dividing cells (G_2/M phase) and results in increased growth rates. Secondly, differences in temperature ("ambient" vs. "anomalous heating") were examined. Heat stress causes DNA damage and arrests cells at cell cycle check points which are regulatory pathways that control order and timing of cell cycle progression and also detect stress and respond to damage (e.g. Elledge 1996). *Symbiodinium* spp. can be particularly susceptible to heat stress events that in turn drive coral bleaching (e.g. Davy et al. 2012). However, the susceptibility to heat stress differs between genetic types (e.g. Goyen et al. 2017). Therefore, it is important to resolve how core cell cycle processes are affected by heat stress across strains. Our analysis provides the first inter-cladal assessment of *Symbiodinium* cell cycle dynamics and the impact of different light and temperature treatments on cell cycle progression. Ultimately, we provide a baseline of the *Symbiodinium* cell cycle in its free-living life stage that also builds the foundation for new insight into the role of pre-mitotic control in maintaining a functional equilibrium between algal symbionts and coral hosts, and thus how differences in phylogeny and environmental conditions potentially influence *Symbiodinium* population dynamics *in hospite*.

4.3. Materials and methods

4.3.1. Culturing conditions

Four strains of *Symbiodinium* (ITS2-type B1, two of C1, and D1a; Table 4.1) were cultured in IMK medium (Daigo's IMK Medium, Nihon Pharmaceutical, Tokyo, Japan) within a climate controlled incubator (model ICC50, LABEC, Marrickville, NSW) set to 26ºC. Cultures were maintained in 200-mL glass conical flasks (n = 3 per strain and per treatment). Two experiments were performed separately to evaluate for the effect of light and temperature on cell cycle progression.

Table 4.1. Summary of *Symbiodinium* sp. type identifiers and source (geographic origin and host species) used for cell cycle analysis.

Clade/ ITS2-type		Identity	Species	Geographic origin	Host taxa
B	B1	UTSB	*S. minutum*	S. Taiwan (Indo-Pacific)	*Euphyllia glabrescens* (Coral)
C	C1	SCF058-04	*S. goreaui*	Magnetic Island (Pacific)	*Acropora millepora* (Coral)
	C1´	SCF055-06	*S. goreaui*	Magnetic Island (Pacific)	*Acropora tenuis* (Coral)
D	D1a	SCF082	*S. trenchii*	Magnetic Island (Pacific)	*Acropora muricata* (Coral)

Cultures were maintained under two different light intensities within the same incubator by placing the flasks at one of two distances from the light source (cool white LED lights, Hydra FiftyTwo HD, AquaIllumination, Ames, IA), 80 ± 16 µmol photon m^{-2} s^{-1} (mean ± SD, n = 12) and 262 ± 54 µmol photon m^{-2} s^{-1}, yielding a "low" and "high" light treatment, respectively (note approx. 300 µmol photon m^{-2} s^{-1} is potentially not saturating for growth and hence not considered as "stressful"– as per Hennige et al. 2009). The position of the flasks within each light treatment was moved daily to ensure randomisation within each light field. All cultures were acclimated to

each light treatment under a 12 h light: 12 h dark cycle for three weeks prior to sampling. Temperature was maintained at 26ºC (26.1 ± 0.26ºC and 26.1 ± 0.36ºC (mean ± SD)) for "low" and "high" light treatments, respectively; daily average temperature was measured using iButton® temperature logger (Thermochron, model DS1922L, Maxim Integrated, San Jose, CA) for the experimental period.

All cultures were subsequently grown within one of two incubators (model ICC50, LABEC) maintained at either "ambient" 26.4 ± 0.12ºC (mean ± SD) (referred to hereafter as "control") vs. "heat treatment", where the temperature was ramped up from 26ºC to 32ºC (2ºC per day at the beginning of the light period) over three days and then maintained for four days at 32.0 ± 0.16ºC (as per Robison and Warner 2006). Light intensity for both incubators was set at 324 ± 50 μmol photon m^{-2} s^{-1} (mean ± SD, n = 12) and 334 ± 106 μmol photon m^{-2} s^{-1} for the control and treatment incubator, respectively. The position of the flasks within each incubator was moved daily to ensure randomisation within each light field.

4.3.2. Monitoring the cultures

Cultures were diluted with growth medium to set the cell density to an equivalent value across all replicates and treatments of approx. 2-5 × 10^4 cells mL^{-1} at the beginning of each experiment. Cell counts to monitor growth were performed daily using a haemocytometer and light microscope (ECLIPSE Ni-E, Nikon, Tokyo, Japan) with automated capturing system (NIS-Elements Advanced Research, version 4.30, Nikon, Tokyo, Japan). For this, cultures were sampled at the same time every day (13:00-14:00 local time) when motile cells were the most abundant (> 80%). Samples were fixed with glutaraldehyde (Sigma-Aldrich, St. Louis, MO) to stop cells from

swimming and allow longer term preservation. Cell density was calculated using the cell counting script on Image J software FIJI (Suggett et al. 2015). Growth rate (μ, d^{-1}) were calculated from the cell count data using equation 1,

$$\mu = \ln\left(\frac{N2}{N1}\right)/(t2 - t1) \quad [1]$$

where N1 and N2 are cell number at time 1 (t1) and time 2 (t2), respectively. Cell volume (μm^3) data were also collected and analysed by Image J FIJI (Suggett et al. 2015) from the same samples used for cell counts to account for differences in cell volume amongst motile cells. Dark acclimated (ca. 15 min) measurements of the maximum quantum yield of photosystem II (F_v/F_m; dimensionless) were performed routinely at midday using Fast Repetition Rate fluorometry (FRRf: FastOcean, Chelsea Technologies Group, Surrey, UK) to verify the physiological status of the cultures (as described previously; Robinson et al. 2014; Suggett et al. 2015; Goyen et al. 2017). Sampling was conducted on days 2, 4, 6, and 7 (following inoculation) for the light intensity comparison experiment and days 2-7 for the heat stress experiment.

4.3.3. Cell cycle analysis using flow cytometry

After six days of culturing and during exponential growth, 10 mL (ca. 10^5-10^6 cells) from each replicate were collected into a 15-mL centrifuge tube throughout a diel cycle (3 h intervals over 24 h). Sampling time points were thus T0 (beginning of the light period), T3, T6, T9, T12 (end of the light/start of the dark period), T15, T18, T21, T24 (beginning of the light period). All samples were immediately fixed with 1% paraformaldehyde (Sigma-Aldrich) and chlorophyll was extracted with cold methanol (Chem-Suppy, Gillman, SA) following the protocol described by Figueroa et al. (2010) and stored in 4ºC until later analysis using flow cytometry. Cells were washed twice in phosphate buffer saline (PBS, pH 7) and stained with propidium iodide (PI, Sigma-

Aldrich) (3 μg mL^{-1}) with RNase (Sigma-Aldrich) (1.1 μg mL^{-1}) in PBS for at least 3 h at the room temperature (20ºC). DNA content was analysed using a flow cytometer (BD LSR II, BD Biosciences, San Jose, CA) with a flow rate of 35 μL min^{-1}. PI-stained DNA was excited with a blue (488 nm) laser, and PI fluorescence (636 nm) detected using a 695/40 nm bandpass filter with PerCP channel of the BD LSR II. A total of 30,000 events were acquired for each replicate. Initial gating of *Symbiodinium* cells was performed based on forward and side scatter (Fig. S4.1). Histograms of relative DNA content were analysed using ModFit LT (version 5.0, Verity Software House, Topsham, ME) in order to calculate the percentage of cells in each cell cycle phase; G_1, S, and G_2/M.

4.3.4. Statistical analysis

Two-way ANOVA was used to investigate differences in cell cycle parameters (peak proportion of G_1, S, G_2/M phases), growth rate and cell volume (at day 6, when cell cycle samples were collected) based on variables of culture identity (four strains) and environment (either "low" vs. "high" light, or "control" vs. "heat treatment") with Bonferroni multiple comparison *post-hoc* tests. Potential relationships between the cell cycle parameters, growth rate and cell volume were evaluated with Pearson correlations by combining low light and high light data sets. Repeated measures ANOVA were used to investigate the daily change and effect of the treatment on F_v/F_m. All the statistical analyses above were performed in SPSS Statistics 24 (IBM, Armonk, NY) ($P < 0.05$) ($n = 3$). To identify groupings amongst culture strains and treatments based on cell cycle proportion at G_2/M peak time, cluster analysis and multi-dimensional scaling (MDS) was performed on the average of each variable (PRIMER v6, PRIMER-E, Plymouth, UK). The G_2/M peak was chosen for this analysis given

that it is the most important phase in the cell cycle in relation to cell division. Values of all cell cycle proportions and F_v/F_m were arcsine transformed and cell volumes were square root transformed to stabilize the variance for ANOVA, Pearson correlation and MDS analyses.

4.4. Results

4.4.1. Light treatment (low light vs. high light)

All culture strains exhibited a typical microalgal cell cycle progression: cell division occurred in the early light period (T0-T6) with new G_1 populations being generated. G_1 phase progressed to S phase during the late light period (T6-12), and cells subsequently entered G_2/M phase during the dark period (T12-24) for preparation of cytokinesis. Hence, cell cycle "progression" was consistent across all tested strains (genetic types/species). An example of the DNA histograms produced through time is shown in Fig. 4.1 for *Symbiodinium* type B1 (*S. minutum*). Percentages of the different cell cycle phases are plotted through time for all strains in Fig. 4.2.

Differences in growth light intensity did not appear to affect the cell cycle patterns, as the G_2/M peak proportion was the same for the low and high light treatments (Table 4.2) (two-way ANOVA, $P > 0.05$, also see Table S4.1 for summary of two-way ANOVA), and data generally clustered independent of light treatment (with 96% similarity for each strain; Fig. 4.3A). Thus, cell cycle patterns were not affected by the tested light intensities, an observation that was largely consistent with a lack of light treatment response upon both growth rate (Fig. S4.2 for cell density plot) and values of F_v/F_m (Fig. 4.4, upper panels) (repeated measures ANOVA, $P > 0.05$). An exception

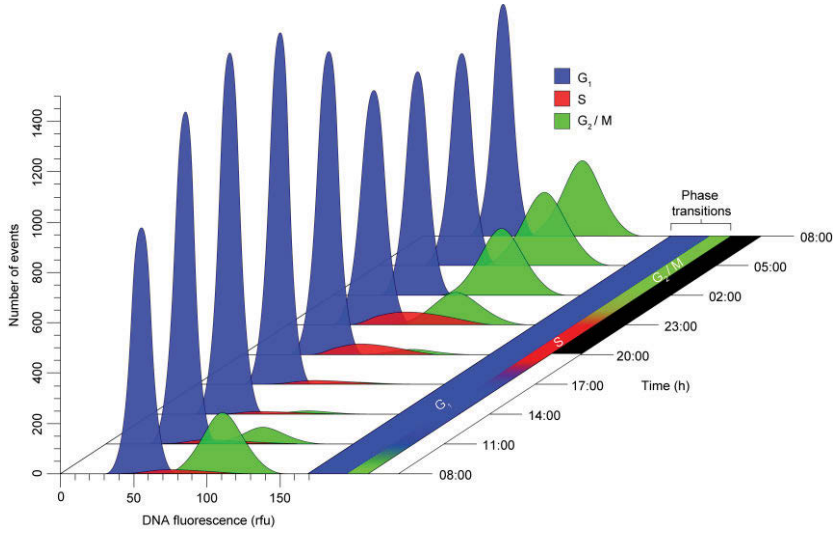

Figure 4.1. DNA histograms of cell cycle progression through 24 h. Example cell cycle analysis of *Symbiodinium* type B1 under high light treatment. First distribution (blue) are cells in G_1 phase with 1n DNA content. Second distribution (green) is G_2/M phase, where cells have 2n DNA content (twice as much as G_1 phase cells). S phase cells (red) have intermediate DNA content between G_1 and G_2/M phase cells. White bar shows the light period (8:00-20:00) and black bar shows the dark period (20:00-8:00). All distributions were produced using ModFit LT.

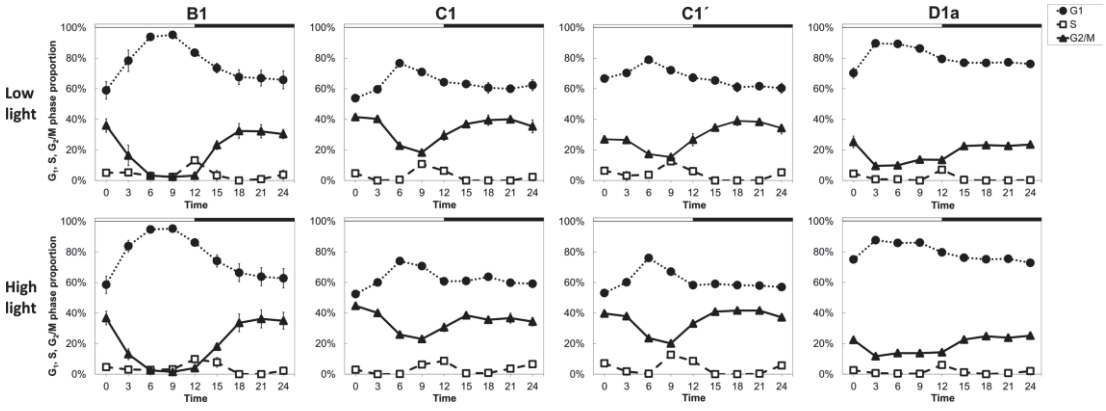

Figure 4.2. Cell cycle progression of four *Symbiodinium* culture strains through 24 h under two light treatments (low light vs. high light). Y axis is percentage of G_1, S and G_2/M phase, and X axis is the sampling time points (T0-24). White and black bars on the top of each graph show the light period (T0-12) and dark period (T12-24), respectively. G_1 phase is shown as dotted lines with black circles, S phase as dashed lines with open squares, and G_2/M phase as solid lines with black rectangles. Values represent mean ± SD (n = 3).

Table 4.2. Cell cycle and growth characteristics across four *Symbiodinium* culture strains under the light treatments (low light vs. high light). Cell cycle parameters: G_1 peak, S peak and G_2/M peak proportions (the maximum % of cells, for each phase, reached throughout a diel cycle) were obtained from analysis using cell cycle software: ModFit LT. Growth rates were calculated with equation 1 using cell densities. Mean ± SD (n = 3) are shown for all parameters except for cell volume (μm^3): median (upper–lower quartile ranges) are shown. Two-way ANOVA (strains × treatments) across variants is also shown where superscript letters indicate *post-hoc* groupings of strain effects within each treatment.

		Low light					High light				
Genotype		G_1 peak (%)	S peak (%)	G_2/M peak (%)	Growth rate (μ, d^{-1})	Cell volume (μm^3)	G_1 peak (%)	S peak (%)	G_2/M peak (%)	Growth rate (μ, d^{-1})	Cell volume (μm^3)
B	B1	95.3 (0.7)^{a}	13.2 (1.0)^{a}	32.6 (4.5)^{a}	0.28 (0.10)$^{a, b}$	215 (167-290)^{a}	95.3 (0.8)^{a}	10.2 (0.4)^{a}	36.2 (6.0)^{a}	0.34 (0.04)$^{a, b}$	177 (133-246)^{a}
C	C1	76.7 (1.2)^{b}	10.8 (1.3)^{a}	40.2 (2.8)^{a}	0.17 (0.05)^{a}	308 (230-396)^{b}	74.0 (1.0)^{b}	8.7 (0.8)^{a}	39.1 (1.1)^{a}	0.17 (0.02)^{c}	256 (201-328)^{b}
	C1′	79.0 (0.9)^{b}	12.5 (0.5)^{a}	39.0 (3.0)^{a}	0.22 (0.02)$^{a, b}$	306 (239-392)^{b}	76.1 (0.6)^{b}	12.7 (1.3)^{b}	42.2 (0.7)^{a}	0.21 (0.04)$^{a, c}$	258 (188-344)^{b}
D	D1a	89.9 (1.3)^{c}	7.0 (0.9)^{b}	23.5 (1.1)^{b}	0.31 (0.09)^{b}	230 (175-300)^{b}	87.6 (1.0)^{c}	6.0 (0.9)^{c}	25.3 (1.4)^{b}	0.35 (0.01)^{b}	246 (185-328)^{a}
ANOVA (F, P = 0.05)		228.39	26.61	18.88	3.78	11.33	277.94	28.98	17.08	8.46	13.63

was observed for type D1a (*S. trenchii*) which F_v/F_m was 3.1-7.8% lower under high light than under low light conditions through experiment (repeated measures ANOVA, P = 0.0074, P = 0.0013, P = 0.0035, P = 0.00019 for day 2, 4, 6, and 7, respectively).

In contrast to light intensity, strain identity resulted in differences in the "proportion" of each phase within the cell cycle (Table 4.2; Fig. 4.2). Strains C1 and C1′, which are the same ITS2-type and species (*S. goreaui*) but isolated from different hosts, exhibited 96% similarity of cell cycle proportions at the peak of the G_2/M phase (Fig. 4.3A). These two strains also shared slightly less similarity (93%) in the proportions of each phase at the G_2/M peak time with type B1, which appeared to reflect a relatively

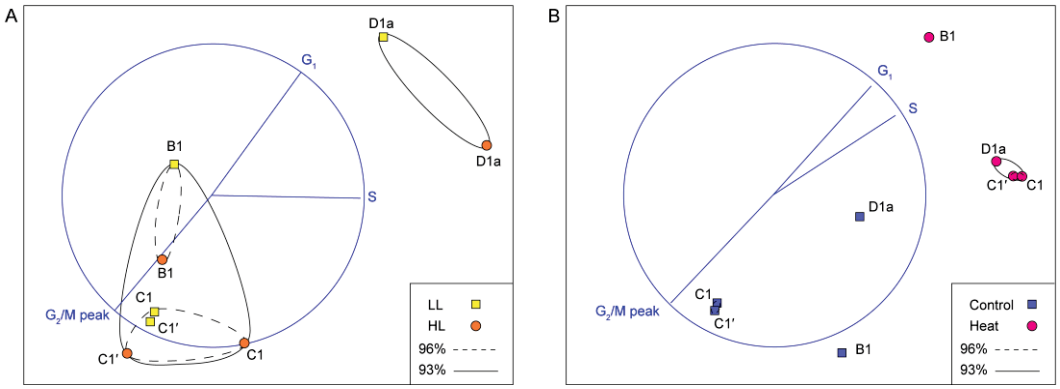

Figure 4.3. Multi-dimensional scaling (MDS) plots of four *Symbiodinium* culture strains with cell cycle proportions corresponding to the time of the G_2/M peak. **A.** Light treatment (low light (LL) vs. high light (HL)). **B.** Temperature treatment (control vs. heat). Cluster analysis and MDS were performed on the average of each variable per variant; similarity is shown at the 93% (solid lines) and 96% (dashed lines) levels and vectors driving the clustering are shown as blue lines. Low light and high light are represented by yellow squares and orange circles, respectively. Control temperatures and heat treatments are represented by blue squares and pink circles, respectively.

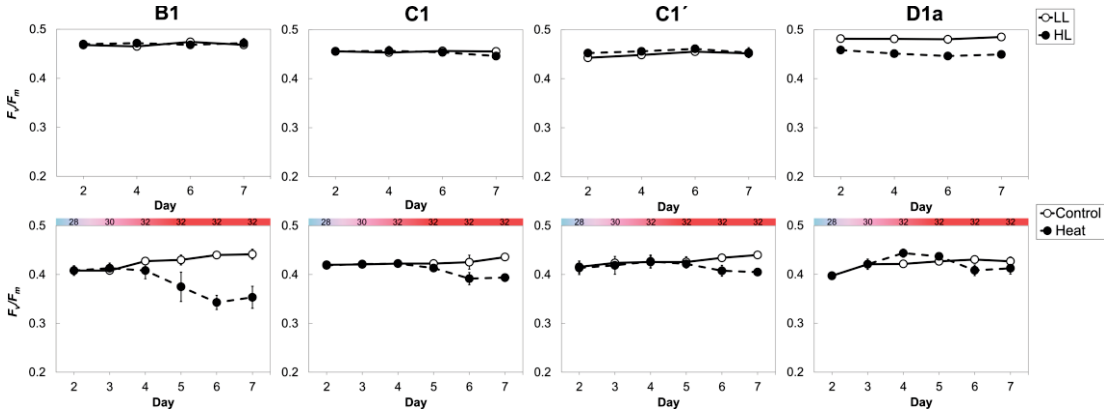

Figure 4.4. F_v/F_m of four *Symbiodinium* culture strains. Changes in photophysiology under light (low light (LL) vs. high light (HL), upper panels) and temperature (control vs. heat, lower panels) treatment. Low light and control temperatures are shown as solid lines with open circles and high light and heat treatments are shown as dashed lines with black circles. Values represent mean ± SD (n = 3). The temperature increase is shown on the top X axis of each graph for heat treatment (lower panel). The temperatures for heat treatments were; day 2: 27.7 ± 0.75°C, day 3: 29.7 ± 0.87°C, day 4: 31.9 ± 0.89°C, day 5: 32.0 ± 0.81°C, day 6: 32.1 ± 0.56°C, day 7: 32.3 ± 0.84°C (± SD for daily mean temperature measured using iButton® temperature logger).

reduced G_2/M peak proportion (ca. 39-42% for C1 and C1′ compared to ca. 33-36% for B1 including both low and high light values) and increased G_1 peak proportion (ca. 74-79% for C1 and C1′ compared to ca. 95% for B1) (Table 4.2) (two-way ANOVA, $P < 0.05$). Type D1a was separated from the three strains since it had the lowest G_2/M peak proportion (ca. 24-25%) compared to the other culture strains (Table 4.2) (two-way ANOVA, $P < 0.05$).

Cell cycle phasing during the diel cycle (G_1 to S to G_2/M phases) was conserved, whereas G_1 and G_2/M peak proportions reflected strain-specific differences in maximum growth rate. Strains inducing higher G_1 and lower G_2/M peak proportion exhibited a higher growth rate (Fig. S4.3A, B) (Pearson correlation, G_1 peak proportion and growth rate: $R^2 = 0.67$, $P = 0.00036$, G_2/M peak proportion and growth rate: $R^2 = -0.53$, $P = 0.0082$, $n = 24$). Cell volume was negatively correlated with the G_1 peak proportion and also growth rate (Fig. S4.3C, D) (Pearson correlation, G_1 peak proportion and cell volume: $R^2 = -0.78$, $P = 7.0 \times 10^{-6}$; growth rate and cell volume: $R^2 = -0.49$, $P = 0.015$, $n = 24$).

An additional feature observed was the existence of undivided cells with 3n DNA content, rarely in type B1, and more obviously in type D1a with larger cell size (Fig. S4.1A, D, also see Appendix E4.1A, D for image series of DNA contents shifting through 24 h). For D1a, the phasing of this 3n population was similar to the G_2/M phase: decreasing in the early light period and increased during the dark period, fluctuating between 2.2 to 8.0% of the total distribution under high light conditions.

4.4.2. Temperature treatment (control versus heat stress)

Under the ambient growth temperature (26ºC), cell cycle parameters (G_1, S and G_2/M peak proportion), growth rate and cell volume (Table 4.3) showed similar patterns as seen for the light treatment experiment (Table 4.2). Cell cycles exhibited characteristic transition across the phases throughout the diel cycle (Fig. 4.5). Under the heat stress (32ºC), cell cycle progression was not observed for any strain (Table 4.3; Fig. 4.5), whereby the G_2/M peak proportion significantly decreased compared to the control (ca. 25-50% for the control compared to ca. 4.3-14% for the treatment across all strains). MDS demonstrated different clustering for the control vs. heat treatment (Fig. 4.3B), with a consistent decrease of G_2/M and increase of G_1 proportions at the G_2/M peak time, suggesting cells were arrested in G_1 phase under heat stress. Slightly different cell cycle patterns were observed across the strains. Type B1 was clustered away

Table 4.3. Cell cycle and growth characteristics across four *Symbiodinium* culture strains under the temperature treatments (control vs. heat). Cell cycle parameters: G_1 peak, S peak and G_2/M peak proportions (the maximum % of cells, for each phase, reached throughout a diel cycle) were obtained from analysis using cell cycle software: ModFit LT. Growth rates were calculated with equation 1 using cell densities. Mean ± SD (n = 3) are shown for all parameters except for cell volume (µm^3): median (upper–lower quartile ranges) are shown. Two-way ANOVA (strains × treatments) across variants is also shown where superscript letters indicate *post-hoc* groupings of strain effects within each treatment.

		Temperature treatment									
		Control (26.4 ± 0.12°C)					Heat (32.0 ± 0.16°C)				
Genotype		G_1 peak (%)	S peak (%)	G_2/M peak (%)	Growth rate (µ, d^{-1})	Cell volume (µm^3)	G_1 peak (%)	S peak (%)	G_2/M peak (%)	Growth rate (µ, d^{-1})	Cell volume (µm^3)
B	B1	94.3 (0.8)^{a}	13.4 (1.4)^{a}	36.3 (2.2)^{a}	0.35 (0.06)	194 (151-258)^{a}	94.7 (0.4)^{a}	7.2 (2.2)^{a}	4.3 (1.4)^{a}	0.03 (0.10)	341 (256-437)^{a}
C	C1	74.4 (4.4)^{b}	13.6 (0.9)^{a}	47.9 (1.4)^{b}	0.26 (0.06)	345 (253-464)^{b}	80.5 (0.8)^{b}	13.7 (0.2)^{b}	12.5 (1.2)^{b}	0.07 (0.10)	423 (332-533)$^{a, b}$
	C1´	76.0 (1.7)^{b}	11.9 (2.9)$^{a, b}$	49.9 (6.2)^{b}	0.24 (0.07)	320 (247-409)^{b}	81.2 (0.8)^{b}	14.8 (0.3)^{b}	14.2 (1.9)^{b}	0.07 (0.05)	403 (328-485)$^{a, b}$
D	D1a	89.3 (0.7)^{c}	9.0 (0.9)^{b}	25.4 (0.7)^{c}	0.32 (0.04)	266 (207-363)^{b}	87.4 (0.5)^{c}	5.3 (0.5)^{a}	13.8 (1.5)^{b}	0.13 (0.18)	464 (367-653)^{b}
ANOVA (F, P = 0.05)		130.70	5.94	45.82	ns	14.05	73.25	33.48	23.97	ns	5.90

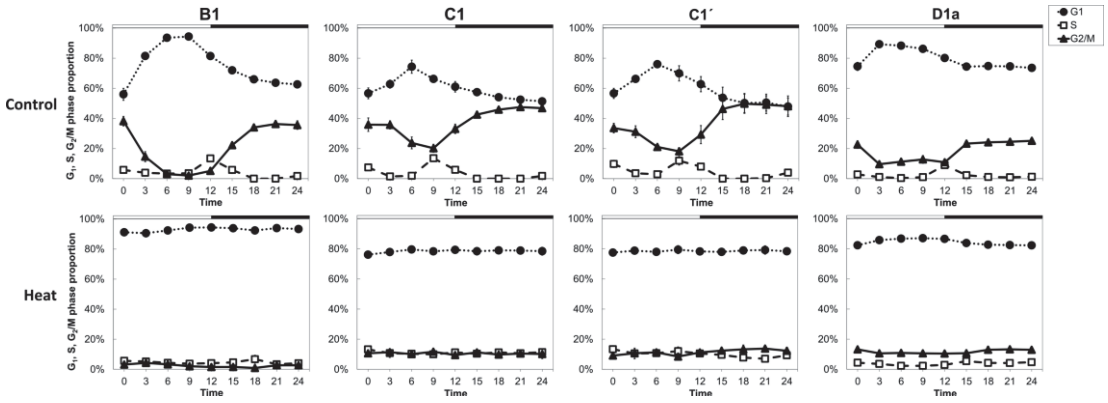

Figure 4.5. Cell cycle progression of four *Symbiodinium* culture strains through 24 h under the temperature treatment (control vs. heat). Y axis is percentage of G_1, S and G_2/M phase, and X axis is the sampling time points (T0-24). White and black bars on the top of each graph show the light period (T0-12) and dark period (T12-24), respectively. G_1 phase is shown as dotted lines with black circles, S phase as dashed lines with open squares, and G_2/M phase as solid lines with black rectangles. Values represent mean ± SD (n = 3).

from the two C1 and D1a types, as a result of significantly lower G_2/M peak proportion for type B1 compared to the other isolates (Table 4.3) (two-way ANOVA, $P < 0.05$, also see Table S4.2 for summary of two-way ANOVA).

Measurements of growth rate, cell volume (Table 4.3; Fig. S4.4) and F_v/F_m (Fig. 4.4, lower panels) supported the impact of the heat stress on cell cycle progression and cell viability. Growth rates were significantly lower (0.03-0.13 d^{-1}) under heat stress than for ambient temperature (0.24-0.35 d^{-1}) for all strains (two-way ANOVA, $P < 0.05$). Cell volume increased under heat stress for all strains; however, this increase was only significant for types B1 and D1a (two-way ANOVA, $P = 8.0 \times 10^{-5}$, $P = 0.056$, $P = 0.20$, $P = 1.0 \times 10^{-4}$, for B1, C1, C1´ and D1a, respectively). F_v/F_m decreased once the temperature reached 32ºC on day 4, and was significantly lower than for the control at

day 5, 6, and 7 for B1 which is relatively sensitive to heat stress, day 6 and 7 for C1, day 7 for C1′, and day 6 for D1a which is relatively resistant to heat stress (repeated measures ANOVA, $P < 0.05$). Values of F_v/F_m were lower for heat stress compared to controls by 78 ± 4.1%, 90 ± 3.0%, 92 ± 0.4%, 95 ± 4.0% (B1, C1, C1′ and D1a, respectively) at the end of experimentation.

4.5. Discussion

Functional equilibrium between hosts and *Symbiodinium* results from the continuous regulation of symbiont density *in hospite* (e.g. Baghdasarian and Muscatine 2000; Davy et al. 2012). Whilst hosts are considered to control *Symbiodinium* growth to maintain optimum densities, the potential for pre-mitotic control of cell proliferation is not well studied (Davy et al. 2012). Data do not yet exist for a generalized framework describing *Symbiodinium* cell cycle dynamics despite immense phylogenetic (e.g. Pochon and Gates 2010) and functional (Suggett et al. 2015; Warner and Suggett 2016; Goyen et al. 2017) diversity. Such a framework could function as a baseline of *Symbiodinium* cell proliferation and help to resolve how hosts exert control over *Symbiodinium* cellular growth cycles (Cunning et al. 2017; Suggett et al. 2017).

Cell cycle progression is a core biological process with conserved control and regulatory mechanisms across microalgae, other eukaryotic microorganisms, plants, and animals (Vaulot 1995; Elledge 1996; Griffiths 2010). Our experiments showed highly conserved cell cycle “progression” dynamics across genetically distinct *Symbiodinium* culture strains (ITS2-types/species B1: *S. minutum*, C1: *S. goreaui* and D1a: *S. trenchii*), with all types exhibiting a typical microalgal cell cycle pattern (e.g. Griffiths 2010). Thus, our results are in agreement with current knowledge and are

consistent with cell cycle dynamics previously described for a single *Symbiodinium* isolate (clade B; Wang et al. 2008) and also for many other dinoflagellates (Chang and Carpenter 1988; Van Dolah and Leighfield 1999; Van Dolah et al. 2008; Dapena et al. 2015). However, we did observe differences in how key cell cycle phases were proportioned amongst genetic types/species and environmental conditions.

The two strains of ITS2-type C1 (originally isolated from different coral hosts) exhibited similar cell cycle phasing proportions, which were different to those observed for types B1 and D1a. Whilst it is tempting to suggest conserved intra- but not inter-cladal phasing proportions, functional diversity of key physiological and biological properties is often difficult to assign to phylogenetic differences (Suggett et al. 2017). Comparing a larger number of strains is inevitably required to resolve the extent with which phylogeny may explain functional diversity (Suggett et al. 2015; Goyen et al. 2017). Cell cycle phasing proportions were particularly different for type D1a, which displayed a significantly lower G_2/M peak proportion and a population of larger cells with 3n DNA content. 3n/4n cells are not unusual in the cell cycle of *Symbiodinium* spp. but are typically rare in abundance (Freudenthal 1962; Fitt and Trench 1983; Wang et al. 2008). Based on studies from Freundenthal (1962) and Fitt and Trench (1983), 3n/4n cells have undergone complete karyokinesis and cytokinesis as they contain 3-4 distinct nuclei, separated into 3-4 cells but still held together by the parent cell wall. Interestingly, Wang et al. (2008) showed that constant light temporarily inhibited cytokinesis in a clade B *Symbiodinium* strain, leading to a substantial, transient increase in the abundance of 3n/4n stages. Hence, the *Symbiodinium* cell cycle was entrained by the light-dark photoperiod rather than an endogenous circadian clock and the dark period was shown to be an important cue for

cytokinesis into zoospores (G_1 phase cells). An interpretation of why type D1a formed more 3n stages under a regular 12 h light:12 h dark cycle than the other three strains is difficult without further experiments. However, it is possible that the uncoupling of biomass growth and DNA synthesis from final cytokinesis into multiple zoospores provides *Symbiodinium* (especially for the type D1a) with flexibility in optimizing growth under different growth conditions as they transition from endosymbionts in the host to free-living entity in the environment. However, to unravel the true biological relevance of 3n/4n stages and their control will require more targeted investigation.

Variability was observed in the proportion of cell cycle between strains with a higher proportion of G_1 phase correlating with higher growth rate. We also consistently observed that cells with a greater proportion of G_1 and higher growth rates were of generally smaller cells, which is typically seen for other eukaryotic algae (Cavalier-Smith 1978). In parallel to this, we observed a negative correlation between the G_2/M peak proportion and growth rate. The G_2/M phase precedes division and hence the G_2/M proportion typically relates to (and can be used to calculate) growth rate (Carpenter and Change 1988; see also, Chang and Carpenter 1988; Van Bleijswijk and Veldhuis 1995; Van Dolah et al. 2008). However, why we found different trends can be possibly explained by the complexity of the cell cycle patterns. Cells with 3n DNA content were observed especially in type D1a which had the highest growth rate but the lowest G_2/M peak proportion. In addition, 15-23% of G_2/M phase cells in the slower growth rate strains (C1 and C1′) appeared to stay in this phase for more than one full light cycle. As there are clear differences in the cell cycle patterns between types, population models that incorporate cell cycle information from *Symbiodinium* in culture (free-living) to understand the role of pre-mitotic control and the population

dynamics of *Symbiodinium* when *in hospite* will need to be specific to functional groups.

Lack of correlation between G_2/M and growth was further evident in attempting to identify differences between growth light intensity; specifically, the two light treatments did not yield significant differences between either G_2/M proportion or growth rate for the strains. From previous studies, it is clear that *Symbiodinium* growth rate can be influenced by changes in light intensity, for example, increased rates under higher light conditions for 180 vs. 15 μmol photon m^{-2} s^{-1} for *Symbiodinium* spp. isolated from *Aiptasia tagete*s, *Heteractis lucida*, and *Cassiopeia xamachana* (Fitt and Trench 1983), and 650 vs. 100 μmol photon m^{-2} s^{-1} for a broad range of ITS2-types from clades A, B and F (Hennige et al. 2009). However, this response is by no means universal, with other studies highlighting highly conserved growth rates across high and low light (e.g. clade A; Robison and Warner 2006). Most likely these differences reflect either complex confounding factors in the culture experiments, e.g. nutrient starvation (Rodríguez-Román and Iglesias-Prieto 2005) or more likely that certain types have a restricted breadth in light niche (Suggett et al. 2015), and hence growth rate becomes saturated at relatively low light intensities. Suggett et al. (2015) identified that strains B1 and D1a which have been used here fall into a similar "photobiological" (and growth) strategy best suited to "intermediate more cosmopolitan light regime types", which presumably would aid acclimation to broad light regimes (as likely commonly experienced as cells transition from free-living to *in hospite* light fields; Roth 2014). Thus, in our study, it is suggested that isolates acclimated to a three-fold increase in light intensity (80 vs. 262 μmol photon m^{-2} s^{-1} for low light and high light, respectively), therefore high light treatment is not enough to induce a change in growth

rate and ultimately cell cycle was constant throughout the light treatment. However, it is a possibility that growth and cell cycle will be affected with a magnitude order difference of the light levels as seen in differences of the light environment between free-living and symbiotic life stage of *Symbiodinium* (Jimenez et al. 2012; Wangpraseurt et al. 2012), thus further study is required.

Heat stress altered the cell cycle progression of all isolates, whereby the G_2/M proportion was significantly decreased and cells were arrested in G_1 phase, resulting in reduced cell proliferation. Addition of DCMU (inhibitor of photosynthesis) (Wang et al. 2008) and cerulenin (inhibitor of lipid synthesis) (Wang et al. 2013b) to *Symbiodinium* cultures was also found to arrest *Symbiodinium* cells in G_1 phase. G_1 arrest under stressful conditions is commonly observed in dinoflagellates (e.g. Zhang et al. 2014; Li et al. 2015) and other eukaryotic organisms (e.g. Nitta et al. 1997; Kühl and Rensing 2000; Lesser and Farrell 2004; Park et al. 2005) and represents the activation of the checkpoint pathway (Elledge 1996). For example, eukaryotic cells maintained in the light under heat stress exhibit up-regulation of cell cycle gene p53, which arrests the cells in G_1 phase for repair of DNA damage or initiate apoptosis (Evan and Littlewood 1998), including corals (Lesser and Farrell 2004). Arresting in G_1 phase was accompanied by the swelling (increased volume) of *Symbiodinium* cells. This symptom of stress was also previously observed in *Symbiodinium* cells exposed to elevated temperatures (30-34°C) and swelling was suggested to be an early (potentially reversible) stage of necrosis-like cell death (Strychar et al. 2004a). Therefore, it is possible that the checkpoint pathways which detect stress-related DNA damage (Elledge 1996) responded to arrest in G_1 phase to prevent replication of damaged templates which then manifested as abnormally large cells.

In spite of the lack of cell proliferation under heat stress, maximum photochemical efficiency only exhibited minor reductions indicating the presence of photosynthetically competent cells (e.g. Robison and Warner 2006; Suggett et al. 2008). Of the strains tested, type B1 was the most heat stress sensitive (greatest reduction of F_v/F_m) and D1a the least sensitive, as expected for these strains (see Goyen et al. 2017). Thus, growth and photosynthesis was clearly and consistently uncoupled across all strains, but with differing severity. McBride et al. (2009) observed that usually 80% of photosynthetically fixed carbon was used for proliferation of *Symbiodinium* cells under optimum temperatures, but was reduced to only ca. 10% under heat stress. Consequently, it is likely this reflects that energy typically derived from photosynthesis to drive growth must be diverted to alternate energy-consuming pathways (e.g. repair machinery or/and protection pathway) under heat stress (Robison and Warner 2006; Suggett et al. 2008). However, it is clear that the mechanisms underpinning such uncoupling of growth and photosynthesis warrant furthermore targeted study.

4.6. Conclusions

Our assessment of *Symbiodinium* culture strains has provided a baseline for cell cycle patterns of *Symbiodinium* free from host control. Cell cycle progression appears well-conserved across genetic types (species) and thus provides an improved baseline with which to consider cell cycle progression *in hospite* and hence better understand host control. Previous studies have identified phased division of *Symbiodinium in hospite* (Wilkerson et al. 1983; Hoegh-Guldberg and Smith 1989; Hoegh-Guldberg 1994; Fitt 2000; Dimond et al. 2013); however, almost all of these studies were based on a "mitotic index" (visual index of doublets or cells undergoing cytokinesis), providing

only a narrow window of cell cycle progression. For example, previous studies showed an increase in the mitotic index of *Symbiodinium in hospite* during increases in water temperature (Suharsono and Brown 1992; Bhagooli and Hidaka 2002; Strychar et al. 2004b). However, as mitotic indices are endpoint measurements, it is not possible to identify the underlying mechanisms responsible for the shift in growth rate. Application of cell cycle analysis is thus critical to understand how cell phases cycle, how stressor affects cell cycling (i.e. arresting in specific phases), cell proliferation and thus ultimately growth rates. Furthermore, it is known that intracellular pH (pH_i) regulates the eukaryotic cell cycle (Madshus 1988), and since pH_i differs across genetically distinct *Symbiodinium* types (Gibbin and Davy 2013), further characterisation of the *Symbiodinium* cell cycle in the context of other environmental pressures such as ocean acidification is required. This is particularly important as increased pCO_2 (decreased pH) has been shown to alter the growth rate of both free-living and endosymbiotic *Symbiodinium* (Brading et al. 2011; Towanda and Thuesen 2012). Given the differences in growth rate and cell cycle patterns between strains, any baseline will need to consider subtle changes associated with phylogeny. Examining more strains (as per Suggett et al. 2015; Goyen et al. 2017) will be needed to establish whether differences operate in a purely taxonomic sense or represent functional groupings that stem from localized environmental pressures (see Suggett et al. 2017).

Despite the ever-intensifying interest in resolving *Symbiodinium* biology (e.g. Davy et al. 2012; Frommlet et al. 2015; Suggett et al. 2017), few studies have yet examined the *Symbiodinium* cell cycle to resolve pre-mitotic control of *Symbiodinium* cell densities by their hosts (Smith and Muscatine 1999; Dimond et al. 2013). Growth status of *Symbiodinium* is important for maintaining a stable symbiosis with the host (e.g.

Cunning and Baker 2014). Consequently, application of cell cycle analysis to *Symbiodinium in hospite*, not only under steady-state conditions but also under periodic stress, is further needed to better understand mechanisms of maintenance and hence of breakdown of symbiosis at the level of individual cells.

4.7. Acknowledgements

The authors thank Mickael Ros and Nerissa Fisher for providing assistance with cell cycle sampling, David Hughes for assistance with FRRf measurements, Christian Evenhuis for assistance with cell volume measurements, and Paul Brooks for assistance with the experimental setup. Climate Change Cluster (University of Technology Sydney) and Yoshida Scholarship Foundation (Japan) contributed financial support for this study. Further support was provided by the Portuguese Foundation for Science and Technology (FCT/MCTES) and co-financed by FEDER (POCI-01-0145-FEDER-016748), within PT2020, and Compete 2020 through project "Symbiolite" (PTDC/MAR-EST/3726/2014). JF was supported by a FCT-funded postdoctoral fellowship (SFRH/BPD/111685/2015) and DJS was supported through an ARC Discovery Grant (DP160100271).

(This page is intentionally left blank)

Chapter 5

General Discussion: Synthesis, perspectives and future directions

5.1. Addressing knowledge gaps in free-living life stage of *Symbiodinium*

Free-living *Symbiodinium* populations fundamentally sustain coral reef ecosystems as the source material for endosymbiosis of many reef-building corals (e.g. Coffroth et al. 2006; Nitschke et al. 2016; Quigley et al. 2017) as well as trophic and biogeochemical structuring of the reef microbial biosphere (Frommlet et al. 2015). However, the underlying biodiversity and ecology of these free-living populations still largely remains a black box. Little is known about how free-living *Symbiodinium* communities are structured spatially, temporally (e.g. Sweet 2014; Granados-Cifuentes et al. 2015), and also regionally (temperate vs. tropical), and how those communities thereby ultimately contribute to shaping the flexibility and resilience of host-symbiont holobionts as reef ecosystems continue to decline (addressed in **Chapters 2 and 3**). Furthermore, how *Symbiodinium* population dynamics within these complex community structures are regulated and influenced by changing environmental conditions, which can determine the survival of *Symbiodinium* as well as the host-symbiont functional equilibrium (e.g. Davy et al. 2012) when *Symbiodinium* shift their life stage from free-living to symbiotic, is poorly understood. This is because information of *Symbiodinium* population (cell cycle) dynamics is still limited (Wang et al. 2008) (addressed in **Chapter 4**). Therefore in this thesis, the distribution, abundance and life cycle of free-living *Symbiodinium* were explored to advance understanding and fill these major knowledge gaps.

I applied novel dual NGS- and qPCR-based approaches to initially explore distribution and abundance of free-living *Symbiodinium* qualitatively and quantitatively for a well-studied tropical reef (Heron Island, 23°S), southern Great

Barrier Reef (**Chapter 2**), and a temperate coral community (Sydney Harbour, 33°S), east coast of Australia (**Chapter 3**). In these two chapters, free-living *Symbiodinium* community was assessed not only spatially but also temporally: spawning vs. summer season (**Chapter 2**) and pre-bleaching vs. bleaching (**Chapter 3**), to contrast diversity when host-symbiont recombination events are likely the highest through reproduction events and environmental stress events, respectively. **Chapters 2 and 3** revealed incredibly high diversity for both tropical and temperate free-living *Symbiodinium* communities and those communities were spatially complex and temporally dynamic. Such diversity is of course still only a snap shot of the population dynamics over time and does not convey how this genetic diversity is sustained through individual population turnover. To further address, this requires knowledge of how population dynamics are regulated across genetically and functionally diverse *Symbiodinium* species. Therefore in **Chapter 4**, I stepped back to the laboratory to establish a baseline for *Symbiodinium* cell cycle dynamics that represents the fundamental mechanism governing the population dynamics and life cycle for free-living unicellular microalgae (hence free from host control), and under different environmental scenarios also relevant to **Chapter 2** (light) and **Chapter 3** (heat stress). This analysis provides the first inter-cladal assessment of *Symbiodinium* cell cycle dynamics and the impact of environmental conditions on cell cycle progression, and therefore delivers significant new information on the contribution of free-living *Symbiodinium* to the coral reef ecosystem and regulation of population dynamics. The following discussion synthesizes the key findings from these novel studies and considers how they expand our knowledge and/or change our perspectives of the role of *Symbiodinium* in healthy coral reef functioning.

5.2. Key findings

Highly diverse free-living *Symbiodinium* communities were detected (eight clades from A to I except E) across water, sediment and macroalgae habitats at Heron Island reef (southern GBR, 23°S; **Chapter 2**). *Symbiodinium* community compositions were clearly separated by habitats where "transiently" free-living types (Yamashita and Koike 2013) were more abundant in the water column and upon macroalgae, whereas "exclusively" free-living types (Takabayashi et al. 2012) dominated in the sediment. *Symbiodinium* taxa specific to key coral hosts were always presented in the surrounding environmental habitats (and hence available to the hosts), presumably through continuous expulsion and hence population turnover by the hosts (e.g. Jones and Yellowlees 1997; Fujise et al. 2014), with the quantitative analysis (qPCR analysis for examining abundance of free-living *Symbiodinium*) revealing macroalgae as a key habitat for coral symbionts and a major reservoir likely aiding wider dispersal.

To verify whether such patterns for tropical reef systems are also maintained in temperate reef systems where coral diversity is lower (Veron 1993; Harriott and Banks 2002; Butler et al. 2010) and benthic ecological structuring very different (Zann 2000; Harriott and Banks 2002; Cresswell et al. 2017), *Symbiodinium* diversity and distribution were further examined for a high-latitude temperate reef (Sydney Harbour, 33°S; **Chapter 3**). This research provided the first ever baseline for community composition of *Symbiodinium* in high-latitude temperate reefs. Unique free-living *Symbiodinium* communities were detected, whereby the free-living *Symbiodinium* pool was strongly influenced by the dominant host assemblage (association with temperate specific *Symbiodinium* types), but also inherently

characterised by distinct temperate *Symbiodinium* taxa (including clade E, *Symbiodinium voratum*). In addition, community shifts were observed during the 2015/2016 El Niño heat wave-induced bleaching event with a decrease of clade E (*S. voratum*) frequency. Consequently, reef structure (hosts assemblage) and environmental conditions (not only globally but locally) shape the free-living *Symbiodinium* community.

Detailed knowledge of the free-living diversity and community structure from the neighbouring tropical (**Chapter 2**) and temperate (**Chapter 3**) reefs, which are periodically connected through seasonal extensions of the Eastern Australian Current (EAC) (Ridgway and Godfrey 1997; Ridgway and Hill 2009), provided a unique opportunity to further assess whether and how free-living *Symbiodinium* diversity may be shared between latitudes. Here, almost exclusive geographical separation of *Symbiodinium* genetic types was detected, with only 1% of OTUs being shared between two regions. This finding flags the importance of the free-living pools with specific types of *Symbiodinium* for persistence of coral hosts in specific area. This is crucial for high-latitude marginal reef systems, including those of southern eastern Australia (Baird et al. 2012; Beger et al. 2014), to act as refugia for tropical coral populations under future climate projections; more specifically, free-living populations also need to migrate together with hosts and adapt to marginal conditions to provide a source of symbionts which can associate with tropical corals.

Analysis of *Symbiodinium* cell cycle dynamics for free-living life stages across genetically distinct strains (species) (**Chapter 4**) revealed how diverse *Symbiodinium* populations are maintained over time via individual population turnover. Cell cycle

progression was conserved across species, and hence provides a reliable baseline for how cells proliferate through cell cycle phasing. However, cell cycle proportions differed between species, with a distinct cell cycle pattern detected for a key species, type D1a (*S. trenchii*), recognised to be highly stress resilient (e.g. LaJeunesse et al. 2014; Silverstein et al. 2015; Goyen et al. 2017). How such functional diversity further spans other ecologically key, but genetically diverse types of *Symbiodinium* is clearly warranted, and to identify how such differences contribute to ecological resilience. Furthermore, cell cycle progression was impacted by heat stress (cells commonly arrested in G_1 phase) for all tested species, revealing that environmental conditions supress growth at the individual cellular level.

The key findings of each chapter are summarised in a diagram (Fig. 5.1) on the following page.

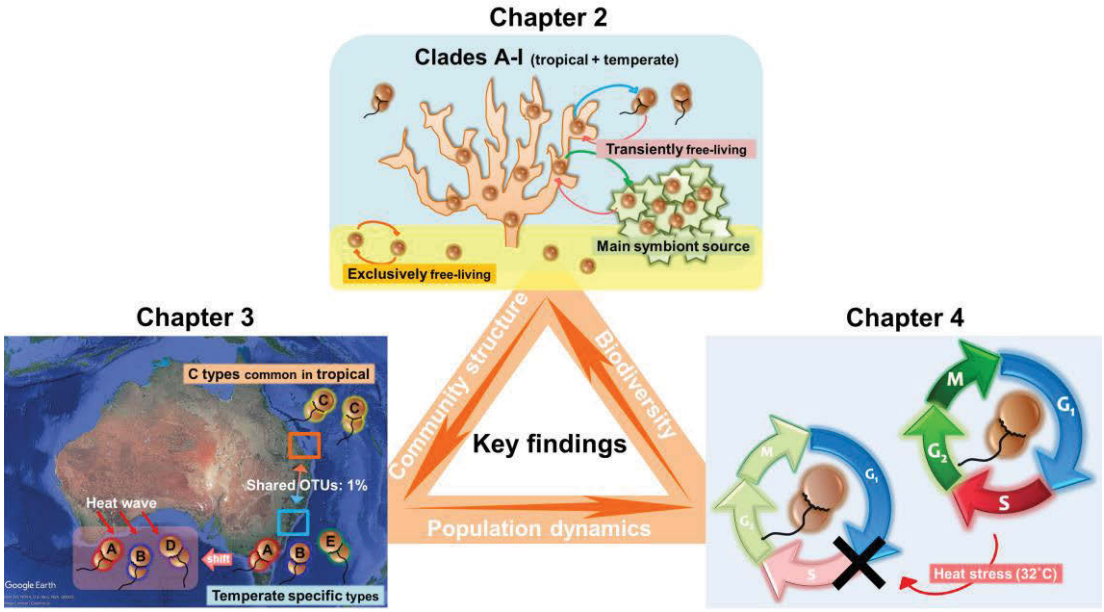

Figure 5.1. Key findings from the thesis. **Chapter 2**: Transiently free-living *Symbiodinium* mainly existed in water and macroalgae habitats (seems to be a main source of symbionts for hosts), in contrast, exclusively free-living types dominated in sediment. **Chapter 3**: Unique free-living populations (temperate specific types) dominated in the high-latitude temperate coral communities and the populations would shift due to an impact of the heat wave. **Chapter 4**: Cell cycle progressions of *Symbiodinium* were conserved across species, but proportions differed by species. Heat stress arrested cells in G_1 phase and supressed the growth. Arrows indicate the linkages between the chapters: Chapter 1 → 2: **Community structure** of free-living *Symbiodinium* is shaped by reef structures and environmental conditions; Chapter 2 → 3: **Population dynamic** seems to contribute for regulating community structure of *Symbiodinium* via cell cycle; Chapter 3 → 1: **Biodiversity** of free-living *Symbiodinium* is maintained via individual population turnover.

5.3. Synthesis and perspectives

Together, these findings can be synthesised around consideration of **vectors of population propagation** to better understand how free-living *Symbiodinium* populations contribute to coral reef ecosystems as they face this era of "ecological crisis" (Suggett et al. 2017). The first vector driving how free-living *Symbiodinium* communities are structured and function is **habitat variety**. As with other reef taxa, habitat variety is clearly important in maintaining and sustaining diverse pools of free-living *Symbiodinium*. Indeed, each habitat (water, sediment and macroalgae) possesses a variety of genetic types (= niche separation for types) and creates different free-living community that operates along the continuum of life history, from transient to exclusively free-living, within the ecosystem. Genetic diversity is critically important for physiological/functional plasticity (Stat et al. 2006; Stat et al. 2009b; Lesser et al. 2013) and positively associated with the degree of resistance to disturbance (Hughes and Stachowicz 2004; Pauls et al. 2013; Boulotte et al. 2016). Thus, habitat variety which structures diverse free-living pools would be a key for providing "biological insurance" against environmental change (Hughes and Stachowicz 2004) and ultimately surviving in the era of ecological crisis (Suggett et al. 2017).

Macroalgal habitats appear to be the most important habitat for free-living *Symbiodinium*, both qualitatively (community composition) and quantitatively (cell abundance), and thus likely a critical niche linking *Symbiodinium* life stages (free-living and symbiotic) (**Chapter 2**). My analysis confirms that a balanced presence of macroalgae is critical to the long-term viability of free-living population persistence – not only for fuelling new generations of endosymbionts, but also for the

exclusively free-living pool, whose roles and contributions to coral reef functioning are still largely unexplored. Healthy reefs exhibit a careful balance between macroalgae and coral abundance; for example, overly high abundance of macroalgae within reef systems can negatively impact coral fitness and survival (Tanner 1995; Lirman 2001; McCook et al. 2001; Kuffner et al. 2006; Bonaldo and Hay 2014), and thus the health of entire reef systems (Done 1992; Hughes 1994; Hughes et al. 2010; van de Leemput et al. 2016). However, in well balanced coral reefs, macroalgae play important roles and benefits, including provision of a major food source for various herbivores and also secreting organic carbon into the water column to fuel bacterial communities (Diaz-Pulido and McCook 2008). Maintenance of coral dominated reefs, where macroalgae are beneficial components, depends to a large extent on herbivorous fish for balancing coral-macroalgae abundance (Hughes et al. 2010; van de Leemput et al. 2016). Such herbivorous fish is also considered to have a key role in the dispersal of free-living *Symbiodinium* by ingesting macroalgae possessing large abundances of associated *Symbiodinium* (Porto et al. 2008; Castro-Sanguino and Sánchez 2012). Therefore, macroalgae are not only important for habitats of free-living *Symbiodinium*, but also for potential dispersal agents.

Such a step, that macroalgae and also herbivorous fishes seem to be important agents for dispersal of *Symbiodinium*, may be critical to a secondary vector **tropicalisation** of high-latitude temperate reef, which has been proposed as potential refugia for tropical corals (e.g. Beger et al. 2014; Cacciapaglia and Woesik 2015; Tuckett et al. 2017) and result in community structure changes from macroalgal- to coral-dominated (Vergés et al. 2014). Whilst there are reports of poleward expansion of tropical corals to high-latitude reefs correlated with increased water temperature

(e.g. Florida: Precht and Aronson 2004, Japan: Yamano et al. 2011), including eastern Australia (Baird et al. 2012), my findings highlighted clear geographical separation of *Symbiodinium* taxa between the tropical and temperate east coast of Australia (from southern GBR to Sydney) (**Chapter 3**). Corals with horizontal transmission symbionts require a source of suitable free-living *Symbiodinium* types to migrate from tropical to temperate reefs – so the question here is how will tropical *Symbiodinium* communities migrate to enable specific host-symbiont associations to persist? The answer may in fact lie with macroalgae as key dispersal agents acting as stepping stones for migration of free-living *Symbiodinium*. Herbivorous fishes would enhance the long-distance dispersal and many tropical herbivores are already known to migrate (as Eastern Australian Current vagrants) annually from tropical to temperate waters such as Sydney Harbour (Booth et al. 2007; Vergés et al. 2014; Basford et al. 2016). Examining free-living *Symbiodinium* communities and the role of macroalgae and herbivores as dispersal agents at the front line of temperate-tropical reef boundaries (e.g. Coffs Harbour in eastern Australia) is therefore a logical next step.

Even if species successfully migrate, populations need to turnover and persist within marginal environments such as temperate reef boundaries to contribute to reef system resilience. I found that population dynamics, especially the cell cycle proportion which relates to growth rates of *Symbiodinium*, differed between genetically different strains (species) (**Chapter 4**). As such, the third vector sustaining population propagation is **functional trait diversity**. Within their immense phylogenetic diversity, *Symbiodinium* are also highly functionally diverse (e.g. Stat et al. 2008a; Suggett et al. 2017), and therefore a functional trait based approach is important to

connect taxonomic diversity to ecological resilience. Based on my findings, I therefore propose that differences in **cell cycle dynamics** by genetic types would comprise a key functional trait since it governs population turnover (hence population dynamics). Here, specific types (e.g. clade D types) proliferate faster under certain environmental conditions (e.g. increased water temperature, **Chapter 4**) (also *in hospite*; e.g. Núñez-Pons et al. 2017), thereby driving community shifts (**Chapter 3**) whilst simultaneously resisting stress disturbance. Furthermore, Suggett et al. (2017) recently suggested "resource acquisition and utilization" as key functional traits to define functional diversity of *Symbiodinium*. These key traits together with cell cycle dynamics would determine competitive fitness and resolve niche boundaries for *Symbiodinium* both as free-living and *in hospite*, thus help to reconcile ecological success over space and time.

5.4. Future directions

In unlocking this new insight into free-living *Symbiodinium* diversity and its contribution to health reef functioning, a key set of new questions arise:

(1) Detailed examination of free-living *Symbiodinium* populations associated with macroalgae habitats.

Whilst work in this thesis highlights the importance of macroalgae habitats for sustaining pools of coral endosymbionts, it is clear that more insight is needed to fully characterise the functional roles macroalgae habitats play in sustaining free-living *Symbiodinium* cells, e.g. nutritional and resource exchange. The few studies to date that have examined communities of free-living *Symbiodinium* associated with macroalgae (Porto et al. 2008; Venera-Ponton et al. 2010;

Granados-Cifuentes et al. 2015), including work in this thesis, have only identified *Symbiodinium* species diversity. More comprehensive study is specifically required to characterise finer scale community composition (e.g. highly taxonomically resolute as per **Chapters 2 and 3**) alongside quantitative observations of *Symbiodinium* across various macroalgae species (over time and space) is an obvious next point of focus to further resolve how macroalgae serve as habitats. Identifying the potential role of *Symbiodinium* in nutrient exchange with associated macroalgae whilst residing within the surface microbiome (e.g. NanoSIMS; Pernice et al. 2012; Kopp et al. 2013) would be a logical step to better understand the interaction between macroalgae and *Symbiodinium*, and also the transient nature of *Symbiodinium* in this life history stage. Furthermore, infection tests of corals with the presence/absence of macroalgae are also important to examine the potential of macroalgae as a source of endosymbiont species capable of initiating symbiosis (e.g. Nitschke et al. 2016 has previously demonstrated this for sediments). Finally, more studies will be required to better understand the dispersal role of herbivorous fishes feeding on macroalgae, which little is known (Porto et al. 2008; Castro-Sanguino and Sánchez 2012). For example, clarifying important herbivorous fish species, dispersal distance, finer taxonomic composition of *Symbiodinium* in faeces, survivability of ingested *Symbiodinium*, and capacity for infection to new hosts, together likely underpin the capacity of free-living *Symbiodinium* to migrate from tropical to temperate regions over broad scales.

(2) Exploration of free-living *Symbiodinium* diversity across locations with fine scale spatial resolution.

We now know that the diversity and structure of free-living *Symbiodinium* communities are distinct between regions (tropical vs. temperate), and that genetic identities are geographically separated, despite periodic connectivity between sites by the Eastern Australian Current. However, to further understand the potential of high-latitude temperate reef to act as refugia for tropical corals, we need to focus on dispersal of free-living *Symbiodinium* (from tropical to temperate regions), and importantly survival and turnover where they arrive into areas where environmental conditions are very different from their origin. To do this, we must first identify the current edges of separation of free-living population across latitudes, or more specifically across dynamic biogeographical boundaries. Exploring free-living *Symbiodinium* community in reefs that are in a state of transition with a mixture of tropical and temperate hosts exist (such as, Solitary Island Marine Reserve including Coffs Harbour; Harriott et al. 1994; Zann 2000) will be an essential point of focus.

(3) Application of cell cycle analysis to a broader diversity of *Symbiodinium* in both free-living and *in hospite* states.

To fully investigate and resolve functional traits and thus understand functional diversity of *Symbiodinium*, it is inevitably required for examining more strains/species (Suggett et al. 2015; Goyen et al. 2017). In the case of cell cycle dynamics, this may ultimately rest on how well we can improve collections of free-living *Symbiodinium* for species that commonly associate with key coral taxa (see Suggett et al. 2017). Even so, it is important to understand how the *Symbiodinium* population (cell cycle) dynamics are controlled by the coral host, not

only to clarify mechanisms employed to maintain functional equilibrium under steady-state symbioses (Smith and Muscatine 1999; Dimond et al. 2013), but also to examine the impact of stress-induced breakdown of the stable relationship that are becoming increasingly frequent and intense (e.g. Hughes et al. 2018).

5.5. Concluding remarks

In conclusion, this thesis unveils the mysterious life stage of free-living *Symbiodinium* by exploring their **distribution, abundance and life cycle** to provide new insights as to how those populations are structured spatially, temporally and regionally, and thus ultimately contributing to coral reef resilience. Free-living populations appear immensely genetically diverse and my research has improved our knowledge that such diversity is sustained by inherent variety of environmental habitats and conditions. I have revealed that macroalgae habitats should be considered as key habitats for connecting free-living and symbiotic life stages of many *Symbiodinium* taxa, and providing the potential as critical dispersal agents of *Symbiodinium* to migrate, including to refugia. *Symbiodinium* population turnover through cell cycle progression appears to vary across species, thereby suggesting a key role for this process (as a functional trait) in contributing to ecological success, and how selection amongst species supports persistence of reef resilience over space and time. Free-living *Symbiodinium* comprise crucial populations for maintaining healthy coral reef systems, and this thesis sheds new light on how such populations may be critical to the persistence of reefs under an increasingly uncertain future.

Appendix: OTU analysis for *Symbiodinium* culture strains

Background and rationale

Symbiodinium as a genus is taxonomically, physiologically and functionally diverse (e.g. Rowan 1998; LaJeunesse 2001; Stat et al. 2006; LaJeunesse et al. 2012a; LaJeunesse 2017), with research to date particularly focussing on how patterns of *Symbiodinium* community diversity potentially shape coral reef functioning *in hospite* of corals (LaJeunesse et al. 2003; 2004; Tonk et al. 2017) and as free-living cells (Yamashita and Koike 2013; Cunning et al. 2015; Quigley et al. 2017). Assessments of *Symbiodinium* genetic diversity have most commonly used the internal transcribed spacer 2 (ITS2) region of nuclear rDNA, since variation of ITS2-types correlates with physiological and ecological attributes (e.g. LaJeunesse 2001; 2002; 2004; Sampayo et al. 2009). Extensive databases are now available for assigning ITS2 sequences to putative taxonomic diversity (e.g. "SymTyper" which contains 719 ITS2 sequences; Cunning et al. 2015; Boulotte et al. 2016). Therefore, the ITS2 marker is considered useful for exploring unknown diversity, such as free-living *Symbiodinium* diversity (as per Chapters 2 and 3).

Unfortunately, the multi-copy nature of rDNA gene (ITS2 is part of the tandemly-repeated rRNA array) results in intra-genomic variations that affect estimates of *Symbiodinium* biodiversity based purely on ITS2 sequences (Thornhill et al. 2007; Sampayo et al. 2009; Arif et al. 2014). Indeed, Thornhill et al. (2007) assessed the intra-genomic variation and sequence divergence of rDNA genes (ITS2 region) within *Symbiodinium* clonal culture strains and suggested that if the ITS2 sequence variants were each assigned to individual *Symbiodinium* types/species, diversity would be

overestimated by 4 to10-fold relative to the genetic composition of the clonal cell lines (i.e. a single biological entity). Thus, to minimise the influence of intra-genomic variants on estimating *Symbiodinium* biodiversity based on the ITS2 marker, especially when derived by next generation sequencing (NGS) which can collect massive amounts of sequences in parallel from bulk community samples, an OTU (operational taxonomic unit) approach is useful: Arif et al. (2014) demonstrated that clustering sequences (from a high-throughput ITS2 amplicon sequencing) at a 97% similarity threshold could successfully collapse intra-genomic variants into distinct OTUs (by testing with mono-clonal cultures: types A1, B1 and C1). Such an OTU framework phylogenetically and ecologically provides the platform for examining taxonomic resolution and functional variability (Stat et al. 2015) and thus has been increasingly applied to studies of *Symbiodinium* diversity *in hospite* (e.g. Stat et al. 2013; 2015; Lucas et al. 2016; Smith et al. 2017; Ziegler et al. 2017) and in the environment as free-living cells (Cunning et al. 2015; Quigley et al. 2017; Chapters 2 and 3).

While the OTU approach has been widely used based on the observations of Arif et al. (2014) at the 97% cut-off using mono-clonal cultures across clades A, B and C, it has not been validated for clades identified as free-living within this thesis (e.g. clades A-F). I therefore revisited the analysis of Arif et al. (2014), but using more variety of culture strains (14 mono-clonal cultures across clades A, B, D, E and F) to ensure we have minimised the influence of intra-genomic variations and sequencing/PCR noise. This is critical for estimating diversity of free-living *Symbiodinium* which is assumed to contain variety of taxa and functional groups (as per Chapters 2 and 3) and important to check the utility of the approach using culture strains as standards for applying to the field samples.

Next generation sequencing analysis of *Symbiodinium* culture strains

Total genomic DNA was extracted from 14 culture strains of *Symbiodinium* (Table 6.1) using the Wizard DNA prep protocol (Promega, WI, USA). Extracted DNA was submitted to MR DNA (Molecular Research LP, TX, USA) and amplicon sequencing (bTEFAP®) was performed using the ITS2 primer set, ITSD (5′-GTGAATTGCAGAACTCCGTG-3′; Pochon et al. 2001) and ITS2rev2 (5′-CCTCCGCTTACTTATATGCTT-3′; Stat et al. 2009b), that targets the partial 5.8S, entire ITS2, and partial 28S region of nuclear ribosomal DNA of *Symbiodinium*, on the Illumina Miseq platform (Illumina, CA, USA) (2 × 300 paired end).

Table 6.1. *Symbiodinium* culture strains used for the NGS analysis. *I included two identical strains of CCMP2548 (*S. natans*) (X and Y). **SG_37 and SG_40 were isolated from *Plesiastrea versipora*, but the isolates were possibly surface contaminants from the environment, because *P. versipora* was dominated by B18-like types based on the NGS analysis of *in hospite* samples (see Chapter 3, section 3.4.7).

Clade/ITS2-type		Sample label	Species	Identity	Geographic origin	Host taxa
A	A2	CCMP2461	*S. pilosum*	CCMP2461, RT185	Jamaica (Caribbean)	*Zoanthus sociatus* (Zoanthid)
	A2-relative	CCMP2548_X*	*S. natans*	CCMP2548, RT796	Hawai‘i (Pacific)	Free-living
	A2-relative	CCMP2548_Y*	*S. natans*	CCMP2548, RT796	Hawai‘i (Pacific)	Free-living
	A3	CCMP2430	*S. tridacnidorum*	CCMP2430	One Tree Island (Pacific)	*Tridacna maxima* (Giant clam)
	A13	CCMP2469	*S. necroappetens*	CCMP2469, RT80	Jamaica (Caribbean)	*Condylactis gigantea* (Sea anemone)
	-	CCMP2592	*Symbiodinium* sp.	CCMP2592	One Tree Island (Pacific)	*Heliofungia actiniformis* (Coral)
B	B2	SG_37**	*S. psygmophilum*	SG 37	Sydney Harbour (Pacific)	*Plesiastrea versipora* (Coral)
	B2	SG_40**	*S. psygmophilum*	SG 40	Sydney Harbour (Pacific)	*Plesiastrea versipora* (Coral)
D	D1a	CCMP2556	*S. trenchii*	CCMP2556	Florida Key (Caribbean)	*Montastraea faveolata* (Coral)
	D1a	CCMP3408	*S. trenchii*	CCMP3408, RD03	Okinawa (Pacific)	*Acropora* sp. (Coral)
E	-	SVFL_1	*S. voratum*	SVFL 1	Jeju Island (Pacific)	Free-living
	-	SVIC_1	*S. voratum*	SVIC 1	Jeju Island (Pacific)	*Alveopora japonica* (Coral)
F	F1	CCMP2468	*S. kawagutii*	CCMP2468, RT135	Hawai‘i (Pacific)	*Montiprora verrucosa* (Coral)
	-	CCMP2434	*Symbiodinium* sp.	CCMP2434	One Tree Island (Pacific)	*Leptastrea purpurea* (Coral)

OTU analysis at the 97% similarity cut-off

The bioinformatic pipeline is described in Chapter 2 (section 2.3.4) and the detailed pipeline including tools used for the bioinformatic analysis for MiSeq sequences can be found in the following link: Paired end (ITS2) (Kahlke and Fujise 2017): https://doi.org/10.17605/osf.io/hcsp4.

To briefly show the protocol, paired end sequences were demultiplexed, forward and reverse sequences were joined, and quality filtered. To follow the exact protocol used for the field samples, possible non-*Symbiodinium* sequences were removed and then subjected to OTU analysis at 85% similarity cut-off to separate sequences by clade followed by OTU analysis at 97% similarity cut-off for each clade (Arif et al. 2014). OTU taxonomies were assigned using BLAST against the *Symbiodinium* ITS2 reference database "SymTyper" (e.g. Cunning et al. 2015; Boulotte et al. 2016). For additional de-noising step, OTU relative abundance filtering was performed and removed OTUs which contain < 1% reads within each sample to remove spurious OTUs generated by sequencing and PCR errors (e.g. Degnan and Ochman 2012).

Exact sequence variance (zOTU) analysis

Exact sequence variants, also called zero-radius operational taxonomic units (zOTUs) analysis was performed to assess the intra-genomic variation within each culture strain. zOTUs were identified using the QIIME2 framework (Caporaso et al. 2010) and the DADA2 (Callahan et al. 2016) plugin. Forward and reverse read sequences were trimmed to 260 and 220 nucleotides, respectively, using the *--p-trunc-len-f* and *--p-trunc-len-r* parameters. Of the resulting zOTUs only those accounting for ≥1% of the

reads per sample were used in the analysis. Taxonomic classification of representative sequences was performed using a naïve bayes classifier that was trained on a custom ITS2 database. This database includes the complete ITS2 database (Merget et al. 2012) as well as the SymTyper sequences and was further manually curated to remove duplicate sequences and sequences with ambiguous nucleotides. After taxonomic classification, non-*Symbiodinium* sequences were removed from the representative sequences. Sequences for which the classifier did not assign taxonomies below family level were manually investigated using BLAST against SymTyper. Intra-genomic variation was estimated for each culture strain as follows: first all representative sequences (≥1% reads per sample) of a culture strain were aligned with mafft v7 (Katoh and Standley 2013) using *einsi* settings. Second, the percent identity was calculated for all n^2-n pairwise sequence comparisons as the percentage of identical nucleotides in the first sequence.

Outcomes from OTU analysis at the 97% similarity cut-off

Majority of sequences (> 80%) collapsed into one OTU and the representative sequences were assigned to the ITS2 variants which closely related to the expected types of each strain (Table 6.2). However, 24-41 OTUs were detected within each strain and OTUs accounting for < 1% of the reads within each sample were the random OTUs from other clades, which possibly reflected noise, e.g. cross-contamination during sequencing, PCR artifacts of sequencing errors. Note that the negative control did not generate any sequences; sequencing errors; PCR artifacts, etc.

To minimise the influences of potential sources of noise, I performed OTU abundance filtering as an additional denoising step by removing OTUs that contain < 1% of the

Table 6.2. OTU table (97% cut-off) for *Symbiodinium* culture strains. Top three OTUs (based on the number of sequences within each strain) are highlighted with colours and OTUs which contain ≥ 1% of the reads within each sample are shown as bold. Colour coding: red for clade A, blue for clade B, yellow for clade C, purple for clade D, green for clade E, and orange for clade F.

Clade	OTU ID	Taxonomy	CCMP2461	CCMP2548_X	CCMP2548_Y	CCMP2430	CCMP2469	CCMP2592	SG_37	SG_40	CCMP2556	CCMP3408	SVFL_1	SVIC_1	CCMP2468	CCMP2434
			clade A	clade A	clade A	clade A	clade A	clade A	clade B	clade B	clade D	clade D	clade E	clade E	clade F	clade F
A	OTU_A_35	A1	0	1	0	0	178	0	0	0	0	0	0	0	0	1
A	OTU_A_7	A1	9	5	2	2	11	5	6	5	7	4	7	3	1	7
A	OTU_A_19	A1.3	0	53	3	0	0	0	0	0	0	0	0	0	0	0
A	OTU_A_1	A3	0	0	0	13	0	0	0	0	0	0	0	0	0	0
A	OTU_A_5	A3	71	45	45	**35,087**	94	129	51	55	52	8	29	37	34	53
A	OTU_A_45	A5	0	0	0	0	0	4	0	0	0	0	0	0	0	0
A	OTU_A_6	A5	54	55	33	72	78	**43,250**	40	37	40	6	23	16	34	69
A	OTU_A_15	A101	**50,898**	65	44	67	60	78	34	46	62	16	33	27	30	84
A	OTU_A_23	A101	36	0	0	0	0	0	0	0	0	0	0	0	0	0
A	OTU_A_24	A101	60	6	0	0	1	1	24	33	4	3	5	0	0	0
A	OTU_A_47	A109	0	0	0	0	26	0	0	0	0	0	0	0	0	1
A	OTU_A_10	A113	0	**514**	**736**	1	2	2	2	1	1	0	0	0	2	0
A	OTU_A_11	A113	0	96	93	0	0	1	0	0	1	0	0	1	0	0
A	OTU_A_29	A113	2	141	105	0	1	0	0	0	0	0	0	0	0	0
A	OTU_A_36	A113	1	**632**	**688**	0	1	2	3	1	0	0	0	2	0	0
A	OTU_A_4	A113	100	**40,975**	**29,701**	82	100	108	101	63	86	23	41	35	68	100
A	OTU_A_46	A113	0	18	27	0	0	0	0	0	0	0	0	0	0	0
A	OTU_A_57	A113	1	98	151	1	0	0	0	1	1	0	0	0	0	0
A	OTU_A_41	A127	0	0	0	3	2	1	1	0	0	0	0	0	0	0
A	OTU_A_28	A128	1	0	0	0	0	0	0	0	0	0	0	0	0	0
A	OTU_A_3	A13	113	31	73	117	**39,261**	153	76	55	68	15	36	37	65	88
A	OTU_A_16	A133	0	1	0	0	0	2	1	0	0	0	0	0	0	0
A	OTU_A_2	A133	82	77	56	51	84	92	83	52	56	18	32	30	40	76
A	OTU_A_14	A134	5	0	0	0	1	0	0	0	0	0	0	0	0	0
A	OTU_A_60	A135	90	0	0	0	1	0	0	1	1	0	0	0	0	0
A	OTU_A_61	A135	34	0	0	1	0	0	0	0	0	0	0	0	0	0
A	OTU_A_8	A135	24	0	0	0	0	0	0	0	0	0	0	0	0	0
B	OTU_B_10	B1	1	0	11	21	24	0	107	89	60	3	2	1	2	67
B	OTU_B_11	B1	0	0	1	0	0	0	6	3	2	2	0	0	0	1
B	OTU_B_14	B1	34	30	25	14	37	59	54	61	49	8	46	62	75	61
B	OTU_B_15	B1	11	11	5	6	8	9	48	55	21	9	13	11	13	26
B	OTU_B_16	B1	2	0	0	0	1	1	2	1	0	0	0	1	0	5
B	OTU_B_22	B1	0	0	0	0	0	0	0	0	1	0	0	0	0	0
B	OTU_B_27	B1	0	0	0	0	0	0	0	1	0	0	0	0	0	0
B	OTU_B_35	B1	0	0	0	0	0	0	1	0	0	0	0	0	0	0
B	OTU_B_7	B1	2	0	4	2	1	0	7	8	6	1	2	1	0	4
B	OTU_B_9	B1	0	28	13	15	0	0	98	87	0	8	15	0	0	0
B	OTU_B_1	B2	0	0	0	0	1	1	132	111	0	0	0	1	0	0
B	OTU_B_21	B2	0	0	0	0	0	1	2	4	0	0	0	0	0	0
B	OTU_B_30	B2	0	0	0	0	0	0	36	24	0	0	0	0	0	0
B	OTU_B_5	B2	0	1	0	0	0	0	2	1	1	0	0	0	0	0
B	OTU_B_6	B2	117	85	86	74	102	85	**57,534**	**53,780**	154	52	96	74	111	186
B	OTU_B_26	B5	0	0	2	1	0	1	39	3	1	3	1	1	0	0
B	OTU_B_33	B5	5	4	8	1	6	8	3	11	15	1	0	4	13	16
B	OTU_B_29	B19	37	0	0	0	0	0	36	188	1	0	0	3	0	0
B	OTU_B_34	B19	0	0	1	0	0	0	0	0	0	0	0	0	0	0
B	OTU_B_4	B114	0	0	0	0	0	0	0	3	0	0	0	0	0	0
B	OTU_B_43	B114	0	4	0	1	1	0	**604**	487	3	0	1	0	2	1
C	OTU_C_2	C7	0	0	0	0	0	0	0	0	0	0	1	0	0	0
C	OTU_C_3	C131	0	0	21	0	0	0	9	0	0	11	0	0	1	0
D	OTU_D_2	D1	78	74	43	53	40	61	93	114	**80,569**	127	150	122	114	145
D	OTU_D_3	D1a	29	21	9	18	21	12	65	42	7	**23,834**	28	11	35	47
D	OTU_D_10	D2	1	1	1	0	0	2	2	1	721	1	1	1	3	0
D	OTU_D_1	D120	0	0	0	0	0	0	1	1	0	103	1	1	0	1
E	OTU_E_1	E105	99	74	37	53	48	74	81	80	163	45	**65,881**	**55,732**	97	164
E	OTU_E_15	E105	1	2	6	3	12	2	22	11	19	7	0	0	4	10
E	OTU_E_2	E107	32	14	14	13	15	17	17	31	48	12	**14,152**	**11,640**	32	34
E	OTU_E_18	E109	0	0	0	0	0	1	0	0	0	0	510	40	0	0
E	OTU_E_9	E109	0	0	0	0	0	0	0	0	0	0	326	207	0	1
E	OTU_E_19	E111	1	0	0	0	0	0	1	0	2	0	138	447	0	1
E	OTU_E_5	E111	1	0	0	0	0	0	1	0	3	0	708	477	0	1
F	OTU_F_12	F5.1	0	0	0	0	0	0	1	0	0	0	0	0	6	1
F	OTU_F_2	F5.1	0	1	0	0	0	1	0	0	1	0	0	0	230	1
F	OTU_F_4	F5.1	125	87	55	52	79	67	137	133	163	56	119	94	**47,348**	**83,948**
F	OTU_F_16	F5.2	0	0	0	0	0	0	0	0	0	0	0	1	0	13
F	OTU_F_1	F5.2e	0	0	0	0	0	0	0	0	0	0	0	0	0	8
F	OTU_F_15	F5.2e	0	0	0	0	0	0	0	0	0	0	0	0	0	2
		Total sequences	52,157	43,250	32,099	35,824	40,297	44,230	59,563	55,680	82,389	24,376	82,397	69,120	48,360	85,223
		Number ot OTUs	34	32	32	27	31	31	41	38	34	26	28	31	24	33
		Top 1 (% seqs in total)	98%	95%	93%	98%	97%	98%	97%	97%	98%	98%	80%	81%	98%	99%
		Top 2 (% seqs in total)	0.24%	1.5%	2.3%	0.33%	0.44%	0.35%	1.0%	0.87%	0.88%	0.52%	17%	17%	0.48%	0.22%
		Top 3 (% seqs in total)	0.22%	1.2%	2.1%	0.23%	0.25%	0.29%	0.23%	0.34%	0.20%	0.42%	0.86%	0.69%	0.24%	0.19%

reads within each sample. I choose abundance filtering by each sample to account for heterogeneity of read depths and sample features (for example, host samples: dominated by a few OTUs (biological entities) vs. environmental samples: contain various OTUs) to consider how such a step could be applied to the field samples. Applying the OTU abundance filtering step successfully eliminated noise from the other clades, such that the majority of strains (9/14 strains) resulted in one OTU per strain with expected taxonomy (ITS2 variants: A101 (closely related to ITS2-type A2: *S. pilosum*), A113 (closely related to A2-relative: *S. natans*), E105 and E107 (both variants belong to *S. voratum*)) (Table 6.3). CCMP2548 (*S. natans*) resulted in three OTUs per strain (all assigned to the same ITS2 variants A113) and SG_37 (*S. psygmophilum*) in two OTUs per strain (B2 and B114 (closely related to B2)), but second and third abundant OTUs were just above the abundance filtering threshold (1.0-2.4%). However, both clade E strains (*S. voratum*: SVFL_1 and SVIC_1) contained two OTUs with the second OTU accounting for 18% and 17% of the reads within each sample, respectively.

Table 6.3. OTU table (97% cut-off) for *Symbiodinium* culture strains after applying OTU abundance filtering. OTUs which contain < 1% of the reads within each sample were replaced by 0 and removed from the OTU table if those OTUs contain 0 sequence across all samples. OTUs contain sequences are highlighted with colours.

			CCMP2461	CCMP2548_X	CCMP2548_Y	CCMP2430	CCMP2469	CCMP2592	SG_37	SG_40	CCMP2556	CCMP3408	SVFL_1	SVIC_1	CCMP2468	CCMP2434
Clade	OTU ID	Taxonomy	clade A	clade A	clade A	clade A	clade A	clade A	clade B	clade B	clade D	clade D	clade E	clade E	clade F	clade F
A	OTU_A_15	A101	50,898	0	0	0	0	0	0	0	0	0	0	0	0	0
A	OTU_A_4	A113	0	40,975	29,701	0	0	0	0	0	0	0	0	0	0	0
A	OTU_A_36	A113	0	632	688	0	0	0	0	0	0	0	0	0	0	0
A	OTU_A_10	A113	0	514	736	0	0	0	0	0	0	0	0	0	0	0
A	OTU_A_5	A3	0	0	0	35,087	0	0	0	0	0	0	0	0	0	0
A	OTU_A_3	A13	0	0	0	0	39,261	0	0	0	0	0	0	0	0	0
A	OTU_A_6	A5	0	0	0	0	0	43,250	0	0	0	0	0	0	0	0
B	OTU_B_6	B2	0	0	0	0	0	0	57,534	53,780	0	0	0	0	0	0
B	OTU_B_43	B114	0	0	0	0	0	0	604	0	0	0	0	0	0	0
D	OTU_D_2	D1	0	0	0	0	0	0	0	0	80,569	0	0	0	0	0
D	OTU_D_3	D1a	0	0	0	0	0	0	0	0	0	23,834	0	0	0	0
E	OTU_E_1	E105	0	0	0	0	0	0	0	0	0	0	65,881	55,732	0	0
E	OTU_E_2	E107	0	0	0	0	0	0	0	0	0	0	14,152	11,640	0	0
F	OTU_F_4	F5.1	0	0	0	0	0	0	0	0	0	0	0	0	47,348	83,948
		Total sequences	50,898	42,121	31,125	35,087	39,261	43,250	58,138	53,780	80,569	23,834	80,033	67,372	47,348	83,948
		Number ot OTUs	1	3	3	1	1	1	2	1	1	1	2	2	1	1
		Top 1 (% seqs in total)	100%	97%	95%	100%	100%	100%	99%	100%	100%	100%	82%	83%	100%	100%
		Top 2 (% seqs in total)		1.5%	2.4%				1.0%				18%	17%		
		Top 3 (% seqs in total)		1.2%	2.2%											

Outcomes from exact sequence variance (zOTU) analysis

As observed for the OTU analysis at the 97% cut-off, each strain contained dominant zOTUs that assigned to the expected taxonomy (plus random zOTUs from the other clades; see Appendix E6.1 for zOTU table). Therefore, I further applied the OTU abundance filtering with the 1% threshold (see Appendix E6.2 for zOTU table after abundance filtering) and calculated the percent identity to assess sequence variations within each strain. All tested strains, except for two clade E strains, showed > 97% percent identity between sequence variants within each strain (Fig. 6.1), thus further supporting the OTU analysis at the 97% cut-off can successfully collapse intra-genomic variations into a distinct OTU cluster. Percent identity of clade E strains (SVFL_1 and SVIC_1) were 94 ± 4.2% and 95 ± 4.3% (average ± SD), respectively.

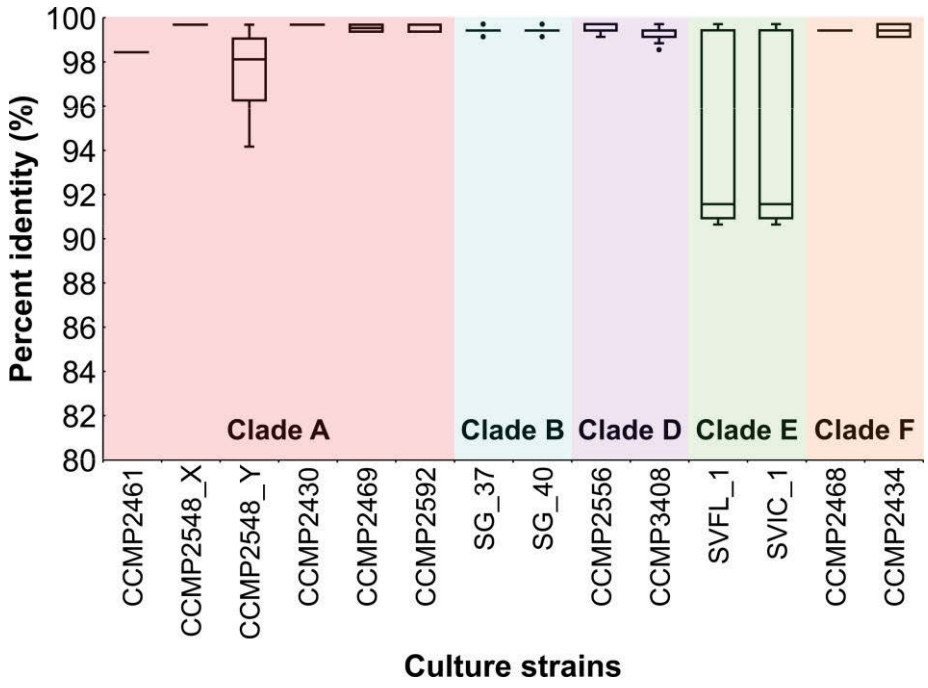

Figure 6.1. Box plots for percent identity of sequences within each strain. Background colour were used to classify the clade of strains: red for clade A, blue for clade B, purple for clade D, green for clade E, and orange for clade F.

Intra-genomic variations successfully collapse into distinct OTUs at the 97% similarity cut-off

Assessing biodiversity by amplicon sequencing using multi-copy genes such as nuclear rDNA faces a challenge in discerning inter- from intra-genomic variation (Thornhill et al. 2007; Sampayo et al. 2009; LaJeunesse and Thornhill 2011; Arif et al. 2014; Ziegler et al. 2017). Using the variety of culture strains spanning clades A, B, D, E and F, and analysing them with two different approaches: OTU analysis at the 97% sequence similarity cut-off and exact sequence variation (zOTU) analysis, the results support the finding from Arif et al. (2014) (who only used culture strains of clades A-C) that clustering sequences at the 97% similarity threshold can successfully collapse intra-genomic variants into distinct OTUs for the majority of tested *Symbiodinium* species. Clade E strains (*S. voratum*) exhibited particularly high intra-genomic variations compared to other strains, a finding also reported by Thornhill et al. (2007) that clade E strains had relatively higher sequence diversity (only 6/24 cloned sequences were identical) and the greatest amount of sequence divergence among clones (up to 45 changes from the most commonly recovered sequence, uncorrected average genetic distances: 0.06) compared to other clades A-D isolates. Also, free-living strains *S. natans* resulted into three OTUs per strain. I acknowledge that the OTU approach does not overcome all problems due to intra-genomic variations and work perfectly for all species (Thornhill et al. 2007; Stat et al. 2011; 2013; Arif et al. 2014; Ziegler et al. 2017). However, it reduces the complexity based on ITS2 sequences and provide an informative framework for assessing *Symbiodinium* diversity with phylogenetic and ecological supports (Stat et al. 2015). Based on my analysis, I suggest that the OTU approach is a powerful and useful tool for estimating diversity and community compositions based on the large amounts of sequence data

generated by NGS technology. The OTU approach has been widely applied not only for *Symbiodinium* studies (e.g. Arif et al. 2014; Thomas et al. 2014; Stat et al. 2015; Cunning et al. 2015; Ziegler et al. 2017), but also for various other prokaryotic (e.g. Sunagawa et al. 2015; Pootakham et al. 2018) and eukaryotic organisms (e.g. de Vargas et al. 2015; Bista et al. 2017).

OTU relative abundance filtering is critical for minimising noise

For estimating the diversity based on NGS analysis, it is required to carefully control the sequence data by quality filtering and OTU abundance filtering to minimise the erroneous reads that can result from systematic errors (e.g. sequencing errors and PCR artifacts) (e.g. Degnan and Ochman 2012; Bokulich 2013). I found that an additional de-noising step: abundance filtering at 1% threshold within each sample, is critical to minimise such potential noise. Indeed, Arif et al. (2014) also reported multiple OTUs within one strain, where rare OTUs originated from other strains in the same sequence run. I acknowledge that removing the rare OTUs (accounting for < 1% of the reads within sample) as noise potentially removes real biological entities resulting in number of biological and ecological questions that are disregarded (Stat et al. 2011; Degnan and Ochman 2012; Boulotte et al. 2016; Auer et al. 2017; Ziegler et al. 2018). However, selecting a more conservative approach and applying stricter filtering steps (both quality filtering and OTU abundance filtering) inevitably provides more robust estimates of diversity.

Summary

According to the findings from the NGS analysis of 'control' *Symbiodinium* culture strains, I have applied OTU approach at the 97% similarity cut-off and OTU abundance filtering at 1% threshold within each sample for the field samples (Chapters 2 and 3; cross-linked the culture analysis as "Appendix: Culture OTU analysis") to minimise the influence of intra-genomic variations and systematic errors for assessing *Symbiodinium* diversity and community composition. Such a step introduced a more conservative treatment of NGS data, but seems critical to ensure relevant and robust conclusions of *Symbiodinium* diversity, as it is distributed both *in hospite* and in environments as free-living cells.

(This page is intentionally left blank)

Appendix

Supplementary Figures

Chapter 4

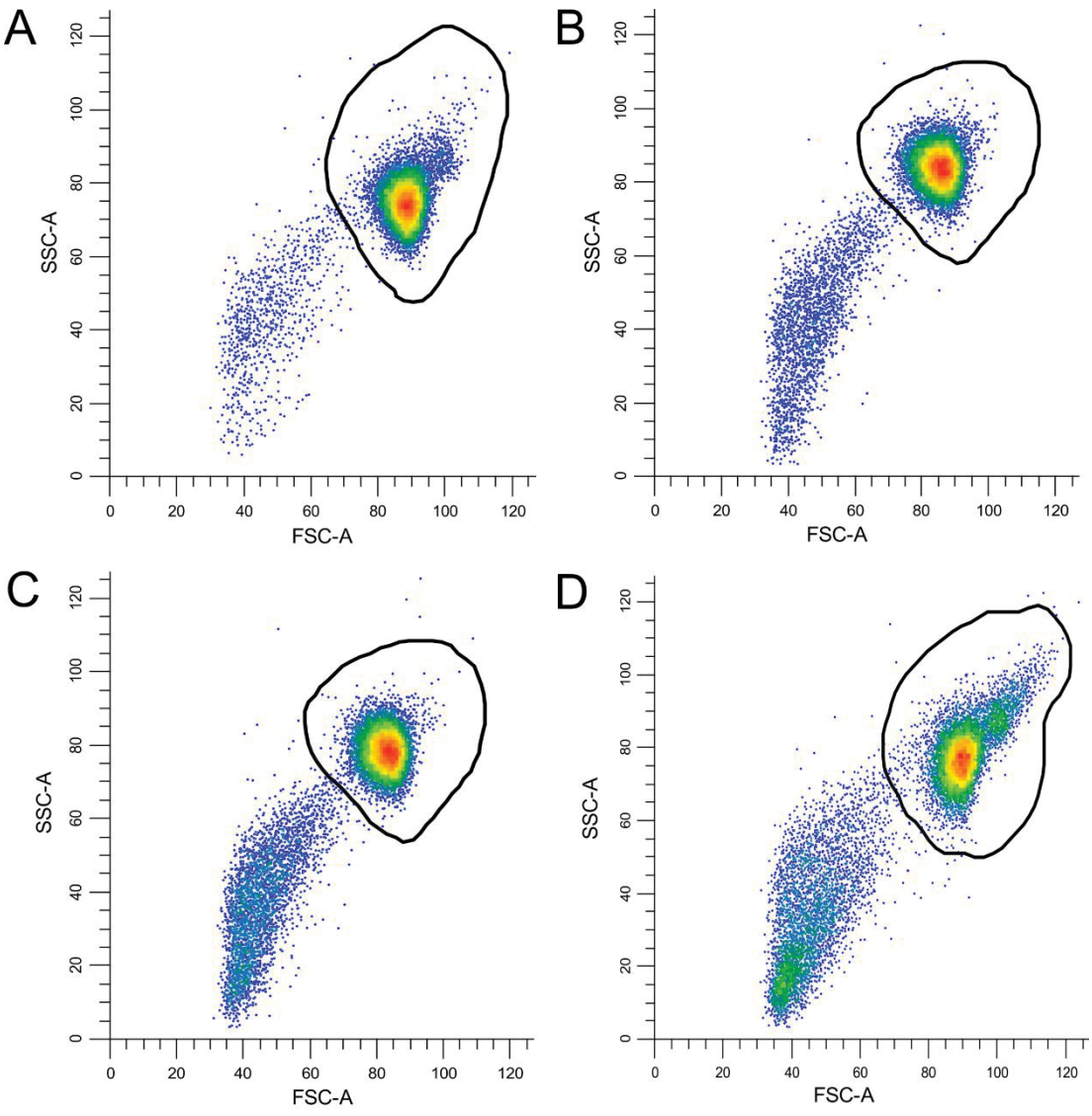

Figure S4.1. Example of manual gating for *Symbiodinium* populations in flow cytometry analysis. The gating for **A.** B1, **B.** C1, **C.** C1′, and **D.** D1a strains under high light treatment at sampling time point T0. X axis is forward scatter, and Y axis is side scatter in log scale for both.

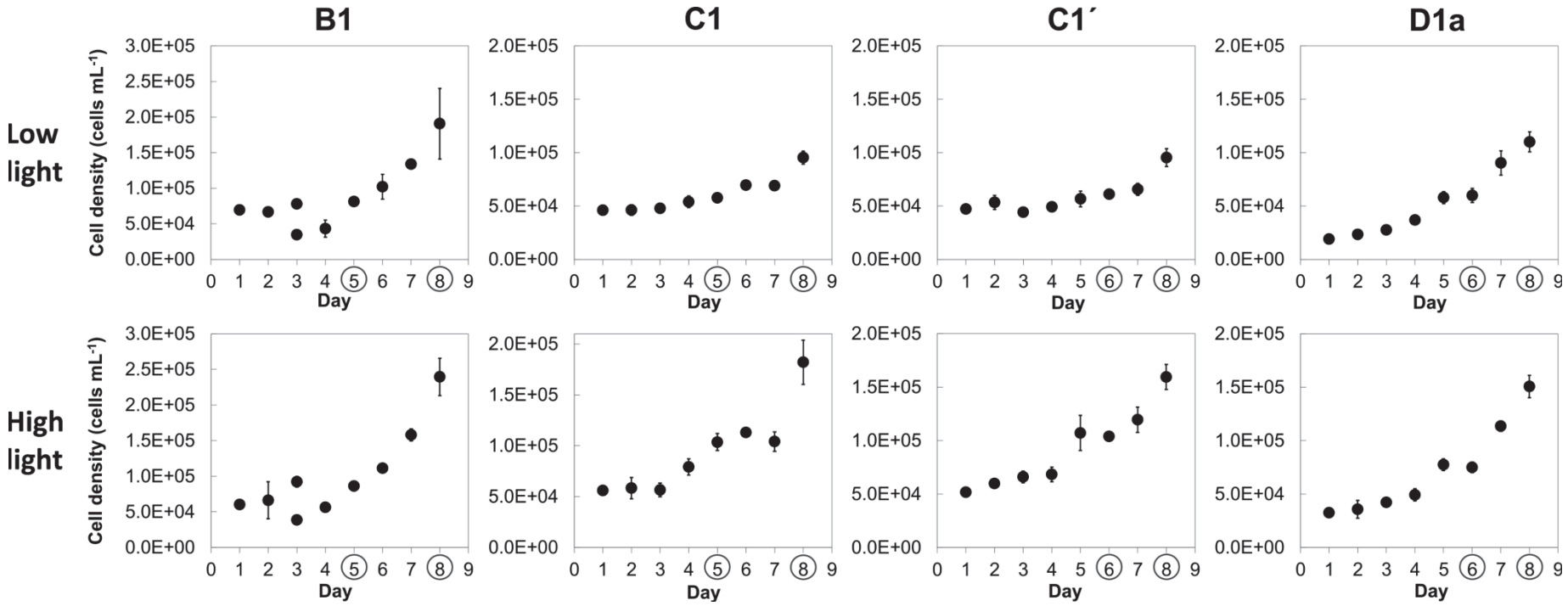

Figure S4.2. Cell densities of four *Symbiodinium* culture strains under the light treatment (low light vs. high light). B1 was diluted into half concentration at day 3 both under low light and high light treatment to prevent the over growth. Cell cycle samples were collected through days 6-7. The days circled on the X axis and corresponding cell densities were used in calculating the growth rate (equation 1). Outliers which deviated from the exponential curve were treated as counting errors and not used for calculating the growth rate. Values represent mean ± SD (n = 3).

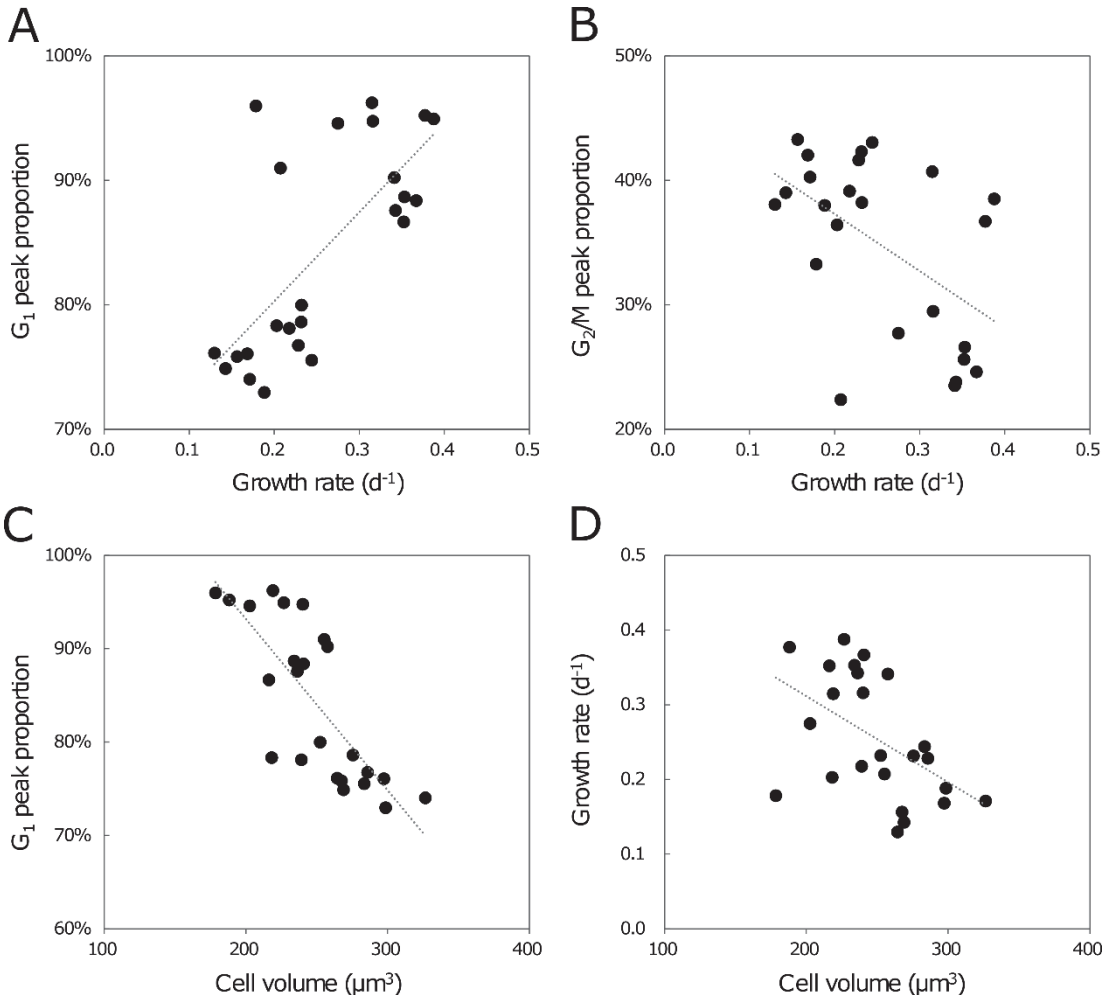

Figure S4.3. Correlation between cell cycle and growth parameters. Relationship between **A.** Growth rate and G_1 peak proportion, **B.** Growth rate and G_2/M peak proportion, **C.** Cell volume and G_1 peak proportion, **D.** Cell volume and growth rate. Values from low light and high light were plotted (n = 24).

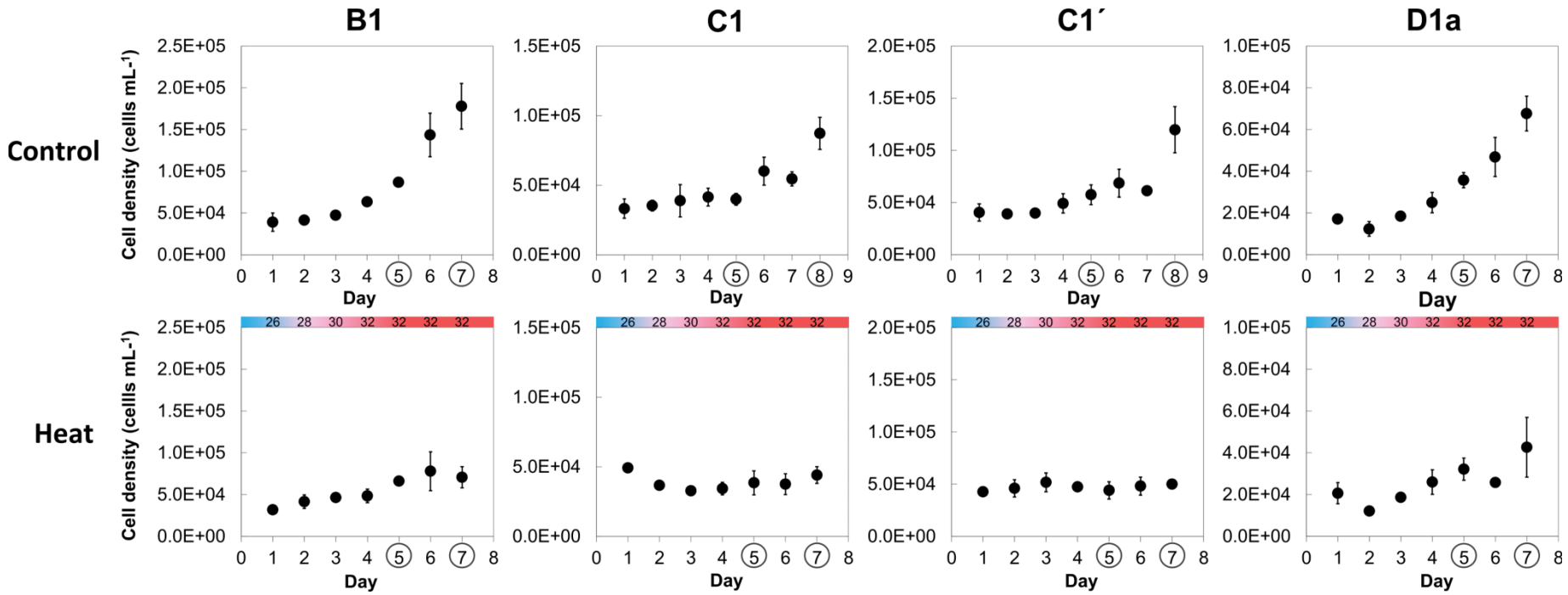

Figure S4.4. Cell densities of four *Symbiodinium* culture strains under the temperature treatment (control vs. heat). Cell cycle samples were collected through days 6-7. The days circled on the X axis and corresponding cell densities were used in calculating the growth rate (equation 1). Outliers which deviated from the exponential curve were treated as counting errors and not used for calculating the growth rate. Values represent mean ± SD (n = 3). The temperature increase is shown on the top X axis of each graph for heat treatment (lower panel). The temperatures were; day 1: 26.4 ± 0.72°C, day 2: 27.7 ± 0.75°C, day 3: 29.7 ± 0.87°C, day 4: 31.9 ± 0.89°C, day 5: 32.0 ± 0.81°C, day 6: 32.1 ± 0.56°C, day 7: 32.3 ± 0.84°C (± SD for daily mean temperature measured using iButton® temperature loggers).

Supplementary Tables

Chapter 2

Table S2.1. Number of sequences, clades, ITS2 variants and OTUs obtained by DNA metabarcoding. Total samples are 96 samples (2 seasons × 3 sites (coral species) × 4 habitats × 4 replicates).

Sample				Number of	Number of	Number of	Number of
Season	Site	Habitat	Replicate	sequences	clades	ITS2 variants	OTUs
Spawning	1	*A. aspera*	a	41,075	1	5	7
			b	36,833	1	6	7
			c	34,052	1	3	6
			d	40,485	1	4	5
	2	*M. digitata*	a	189,027	1	3	5
			b	49,887	1	3	5
			c	52,084	1	4	6
			d	61,475	1	2	3
	3	*P. damicornis*	a	55,736	1	4	7
			b	35,104	1	4	7
			c	72,507	1	4	7
			d	52,134	1	4	8
	1	Water	a	12,378	4	14	19
			b	7,297	4	12	14
			c	6,507	4	13	16
			d	4,793	3	14	20
	2	Water	a	10,486	4	17	19
			b	19,974	3	13	17
			c	11,164	3	14	18
			d	7,899	3	12	18
	3	Water	a	8,776	3	13	16
			b	9,431	3	11	15
			c	30,612	2	10	10
			d	13,120	5	16	20
	1	Sediment	a	1,055	5	14	20
			b	653	5	14	24
			c	8,203	6	15	27
			d	918	6	16	22
	2	Sediment	a	2,860	5	16	20
			b	1,855	7	14	22
			c	1,250	5	15	21
			d	2,110	4	11	13
	3	Sediment	a	2,162	4	13	15
			b	1,978	7	18	23
			c	1,960	6	12	17
			d	2,626	5	15	18
	1	Macroalgae	a	3,139	4	15	19
			b	3,916	4	14	17
			c	5,878	4	16	19
			d	2,383	4	12	17
	2	Macroalgae	a	4,204	3	15	16
			b	9,015	2	10	16
			c	7,342	3	15	24
			d	10,036	3	10	14
	3	Macroalgae	a	1,251	4	14	14
			b	1,684	5	15	21
			c	5,478	4	12	16
			d	4,121	4	10	14

Table S2.1. (continued)

Sample				Number of	Number of	Number of	Number of
Season	Site	Habitat	Replicate	sequences	clades	ITS2 variants	OTUs
Summer	1	*A. aspera*	a	41,292	1	4	7
			b	49,003	1	3	4
			c	48,850	1	3	3
			d	50,632	1	4	5
	2	*M. digitata*	a	72,641	1	2	3
			b	53,638	1	2	3
			c	67,447	1	2	3
			d	68,181	1	3	4
	3	*P. damicornis*	a	68,415	1	6	8
			b	69,931	1	3	6
			c	76,537	1	6	13
			d	78,350	1	4	4
	1	Water	a	3,393	2	10	11
			b	3,084	3	14	15
			c	439	2	11	13
			d	826	4	9	12
	2	Water	a	1,367	2	7	9
			b	906	2	8	12
			c	409	3	8	11
			d	452	3	11	12
	3	Water	a	4,125	3	9	10
			b	2,571	4	14	15
			c	1,656	4	13	17
			d	1,757	4	13	18
	1	Sediment	a	2,638	5	11	12
			b	491	6	13	14
			c	45	6	14	17
			d	298	4	10	12
	2	Sediment	a	138	4	10	13
			b	133	4	10	11
			c	56	5	12	12
			d	159	5	14	17
	3	Sediment	a	31	3	7	9
			b	186	4	14	17
			c	41	5	13	16
			d	24	5	10	11
	1	Macroalgae	a	7,837	4	13	14
			b	12,975	3	12	14
			c	6,511	4	17	19
			d	5,020	4	14	17
	2	Macroalgae	a	1,129	4	16	18
			b	5,132	4	12	18
			c	824	5	16	19
			d	7,238	3	17	22
	3	Macroalgae	a	1,064	5	14	16
			b	37,521	1	4	7
			c	496	3	12	17
			d	3,387	3	9	10

Table S2.2. Summary of Kruskal-Wallis test for number of clades, ITS2 variants and OTUs. **A.** Main effects. **B.** *Post-hoc* pairwise comparison for sites × habitats × seasons. df: degrees of freedom, P value: * for $P < 0.05$, ** for $P < 0.01$.

A. Main effects.

Variables	Test Statistic	df	P value	
Number of clades	73	7	3.1E-13	**
Number of ITS2 variants	62	7	5.4E-11	**
Number of OTUs	66	7	8.5E-12	**

B. Pairwise comparison.

			Spawning						Summer					
			Coral		Water		Sediment	Macroalgae	Coral		Water		Sediment	
Variables	Seasons	Habitats	P value		P value		P value	P value	P value		P value		P value	
Number of clades	Spawning	Coral												
		Water	0.022	*					0.022	*				
		Sediment	5.3E-09	**	0.074				5.3E-09	**	0.0092	**		
		Macroalgae	0.0032	**	1.0		0.34		0.0032	**	1.0		1.0	
	Summer	Coral	1.0											
		Water	0.15		1.0				0.15					
		Sediment	1.1E-06	**	0.94		1.0		1.1E-06	**	0.19			
		Macroalgae	0.0054	**	1.0		0.23	1.0	0.0054	**	1.0		1.0	
Number of ITS2 variants	Spawning	Coral												
		Water	3.8E-04	**					1.2E-04	**				
		Sediment	2.8E-06	**	1.0				6.8E-07	**	0.22			
		Macroalgae	2.2E-04	**	1.0		1.0		6.6E-05	**	1.0		1.0	
	Summer	Coral	1.0											
		Water	0.21		1.0				0.096					
		Sediment	0.039	*	1.0		0.93		0.016	*	1.0			
		Macroalgae	2.8E-04	**	1.0		1.0	1.0	8.4E-05	**	1.0		1.0	
Number of OTUs	Spawning	Coral												
		Water	2.1E-04	**					5.2E-05	**				
		Sediment	3.0E-07	**	1.0				5.2E-08	**	0.029	*		
		Macroalgae	2.0E-04	**	1.0		1.0		5.0E-05	**	1.0		1.0	
	Summer	Coral	1.0											
		Water	0.41		1.0				0.18					
		Sediment	0.22		1.0		0.063		0.088		1.0			
		Macroalgae	0.0014	**	1.0		1.0	1.0	4.0E-04	**	1.0		1.0	

Table S2.3. Summary of PERMANOVA main effects for *Symbiodinium* community compositions. **A.** Clades. **B.** ITS2 variants. **C.** OTUs. Relative abundance of community compositions was square-root transformed and PERMANOVA was performed with sites (coral species) (3 levels), habitats (4 levels) and seasons (2 levels) as fixed factors, using type III sum of squares and unrestricted permutation of raw data with 999 permutations. MS: mean square, df: degrees of freedom, *F*: Fisher statistic, P value: * for $P < 0.05$, ** for $P < 0.01$.

A. Main effects on cladal composition.

Source	MS	df	*F*	P value	
Site	289	2	1.5	0.25	
Habitat	23,545	3	121	0.001	**
Season	858	1	4.4	0.030	*
Site × Habitat	276	6	1.4	0.21	
Site × Season	793	2	4.1	0.015	*
Habitat × Season	429	3	2.2	0.098	
Site × Habitat × Season	335	6	1.7	0.12	

B. Main effects on ITS2 variant composition.

Source	MS	df	*F*	P value	
Site	12,558	2	13	0.001	**
Habitat	34,232	3	37	0.001	**
Season	6,104	1	6.5	0.001	**
Site × Habitat	8,061	6	8.6	0.001	**
Site × Season	2,536	2	2.7	0.003	**
Habitat × Season	4,273	3	4.6	0.001	**
Site × Habitat × Season	1,653	6	1.8	0.003	**

C. Main effects on OTU composition.

Source	MS	df	*F*	P value	
Site	10,678	2	4.6	0.001	**
Habitat	23,117	3	10	0.001	**
Season	19,775	1	8.4	0.001	**
Site × Habitat	6,401	6	2.7	0.001	**
Site × Season	5,972	2	2.5	0.001	**
Habitat × Season	11,622	3	5.0	0.001	**
Site × Habitat × Season	3,938	6	1.7	0.001	**

Table S2.4. Summary of SIMPER analysis for *Symbiodinium* cladal community compositions. Pairwise comparison within **A.** Spawning season and **B.** Summer season. Pairwise comparison **C.** Between spawning and summer seasons. Top two clades which contributed to dissimilarity of community compositions are shown with contribution percentages (%). Clades which were more abundant in variables in columns are shown as bold letter and clades which were more abundant in variables in rows are shown as normal letter.

A. Within spawning season.

			Spawning																					
			Site 1								Site 2								Site 3					
			Coral		Water		Sediment		Macroalgae		Coral		Water		Sediment		Macroalgae		Coral		Water		Sediment		Macroalgae	
Seasons	Site	Habitats	Contri.	%	Contri.	%	Contri.	%	Contri.	%	Contri.	%	Contri.	%	Contri.	%	Contri.	%	Contri.	%	Contri.	%	Contri.	%	Contri.	%
Spawning	1	Coral																						
		Water	**A**, **D**	40, 31							**A**, **D**	40, 31							**A**, **D**	40, 31					
		Sediment	**A**, C	30, 28	C, **A**	33, 27					**A**, C	30, 28	C, **F**	25, 23					**A**, C	30, 28	C, **F**	27, 27			
		Macroalgae	**A**, C	50, 26	**A**, C	54, 35	F, **C**	36, 29			**A**, C	50, 26	**A**, D	35, 33	**C**, F	35, 24			**A**, C	50, 26	**A**, C	36, 33	**C**, G	33, 18	
	2	Coral	-																					
		Water	**D**, **A**	42, 34	**D**, **A**	42, 25					**D**, **A**	42, 34							**D**, **A**	42, 34					
		Sediment	**A**, C	36, 32	C, **A**	36, 34	**C, F**	21, 21			**A**, C	36, 32	C, **A**	27, 24					**A**, C	36, 32	C, **A**	32, 19			
		Macroalgae	**A**, C	62, 29	**A**, C	51, 29	F, **C**	28, 27	**C**, A	33, 30	**A**, C	62, 29	D, **A**	45, 28	**C**, F	33, 20			**A**, C	62, 29	**A**, **C**	32, 31	**C**, A	32, 18	
	3	Coral	-								-													
		Water	**A**, C	51, 26	**A**, C	44, 29					**A**, C	51, 26	D, **A**	35, 32					**A**, C	51, 26					
		Sediment	**A**, C	37, 32	C, **A**	36, 34	G, F	27, 23			**A**, C	37, 32	C, **A**	29, 26	G, **C**	33, 14			**A**, C	37, 32	C, **A**	33, 20			
		Macroalgae	**A**, C	51, 28	**A**, C	53, 35	F, **C**	35, 25	C, **A**	38, 34	**A**, C	51, 28	**A**, D	36, 31	**C**, F	34, 24	C, **A**	34, 31	**A**, C	51, 28	**A**, C	30, 25	**C**, G	31, 21	

B. Within summer season.

			Summer																					
			Site 1								Site 2								Site 3					
			Coral		Water		Sediment		Macroalgae		Coral		Water		Sediment		Macroalgae		Coral		Water		Sediment		Macroalgae	
Seasons	Site	Habitats	Contri.	%	Contri.	%	Contri.	%	Contri.	%	Contri.	%	Contri.	%	Contri.	%	Contri.	%	Contri.	%	Contri.	%	Contri.	%	Contri.	%
Summer	1	Coral																						
		Water	**A**, C	66, 17							**A**, C	66, 17							**A**, C	66, 17						
		Sediment	**A**, C	41, 32	C, **A**	36, 28					**A**, C	41, 32	C, **A**	36, 27					**A**, C	41, 32	C, **A**	35, 35				
		Macroalgae	**A**, C	54, 24	**A**, C	37, 29	**C**, A	35, 20			**A**, C	54, 24	**A**, C	36, 26	**C**, F	33, 21			**A**, C	54, 24	**A**, C	46, 25	**C**, D	26, 22		
	2	Coral	-																					
		Water	**A**, C	65, 20	**A**, C	37, 22					**A**, C	65, 20							**A**, C	65, 20						
		Sediment	**A**, C	44, 31	C, **A**	35, 30	**C**, I	24, 23			**A**, C	44, 31	C, **A**	35, 30					**A**, C	44, 31	**A**, C	35, 35				
		Macroalgae	**A**, C	47, 25	**A**, C	31, 29	**C**, A	32, 20	C, **A**	30, 29	**A**, C	47, 25	**A**, C	30, 26	**C**, A	31, 22			**A**, C	47, 25	**A**, C	40, 27	**C**, D	23, 21		
	3	Coral	-								-													
		Water	**A**, **D**	43, 27	A, **D**		39, 27				**A**, **D**	43, 27	A, **D**	42, 26					**A**, **D**	43, 27						
		Sediment	**A**, C	43, 28	C, **A**	31, 27	**C**, **D**	28, 17			**A**, C	43, 28	C, **A**	32, 28	**C**, **G**	22, 21			**A**, C	43, 28	**A**, C	38, 33				
		Macroalgae	**A**, C	50, 25	A, C	40, 26	**C**, A	34, 33	A, **C**	42, 30	**A**, C	50, 25	A, C	41, 27	A, **C**	36, 33	A, **C**	38, 30	**A**, C	50, 25	**A**, C	42, 25	A, **C**	36, 33		

C. Between spawning and summer seasons.

			Summer																					
			Site 1								Site 2								Site 3					
			Coral		Water		Sediment		Macroalgae		Coral		Water		Sediment		Macroalgae		Coral		Water		Sediment		Macroalgae	
Seasons	Site	Habitats	Contri.	%	Contri.	%	Contri.	%	Contri.	%	Contri.	%	Contri.	%	Contri.	%	Contri.	%	Contri.	%	Contri.	%	Contri.	%	Contri.	%
Spawning	1	Coral	-		A, **C**	66, 17	A, **C**	41, 32	A, **C**	54, 24	-		A, **C**	65, 20	A, **C**	44, 31	A, **C**	47, 25	-		A, D	43, 27	A, **C**	43, 28	A, **C**	50, 25
		Water	**A**, **D**	40, 31	A, **D**	42, 26	A, **C**	37, 36	A, **C**	50, 28	**A**, **D**	40, 31	A, **D**	44, 24	A, **C**	41, 35	A, **C**	43, 29	**A**, **D**	40, 31	A, **C**	45, 23	A, **C**	40, 33	A, **C**	43, 25
		Sediment	**A**, C	30, 28	C, **F**	31, 23	**F**, **G**	25, 19	**F**, C	32, 29	**A**, C	30, 28	C, **F**	31, 24	**F, G**	24, 23	**F**, C	31, 28	**A**, C	30, 28	C, **A**	32, 24	**F**, **G**	31, 23	C, **F**	29, 23
		Macroalgae	**A**, C	50, 26	**A**, C	33, 31	**C**, A	34, 19	C, **A**	32, 31	**A**, C	50, 26	**A**, C	35, 29	**C**, F	33, 25	C, **A**	29, 27	**A**, C	50, 26	**A**, C	53, 34	**C**, A	28, 19	**A**, C	42, 32
	2	Coral	-		A, **C**	66, 17	A, **C**	41, 32	A, **C**	54, 24	-		A, **C**	65, 20	A, **C**	44, 31	A, **C**	47, 25	-		A, D	43, 27	A, **C**	43, 28	A, **C**	50, 25
		Water	**D**, **A**	42, 34	**D**, C	60, 15	A, **C**	28, 27	**D**, A	42, 27	**D**, **A**	42, 34	**D**, A	55, 21	A, **C**	30, 25	**D**, A	35, 25	**D**, **A**	42, 34	**D**, **A**	37, 30	A, **C**	33, 25	**D**, A	39, 26
		Sediment	**A**, C	36, 32	C, **A**	35, 24	**G**, I	21, 18	C, **F**	36, 21	**A**, C	36, 32	C, **A**	35, 23	**G**, C	27, 26	C, **F**	36, 21	**A**, C	36, 32	C, **A**	36, 31	C, **G**	25, 22	C, **A**	34, 29
		Macroalgae	**A**, C	62, 29	**A**, C	42, 35	**C**, A	34, 21	**A**, C	32, 32	**A**, C	52, 29	**A**, C	42, 34	**C**, A	33, 23	**C**, A	29, 27	**A**, C	62, 29	**A**, C	47, 28	**C**, D	28, 23	**A**, C	44, 32
	3	Coral	-		A, **C**	66, 17	A, **C**	41, 32	A, **C**	54, 24	-		A, **C**	65, 20	A, **C**	44, 31	A, **C**	47, 25	-		A, D	43, 27	A, **C**	43, 28	A, **C**	50, 25
		Water	**A**, C	51, 26	**A**, C	31, 28	**C**, A	32, 22	A, C	27, 24	**A**, **C**	51, 26	**A**, C	34, 29	**C**, A	31, 26	A, **C**	25, 23	**A**, C	51, 26	**A**, C	42, 28	**C**, A	27, 23	**A**, C	38, 29
		Sediment	**A**, C	37, 32	C, **A**	35, 24	**G**, C	26, 18	C, **G**	33, 16	**A**, C	37, 32	C, **A**	35, 24	**G**, C	28, 21	C, G	30, 19	**A**, C	37, 32	C, **A**	36, 32	**G**, C	25, 24	C, **A**	33, 29
		Macroalgae	**A**, C	61, 28	**A**, C	37, 33	**C**, I	33, 20	C, **A**	31, 31	**A**, C	51, 28	**A**, C	37, 32	**C**, F	32, 26	**A**, C	27, 27	**A**, C	51, 28	**A**, C	50, 34	**G**, D	22, 21	**A**, C	42, 33

Table S2.5. List of ITS2 variants and relative abundance in each sample. **A.** Spawning season. **B.** Summer season. Compositions of ITS2 variants in each replicate (n = 4) were averaged and top three ITS2 variants in each clade are listed with relative abundance (%) in each sample.

A. Spawning season.

	Spawning																					
	Coral						Water						Sediment						Macroalgae					
Clade	site 1		site 2		site 3		site 1		site 2		site 3		site 1		site 2		site 3		site 1		site 2		site 3	
A							A1	2.1	A1	10.5	A1	19	A113	16	A113	36	A113	31	A112	26	A112	29	A112	32
							A110	1.4	A110	3.0	A110	7.9	A155	14	A155	10	A155	10	A5	9.4	A5	5.8	A1	9.0
							A5	0.28	A114	0.41	A155	6.5	A1	5.6	A112	8.7	A5	8.0	A1	4.6	A1	4.5	A5	9.0
B																	B1	0.33						
C	C1085	81	C15	62	C42	47	C131	22	C131	18	C15.16	16	C1085	6.0	C1085	2.0	C1cstar	2.7	C131	17	C131	15	C131	11
	C131	14	C15.16	34	C1cstar	36	C1085	19	C15.20	13	C131	9.6	C131	2.9	C15.20	1.8	C131	2.4	C1085	6.2	C1085	7.6	C15.20	9.3
	C1cstar	1.6	C15.7	1.4	C1	11	C15.20	14	C15	5.6	C1085	7.2	C90	1.4	C1.11	1.6	C1.11	2.2	C15.20	5.5	C66	7.3	C1cstar	3.2
D							D111	1.3	D1	9.1	D105	3.0	D106	3.0	D106	1.1	D1	2.9	D1a	2.8	D1a	0.53	D1a	1.4
							D1	0.91	D1a	6.3	D111	2.5	D111	0.45	D111	0.87	D111	0.94	D1	0.45			D1	0.28
									D111	4.1	D106	0.86					D106	0.82						
F											F3.2	0.36	F3.2	13	F3.2	6.3	F5.2	1.7					F114	0.9
													F5.2	4.4	F5.2	0.8	F3.2	1.1						
													F4.4a	0.47			F107	0.63						
G							G3.1	1.3	G3.1	0.42	G4	1.0	G4	13	G4	10.4	G4	10.6	G4	2.6	G4	0.72	G4	2.1
									G4	0.39														
H													H2	0.38	H2	0.42	H2	0.32						
I													I2	0.35	I4	0.47	I2	0.49						
																	I4	0.37						

B. Summer season.

	Summer																					
	Coral						Water						Sediment						Macroalgae					
Clade	site 1		site 2		site 3		site 1		site 2		site 3		site 1		site 2		site 3		site 1		site 2		site 3	
A							A1	13	A1	12	A110	7.3	A155	55	A155	59	A155	33	A112	16	A112	17	A112	7.9
							A110	4.8	A110	9.8	A1	6.7	A1	6.5	A5	3.3	A113	11	A1	12	A1	10	A1	5.7
							A155	0.93	A155	1.0			A113	5.2	A113	2.8	A1	6.0	A121	8.1	A121	8.6	A121	5.6
B							B1	0.64											B1	0.52	B1	0.66		
C	C1085	80	C15	76	C1cstar	66	C15.20	23	C15.20	42	C15.20	37	C131	6.8	C131	6.3	C131	11	C131	20	C131	19	C131	52
	C131	17	C15.20	20	C42	16	C15.16	21	C1085	15	C131	9.2	C15	2.2	C15	5.1	C1cstar	5.8	C1085	6.8	C15.20	8.0	C93	7.7
	C3	1.5	C15.7	4.3	C42.2	12	C1085	12	C131	7.8	C1cstar	7.6	C1085	1.6	C15.20	3.4	C15	2.8	C1.11	5.3	C93	7.8	C1cstar	3.2
D									D1a	2.0	D1a	2.4	D1	2.1	D1	2.0	D1	6.9	D1	0.70	D111	0.94	D1	1.0
											D106	0.66			D111	0.45	D111	0.54						
											D1.3	0.36			D2	0.31								
F													F3.2	1.1	F3.2	3.5	F3.2	1.2			F3.1a	0.61	F3.1a	0.31
													F5.2	1.0	F5.2	0.69	F5.2	1.0						
													F5.1a	0.89	F107	0.36								
G							G3.1	1.1	G3.1	0.50	G3.1	1.4	G4	3.0	G4	3.2	G4	3.4	G3.1	2.0	G3	5.4	G3	1.6
													G3.1	0.46			G3	0.61	G3	1.3	G4	0.88	G4	1.2
I													I4	3.2			I4	1.0						

Table S2.6. Summary of SIMPER analysis for *Symbiodinium* ITS2 variant community compositions. Pairwise comparison within **A.** Spawning season and **B.** Summer season. Pairwise comparison **C.** Between spawning and summer seasons. Top two ITS2 variants which contributed to dissimilarity of community compositions are shown with contribution percentages (%). ITS2 variants which were more abundant in variables in columns are shown as bold letter and ITS2 variants which were more abundant in variables in rows are shown as normal letter.

A. Within spawning season.

			Spawning																					
			Site 1								Site 2								Site 3					
			Coral		Water		Sediment		Macroalgae		Coral		Water		Sediment		Macroalgae		Coral		Water		Sediment		Macroalgae	
Seasons	Site	Habitats	Contri.	%	Contri.	%	Contri.	%	Contri.	%	Contri.	%	Contri.	%	Contri.	%	Contri.	%	Contri.	%	Contri.	%	Contri.	%	Contri.	%
Spawning	1	Coral																						
		Water	C1085, **C15.20**	15, 10							C15, **C1085**	14, 10							C42, C1cstar	16, 12						
		Sediment	C1085, **A113**	17, 8	**A113**, **A155**	7, 6					C15, C15.16	16, 8	**A113**, **A155**	7, 7					C42, C1cstar	14, 11	**F3.2**, **A113**	7, 7				
		Macroalgae	C1085, **A112**	17, 13	**A112**, **A5**	11, 6	**A112**, F3.2	8, 8			C15, **A112**	16, 11	**A112**, **A5**	12, 7	A113, **C131**	13, 8			C42, **A112**	15, 11	**A112**, C15.16	12, 6	A113, **A112**	12, 8		
	2	Coral	C1085, **C15**	31, 27																				
		Water	C1085, **A1**	17, 8	**D1a**, **D1**	7, 6					C15, C15.16	13, 10							C42, C1cstar	15, 11						
		Sediment	C1085, **A113**	18, 13	**A113**, C131	10, 8	**A113**, **A112**	10, 7			C15, **A113**	17, 13	**A113**, C131	11, 7					C42, **A113**	15, 12	**A113**, A1	12, 7				
		Macroalgae	C1085, **A112**	19, 13	**A112**, C1085	12, 7	**A112**, F3.2	9, 8	C131, C1085	10, 7	C15, **A112**	17, 12	**A112**, C131	12, 7	A113, **A112**	13, 8			C42, C1cstar	16, 12	**A112**, C15.16	12, 7	A113, **A112**	12, 8		
	3	Coral	C1085, **C42**	31, 24							C15, **C42**	25, 23														
		Water	C1085, **A1**	18, 11	**A1**, C15.20	7, 7					C15, C15.16	17, 10	**C15.16**, D1	7, 7					C42, C1cstar	16, 11						
		Sediment	C1085, **A113**	19, 12	**A113**, C1085	10, 7	F3.2, G4	9, 8			C15, **A113**	16, 12	**A113**, C131	10, 6	G4, A113	8, 7			C42, **A113**	15, 12	**A113**, C1085	11, 5				
		Macroalgae	C1085, **A112**	19, 14	**A112**, C1085	13, 7	**A112**, A113	10, 8	C131, **C15.20**	10, 7	C15, **A112**	17, 13	**A112**, **A5**	15, 7	A113, **A112**	14, 8	C131, C1085	9, 7	C42, **A112**	16, 13	**A112**, C15.16	14, 6	A113, **A112**	13, 9		

B. Within summer season.

			Summer																					
			Site 1								Site 2								Site 3					
			Coral		Water		Sediment		Macroalgae		Coral		Water		Sediment		Macroalgae		Coral		Water		Sediment		Macroalgae	
Seasons	Site	Habitats	Contri.	%	Contri.	%	Contri.	%	Contri.	%	Contri.	%	Contri.	%	Contri.	%	Contri.	%	Contri.	%	Contri.	%	Contri.	%	Contri.	%
Summer	1	Coral																						
		Water	C1085, **C15.20**	17, 11							C15, **C15.20**	19, 11							C1cstar, **C15.20**	14, 9						
		Sediment	C1085, **A155**	22, 20	**A155**, C15.20	16, 8					C15, **A155**	20, 19	**A155**, C15.20	17, 16					C1cstar, **A155**	17, 17	**A155**, C15.20	15, 13				
		Macroalgae	C1085, **A112**	17, 10	C15.20, **A112**	10, 10	A155, **C131**	16, 7			C15, **A112**	18, 8	C15.20, **A112**	15, 10	A155, **A112**	15, 7			C1cstar, **A112**	13, 8	C15.20, **A112**	12, 9	A155, **A112**	10, 8		
	2	Coral	C1085, **C15**	32, 31																						
		Water	**C15.20**, C1085	24, 19	**C15.20**, C15.16	18, 14					C15, **C15.20**	22, 17							C1cstar, **C15.20**	18, 16						
		Sediment	C1085, **A155**	24, 21	**A155**, C15.20	16, 8	I4, **C15**	6, 6			**A155**, C15	21, 19	**A155**, C15.20	18, 13					C1cstar, **A155**	18, 18	**A155**, C15.20	17, 10				
		Macroalgae	C1085, **A112**	19, 9	**A112**, C15.20	9, 9	A155, **C15.20**	15, 7	**C131**, **C93**	10, 6	C15, **C131**	17, 9	**A112**, C15.20	11, 10	A155, **A112**	15, 9			C1cstar, **A112**	14, 8	**A112**, C15.20	9, 8	A155, **A112**	10, 8		
	3	Coral	C1085, **C1cstar**	29, 26							C15, **C1cstar**	28, 27														
		Water	C1085, **C15.20**	19, 18	**C15.20**, C15.16	12, 12					C15, **C15.20**	19, 15	A110, **C15a**	9, 9					**C15.20**, C1cstar	15, 13						
		Sediment	C1085, **A155**	23, 15	**A155**, C15.20	12, 8	**C131**, A155	7, 7			C15, **A155**	18, 14	C15.20, **A155**	16, 12	**A113**, A155	8, 8			C1cstar, **A155**	14, 13	C15.20, **A155**	13, 12				
		Macroalgae	C1085, **C131**	27, 14	**C131**, C15.20	14, 9	A155, **C131**	18, 15	**C131**, A112	15, 8	C15, **C131**	23, 19	C15.20, **C131**	16, 14	A155, **C131**	18, 14	**C131**, A112	14, 8	**C131**, C1cstar	17, 17	C15.20, **C131**	14, 13	A155, **C131**	13, 13		

C. Between spawning and summer seasons.

			Summer																							
			Site 1								Site 2								Site 3							
			Coral		Water		Sediment		Macroalgae		Coral		Water		Sediment		Macroalgae		Coral		Water		Sediment		Macroalgae	
Seasons	Site	Habitats	Contri.	%	Contri.	%	Contri.	%	Contri.	%	Contri.	%	Contri.	%	Contri.	%	Contri.	%	Contri.	%	Contri.	%	Contri.	%	Contri.	%
Spawning	1	Coral	C131, **C1cstar**	27, 16	**C1085**, C15.20	17, 11	**C1085**, A155	21, 19	**C1085**, A112	17, 10	**C1085**, C15	32, 30	C15.20, **C1085**	22, 18	**C1085**, A155	23, 20	**C1085**, A112	19, 9	**C1085**, C1cstar	30, 24	**C1085**, C15.20	18, 18	**C1085**, A155	23, 14	**C1085**, C131	27, 16
		Water	C1085,**C15.20**	16, 11	C15.20, C15.16	10, 9	A155, **C1085**	15, 7	A112, **C131**	9, 7	C15, **C131**	17, 12	C15.20, **C1.11**	11, 7	A155, **C1085**	16, 9	A112, **C1085**	9, 8	C1cstar, **C131**	16, 9	C15.20, **C131**	10, 7	A155, **C1085**	12, 9	C131, **C1085**	10, 9
		Sediment	C1085, **A113**	18, 8	**A113**, **F3.2**	7, 7	A155, **F3.2**	11, 9	**F3.2**, **G4**	7, 7	C15, **A113**	18, 8	C15.20, A**113**	13, 8	A155, **A113**	12, 8	**F3.2**, **A113**	7, 7	C1cstar, **A113**	15, 7	C15.20, **A113**	10, 7	**F3.2**, D1	8, 7	C131, **F3.2**	13, 8
		Macroalgae	C1085, **A112**	17, 13	**A112**, C15.20	11, 8	A155, **A112**	18, 8	**C131**, **A112**	9, 6	C15, **A112**	19, 11	**A112**, C15.20	13, 12	A155, **A112**	17, 11	C93, C131	8, 8	C1cstar, **A112**	14, 11	**A112**, C15.20	13, 10	A155, **A112**	12, 10	C131, **A112**	14, 10
	2	Coral	C1085, **C15**	32, 27	**C15**, **C15.16**	17, 12	A155, **C15**	19, 18	**C15**, **C15.16**	16, 9	**C15.16**, C15	37, 23	C15.20, **C15**	8, 17	A155, **C15**	21, 17	**C15**, **C15.16**	14, 9	C1cstar, **C15**	26, 24	C15.20, **C15**	15, 15	**C15**, A155	16, 14	**C15**, C131	20, 18
		Water	C1085, **A1**	18, 9	C15.20, C15.16	9, 9	A155, **C15.20**	16, 7	A112, **C131**	9, 7	C15, **C15.20**	16, 9	C15.20, **D1**	11, 8	A155, **C131**	17, 5	A112, **D1**	9, 6	C1cstar, **C131**	15, 7	C15.20, **D1**	9, 8	A155, A113	12, 7	C131, **C15.20**	11, 7
		Sediment	C1085, **A113**	19, 19	**A113**, C15.20	12, 7	A155, **A113**	12, 10	**A113**, C131	12, 7	C15, **A113**	19, 13	**A113**, C15.20	13, 11	**A113**, A155	14, 13	**A113**, C131	12, 8	C1cstar, **A113**	16, 12	**A113**, C15.20	11, 9	**A113**, C131	8, 8	C131, **A113**	15, 13
		Macroalgae	C1085, **A112**	19, 14	**A112**, C15.20	12, 9	A155, **A112**	17, 9	C131, **A112**	9, 7	C15, **A112**	20, 12	**A112**, C15.20	14, 12	A155, **A112**	18, 11	C93, C131	8, 8	C1cstar, **A112**	16, 11	**A112**, C15.20	13, 10	A155, **A112**	12, 11	C131, **A112**	14, 10
	3	Coral	C1085, **C42**	31, 24	**C42**, **C1cstar**	18, 9	A155, **C42**	18, 16	**C42**, **C1cstar**	16, 9	C15, **C42**	29, 23	**C42**, C15.20	18, 17	A155, **C42**	19, 17	**C42**, **C1cstar**	15, 9	**C42**, C42.2	22, 18	**C42**, C15.20	18, 16	**C42**, A155	17, 14	**C42**, C131	20, 16
		Water	C1085, **A1**	18, 12	C15.16, C15.20	11, 10	A155, **C15.16**	13, 6	A112, **C131**	9, 8	C15, **A1**	18, 10	C15.20, **C15.16**	17, 7	A155, **A1**	14, 7	A112, C131	10, 6	C1cstar, **A1**	16, 9	C15.20, **A1**	13, 6	A155, A113	9, 7	C131, **A1**	14, 7
		Sediment	C1085, **A113**	19, 12	**A113**, C15.20	11, 7	A155, **A113**	14, 9	**A113**, C131	11, 6	C15, **A113**	18, 12	C15.20, **A113**	13, 12	A155, **A113**	14, 12	**A113**, C131	11, 6	C1cstar, **A113**	15, 11	C15.20, **A113**	11, 10	A155, **A113**	9, 7	C131, **A113**	14, 12
		Macroalgae	C1085, **A112**	20, 14	**A112**, C15.20	14, 9	A155, **A112**	18, 10	C131, **A112**	9, 7	C15, **A112**	20, 13	**A112**, C15.20	16, 11	A155, **A112**	18, 12	C93, C131	9, 8	C1cstar, **A112**	15, 12	**A112**, C15.20	15, 9	A155, **A112**	13, 12	C131, **A112**	15, 11

Table S2.7. Summary of PERMANOVA main effects for *Symbiodinium* community compositions based on the abundance of clades A, C and D obtained by qPCR. Cell densities of *Symbiodinium* belong to clades A, C and D in each environmental habitat, which were normalized by cm^3, were square-root transformed and PERMANOVA was performed with sites (coral species) (3 levels), habitats (4 levels), and seasons (2 levels) as fixed factors, using type III sum of squares and unrestricted permutation of raw data with 999 permutations. MS: mean square, df: degrees of freedom, *F*: Fisher statistic, P value: * for $P < 0.05$, ** for $P < 0.01$.

Source	MS	df	*F*	P value	
Site	869	2	2.9	0.022	*
Habitat	66,437	2	221	0.001	**
Season	214	1	0.7	0.48	
Site × Habitat	618	4	2.1	0.053	
Site × Season	352	2	1.2	0.29	
Habitat × Season	1,841	2	6.1	0.001	**
Site × Habitat × Season	479	4	1.6	0.14	

Chapter 3

Table S3.1. Number of sequences, clades and OTUs obtained by DNA metabarcoding using the cp23S primer set. Total samples which were successfully amplified and sequenced are 109/120 samples (4 replicates × 3 sites × 5 habitats × 2 sampling times).

Sample				Number of	Number of	Number of
Season	Site	Habitat	Replicate	sequences	clades	OTUs
Pre-bleaching	1	*P. versipora*	a	7,588	1	1
			b	16,107	1	1
			c	16,217	1	1
			d	16,992	1	1
	2	*P. versipora*	a	6,438	1	2
			b	17,978	1	1
			c	18,622	1	1
			d	14,039	1	2
	3	*P. versipora*	a	17,700	1	1
			b	18,404	1	1
			c	23,462	1	2
			d	19,446	1	2
	1	*C. gaboensis*	a	11,596	1	2
			b	9,849	1	1
			c	12,061	1	1
			d	12,719	1	2
	2	*C. gaboensis*	a	7,207	1	2
			b	14,693	1	1
			c	14,934	1	1
			d	16,090	1	1
	3	*C. gaboensis*	a	6,703	1	2
			b	11,821	1	1
			c	11,990	1	1
			d	12,353	1	1
	1	Water	a	10,486	1	3
			b	11,789	2	3
			c	10,420	1	2
			d	7,384	1	1
	2	Water	a	7,573	1	4
			b	8,640	3	10
			c	14,005	1	3
			d	6,990	1	3
	3	Water	a	5,439	1	1
			b	5,712	2	3
			c	5,342	3	4
			d	6,326	2	2
	1	Sediment	a	5,132	2	2
			b	18,655	3	3
			c	6,066	2	2
			d	5,098	2	3
	2	Sediment	a	4,824	2	2
			c	7,099	2	2
			d	7,495	3	5
	3	Sediment	a	6,995	2	5
			b	1,036	2	4
			c	5,924	3	6
			d	3,443	4	6
	1	Macroalgae	a	1,761	2	3
			b	7,559	4	6
			c	6,934	1	2
			d	9,127	1	2
	2	Macroalgae	a	3,384	3	5
			b	6,363	2	2
			c	8,267	4	12
			d	4,574	2	4
	3	Macroalgae	a	6,723	2	6
			b	22,778	1	4
			c	10,068	2	4
			d	7,464	2	5

Table S3.1. (continued)

Sample				Number of	Number of	Number of
Season	Site	Habitat	Replicate	sequences	clades	OTUs
Bleaching	1	*P. versipora*	a	22,843	1	1
			b	19,824	1	3
			c	15,662	1	1
			d	13,774	1	2
	2	*P. versipora*	a	17,728	1	1
			b	15,461	1	2
			c	15,700	1	1
			d	16,454	1	1
	3	*P. versipora*	a	20,407	1	2
			b	22,115	1	1
			c	18,085	1	2
			d	26,044	1	2
	2	*C. gaboensis*	a	18,294	1	1
			b	10,592	1	1
			c	14,995	1	1
			d	11,654	1	1
	3	*C. gaboensis*	a	12,143	1	1
			b	15,813	1	1
			c	12,902	1	1
			d	10,773	1	1
	1	Water	a	9,040	1	3
			b	10,601	1	4
			c	18,418	1	3
			d	9,200	1	3
	2	Water	a	7,068	2	4
			b	7,041	2	7
			c	3,183	2	8
			d	8,527	2	4
	3	Water	a	38,610	3	5
			b	32,043	2	5
			c	13,338	1	3
			d	5,315	2	4
	1	Sediment	c	4,863	1	1
			d	9,333	2	2
	2	Sediment	c	2,799	1	1
			d	2,516	1	1
	3	Sediment	a	5,073	2	4
			b	1,972	2	6
			c	3,205	2	3
			d	2,779	3	7
	1	Macroalgae	a	7,915	4	8
			b	4,466	3	4
			c	7,649	3	5
			d	10,793	2	3
	2	Macroalgae	a	7,705	2	3
			c	8,383	1	3
			d	8,755	1	1
	3	Macroalgae	b	4,202	1	3
			c	804	1	3
			d	3,359	1	2

Table S3.2. Summary of Kruskal-Wallis test for number of clades and OTUs based on the cp23S marker. **A.** Main effects. **B.** *Post-hoc* pairwise comparison for sites × habitats × seasons. df: degrees of freedom, P value: * for $P < 0.05$, ** for $P < 0.01$.

A. Main effects.

Variables	Test Statistic	df	P value	
Number of clades	53	9	2.6E-08	**
Number of OTUs	62	9	5.8E-10	**

B. Pairwise comparison.

			Pre-bleaching								Bleaching							
			P. versipora		*C. gaboensis*		Water	Sediment	Macroalgae	*P. versipora*		*C. gaboensis*		Water	Sediment			
Variables	Seasons	Habitats	P value		P value		P value	P value	P value	P value		P value		P value	P value			
Number of clades	Pre-bleaching	*P. versipora*																
		C. gaboensis	1.0							1.0								
		Water	1.0		1.0					1.0		1.0						
		Sediment	6.6E-05	**	6.6E-05	**	0.22			6.6E-05	**	6.8E-04	**	1.0				
		Macroalgae	0.0091	**	0.0091	**	1.0	1.0		0.0091	**	0.040	*	1.0	1.0			
	Bleaching	*P. versipora*	1.0															
		C. gaboensis	1.0		1.0					1.0								
		Water	0.39		0.39		1.0			0.39		0.86						
		Sediment	0.46		0.46		1.0	1.0		0.46		0.86		1.0				
		Macroalgae	0.45		0.45		1.0	1.0	1.0	0.45		0.91		1.0	1.0			
Number of OTUs	Pre-bleaching	*P. versipora*																
		C. gaboensis	1.0							1.0								
		Water	0.23		0.23					1.0		0.059						
		Sediment	0.019	*	0.019	*	1.0			0.12		0.0049	**	1.0				
		Macroalgae	0.0013	**	0.0013	**	1.0	1.0		0.012	*	3.7E-04	**	1.0	1.0			
	Bleaching	*P. versipora*	1.0															
		C. gaboensis	1.0		1.0					1.0								
		Water	2.8E-04	**	2.8E-04	**	1.0			0.0031	**	8.9E-05	**					
		Sediment	1.0		1.0		1.0	1.0		1.0		0.45		1.0				
		Macroalgae	0.066		0.066		1.0	1.0	1.0	0.34		0.017	*	1.0	1.0			

Table S3.3. Number of sequences, clades, ITS2 variants and OTUs obtained by DNA metabarcoding using the ITS2 primer set. Total samples which were successfully amplified and sequenced are 105/120 samples (4 replicates × 3 sites × 5 habitats × 2 sampling times).

Sample				Number of	Number of	Number of	Number of
Season	Site	Habitat	Replicate	sequences	clades	ITS2 variants	OTUs
Pre-bleaching	1	*P. versipora*	a	87,970	1	3	14
			b	29,622	1	3	13
			c	31,538	1	3	12
			d	35,754	1	2	15
	2	*P. versipora*	a	79,478	1	3	12
			b	36,930	1	3	11
			c	30,418	1	3	11
			d	31,889	1	3	15
	3	*P. versipora*	a	112,593	1	4	13
			b	60,270	1	3	11
			c	55,859	1	3	19
			d	39,474	1	3	7
	1	*C. gaboensis*	a	63,012	1	1	14
			b	51,687	1	1	14
			c	62,907	1	1	5
			d	52,997	1	1	10
	2	*C. gaboensis*	a	184,671	1	1	7
			b	51,059	1	1	5
			c	50,522	1	1	10
			d	50,493	1	1	6
	3	*C. gaboensis*	a	81,101	1	1	12
			b	57,206	1	1	10
			c	50,478	1	1	14
			d	57,136	1	1	15
	1	Water	a	6,515	2	3	10
			b	260	1	3	12
			c	24,994	1	3	10
			d	1,104	1	2	8
	2	Water	a	1,589	2	6	17
			b	34	2	6	14
			c	50	2	4	12
			d	92	2	6	26
	3	Water	a	7,695	1	1	8
			b	4,483	1	1	12
			c	3,549	1	1	15
			d	412	1	2	11
	1	Sediment	b	51,317	2	2	2
			c	421	1	1	1
			d	24,787	2	4	7
	2	Sediment	a	638	3	4	5
			c	302	1	1	1
			d	2,843	1	2	3
	3	Sediment	a	1,533	2	2	2
			b	736	1	2	3
			c	613	2	2	6
			d	106	2	3	5
	1	Macroalgae	a	349	2	3	3
			b	645	2	3	4
			c	456	4	6	10
			d	474	2	2	2
	2	Macroalgae	a	327	2	3	10
			b	278	2	3	4
			c	440	2	4	10
			d	476	1	1	7
	3	Macroalgae	a	5,295	3	3	6
			b	7,551	1	2	8
			c	15,842	1	1	13
			d	9,474	2	2	15

Table S3.3. (continued)

Sample				Number of	Number of	Number of	Number of
Season	Site	Habitat	Replicate	sequences	clades	ITS2 variants	OTUs
Bleaching	1	*P. versipora*	a	72,057	1	2	12
			b	70,678	1	2	13
			c	34,749	1	2	12
			d	39,818	1	2	14
	2	*P. versipora*	a	67,228	1	2	12
			b	48,798	1	3	10
			c	52,661	1	3	13
			d	37,293	1	3	11
	3	*P. versipora*	a	64,026	1	3	11
			b	56,813	1	3	11
			c	34,708	1	3	11
			d	55,268	1	2	9
	2	*C. gaboensis*	a	50,414	1	1	15
			b	62,195	1	1	9
			c	49,445	1	1	18
			d	64,262	1	1	15
	3	*C. gaboensis*	a	63,293	1	1	11
			b	51,900	1	1	12
			c	70,140	1	1	4
			d	52,522	1	1	8
	1	Water	a	10,761	1	3	10
			b	67,740	1	3	9
			c	14,209	1	3	11
			d	10,276	1	3	11
	2	Water	a	1,503	2	3	9
			b	961	2	3	9
			c	867	2	2	7
			d	3,060	2	4	7
	3	Water	a	169	2	2	17
			b	107	1	1	11
			c	28	1	1	10
	1	Sediment	d	45,186	1	2	5
	2	Sediment	a	3,076	1	1	2
			d	16,794	1	1	1
	3	Sediment	a	21	4	4	7
			b	30	1	3	4
			c	27	3	4	5
			d	171	2	3	4
	1	Macroalgae	a	1,267	3	6	7
			b	1,906	1	2	4
			c	1,164	2	3	3
			d	2,733	1	2	3
	2	Macroalgae	a	273	2	2	4
			c	161	1	1	6
	3	Macroalgae	b	2,266	1	1	6
			c	6,132	1	1	5
			d	13,754	2	2	5

Table S3.4. Summary of Kruskal-Wallis test for number of clades, ITS2 variants and OTUs based on the ITS2 marker. **A.** Main effects. **B.** *Post-hoc* pairwise comparison for sites × habitats × seasons. df: degrees of freedom, P value: * for $P < 0.05$, ** for $P < 0.01$.

A. Main effects.

Variables	Test Statistic	df	P value	
Number of clades	37	9	2.5E-05	**
Number of ITS2 variants	42	9	3.0E-06	**
Number of OTUs	59	9	2.5E-09	**

B. Pairwise comparison.

			Pre-bleaching								Bleaching							
			P. versipora		*C. gaboensis*		Water		Sediment	Macroalgae	*P. versipora*		*C. gaboensis*		Water		Sediment	
Variables	Seasons	Habitats	P value		P value		P value		P value	P value	P value		P value		P value		P value	
Number of clades	Pre-bleaching	*P. versipora*																
		C. gaboensis	1.0								1.0							
		Water	1.0		1.0						1.0		1.0					
		Sediment	0.13		0.13		1.0				0.13		0.33		1.0			
		Macroalgae	0.0031	**	0.0031	**	1.0		1.0		0.0031	**	0.017	*	1.0		1.0	
	Bleaching	*P. versipora*	1.0															
		C. gaboensis	1.0		1.0						1.0							
		Water	1.0		1.0		1.0				1.0		1.0					
		Sediment	1.0		1.0		1.0		1.0		1.0		1.0		1.0			
		Macroalgae	1.0		1.0		1.0		1.0	1.0	1.0		1.0		1.0		1.0	
Number of ITS2 variants	Pre-bleaching	*P. versipora*																
		C. gaboensis	6.8E-05	**							0.012	*						
		Water	1.0		0.0033	**					1.0		0.017	*				
		Sediment	1.0		0.18		1.0				1.0		0.41		1.0			
		Macroalgae	1.0		0.0069	**	1.0		1.0		1.0		0.032	*	1.0		1.0	
	Bleaching	*P. versipora*	1.0															
		C. gaboensis	7.7E-04	**	1.0						0.050	*						
		Water	1.0		0.013	*	1.0				1.0		0.052					
		Sediment	1.0		0.082		1.0		1.0		1.0		0.19		1.0			
		Macroalgae	1.0		1.0		1.0		1.0	1.0	1.0		1.0		1.0		1.0	
Number of OTUs	Pre-bleaching	*P. versipora*																
		C. gaboensis	1.0								1.0							
		Water	1.0		1.0						1.0		1.0					
		Sediment	3.5E-05	**	0.021	*	2.4E-04	**			5.4E-04	**	0.0093	**	0.070			
		Macroalgae	0.12		1.0		0.44		1.0		0.73		1.0		1.0		1.0	
	Bleaching	*P. versipora*	1.0															
		C. gaboensis	1.0		1.0						1.0							
		Water	1.0		1.0		1.0				1.0		1.0					
		Sediment	9.1E-04	**	0.14		0.0042	**	1.0		0.0079	**	0.056		0.34			
		Macroalgae	8.2E-04	**	0.18		0.0043	**	1.0	1.0	0.0084	**	0.072		0.46		1.0	

Table S3.5. Summary of PERMANOVA main effects for *Symbiodinium* community compositions based on the cp23S marker. **A.** Clades. **B.** OTUs. Relative abundance of community compositions was square-root transformed and PERMANOVA was performed with sites (3 levels), habitats (5 levels), and seasons (2 levels) as fixed factors, using type III sum of squares and unrestricted permutation of raw data with 999 permutations. MS: mean square, df: degrees of freedom, *F*: Fisher statistic, P value: * for $P < 0.05$, ** for $P < 0.01$.

A. Main effects on cladal composition.

Source	MS	df	*F*	P value	
Site	11,230	2	19	0.001	**
Habitat	25,179	4	43	0.001	**
Season	1,115	1	1.9	0.15	
Site × Habitat	3,074	8	5.3	0.001	**
Site × Season	482	2	0.83	0.46	
Habitat × Season	201	4	0.35	0.90	
Site × Habitat × Season	1,115	7	1.9	0.057	

B. Main effects on OTU composition.

Source	MS	df	*F*	P value	
Site	17,901	2	16	0.001	**
Habitat	25,770	4	23	0.001	**
Season	1,282	1	1.2	0.28	
Site × Habitat	4,983	8	4.5	0.001	**
Site × Season	1,976	2	1.8	0.099	
Habitat × Season	1,159	4	1.0	0.38	
Site × Habitat × Season	2,148	7	1.9	0.010	**

Table S3.6. Summary of SIMPER analysis for *Symbiodinium* cladal community compositions based on the cp23S marker. Pairwise comparison within **A.** Pre-bleaching and **B.** Bleaching. Pairwise comparison **C.** Between pre-bleaching and bleaching sampling time points. Top two clades which contributed to dissimilarity of community compositions are shown with contribution percentages (%). Clades which were more abundant in variables in columns are shown as bold letter and clades which were more abundant in variables in rows are shown as normal letter.

A. Within pre-bleaching sampling time point.

			Pre-bleaching																											
			Site 1										Site 2										Site 3							
			P. versipora		*C. gaboensis*		Water		Sediment		Macroalgae		*P. versipora*		*C. gaboensis*		Water		Sediment		Macroalgae		*P. versipora*		*C. gaboensis*		Water		Sediment		Macroalgae	
Seasons	Site	Habitats	Contri.	%	Contri.	%	Contri.	%	Contri.	%	Contri.	%	Contri.	%	Contri.	%	Contri.	%	Contri.	%	Contri.	%	Contri.	%	Contri.	%	Contri.	%	Contri.	%	Contri.	%
Pre-bleaching	1	*P. versipora*																												
		C. gaboensis	**A**, B	50, 50									**A**, B	50, 50									**A**, B	50, 50						
		Water	**C**	94	A, **B**	49, 49							**C**	94	A, **B**	49, 49							**C**	94	A, **B**	49, 49				
		Sediment	**E**, B	63, 31	A, **B**	44, 34	**E**, B	62, 30					**E**, B	63, 31	A, **B**	44, 34	**E**, B	56, 27					**E**, B	63, 31	A, **B**	44, 34	A, **B**	46, 29		
		Macroalgae	**C**, B	46, 44	A, **C**	46, 28	**C**, B	46, 44	**C**, B	33, 31			**C**, B	46, 44	A, **C**	46, 28	**C**, B	45, 42	**C**, B	35, 32			**C**, B	46, 44	A, **C**	46, 28	A, **C**	45, 28	A, **C**	30, 27
	2	*P. versipora*	-																											
		C. gaboensis	**A**, B	50, 50	-								**A**, B	50, 50									**A**, B	50, 50						
		Water	**A**, **F**	52, 38	**B**, A	50, 48	**A**, **F**	40, 29					**A**, **F**	52, 38	**B**, A	50, 48							**A**, **F**	52, 38	**B**, A	50, 48				
		Sediment	**A**, **F**	55, 24	**B**, A	52, 37	**A**, **F**	53, 23	E, **A**	36, 31			**A**, **F**	55, 24	**B**, A	52, 37	**A**, **F**	53, 23					**A**, **F**	55, 24	**B**, A	52, 37	**B**, A	47, 40		
		Macroalgae	B, **A**	37, 34	A, **B**	36, 32	B, **A**	37, 34	**A**, B	32, 31	C, B	29, 27	B, **A**	37, 34	A, **B**	36, 32	B, **A**	38, 32	B, **E**	37, 23			B, **A**	37, 34	A, **B**	36, 32	A, **B**	34, 33	**B**, F	29, 23
	3	*P. versipora*	-										-																	
		C. gaboensis	**A**, B	50, 50	-								**A**, B	50, 50	-								**A**, B	50, 50						
		Water	**A**, B	53, 45	**B**, **F**	75, 13	**A**, B	52, 45					**A**, B	53, 45	**B**, **F**	75, 13	**A**, B	52, 45					**A**, B	53, 45	**B**, **F**	75, 13				
		Sediment	**A**, B	41, 38	**B**, **F**	34, 34	**A**, B	40, 37	**A**, B	34, 23			**A**, B	41, 38	**B**, **F**	34, 34	**A**, B	39, 38	B, **A**	39, 29			**A**, B	41, 38	**B**, **F**	34, 34	**F**, A	39, 32		
		Macroalgae	**A**, B	51, 41	**B**, A	52, 28	**A**, B	50, 40	**A**, B	25, 29	**A**, C	38, 29	**A**, B	51, 41	**B**, A	52, 28	**A**, B	48, 41	B, **A**	41, 33	B, **A**	35, 29	**A**, B	51, 41	**B**, A	52, 28	**B**, A	51, 26	B, F	31, 30

B. Within bleaching sampling time point.

			Bleaching																											
			Site 1										Site 2										Site 3							
			P. versipora		*C. gaboensis*		Water		Sediment		Macroalgae		*P. versipora*		*C. gaboensis*		Water		Sediment		Macroalgae		*P. versipora*		*C. gaboensis*		Water		Sediment		Macroalgae	
Seasons	Site	Habitats	Contri.	%	Contri.	%	Contri.	%	Contri.	%	Contri.	%	Contri.	%	Contri.	%	Contri.	%	Contri.	%	Contri.	%	Contri.	%	Contri.	%	Contri.	%	Contri.	%	Contri.	%
Bleaching	1	*P. versipora*																												
		C. gaboensis																												
		Water	-										-		A, **B**	50, 50							-		A, **B**	50, 50				
		Sediment	**F**, B	79, 21			**F**, B	79, 21					**F**, B	79, 21	A, **B**	46, 43	A, **F**	54, 35					**F**, B	79, 21	A, **B**	46, 43	A, **B**	50, 36		
		Macroalgae	**A**, B	50, 23			**A**, B	50, 23	**A**, F	44, 26			**A**, B	50, 23	**B**, A	50, 36	**A**, B	36, 27	A, **B**	41, 41			**A**, B	50, 23	**B**, A	50, 36	**B**, A	41, 39	**B**, F	35, 30
	2	*P. versipora*	-																											
		C. gaboensis	**A**, B	50, 50									**A**, B	50, 50									**A**, B	50, 50						
		Water	**A**, B	83, 17			**A**, B	83, 17					**A**, B	83, 17	**B**, A	59, 41							**A**, B	83, 17	**B**, A	59, 41				
		Sediment	**A**, B	50, 50			A, **B**	50, 50	**B**, A	41, 41			**A**, B	50, 50	A, **B**	50, 50	**A**, B	48, 48					**A**, B	50, 50	A, **B**	50, 50	**A**, B	48, 48		
		Macroalgae	B, **F**	44, 40			B, **F**	44, 40	**F**, B	45, 40	B, **F**	32, 31	B, **F**	44, 40	A, **B**	47, 34	B, **F**	36, 35	A, **B**	37, 37			B, **F**	44, 40	A, **B**	47, 34	A, **B**	44, 33	**B**, F	35, 35
	3	*P. versipora*	-										-																	
		C. gaboensis	**A**, B	50, 50									**A**, B	50, 50	-								**A**, B	50, 50						
		Water	**A**, B	55, 42			**A**, B	56, 42					**A**, B	55, 42	**B**, A	60, 32	B, **A**	51, 44					**A**, B	55, 42	**B**, A	60, 32				
		Sediment	**A**, B	39, 34			**A**, B	39, 34	**A**, B	40, 32			**A**, B	39, 34	**B**, A	41, 37	B, **F**	39, 34	A, **B**	38, 38			**A**, B	39, 34	**B**, A	41, 37	**B**, A	38, 36		
		Macroalgae	**A**, B	50, 50			**A**, B	50, 50	**A**, B	46, 43	B, **A**	50, 36	**A**, B	50, 50	-		B, **A**	59, 41	**A**, B	50, 50	**A**, B	47, 34	**A**, B	50, 50	-		B, **A**	60, 32	B, **A**	41, 37

C. Between pre-bleaching and bleaching sampling time points.

			Bleaching																											
			Site 1										Site 2										Site 3							
			P. versipora		*C. gaboensis*		Water		Sediment		Macroalgae		*P. versipora*		*C. gaboensis*		Water		Sediment		Macroalgae		*P. versipora*		*C. gaboensis*		Water		Sediment		Macroalgae	
Seasons	Site	Habitats	Contri.	%	Contri.	%	Contri.	%	Contri.	%	Contri.	%	Contri.	%	Contri.	%	Contri.	%	Contri.	%	Contri.	%	Contri.	%	Contri.	%	Contri.	%	Contri.	%	Contri.	%
Pre-bleaching	1	*P. versipora*	-				-		F, **B**	79, 21	A, **B**	50, 23	-		A, **B**	50, 50	A, **B**	83, 17	A, **B**	50, 50	**B**, F	44, 40	-		A, **B**	50, 50	A, **B**	55, 42	A, **B**	39, 34	A, **B**	50, 50
		C. gaboensis	**A**, B	50, 50			**A**, B	50, 50	**A**, B	46, 43	B, **A**	50, 36	**A**, B	50, 50	-		B, **A**	59, 41	**A**, B	50, 50	**A**, B	47, 34	**A**, B	50, 50	-		B, **A**	60, 32	B, **A**	41, 37	-	
		Water	**C**	94			**C**	94	F, **B**	71, 19	A, **B**	49, 23	**C**	94	**B**, A	49, 49	A, **B**	78, 16	A, **B**	49, 49	**B**, F	43, 29	**C**	94	A, **B**	49, 49	A, **B**	54, 41	A, **B**	38, 33	A, **B**	49, 49
		Sediment	**E**, B	63, 31			**E**, B	63, 31	**E**, F	48, 24	**E**, A	34, 30	**E**, B	63, 31	A, **B**	44, 34	**E**, A	43, 33	A, **B**	33, 33	**E**, **B**	33, 29	**E**, B	63, 31	A, **B**	44, 34	A, **B**	43, 27	A, **E**	28, 27	A, **B**	44, 34
		Macroalgae	**C**, B	46, 44			**C**, B	46, 44	**C**, B	40, 37	**C**, B	35, 33	**C**, B	46, 44	A, **C**	46, 28	**C**, B	40, 36	**C**, A	35, 31	**C**, B	35, 31	**C**, B	46, 44	A, **C**	46, 28	A, **C**	39, 30	**C**, B	31, 28	A, **C**	46, 28
	2	*P. versipora*	-				-		F, **B**	79, 21	A, **B**	50, 23	-		A, **B**	50, 50	A, **B**	83, 17	A, **B**	50, 50	**B**, F	44, 40	-		A, **B**	50, 50	A, **B**	55, 42	A, **B**	39, 34	A, **B**	50, 50
		C. gaboensis	**A**, B	50, 50			**A**, B	50, 50	**A**, B	46, 43	B, **A**	50, 36	**A**, B	50, 50	-		B, **A**	59, 41	**A**, B	50, 50	**A**, B	47, 34	**A**, B	50, 50	-		B, **A**	60, 32	B, **A**	41, 37	-	
		Water	**A**, **F**	52, 38			**A**, **F**	52, 38	F, **B**	66, 18	A, **B**	47, 24	**A**, **F**	52, 38	**B**, A	50, 48	A, **B**	74, 16	A, **B**	48, 48	**B**, F	42, 40	**A**, **F**	52, 38	**B**, A	50, 48	A, **B**	52, 43	A, **B**	37, 35	**B**, A	50, 48
		Sediment	**A**, **F**	55, 24			**A**, **F**	56, 24	**A**, F	53, 35	**F**, A	31, 31	**A**, **F**	55, 24	**B**, A	52, 37	**F**, **A**	46, 33	**B**, A	42, 42	F, **B**	38, 34	**A**, **F**	55, 24	**B**, A	52, 37	**B**, A	44, 39	**B**, F	37, 37	**B**, A	53, 37
		Macroalgae	B, **A**	37, 34			B, **A**	37, 34	**A**, B	32, 32	B, **A**	37, 22	B, **A**	37, 34	A, **B**	36, 32	B, **E**	43, 25	**A**, B	35, 35	B, **A**	30, 26	B, **A**	37, 34	A, **B**	36, 32	**B**, A	35, 30	**B**, F	32, 22	A, **B**	36, 32
	3	*P. versipora*	-				-		F, **B**	79, 21	A, **B**	50, 23	-		A, **B**	50, 50	A, **B**	83, 17	A, **B**	50, 50	**B**, F	44, 40	-		A, **B**	50, 50	A, **B**	55, 42	A, **B**	39, 34	A, **B**	50, 50
		C. gaboensis	**A**, B	50, 50			**A**, B	50, 50	**A**, B	46, 43	B, **A**	50, 36	**A**, B	50, 50	-		B, **A**	59, 41	**A**, B	50, 50	**A**, B	47, 34	**A**, B	50, 50	-		B, **A**	60, 32	B, **A**	41, 37	-	
		Water	**A**, B	53, 45			**A**, B	53, 45	**A**, B	49, 39	B, **A**	45, 39	**A**, B	53, 45	**B**, **F**	75, 13	B, **A**	54, 44	B, **A**	49, 49	**A**, B	47, 32	**A**, B	53, 45	**B**, **F**	75, 13	B, **A**	55, 34	B, **A**	38, 38	**B**, **F**	75, 13
		Sediment	**A**, B	41, 38			**A**, B	41, 38	**A**, B	41, 35	B, **A**	35, 29	**A**, B	41, 38	**B**, **F**	34, 34	B, **A**	43, 28	**A**, B	36, 36	**A**, B	37, 32	**A**, B	41, 38	**B**, **F**	34, 34	**F**, A	35, 31	B, **A**	35, 32	**B**, **F**	34, 34
		Macroalgae	**A**, B	51, 41			**A**, B	51, 41	**A**, B	46, 34	B, **A**	41, 32	**A**, B	51, 41	**B**, A	52, 28	B, **A**	50, 39	**A**, B	44, 44	**A**, B	40, 31	**A**, B	51, 41	**B**, A	52, 28	B, **A**	49, 30	B, **A**	36, 28	**B**, A	52, 28

Table S3.7. Summary of PERMANOVA main effects for *Symbiodinium* community compositions based on the ITS2 marker. **A.** Clades. **B.** ITS2 variants. **C.** OTUs. Relative abundance of community compositions was square-root transformed and PERMANOVA was performed with sites (3 levels), habitats (5 levels) and seasons (2 levels) as fixed factors, using type III sum of squares and unrestricted permutation of raw data with 999 permutations. MS: mean square, df: degrees of freedom, *F*: Fisher statistic, P value: * for $P < 0.05$, ** for $P < 0.01$.

A. Main effects on cladal composition.

Source	MS	df	*F*	P value	
Site	11,076	2	23	0.001	**
Habitat	27,730	4	57	0.001	**
Season	755	1	1.5	0.20	
Site × Habitat	4,205	8	8.6	0.001	**
Site × Season	1,174	2	2.4	0.08	
Habitat × Season	1,838	4	3.8	0.008	**
Site × Habitat × Season	1,214	7	2.5	0.020	*

B. Main effects on ITS2 variant composition.

Source	MS	df	*F*	P value	
Site	15,356	2	18	0.001	**
Habitat	27,326	4	32	0.001	**
Season	761	1	0.89	0.40	
Site × Habitat	5,127	8	6.0	0.001	**
Site × Season	1,854	2	2.2	0.069	
Habitat × Season	1,922	4	2.2	0.025	*
Site × Habitat × Season	1,769	7	2.1	0.030	*

C. Main effects on OTU composition.

Source	MS	df	*F*	P value	
Site	6,194	2	1.8	0.001	**
Habitat	15,770	4	4.6	0.001	**
Season	12,070	1	3.6	0.001	**
Site × Habitat	5,836	8	1.7	0.001	**
Site × Season	5,823	2	1.7	0.001	**
Habitat × Season	11,187	4	3.3	0.001	**
Site × Habitat × Season	5,010	7	1.5	0.001	**

Table S3.8. Summary of SIMPER analysis for *Symbiodinium* cladal community compositions based on the ITS2 marker. Pairwise comparison within **A.** Pre-bleaching and **B.** Bleaching. Pairwise comparison **C.** Between pre-bleaching and bleaching sampling time points. Top two clades which contributed to dissimilarity of community compositions are shown with contribution percentages (%). Clades which were more abundant in variables in columns are shown as bold letter and clades which were more abundant in variables in rows are shown as normal letter.

A. Within pre-bleaching sampling time point.

			Pre-bleaching																											
			Site 1										Site 2										Site 3							
			P. versipora		*C. gaboensis*		Water		Sediment		Macroalgae		*P. versipora*		*C. gaboensis*		Water		Sediment		Macroalgae		*P. versipora*		*C. gaboensis*		Water		Sediment		Macroalgae	
Seasons	Site	Habitats	Contri.	%	Contri.	%	Contri.	%	Contri.	%	Contri.	%	Contri.	%	Contri.	%	Contri.	%	Contri.	%	Contri.	%	Contri.	%	Contri.	%	Contri.	%	Contri.	%	Contri.	%
Pre-bleaching	1	*P. versipora*																												
		C. gaboensis	**A**, B	50, 50									**A**, B	50, 50									**A**, B	50, 50						
		Water	**A**	94	**B**, A	51, 49							**A**	94	**B**, A	51, 49							**A**	94	**B**, A	51, 49				
		Sediment	**E**, B	79, 21	A, **B**	45, 41	**E**, B	73, 20					**E**, B	79, 21	A, **B**	45, 41	A, **E**	50, 30					**E**, B	79, 21	A, **B**	45, 41	A, **B**	45, 41		
		Macroalgae	B, **A**	39, 29	A, **C**	36, 28	B, **A**	39, 29	B, **A**	31, 26			B, **A**	39, 29	A, **C**	36, 28	B, A	35, 28	A, **C**	34, 27			B, **A**	39, 29	A, **C**	36, 28	A, **C**	36, 28	B, A	31, 31
	2	*P. versipora*	-																											
		C. gaboensis	**A**, B	50, 50	-								**A**, B	50, 50									**A**, B	50, 50						
		Water	**A**, B	69, 31	**B**, A	62, 38	**A**, B	68, 32					**A**, B	69, 31	**B**, A	62, 38							**A**, B	69, 31	**B**, A	62, 38				
		Sediment	**A**, B	52, 46	**B**, **E**	64, 19	**A**, B	51, 47	**A**, B	47, 38			**A**, B	52, 46	**B**, **E**	64, 19	B, **A**	57, 40					**A**, B	52, 46	**B**, **E**	64, 19	**B**, **E**	64, 19		
		Macroalgae	**A**, B	44, 43	**B**, A	37, 36	B, **A**	44, 43	**A**, B	42, 36	**A**, C	30, 24	**A**, B	44, 43	**B**, A	37, 36	B, **A**	43, 39	A, **B**	36, 34			**A**, B	44, 43	**B**, A	37, 36	**B**, A	37, 36	B, A	41, 38
	3	*P. versipora*	-										-																	
		C. gaboensis	**A**, B	50, 50	-								**A**, B	50, 50	-								**A**, B	50, 50						
		Water	**A**, B	50, 50	-		B, **A**	51, 49					**A**, B	50, 50	-		B, **A**	62, 38					**A**, B	50, 50	-					
		Sediment	**A**, B	59, 41	**B**, A	65, 35	**A**, B	58, 42	**A**, B	49, 30			**A**, B	59, 41	**B**, A	65, 35	B, **A**	53, 47	**B**, A	60, 35			**A**, B	59, 41	**B**, A	65, 35	**B**, A	65, 35		
		Macroalgae	B, **A**	47, 45	**E**, **C**	48, 37	B, **A**	47, 44	**A**, B	43, 41	**A**, C	33, 24	B, **A**	47, 45	**E**, **C**	48, 37	B, **A**	55, 32	B, **E**	34, 33	B, **A**	32, 30	B, **A**	47, 45	**E**, **C**	48, 37	**E**, **C**	48, 37	B, **A**	53, 28

B. Within bleaching sampling time point.

			Bleaching																											
			Site 1										Site 2										Site 3							
			P. versipora		*C. gaboensis*		Water		Sediment		Macroalgae		*P. versipora*		*C. gaboensis*		Water		Sediment		Macroalgae		*P. versipora*		*C. gaboensis*		Water		Sediment		Macroalgae	
Seasons	Site	Habitats	Contri.	%	Contri.	%	Contri.	%	Contri.	%	Contri.	%	Contri.	%	Contri.	%	Contri.	%	Contri.	%	Contri.	%	Contri.	%	Contri.	%	Contri.	%	Contri.	%	Contri.	%
Bleaching	1	*P. versipora*																												
		C. gaboensis																												
		Water	-										-		A, **B**	50, 50							-		A, **B**	50, 50				
		Sediment	-				-						-		A, **B**	50, 50	**A**, B	56, 44					-		A, **B**	50, 50	**B**, A	49, 49			
		Macroalgae	**A**, B	45, 43			**A**, B	45, 43	**A**, B	45, 43			**A**, B	45, 43	**B**, A	46, 44	A, **B**	46, 42	F, **B**	47, 27			**A**, B	45, 43	**B**, A	46, 44	**B**, A	45, 44	A, **B**	35, 33		
	2	*P. versipora*	-																											
		C. gaboensis	**A**, B	50, 50									**A**, B	50, 50									**A**, B	50, 50						
		Water	**A**, B	56, 44			**A**, B	56, 44					**A**, B	56, 44	**B**, A	89, 11							**A**, B	56, 44	**B**, A	89, 11					
		Sediment	B, **F**	50, 50			B, **F**	50, 50	B, **F**	50, 50			B, **F**	50, 50	A, **F**	50, 50	**F**, A	46, 44					B, **F**	50, 50	A, **F**	50, 50	**F**, A	49, 49				
		Macroalgae	**A**, B	56, 44			**A**, B	56, 44	**A**, B	56, 44	**A**, B	45, 44	**A**, B	56, 44	**B**, A	64, 36	**B**, A	65, 35	F, **A**	46, 36			**A**, B	56, 44	**B**, A	64, 36	**B**, A	61, 34	B, **A**	38, 33		
	3	*P. versipora*	-										-																	
		C. gaboensis	**A**, B	50, 50									**A**, B	50, 50	-								**A**, B	50, 50						
		Water	B, **A**	49, 49			B, **A**	49, 49					B, **A**	49, 49	**C**	95	B, **C**	79, 12					B, **A**	49, 49	**C**	95					
		Sediment	**A**, B	37, 37			**A**, B	37, 37	**A**, B	37, 37			**A**, B	37, 37	**B**, A	37, 37	A, **B**	41, 29	F, **A**	42, 24			**A**, B	37, 37	**B**, A	37, 37	**B**, A	37, 36				
		Macroalgae	B, **A**	47, 45			B, **A**	47, 45	B, **A**	47, 45	B, **A**	42, 40	B, **A**	47, 45	**D**, A	76, 24	B, **D**	49, 37	F, **A**	47, 46	B, **A**	50, 28	B, **A**	47, 45	**D**, A	76, 24	**D**, A	66, 21	B, **A**	33, 32		

C. Between pre-bleaching and bleaching sampling time points.

			Bleaching																											
			Site 1										Site 2										Site 3							
			P. versipora		*C. gaboensis*		Water		Sediment		Macroalgae		*P. versipora*		*C. gaboensis*		Water		Sediment		Macroalgae		*P. versipora*		*C. gaboensis*		Water		Sediment		Macroalgae	
Seasons	Site	Habitats	Contri.	%	Contri.	%	Contri.	%	Contri.	%	Contri.	%	Contri.	%	Contri.	%	Contri.	%	Contri.	%	Contri.	%	Contri.	%	Contri.	%	Contri.	%	Contri.	%	Contri.	%
Pre-bleaching	1	*P. versipora*	-				-		-		A, **B**	45, 43	-		A, **B**	50, 50	A, **B**	56, 44	B, F	50, 50	A, **B**	56, 44	-		A, **B**	50, 50	**B**, A	49, 49	A, **B**	37, 37	**B**, A	47, 45
		C. gaboensis	**A**, B	50, 50			**A**, B	50, 50	**A**, B	50, 50	B, **A**	46, 44	**A**, B	50, 50	-		B, **A**	89, 11	**A**, F	50, 50	B, **A**	64, 36	**A**, B	50, 50	-		C	95	B, **A**	37, 37	D, **A**	76, 24
		Water	**A**	94			**A**	94	**A**	94	A, **B**	45, 43	**A**	94	**B**, A	51, 49	A, **B**	55, 45	F, **B**	49, 49	A, **B**	55, 45	**A**	94	**B**, A	51, 49	**B**, A	50, 48	**B**, A	37, 37	**B**, A	48, 44
		Sediment	**E**, B	79, 21			**E**, B	79, 21	**E**, B	79, 21	A, **B**	34, 33	**E**, B	79, 21	A, **B**	45, 41	A, **B**	49, 35	F, **B**	45, 41	A, **B**	48, 33	**E**, B	79, 21	A, **B**	45, 41	A, **B**	44, 41	**B**, A	33, 31	A, **B**	40, 39
		Macroalgae	B, **A**	39, 29			B, **A**	39, 29	B, **A**	39, 29	B, **A**	32, 30	B, **A**	39, 29	A, **C**	36, 28	A, **C**	34, 29	F, **A**	41, 25	A, B	32, 30	B, **A**	39, 29	A, **C**	36, 28	A, **C**	36, 27	**A**, B	28, 26	A, **C**	31, 26
	2	*P. versipora*	-				-		-		A, **B**	45, 43	-		A, **B**	50, 50	A, **B**	56, 44	B, F	50, 50	A, **B**	56, 44	-		A, **B**	50, 50	**B**, A	49, 49	A, **B**	37, 37	**B**, A	47, 45
		C. gaboensis	**A**, B	50, 50			**A**, B	50, 50	**A**, B	50, 50	B, **A**	46, 44	**A**, B	50, 50	-		B, **A**	89, 11	**A**, F	50, 50	B, **A**	64, 36	**A**, B	50, 50	-		C	95	B, **A**	37, 37	D, **A**	76, 24
		Water	**A**, B	69, 31			**A**, B	69, 31	**A**, B	69, 31	**A**, B	46, 42	**A**, B	69, 31	**B**, A	62, 38	**B**, A	55, 45	F, **B**	44, 33	**B**, A	57, 43	**A**, B	69, 31	**B**, A	62, 38	**B**, A	60, 37	**B**, A	36, 34	**B**, A	56, 32
		Sediment	**A**, B	52, 46			**A**, B	52, 46	**A**, B	52, 46	B, **A**	43, 43	**A**, B	52, 46	**B**, E	64, 19	B, A	73, 14	F, **A**	47, 45	B, **A**	61, 33	**A**, B	52, 46	**B**, E	64, 19	**B**, E	54, 16	**A**, B	37, 34	D, **B**	42, 32
		Macroalgae	**A**, B	44, 43			**A**, B	44, 43	**A**, B	44, 43	**A**, B	38, 37	**A**, B	44, 43	**B**, A	37, 36	A, **E**	40, 31	F, **A**	45, 32	B, A	42, 36	**A**, B	44, 43	**B**, A	37, 36	**B**, A	35, 34	**A**, B	36, 27	**B**, A	30, 30
	3	*P. versipora*	-				-		-		A, **B**	45, 43	-		A, **B**	50, 50	A, **B**	56, 44	B, F	50, 50	A, **B**	56, 44	-		A, **B**	50, 50	**B**, A	49, 49	A, **B**	37, 37	**B**, A	47, 45
		C. gaboensis	**A**, B	50, 50			**A**, B	50, 50	**A**, B	50, 50	B, **A**	46, 44	**A**, B	50, 50	-		B, **A**	89, 11	**A**, F	50, 50	B, **A**	64, 36	**A**, B	50, 50	-		C	95	B, **A**	37, 37	D, **A**	76, 24
		Water	**A**, B	50, 50			**A**, B	50, 50	**A**, B	50, 50	B, **A**	46, 44	**A**, B	50, 50	-		B, **A**	89, 11	**A**, F	50, 50	B, **A**	64, 36	**A**, B	50, 50	-		C	95	B, **A**	37, 37	D, **A**	76, 24
		Sediment	**A**, B	59, 41			**A**, B	59, 41	**A**, B	59, 41	**A**, B	45, 43	**A**, B	59, 41	**B**, A	65, 35	**B**, A	61, 39	F, **A**	45, 33	B, **A**	61, 39	**A**, B	59, 41	**B**, A	65, 35	**B**, A	62, 34	**B**, A	36, 35	**B**, A	53, 28
		Macroalgae	B, **A**	47, 45			B, **A**	47, 46	B, **A**	47, 45	B, **A**	41, 39	B, **A**	47, 45	**E**, C	48, 37	B, **E**	51, 23	F, **A**	47, 46	B, **A**	49, 28	B, **A**	47, 45	**E**, C	48, 37	**E**, C	47, 37	B, **A**	35, 34	D, **E**	41, 25

Table S3.9. List of ITS2 variants and relative abundance in each sample. **A.** Pre-bleaching. **B.** Bleaching. Compositions of ITS2 variants in each replicate (n = 2-4, depends on the samples) were averaged and top three ITS2 variants in each clade are listed with relative abundance (%) in each sample.

A. Pre-bleaching.

	Pre-bleaching																											
	P. versipora						*C. gaboensis*						Water						Sediment						Macroalgae			
Clade	site 1		site 2		site 3		site 1		site 2		site 3		site 1		site 2		site 3		site 1		site 2		site 3		site 1		site 2		site 3	
A							A136	100	A136	100	A136	100	A5	0.34	A136	26	A136	99.7			A126	57	A136	51	A5	43	A136	55	A136	93
															A5	7.7	A126	0.30			A136	36	A101	8.5	A3	0.33	A144	9.6	A1	0.44
															A126	2.2									A101	0.27	A126	1.9		
B	B18	53	B18a	49	B18a	64							B18a	60	B18a	41			B18a	50	B19	3.9	B18a	26	B18	15	B19	6.4		
	B18a	46	B18	45	B18	27							B18	39	B18	20			B18	34	B18a	2.5	B18	12	B18a	9.3	B18	5.2		
	B119	0.9	B119	5.8	B119	7.9							B119	0.92	B119	1.1							B2	2.4			B18a	1.6		
C																									C1085	22			C1cstar	1.3
																									C131	1.4			C8a	0.26
E																			E106	12	E105	0.57					E105	19	E105	5.4
																			E105	4.9							E107	1.7		
F																									F5.2	8.5				
G																									G4	0.33				

B. Bleaching.

	Bleaching																											
	P. versipora						*C. gaboensis*						Water						Sediment						Macroalgae					
Clade	site 1		site 2		site 3		site 1		site 2		site 3		site 1		site 2		site 3		site 1		site 2		site 3		site 1		site 2		site 3	
A								A136	100	A136	100			A136	94	A136	100					A136	31	A101	21	A136	50	A136	89
																						A126	7.3	A3	18	A5	14		
																								A5	6.1				
B	B18a	51	B18a	50	B18a	55							B18a	54	B18	2.7			B18a	79		B19	17	B18	34	B18a	36		
	B18	49	B18	46	B18	43							B18	40	B18a	1.9			B18	21		B18a	9.1	B18a	17				
			B119	4.2	B119	1.4							B119	6.2	B19	0.52						B18	8.4						
C																C1cstar	0.39					C1cstar	1.2	C1234	1.3				
D																								D1	2.4			D1a	11
E																						E106	17						
F																			F5.2	100		F5.2	9.3						

Table S3.10. Summary of SIMPER analysis for *Symbiodinium* ITS2 variants community compositions based on the ITS2 marker. Pairwise comparison within **A.** Pre-bleaching and **B.** Bleaching. Pairwise comparison **C.** Between pre-bleaching and bleaching sampling time points. Top two ITS2 variants which contributed to dissimilarity of community compositions are shown with contribution percentages (%). ITS2 variants which were more abundant in variables in columns are shown as bold letter and ITS2 variants which were more abundant in variables in rows are shown as normal letter.

A. Within pre-bleaching sampling time point.

			Pre-bleaching																											
			Site 1										Site 2										Site 3							
			P. versipora		*C. gaboensis*		Water		Sediment		Macroalgae		*P. versipora*		*C. gaboensis*		Water		Sediment		Macroalgae		*P. versipora*		*C. gaboensis*		Water		Sediment		Macroalgae	
Seasons	Site	Habitats	Contri.	%	Contri.	%	Contri.	%	Contri.	%	Contri.	%	Contri.	%	Contri.	%	Contri.	%	Contri.	%	Contri.	%	Contri.	%	Contri.	%	Contri.	%	Contri.	%	Contri.	%
Pre-bleaching	1	*P. versipora*																												
		C. gaboensis	**A136**, B18	41, 29									**A136**, B18a	39, 27									**A136**, B18a	39, 31						
		Water	B18, **B18a**	52, 32	A136, **B18a**	42, 32							B18, B119	40, 28	A136, **B18a**	42, 32							**B18**, B119	44, 25	A136, **B18a**	42, 32				
		Sediment	B18a, B18	33, 31	A136, **B18a**	43, 25	B18, B18a	31, 31					B18a, B18	29, 26	A136, **B18a**	43, 25	A136, B18a	22, 21					B18a, B18	28, 25	A136, **B18a**	43, 25	A136, **B18a**	42, 25		
		Macroalgae	B18a, B18	23, 23	A136, **A5**	39, 19	B18a, **A5**	27, 22	B18a, **A5**	22, 20			B18a, **A5**	22, 21	A136, **A5**	39, 19	**A5**, B18a	18, 18	A126, **A5**	21, 17			B18a, **A5**	26, 20	A136, **A5**	39, 19	A136, **A5**	39, 19	A136, **A5**	25, 18
	2	*P. versipora*	**B119**, **B18a**	41, 30																										
		C. gaboensis	**A136**, B18	41, 29	-								**A136**, B18a	39, 27									**A136**, B18a	39, 31						
		Water	**A136**, B18	31, 20	**B18a**, A136	29, 27	**A136**, B18	30, 22					**A136**, **A5**	30, 16	**B18a**, A136	29, 27							**A136**, B18a	30, 17	**B18a**, A136	29, 27				
		Sediment	B18, **A126**	28, 23	**A126**, A136	44, 40	B18a, **A126**	28, 23	**A126**, B18a	24, 22			B18, B18a	25, 23	**A126**, A136	44, 40	**A126**, B18a	23, 21					B18a, **A126**	27, 22	**A126**, A136	44, 40	**A126**, A136	43, 40		
		Macroalgae	**A136**, B18	25, 24	A136, **E105**	30, 18	B18a, **A136**	27, 25	**A136**, B18a	26, 22	**A136**, A5	23, 17	**A136**, B18a	24, 24	A136, **E105**	30, 18	B18a, **A136**	23, 18	A126, **A136**	30, 26			B18a, **A136**	27, 24	A136, **E105**	30, 18	A136, **E105**	30, 18	A136, B18a	20, 19
	3	*P. versipora*	B18, **B119**	38, 29									B18, **B119**	34, 32	B18a, **A136**															
		C. gaboensis	**A136**, B18	41, 29	-								**A136**, B18a	39, 27	-								**A136**, B18a	39, 31						
		Water	**A136**, B18	40, 29	**A126**	95	**A136**, B18a	41, 32					**A136**, B18a	38, 27	**A126**	95	B18a, **A136**	29, 27					**A136**, B18a	38, 31	**A126**	95				
		Sediment	**A136**, B18	33, 28	**B18a**, A136	32, 31	**A136**, B18a	34, 27	**A136**, B18a	31, 23			**A136**, B18	32, 24	**B18a**, A136	32, 31	B18a, B18	24, 21	A126, **A136**	31, 24			**A136**, B18a	31, 25	**B18a**, A136	32, 31	**B18a**, A136	31, 30		
		Macroalgae	**A136**, B18	36, 27	**E105**, **C1cstar**	41, 22	**A136**, B18a	37, 30	**A136**, B18a	39, 24	**A136**, A5	35, 18	**A136**, B18a	35, 25	**E105**, **C1cstar**	41, 22	B18a, **A136**	27, 24	A126, **A136**	38, 35	**A136**, E105	25, 20	**A136**, B18a	35, 29	**E105**, **C1cstar**	41, 22	**E105**, **C1cstar**	37, 20	B18a, **A136**	27, 24

B. Within bleaching sampling time point.

			Bleaching																											
			Site 1										Site 2										Site 3							
			P. versipora		*C. gaboensis*		Water		Sediment		Macroalgae		*P. versipora*		*C. gaboensis*		Water		Sediment		Macroalgae		*P. versipora*		*C. gaboensis*		Water		Sediment		Macroalgae	
Seasons	Site	Habitats	Contri.	%	Contri.	%	Contri.	%	Contri.	%	Contri.	%	Contri.	%	Contri.	%	Contri.	%	Contri.	%	Contri.	%	Contri.	%	Contri.	%	Contri.	%	Contri.	%	Contri.	%
Bleaching	1	*P. versipora*																												
		C. gaboensis																												
		Water	**B119**, **B18a**	53, 24									**B119**, **B18a**	43, 31	A136, **B18a**	39, 28							**B119**, B18a	41, 26	A136, **B18a**	39, 28				
		Sediment	B18, **B18a**	58, 42			B119, B18	39, 32					B18, **B18a**	39, 32	A136, **B18a**	43, 38	A136, **B18a**	45, 36					B18, **B18a**	43, 32	A136, **B18a**	43, 38	A136, **B18a**	42, 37				
		Macroalgae	B18a, B18	27, 24			B18a, B18	24, 20	B18a, B18	34, 22			B18a, B18	24, 21	A136, **B18**	39, 18	A136, **B18**	39, 16	F5.2, **B18**	39, 18			B18a, B18	26, 22	A136, **B18**	39, 18	A136, **B18**	39, 18	A136, **B18**	18, 16		
	2	*P. versipora*	**B119**, B18a	73, 17																										
		C. gaboensis	**A136**, B18a	41, 30									**A136**, B18a	39, 28									**A136**, B18a	40, 29						
		Water	**A136**, B18a	44, 27			**A136**, B18a	42, 27					**A136**, B18a	42, 26	**B18**, **B18a**	38, 33							**A136**, B18a	43, 27	**B18**, **B18a**	38, 33				
		Sediment	**F5.2**, B18a	41, 30			**F5.2**, B18a	39, 28	**F5.2**, B18a	43, 38			**F5.2**, B18a	39, 28	A136, **F5.2**	50, 50	**F5.2**, A136	44, 42					**F5.2**, B18a	40, 29	A136, **F5.2**	50, 50	**F5.2**, A136	49, 49		
		Macroalgae	B18, **A136**	36, 28			B18, **A136**	30, 26	**A136**, B18a	31, 29	**A136**, B18	23, 20	B18, **A136**	33, 26	A136, **B18a**	42, 36	A136, **B18a**	35, 31	F5.2, **A136**	46, 25			B18, **A136**	33, 27	A136, **B18a**	42, 36	A136, **B18a**	41, 35	**A136**, **B18a**	24, 20		
	3	*P. versipora*	**B119**, B18	40, 24									B119, **B18a**	55, 17																
		C. gaboensis	**A136**, B18a	41, 30									**A136**, B18a	39, 28	-								**A136**, B18a	40, 29						
		Water	**A136**, B18a	41, 29			**A136**, B18a	38, 28					**A136**, B18a	39, 27	**C1estar**	95	B18, B18a	35, 30					**A136**, B18a	39, 29	**C1estar**	95				
		Sediment	B18, **A136**	23, 22			**A136**, B18a	20, 20	B18a, **A136**	29, 22			B18, **A136**	21, 20	A136, **B18a**	31, 15	A136, **B19**	30, 14	F5.2, **A136**	36, 20			B18a, B18	21, 21	A136, **B18a**	31, 15	A136, **B18a**	30, 15		
		Macroalgae	**A136**, B18a	37, 28			**A136**, B18a	35, 27	**A136**, B18a	38, 36	**A136**, B18	36, 18	**A136**, B18a	36, 26	**D1a**, A136	76, 24	**D1a**, B18	31, 24	F5.2, **A136**	47, 45	**A136**, B18a	37, 31	**A136**, B18a	36, 28	**D1a**, A136	76, 24	**D1a**, A136	66, 21	**A136**, B18a	26, 14		

C. Between pre-bleaching and bleaching sampling time points.

			Bleaching																											
			Site 1										Site 2										Site 3							
			P. versipora		*C. gaboensis*		Water		Sediment		Macroalgae		*P. versipora*		*C. gaboensis*		Water		Sediment		Macroalgae		*P. versipora*		*C. gaboensis*		Water		Sediment		Macroalgae	
Seasons	Site	Habitats	Contri.	%	Contri.	%	Contri.	%	Contri.	%	Contri.	%	Contri.	%	Contri.	%	Contri.	%	Contri.	%	Contri.	%	Contri.	%	Contri.	%	Contri.	%	Contri.	%	Contri.	%
Pre-bleaching	1	*P. versipora*	B18a, **B18**	38, 31			**B18**, B18a	36, 31	**B18**, B18a	46, 39	**B18a**, **B18**	24, 24	B119, B18a	41, 35	A136, **B18a**	41, 29	A136, **B18**	44, 26	F5.2, **B18**	41, 29	**B18**, A136	36, 26	B18a, **B18**	33, 29	A136, **B18**	41, 29	A136, **B18**	40, 29	**B18**, A136	24, 21	A136, **B18**	37, 28
		C. gaboensis	**A136**, B18a	41, 30			**A136**, B18a	39, 28	**A136**, B18a	43, 38	**A136**, B18	39, 18	**A136**, B18a	39, 28	-		B18, B18a	38, 33	**A136**, F5.2	50, 50	**A136**, B18a	42, 36	**A136**, B18a	40, 29	-		C1estar	95	**A136**, B18a	31, 15	D1a, **A136**	76, 24
		Water	B18, **B18a**	50, 24			B18, **B18a**	44, 26	**B18**, B18a	52, 29	**B18a**, **B18**	27, 23	B18, B119	45, 26	A136, **B18a**	42, 32	A136, **B18a**	44, 29	F5.2, **B18a**	42, 32	A136, **B18**	29, 28	B18, **B18a**	47, 22	A136, **B18a**	42, 32	A136, **B18a**	41, 32	**B18a**, A136	22, 21	A136, **B18a**	37, 31
		Sediment	B18a, B18	35, 33			B18a, B18	30, 27	B18a, **B18**	37, 32	**B18a**, **B18**	24, 21	B18a, B18	30, 28	A136, **B18a**	43, 25	A136, **B18a**	42, 23	F5.2, **B18a**	43, 25	A136, **B18a**	26, 24	B18a, B18	32, 29	A136, **B18a**	43, 25	A136, **B18a**	42, 25	**B18a**, A136	21, 20	A136, **B18a**	38, 24
		Macroalgae	B18a, **A5**	25, 22			B18a, **A5**	24, 21	B18a, **A5**	33, 22	**A5**, B18	19, 17	B18a, **A5**	23, 21	A136, **A5**	39, 19	A136, **A5**	37, 18	F5.2, **A5**	38, 21	A136, **A5**	23, 20	B18a, **A5**	25, 21	A136, **A5**	39, 19	A136, **A5**	39, 19	**A5**, A136	17, 17	A136, **A5**	35, 18
	2	*P. versipora*	**B119**, B18a	64, 16			B119, B18a	42, 28	**B18**, **B119**	34, 31	**B18a**, **B18**	23, 20	**B119**, B18a	62, 20	A136, **B18a**	39, 27	A136, **B18a**	42, 25	F5.2, **B18a**	39, 27	**B18**, A136	32, 25	**B119**, B18a	54, 18	A136, **B18a**	39, 27	A136, **B18a**	38, 27	**B18**, A136	20, 20	A136, **B18a**	35, 26
		C. gaboensis	**A136**, B18a	41, 30			**A136**, B18a	39, 28	**A136**, B18a	43, 38	**A136**, B18	39, 18	**A136**, B18a	39, 28	-		B18, B18a	38, 33	**A136**, F5.2	50, 50	**A136**, B18a	42, 36	**A136**, B18a	40, 29	-		C1estar	95	**A136**, B18a	31, 15	D1a, **A136**	76, 24
		Water	**A136**, B18	31, 18			**A136**, **A5**	31, 17	**A136**, B18a	34, 23	**A136**, **B18a**	19, 17	**A136**, **A5**	31, 17	**B18a**, A136	29, 27	A136, **B18a**	30, 27	F5.2, **B18a**	34, 21	A136, **B18**	27, 24	**A136**, **A5**	31, 17	**B18a**, A136	29, 27	**B18a**, A136	29, 27	**B18a**, A136	17, 16	**B18a**, A136	27, 23
		Sediment	B18, B18a	28, 25			B18a, B18	24, 23	B18a, **A126**	33, 24	**A126**, B18	22, 17	B18, B18a	26, 24	**A126**, A136	44, 40	**A126**, A136	37, 34	F5.2, **A126**	44, 25	**A126**, A136	31, 27	B18a, B18	25, 25	**A126**, A136	44, 40	**A126**, A136	43, 39	**A126**, A136	26, 21	**A126**, A136	39, 25
		Macroalgae	B18a, **A136**	26, 26			B18a, **A136**	25, 24	B18a, **A136**	34, 26	**A136**, B18	23, 16	**A136**, B18a	24, 24	A136, **E105**	30, 18	A136, **E105**	26, 16	F5.2, **A136**	41, 27	**A136**, B18a	26, 21	B18a, **A136**	26, 25	A136, **E105**	30, 18	A136, **E105**	29, 18	**A136**, B19	20, 14	A136, **E105**	25, 16
	3	*P. versipora*	**B119**, B18	43, 33			B18, **B119**	36, 29	**B119**, **B18**	47, 27	**B18a**, **B18**	26, 19	B18, **B119**	37, 33	A136, **B18a**	39, 31	A136, **B18a**	42, 30	F5.2, **B18a**	39, 31	A136, **B18**	26, 25	**B119**, B18	38, 33	A136, **B18a**	39, 31	A136, **B18a**	38, 31	**B18a**, A136	22, 20	A136, **B18a**	35, 30
		C. gaboensis	**A136**, B18a	41, 30			**A136**, B18a	39, 28	**A136**, B18a	43, 38	**A136**, B18	39, 18	**A136**, B18a	39, 28	-		B18, B18a	38, 33	**A136**, F5.2	50, 50	**A136**, B18a	42, 36	**A136**, B18a	40, 29	-		C1estar	95	**A136**, B18a	31, 15	D1a, **A136**	76, 24
		Water	**A136**, B18a	41, 29			**A136**, B18a	39, 28	**A136**, B18a	42, 28	**A136**, B18	39, 18	**A136**, B18a	39, 27	**A126**	95	B18a, B18	36, 31	F5.2, **A136**	49, 49	**A136**, B18a	41, 35	**A136**, B18a	39, 29	**A126**	95	C1estar, **A126**	55, 41	**A136**, B18a	31, 15	D1a, **A126**	68, 21
		Sediment	**A136**, B18	35, 28			**A136**, B18	32, 24	**A136**, B18a	36, 31	**A136**, B18	29, 19	**A136**, B18	32, 25	**B18a**, A136	32, 31	**B18a**, A136	29, 25	F5.2, **A136**	42, 28	**A136**, B18a	31, 28	**A136**, B18	33, 25	**B18a**, A136	32, 31	**B18a**, A136	31, 30	**A136**, **B18a**	18, 18	**B18a**, A136	28, 25
		Macroalgae	**A136**, B18a	37, 28			**A136**, B18a	35, 27	**A136**, B18a	38, 35	**A136**, B18	36, 17	**A136**, B18a	35, 26	**E105**, **C1estar**	41, 22	B18, B18a	23, 20	F5.2, **A136**	46, 44	**A136**, B18a	35, 30	**A136**, B18a	36, 27	**E105**, **C1estar**	41, 22	**E105**, **C1estar**	39, 27	**A136**, B18a	25, 14	D1a, **E105**	37, 23

Table S4.1. Summary of two-way ANOVA for cell cycle and growth parameters under the light treatments. **A.** Main effects. *Post-hoc* pairwise comparison for **B.** strain effects and **C.** treatment effects. Factors: strain (B1, C1, C1′ and D1a), treatment (low light, high light). Cell cycle parameters (G_1 peak, S peak and G_2/M peak proportions) were arcsine transformed and cell volume was square root transformed. MS: mean square, df: degrees of freedom, *F*: Fisher statistic, P value: * for $P < 0.05$, ** for $P < 0.01$.

A. Main effects.

Source	Variables	MS	df	*F*	P value	
Strain	G_1 peak	0.12	3	504	4.8E-16	**
	S peak	0.013	3	53	1.6E-08	**
	G_2/M peak	0.038	3	35	2.8E-07	**
	Growth rate	0.034	3	12	2.7E-04	**
	Cell volume	5.9	3	20	1.2E-05	**
Treatment	G_1 peak	0.0038	1	16	0.0010	**
	S peak	0.0038	1	15	0.0012	**
	G_2/M peak	0.0025	1	2.3	0.15	
	Growth rate	0.0036	1	1.2	0.29	
	Cell volume	3.6	1	12	0.0031	**
Strain × Treatment	G_1 peak	4.6E-04	3	2.0	0.16	
	S peak	7.0E-04	3	2.8	0.072	
	G_2/M peak	7.3E-04	3	0.68	0.58	
	Growth rate	0.0018	3	0.61	0.62	
	Cell volume	1.5	3	5.0	0.012	*

B. Pairwise comparison: strain effects.

		Low light						High light					
		B1		C1		C1′		B1		C1		C1′	
Variables	Strain	P value		P value		P value		P value		P value		P value	
G_1 peak	B1												
	C1	7.8E-13	**					1.4E-13	**				
	C1′	3.8E-12	**	0.26				5.1E-13	**	0.38			
	D1a	2.0E-06	**	8.5E-10	**	9.7E-09	**	3.0E-08	**	1.2E-09	**	1.1E-08	**
S peak	B1												
	C1	0.061						0.39					
	C1′	1.0		0.29				0.039	*	6.3E-04	**		
	D1a	3.0E-06	**	5.5E-04	**	1.0E-05	**	1.2E-04	**	0.0064	**	6.1E-07	**
G_2/M peak	B1												
	C1	0.055						1.0					
	C1′	0.14		1.0				0.20		1.0			
	D1a	0.011	*	3.1E-05	**	6.9E-05	**	0.0028	**	2.9E-04	**	3.1E-05	**
Growth rate	B1												
	C1	0.15						0.0077	**				
	C1′	1.0		1.0				0.070		1.0			
	D1a	1.0		0.041	*	0.47		1.0		0.0049	**	0.044	*
Cell volume	B1												
	C1	6.8E-04	**					0.0012	**				
	C1′	0.0024	**	1.0				0.0038	**	1.0			
	D1a	0.0015	**	1.0		1.0		1.0		0.0012	**	0.0040	**

C. Pairwise comparison: treatment effects.

			High light	
Variables	Strain	Treatment	P value	
G_1 peak	B1	Low light	0.93	
	C1	Low light	0.022	*
	C1′	Low light	0.015	*
	D1a	Low light	0.012	*
S peak	B1	Low light	0.0019	**
	C1	Low light	0.014	*
	C1′	Low light	0.85	
	D1a	Low light	0.13	
G_2/M peak	B1	Low light	0.17	
	C1	Low light	0.69	
	C1′	Low light	0.23	
	D1a	Low light	0.44	
Growth rate	B1	Low light	0.18	
	C1	Low light	0.99	
	C1′	Low light	0.85	
	D1a	Low light	0.33	
Cell volume	B1	Low light	0.0080	**
	C1	Low light	0.014	*
	C1′	Low light	0.013	*
	D1a	Low light	0.12	

Table S4.2. Summary of two-way ANOVA for cell cycle and growth parameters under the temperature treatments. **A.** Main effects. *Post-hoc* pairwise comparison for **B.** strain effects and **C.** treatment effects. Factors: strain (B1, C1, C1′ and D1a), treatment (control, heat). Cell cycle parameters (G_1 peak, S peak and G_2/M peak proportions) were arcsine transformed and cell volume was square root transformed. MS: mean square, df: degrees of freedom, *F*: Fisher statistic, P value: * for $P < 0.05$, ** for $P < 0.01$.

A. Main effects.

Source	Variables	MS	df	*F*	P value	
Strain	G_1 peak	0.089	3	196	7.9E-13	**
	S peak	0.016	3	27	2.0E-06	**
	G_2/M peak	0.037	3	40	1.1E-07	**
	Growth rate	0.0053	3	0.60	0.63	
	Cell volume	16	3	16	4.8E-05	**
Treatment	G_1 peak	0.0050	1	11	0.0044	**
	S peak	0.0065	1	11	0.0042	**
	G_2/M peak	0.72	1	788	4.9E-15	**
	Growth rate	0.29	1	33	3.1E-05	**
	Cell volume	47	1	47	4.0E-06	**
Strain × Treatment	G_1 peak	0.0034	3	7.6	0.0022	**
	S peak	0.0070	3	12	2.3E-04	**
	G_2/M peak	0.027	3	30	9.3E-07	**
	Growth rate	0.0076	3	0.86	0.48	
	Cell volume	4.1	3	4.1	0.024	*

B. Pairwise comparison: strain effects.

		Control						Heat					
		B1		C1		C1′		B1		C1		C1′	
Variables	Strain	P value		P value		P value		P value		P value		P value	
G_1 peak	B1												
	C1	9.4E-11	**					3.7E-09	**				
	C1′	2.6E-10	**	1.0				6.4E-09	**	1.0			
	D1a	4.2E-04	**	2.7E-08	**	1.1E-07	**	6.0E-06	**	3.3E-04	**	8.7E-04	**
S peak	B1												
	C1	1.0						2.5E-04	**				
	C1′	1.0		1.0				5.8E-05	**	1.0			
	D1a	0.015	*	0.011	*	0.18		0.42		7.0E-06	**	2.0E-06	**
G_2/M peak	B1												
	C1	0.0013	**					6.8E-05	**				
	C1′	2.5E-04	**	1.0				1.1E-05	**	1.0			
	D1a	0.0012	**	3.3E-07	**	1.0E-07	**	1.6E-05	**	1.0		1.0	
Growth rate	B1												
	C1	1.0						1.0					
	C1′	1.0		1.0				1.0		1.0			
	D1a	1.0		1.0		1.0		1.0		1.0		1.0	
Cell volume	B1												
	C1	1.8E-04	**					0.13					
	C1′	3.3E-04	**	1.0				0.85		1.0			
	D1a	0.0040	**	0.87		1.0		0.0052	**	0.88		0.13	

C. Pairwise comparison: treatment effects.

			Heat	
Variables	Strain	Treatment	P value	
G_1 peak	B1	Control	0.58	
	C1	Control	6.9E-04	**
	C1´	Control	0.0024	**
	D1a	Control	0.10	
S peak	B1	Control	6.7E-05	**
	C1	Control	0.90	
	C1´	Control	0.041	*
	D1a	Control	0.0020	**
G_2/M peak	B1	Control	5.7E-12	**
	C1	Control	2.2E-11	**
	C1´	Control	2.6E-11	**
	D1a	Control	2.0E-05	**
Growth rate	B1	Control	6.1E-04	**
	C1	Control	0.027	*
	C1´	Control	0.036	*
	D1a	Control	0.024	*
Cell volume	B1	Control	8.0E-05	**
	C1	Control	0.056	
	C1´	Control	0.20	
	D1a	Control	1.0E-04	**

Electronic Files

Chapter 2

Appendix E2.1. (Cladal composition, NGS) PERMANOVA pairwise comparison (habitat, season)

Appendix E2.2. (ITS2 variants composition, NGS) PERMANOVA pairwise comparison (site, habitat, season)

Appendix E2.3. (OTU composition, NGS) PERMANOVA pairwise comparison (site, habitat, season)

Appendix E2.4. (Cladal composition, qPCR) PERMANOVA pairwise comparison (site, habitat)

Appendix E2.5. (Cladal composition, qPCR vs. NGS) PERMANOVA pairwise comparison (technique)

Chapter 3

Appendix E3.1. (Cladal composition, cp23S) PERMANOVA pairwise comparison (site, habitat)

Appendix E3.2. (OTU composition, cp23S) PERMANOVA pairwise comparison (site, habitat)

Appendix E3.3. (Cladal composition, ITS2) PERMANOVA pairwise comparison (site, habitat)

Appendix E3.4. (Cladal composition, cp23S vs. ITS2) PERMANOVA pairwise comparison (amplicon)

Appendix E3.5. (ITS2 variant composition, ITS2) PERMANOVA pairwise comparison (site, habitat)

Appendix E3.6. (OTU composition, ITS2) PERMANOVA pairwise comparison (site, habitat, season)

Chapter 4

Appendix E4.1A. (B1) Cell cycle progression through 24 h

Appendix E4.1B. (C1) Cell cycle progression through 24 h

Appendix E4.1C. (C1') Cell cycle progression through 24 h

Appendix E4.1D. (D1a) Cell cycle progression through 24 h

Appendix: OTU analysis for *Symbiodinium* culture strains

Appendix E6.1. zOTU table

Appendix E6.2. zOTU table after abundance filtering

(This page is intentionally left blank)

References

Abrego, D., van Oppen, M. J. & Willis, B. L. 2009. Highly infectious symbiont dominates initial uptake in coral juveniles. Mol. Ecol., 18:3518-3531.

Adams, L. M., Cumbo, V. R. & Takabayashi, M. 2009. Exposure to sediment enhances primary acquisition of *Symbiodinium* by asymbiotic coral larvae. Mar. Ecol. Prog. Ser., 377:149-156.

Al-Horani, F. A., Al-Moghrabi, S. M. & de Beer, D. 2003. The mechanism of calcification and its relation to photosynthesis and respiration in the scleractinian coral *Galaxea fascicularis*. Mar. Biol., 142:419-426.

Aligizaki, K. & Nikolaidis, G. 2006. The presence of the potentially toxic genera *Ostreopsis* and *Coolia* (Dinophyceae) in the North Aegean Sea, Greece. Harmful Algae, 5:717-730.

Apprill, A. M. & Gates, R. D. 2007. Recognizing diversity in coral symbiotic dinoflagellate communities. Mol. Ecol., 16:1127-1134.

Arif, C., Daniels, C., Bayer, T., Banguera-Hinestroza, E., Barbrook, A., Howe, C. J., LaJeunesse, T. C. & Voolstra, C. R. 2014. Assessing *Symbiodinium* diversity in scleractinian corals via next-generation sequencing-based genotyping of the ITS2 rDNA region. Mol. Ecol., 23:4418-4433.

Atkinson, M. J. & Grigg, R. W. 1984. Model of a coral reef ecosystem. II. Gross and Net Benthic Primary Production at French Frigate Shoals, Hawaii. Coral Reefs, 3:13-22.

Auer, L., Mariadassou, M., O'Donohue, M., Klopp, C. & Hernandez-Raquet, G. 2017. Analysis of large 16S rRNA Illumina data sets: Impact of singleton read filtering on microbial community description. Mol. Ecol. Resour., 17:e122-e132.

Baghdasarian, G. & Muscatine, L. 2000. Preferential expulsion of dividing algal cells

as a mechanism for regulating algal-cnidarian symbiosis. Biol. Bull., 199:278-286.

Baillie, B. K., Monje, V., Silvestre, V., Sison, M. & Belda-Baillie, C. A. 1998. Allozyme electrophoresis as a tool for distinguishing different zooxanthellae symbiotic with giant clams. Proc. R. Soc. Lond., B, 265:1949-1956.

Baillie, B. K., Belda-Baillie, C. A. & Maruyama, T. 2000a. Conspecificity and Indo-Pacific distribution of *Symbiodinium* genotypes (Dinophyceae) from giant clams. J. Phycol., 36:1153-1161.

Baillie, B. K., Belda-Baillie, C. A., Silvestre, V., Sison, M., Gomez, A. V., Gomez, E. D. & Monje, V. 2000b. Genetic variation in *Symbiodinium* isolates from giant clams based on random-amplified-polymorphic DNA (RAPD) patterns. Mar. Biol., 136:829-836.

Bainbridge, S. J. 2017. Temperature and light patterns at four reefs along the Great Barrier Reef during the 2015–2016 austral summer: understanding patterns of observed coral bleaching. J. Oper. Oceanogr., 10:16-29.

Bainbridge, S., Steinberg, C. & Furnas, M. 2010. GBROOS–an ocean observing system for the Great Barrier Reef. International Coral Reef Symposium.

Baird, A. H., Cumbo, V. R., Leggat, W. & Rodriguez-Lanetty, M. 2007. Fidelity and flexibility in coral symbioses. Mar. Ecol. Prog. Ser., 347:307-309.

Baird, A. H., Guest, J. R. & Willis, B. L. 2009. Systematic and biogeographical patterns in the reproductive biology of scleractinian corals. Annu. Rev. Ecol. Evol. Syst., 40:551-571.

Baird, A. H., Sommer, B. & Madin, J. S. 2012. Pole-ward range expansion of *Acropora* spp. along the east coast of Australia. Coral Reefs, 31:1063

Baker, A. C. 2003. Flexibility and specificity in coral-algal symbiosis: diversity,

ecology, and biogeography of Symbiodinium. Annu. Rev. Ecol. Evol. Syst., 34:661-689.

Baker, A. & Rowan, R. 1997. Diversity of symbiotic dinoflagellates (zooxanthellae) in scleractinian corals of the Caribbean and eastern Pacific. Proc. 8th Int. Coral Reef Symp.

Baker, A. C., Starger, C. J., McClanahan, T. R. & Glynn, P. W. 2004. Coral reefs: corals' adaptive response to climate change. Nature, 430:741-741.

Baker, A. C., Glynn, P. W. & Riegl, B. 2008. Climate change and coral reef bleaching: An ecological assessment of long-term impacts, recovery trends and future outlook. Estuar. Coast. Shelf Sci., 80:435-471.

Banaszak, A. T., Iglestas-Prieto, R. & Trench, R. K. 1993. *Scrippsiella velellae* sp. nov. (Peridiniales) and *Gloeokinium viscum* sp. nov. (Phytodiniales), dinoflagellate symbionts of two hydrozoans (Cnidiaria). J. Phycol., 29:517-528.

Basford, A. J., Feary, D. A., Truong, G., Steinberg, P. D., Marzinelli, E. M. & Vergés, A. 2016. Feeding habits of range-shifting herbivores: tropical surgeonfishes in a temperate environment. Mar. Freshw. Res., 67:75-83.

Beger, M., Sommer, B., Harrison, P. L., Smith, S. D. & Pandolfi, J. M. 2014. Conserving potential coral reef refuges at high latitudes. Divers. Distrib., 20:245-257.

Berkelmans, R. & van Oppen, M. J. 2006. The role of zooxanthellae in the thermal tolerance of corals: a ‘nugget of hope’ for coral reefs in an era of climate change. Proc. R. Soc. B., 273:2305-2312.

Bhagooli, R. & Hidaka, M. 2002. Physiological responses of the coral *Galaxea fascicularis* and its algal symbiont to elevated temperatures. Galaxea, 4:33-42.

Bista, I., Carvalho, G. R., Walsh, K., Seymour, M., Hajibabaei, M., Lallias, D.,

Christmas, M. & Creer, S. 2017. Annual time-series analysis of aqueous eDNA reveals ecologically relevant dynamics of lake ecosystem biodiversity. Nat. commun., 8:14087.

Blank, R. J. 1987. Cell architecture of the dinoflagellate *Symbiodinium* sp. inhabiting the Hawaiian stony coral *Montipora verrucosa*. Mar. Biol., 94:143-155.

Blank, R. J. & Huss, V. A. 1989. DNA divergency and speciation in *Symbiodinium* (Dinophyceae). Plant Syst. Evol., 163:153-163.

Bo, M., Baker, A. C., Gaino, E., Wirshing, H. H., Scoccia, F. & Bavestrello, G. 2011. First description of algal mutualistic endosymbiosis in a black coral (Anthozoa: Antipatharia). Mar. Ecol. Prog. Ser., 435:1-11.

Bokulich, N. A., Subramanian, S., Faith, J. J., Gevers, D., Gordon, J. I., Knight, R., Mills, D. A. & Caporaso, J. G. 2013. Quality-filtering vastly improves diversity estimates from Illumina amplicon sequencing. Nat. Methods, 10:57-59.

Bonaldo, R. M. & Hay, M. E. 2014. Seaweed-coral interactions: variance in seaweed allelopathy, coral susceptibility, and potential effects on coral resilience. PLoS One, 9: e85786.

Booth, D. J., Figueira, W. F., Gregson, M. A., Brown, L. & Beretta, G. 2007. Occurrence of tropical fishes in temperate southeastern Australia: role of the East Australian Current. Estuar. Coast. Shelf Sci., 72:102-114.

Boulotte, N. M., Dalton, S. J., Carroll, A. G., Harrison, P. L., Putnam, H. M., Peplow, L. M. & van Oppen, M. J. 2016. Exploring the *Symbiodinium* rare biosphere provides evidence for symbiont switching in reef-building corals. ISME J, 10:2693-2701.

Brading, P., Warner, M. E., Davey, P., Smith, D. J., Achterberg, E. P. & Suggett, D. J. 2011. Differential effects of ocean acidification on growth and photosynthesis

among phylotypes of *Symbiodinium* (Dinophyceae). Limnol. Oceanogr., 56:927-938.

Brown, B. E. 1997. Coral bleaching: causes and consequences. Coral Reefs, 16: S129-S138.

Brown, B. E., Dunne, R. P., Goodson, M. & Douglas, A. 2000. Marine ecology: Bleaching patterns in reef corals. Nature, 404:142-143.

Buddemeier, R. W. & Fautin, D. G. 1993. Coral bleaching as an adaptive mechanism. Bioscience, 43:320-326.

Burnett, W. J. 2002. Longitudinal variation in algal symbionts (zooxanthellae) from the Indian Ocean zoanthid *Palythoa caesia*. Mar. Ecol. Prog. Ser., 234:105-109.

Butler, A. J., Rees, T., Beesley, P. & Bax, N. J. 2010. Marine biodiversity in the Australian region. PLoS One, 5: e11831.

Cacciapaglia, C. & Woesik, V. R. 2015. Reef-coral refugia in a rapidly changing ocean. Global Change Biol., 21:2272-2282.

Callahan, B. J., McMurdie, P. J., Rosen, M. J., Han, A. W., Johnson, A. J. A. & Holmes, S. P. 2016. DADA2: high-resolution sample inference from Illumina amplicon data. Nat. Methods, 13:581-583.

Cantin, N. E., van Oppen, M. J. H, Willis, B. L., Mieog, J. C. & Negri, A. P. 2009. Juvenile corals can acquire more carbon from high-performance algal symbionts. Coral Reefs, 28:405-414.

Caporaso, J. G., Kuczynski, J., Stombaugh, J., Bittinger, K., Bushman, F. D., Costello, E. K., Fierer, N., Peña, A. G., Goodrich, J. K. & Gordon, J. I. 2010. QIIME allows analysis of high-throughput community sequencing data. Nat. Methods, 7:335-336.

Carlos, A. A., Baillie, B. K., Kawachi, M. & Maruyama, T. 1999. Phylogenetic position

of *Symbiodinium* (Dinophyceae) isolates from tridacnids (Bivalvia), cardiids (Bivalvia), a sponge (Porifera), a soft coral (Anthozoa), and a free-living strain. J. Phycol., 35:1054-1062.

Carpenter, E. J. & Chang, J. 1988. Species-specific phytoplankton growth rates via diel DNA synthesis cycles. I. Concept of the method. Mar. Ecol. Prog. Ser., 43:105-111.

Casado-Amezúa, P., Machordom, A., Bernardo, J. & González-Wangüemert, M. 2014. New insights into the genetic diversity of zooxanthellae in Mediterranean anthozoans. Symbiosis, 63:41-46.

Castro-Sanguino, C. & Sánchez, J. A. 2012. Dispersal of *Symbiodinium* by the stoplight parrotfish *Sparisoma viride*. Biol. Lett., 8:282-286.

Cavalier-Smith, T. 1978. Nuclear volume control by nucleoskeletal DNA, selection for cell volume and cell growth rate, and the solution of the DNA C-value paradox. J. Cell Sci., 34:247-278.

Cesar, H., Burke, L. & Pet-Soede, L. (2003) The economics of worldwide coral reef degradation. Cesar environmental economics consulting (CEEC).

Chakravarti, L. J., Beltran, V. H. & van Oppen, M. J. H. 2017. Rapid thermal adaptation in photosymbionts of reef-building corals. Global Change Biol., 23:4675-4688.

Chang, F. H. 1983. Winter phytoplankton and microzooplankton populations off the coast of Westland, New Zealand, 1979. N. Z. J. Mar. Freshwat. Res., 17:279-304.

Chang, J. & Carpenter, E. J. 1988. Species-specific phytoplankton growth rates via diel DNA synthesis cycles. II. DNA quantification and model verification in the dinoflagellate *Heterocapsa triquetra*. Mar. Ecol. Prog. Ser., 44:287-296.

Chang, S. S., Prezelin, B. B. & Trench, R. K. 1983. Mechanisms of photoadaptation

in three strains of the symbiotic dinoflagellate *Symbiodinium microadriaticum*. Mar. Biol., 76:219-229.

Chi, J., Parrow, M. W. & Dunthorn, M. 2014. Cryptic sex in *Symbiodinium* (Alveolata, Dinoflagellata) is supported by an inventory of meiotic genes. J. Eukaryot. Microbiol., 61:322-327.

Coffroth, M. A. & Santos, S. R. 2005. Genetic diversity of symbiotic dinoflagellates in the genus *Symbiodinium*. Protist, 156:19-34.

Coffroth, M. A., Santos, S. R. & Goulet, T. L. 2001. Early ontogenetic expression of specificity in a cnidarian-algal symbiosis. Mar. Ecol. Prog. Ser., 222:85-96.

Coffroth, M. A., Lewis, C. F., Santos, S. R. & Weaver, J. L. 2006. Environmental populations of symbiotic dinoflagellates in the genus *Symbiodinium* can initiate symbioses with reef cnidarians. Curr. Biol., 16:R985-R987.

Correa, A. M. S & Baker, A. C. 2009. Understanding diversity in coral-algal symbiosis: a cluster-based approach to interpreting fine-scale genetic variation in the genus *Symbiodinium*. Coral Reefs, 28:81-93.

Cresswell, A. K., Edgar, G. J., Stuart-Smith, R. D., Thomson, R. J., Barrett, N. S. & Johnson, C. R. 2017. Translating local benthic community structure to national biogenic reef habitat types. Global Ecol. Biogeogr., 26:1112-1125.

Cristescu, M. E. 2014. From barcoding single individuals to metabarcoding biological communities: towards an integrative approach to the study of global biodiversity. Trends Ecol. Evol., 29:566-571.

Cumbo, V. R, Baird, A. H. & van Oppen, M. J. H. 2013. The promiscuous larvae: flexibility in the establishment of symbiosis in corals. Coral Reefs, 32:111-120.

Cunning, R. & Baker, A. C. 2014. Not just who, but how many: the importance of partner abundance in reef coral symbioses. Front. Microbiol., 5.

doi:10.3389/fmicb.2014.00400

Cunning, R., Yost, D. M., Guarinello, M. L., Putnam, H. M. & Gates, R. D. 2015. Variability of *Symbiodinium* communities in waters, sediments, and corals of thermally distinct reef pools in American Samoa. PLoS One, 10:e0145099.

Cunning, R., Muller, E. B., Gates, R. D. & Nisbet, R. M. 2017. A dynamic bioenergetic model for coral-*Symbiodinium* symbioses and coral bleaching as an alternate stable state. J. Theor. Biol., 431:49-62.

Dapena, C., Bravo, I., Cuadrado, A. & Figueroa, R. I. 2015. Nuclear and cell morphological changes during the cell cycle and growth of the toxic dinoflagellate *Alexandrium minutum*. Protist, 166:146-160.

Davy, S. K., Lucas, I. A. N. & Turner, J. R. 1996. Carbon budgets in temperate anthozoan-dinoflagellate symbioses. Mar. Biol., 126:773-783.

Davy, S. K., Allemand, D. & Weis, V. M. 2012. Cell biology of cnidarian-dinoflagellate symbiosis. Microbiol. Mol. Biol. Rev., 76:229-261.

de Vargas, C., Audic, S., Henry, N., Decelle, J., Mahé, F., Logares, R., Lara, E., Berney, C., Le Bescot, N., Probert, I., et al. 2015. Eukaryotic plankton diversity in the sunlit ocean. Science, 348:1261605.

De'ath, G., Fabricius, K. E., Sweatman, H. & Puotinen, M. 2012. The 27–year decline of coral cover on the Great Barrier Reef and its causes. Proc. Natl. Acad. Sci., 109:17995-17999.

Degnan, P. H. & Ochman, H. 2012. Illumina-based analysis of microbial community diversity. ISME J, 6:183-194.

Descombes, P., Wisz, M. S., Leprieur, F., Parravicini, V., Heine, C., Olsen, S. M., Swingedouw, D., Kulbicki, M., Mouillot, D. & Pellissier, L. 2015. Forecasted coral reef decline in marine biodiversity hotspots under climate change. Global

Change Biol., 21:2479-2487.

Diaz-Pulido, G. & McCook, L. J. 2008. Macroalgae (Seaweeds)' in Chin. A, (ed) The State of the Great Barrier Reef On-line, Great Barrier Reef Marine Park Authority, Townsville.

Dimond, J. & Carrington, E. 2008. Symbiosis regulation in a facultatively symbiotic temperate coral: zooxanthellae division and expulsion. Coral Reefs, 27:601-604.

Dimond, J. L., Pineda, R. R., Ramos-Ascherl, Z. & Bingham, B. L. 2013. Relationships between host and symbiont cell cycles in sea anemones and their symbiotic dinoflagellates. Biol. Bull., 225:102-112.

Done, T. J. 1992. Phase shifts in coral reef communities and their ecological significance. Hydrobiologia, 247:121-132.

Douglas, A. E. 2003. Coral bleaching—how and why? Mar. Pollut. Bull., 46:385-392.

Drew, E. A. 1972. The biology and physiology of alga-invertebrates symbioses. II. The density of symbiotic algal cells in a number of hermatypic hard corals and alcyonarians from various depths. J. Exp. Mar. Biol. Ecol., 9:71-75.

Elledge, S. J. 1996. Cell cycle checkpoints: preventing an identity crisis. Science, 274:1664-1672.

Evan, G. & Littlewood, T. 1998. A matter of life and cell death. Science, 281:1317-1322.

Fabricius, K. & De'ath, G. 2001. Biodiversity on the Great Barrier Reef: large-scale patterns and turbidity-related local loss of soft coral taxa. Oceanographic Processes of Coral Reefs, Physical and Biological Links in the Great Barrier Reef:127-144.

Falkowski, P. G., Dubinsky, Z., Muscatine, L. & McCloskey, L. 1993. Population control in symbiotic corals. Bioscience, 43:606-611.

Farrant, P. A. 1986. Gonad development and the planulae of the temperate Australian soft coral *Capnella gaboensis*. Mar. Biol., 92:381-392.

Farrant, P. A. 1987. Population dynamics of the temperate Australian soft coral *Capnella gaboensis*. Mar. Biol., 96:401-407.

Farrant, P. A., Borowitzka, M. A., Hinde, R. & King, R. J. 1987. Nutrition of the temperate Australian soft coral *Capnella gaboensis*. Mar. Biol., 95:565-574.

Fautin, D. G. & Buddemeier, R. W. 2004. Adaptive bleaching: a general phenomenon. Hydrobiologia, 530:459-467.

Figueroa, R. I., Garcés, E. & Bravo, I. 2010. The use of flow cytometry for species identification and life-cycle studies in dinoflagellates. Deep Sea Res., Part II, 57:301-307.

Fisher, P. L., Malme, M. K. & Dove, S. 2012. The effect of temperature stress on coral–*Symbiodinium* associations containing distinct symbiont types. Coral Reefs, 31:473-485.

Fitt, W. K. 2000. Cellular growth of host and symbiont in a cnidarian-zooxanthellar symbiosis. Biol. Bull., 198:110-120.

Fitt, W. K. & Cook, C. B. 2001. The effects of feeding or addition of dissolved inorganic nutrients in maintaining the symbiosis between dinoflagellates and a tropical marine cnidarian. Mar. Biol., 139:507-517.

Fitt, W. K. & Trench, R. K. 1983. The relation of diel patterns of cell division to diel patterns of motility in the symbiotic dinoflagellate *Symbiodinium microadriaticum* Freudenthal in culture. New Phytol., 94:421-432.

Fransolet, D., Roberty, S. & Plumier, J.-C. 2012. Establishment of endosymbiosis: The case of cnidarians and *Symbiodinium*. J. Exp. Mar. Biol. Ecol., 420:1-7.

Freeman, L. A. 2015. Robust performance of marginal Pacific coral reef habitats in

future climate scenarios. PLoS One, 10:e0128875.

Freudenthal, H. D. 1962. *Symbiodinium* gen. nov. and *Symbiodinium microadriaticum* sp. nov., a Zooxanthella: Taxonomy, life cycle, and morphology. J. Protozool. 9:45-52.

Frommlet, J. C., Sousa, M. L., Alves, A., Vieira, S. I., Suggett, D. J. & Serôdio, J. 2015. Coral symbiotic algae calcify *ex hospite* in partnership with bacteria. Proc. Natl. Acad. Sci., 112:6158-6163.

Fujise, L., Yamashita, H., Suzuki, G. & Koike, K. 2013. Expulsion of zooxanthellae (*Symbiodinium*) from several species of scleractinian corals: comparison under non-stress conditions and thermal stress conditions. Galaxea, 15:29-36.

Fujise, L., Yamashita, H., Suzuki, G., Sasaki, K., Liao, L. M. & Koike, K. 2014. Moderate thermal stress causes active and immediate expulsion of photosynthetically damaged zooxanthellae (*Symbiodinium*) from corals. PLoS Onev, 9:e114321.

Garcia-Cuetos, L., Pochon, X. & Pawlowski, J. 2005. Molecular evidence for host–symbiont specificity in soritid foraminifera. Protist, 156:399-412.

Gibbin, E. M. & Davy, S. K. 2013. Intracellular pH of symbiotic dinoflagellates. Coral Reefs, 32:859-863.

Gissi, F., Stauber, J., Reichelt-Brushett, A., Harrison, P. L. & Jolley, D. F. 2017. Inhibition in fertilisation of coral gametes following exposure to nickel and copper. Ecotoxicol. Environ. Saf., 145:32-41.

Glynn, P. W. 1993. Coral reef bleaching: ecological perspectives. Coral Reefs, 12:1-17.

Gómez-Cabrera, M. d. C., Ortiz, J. C., Loh, W. K. W., Ward, S. & Hoegh-Guldberg, O. 2008. Acquisition of symbiotic dinoflagellates (*Symbiodinium*) by juveniles of

the coral *Acropora longicyathus*. Coral Reefs, 27:219-226.

Goreau, T. F. 1959. The physiology of skeleton formation in corals. I. A method for measuring the rate of calcium deposition by corals under different conditions. Biol. Bull., 116:59-75.

Gou, W., Sun, J., Li, X., Zhen, Y., Xin, Z., Yu, Z. & Li, R. 2003. Phylogenetic analysis of a free-living strain of *Symbiodinium* isolated from Jiaozhou Bay, PR China. J. Exp. Mar. Biol. Ecol., 296:135-144.

Goulet, T. L. & Coffroth, M. A. 2003. Genetic composition of zooxanthellae between and within colonies of the octocoral *Plexaura kuna*, based on small subunit rDNA and multilocus DNA fingerprinting. Mar. Biol., 142:233-239.

Goyen, S., Pernice, M., Szabó, M., Warner, M. E., Ralph, P. J. & Suggett, D. J. 2017. A molecular physiology basis for functional diversity of hydrogen peroxide production amongst *Symbiodinium* spp.(Dinophyceae). Mar. Biol., 164:46.

Goyen, S., Camp, E., Fujise, L., Lloyd, A., Nitschke, M., LaJeunesse, T., Kahlke, T., Ralph, P. J., Suggett, D. J. First high-latitude mass coral bleaching in Sydney Harbour driven by the 2015–2016 heatwave. In prep.

Granados-Cifuentes, C., Neigel, J., Leberg, P. & Rodriguez-Lanetty, M. 2015. Genetic diversity of free-living *Symbiodinium* in the Caribbean: the importance of habitats and seasons. Coral Reefs, 34:927-939.

Great Barrier Reef Marine Park Authority 2017. Final report: 2016 coral bleaching event on the Great Barrier Reef, GBRMPA, Townsville.

Griffiths, D. J. 2010. Microalgal cell cycle. Nova Science Publishers, New York

Grzebyk, D., Berland, B., Thomassin, B. A., Bosi, C. & Arnoux, A. 1994. Ecology of ciguateric dinoflagellates in the coral reef complex of Mayotte Island (SW Indian Ocean). J. Exp. Mar. Biol. Ecol., 178:51-66.

Guinotte, J. M., Buddemeier, R. W. & Kleypas, J. A. 2003. Future coral reef habitat marginality: temporal and spatial effects of climate change in the Pacific basin. Coral Reefs, 22:551-558.

Halfar, J., Godinez-Orta, L., Riegl, B., Valdez-Holguin, J. E. & Borges, J. M. 2005. Living on the edge: high-latitude *Porites* carbonate production under temperate eutrophic conditions. Coral Reefs, 24:582-592.

Hansen, G. & Daugbjerg, N. 2009. *Symbiodinium natans* sp. nov.: a "free-living" dinoflagellate from Tenerife (northeast-Atlantic Ocean). J. Phycol., 45:251-263.

Harriott, V. J. & Banks, S. A. 2002. Latitudinal variation in coral communities in eastern Australia: a qualitative biophysical model of factors regulating coral reefs. Coral Reefs, 21:83-94.

Harriott, V. J., Smith, S. D. A. & Harrison, P. L. 1994. Patterns of coral community structure of subtropical reefs in the Solitary Islands Marine Reserve, Eastern Australia. Mar. Ecol. Prog. Ser., 109:67-76.

Harrison, P. L. 2011. Sexual reproduction of scleractinian corals. Coral reefs: an ecosystem in transition. Springer.59-85.

Hartmann, A. C., Baird, A. H., Knowlton, N. & Huang, D. 2017. The paradox of environmental symbiont acquisition in obligate mutualisms. Curr. Biol., 27:3711-3716. e3.

Hennige, S. J., Suggett, D. J., Warner, M. E., McDougall, K. E. & Smith, D. J. 2009. Photobiology of *Symbiodinium* revisited: bio-physical and bio-optical signatures. Coral Reefs, 28:179-195.

Hennige, S. J., Smith, D. J., Walsh, S.-J., McGinley, M. P., Warner, M. E. & Suggett, D. J. 2010. Acclimation and adaptation of scleractinian coral communities along environmental gradients within an Indonesian reef system. J. Exp. Mar. Biol.

Ecol., 391:143-152.

Hill, M., Allenby, A., Ramsby, B., Schönberg, C. & Hill, A. 2011. *Symbiodinium* diversity among host clionaid sponges from Caribbean and Pacific reefs: evidence of heteroplasmy and putative host-specific symbiont lineages. Mol. Phylogen. Evol., 59:81-88.

Hirose, M., Reimer, J. D., Hidaka, M. & Suda, S. 2008. Phylogenetic analyses of potentially free-living *Symbiodinium* spp. isolated from coral reef sand in Okinawa, Japan. Mar. Biol., 155:105-112.

Hoegh-Guldberg, O. 1994. Population dynamics of symbiotic zooxanthellae in the coral *Pocillopora damicornis* exposed to elevated ammonium [$(NH_4)_2$ SO_4] concentrations. Pac. Sci., 48:263-272

Hoegh-Guldberg, O. 1999. Climate change, coral bleaching and the future of the world's coral reefs. Mar. Freshw. Res., 50:839-866.

Hoegh-Guldberg, O. & Smith, G. J. 1989. Influence of the population density of zooxanthellae and supply of ammonium on the biomass and metabolic characteristics of the reef corals *Seriatopora hystrix* and *Stylophora pistillata*. Mar. Ecol. Prog. Ser., 57:173-186.

Hoegh-Guldberg, O., McCloskey, L. R. & Muscatine, L. 1987. Expulsion of zooxanthellae by symbiotic cnidarians from the Red Sea. Coral Reefs, 5:201-204.

Hofmann, L. C., Fink, A., Bischof, K. & de Beer, D. 2015. Microsensor studies on *Padina* from a natural CO_2 seep: implications of morphology on acclimation to low pH. J. Phycol., 51:1106-1115.

Howells, E. J., van Oppen, M. J. H. & Willis, B. L. 2009. High genetic differentiation and cross-shelf patterns of genetic diversity among Great Barrier Reef

populations of *Symbiodinium*. Coral Reefs, 28:215-225.

Howells, E. J., Beltran, V. H., Larsen, N. W., Bay, L. K., Willis, B. L. & van Oppen, M. J. H. 2012. Coral thermal tolerance shaped by local adaptation of photosymbionts. Nature Climate Change, 2:116-120.

Huang, H., Zhou, G., Yang, J., Liu, S., You, F. & Lei, X. 2013. Diversity of free-living and symbiotic *Symbiodinium* in the coral reefs of Sanya, South China Sea. Mar. Biol. Res., 9:117-128.

Hughes, T. P. 1994. Catastrophes, phase shifts, and large-scale degradation of a Caribbean coral reef. Science-AAAS-Weekly Paper Edition, 265:1547-1551.

Hughes, A. R. & Stachowicz, J. J. 2004. Genetic diversity enhances the resistance of a seagrass ecosystem to disturbance. Proc. Natl. Acad. Sci. U.S.A., 101:8998-9002.

Hughes, T. P., Graham, N. A., Jackson, J. B., Mumby, P. J. & Steneck, R. S. 2010. Rising to the challenge of sustaining coral reef resilience. Trends Ecol. Evol., 25:633-642.

Hughes, T. P., Kerry, J. T., Álvarez-Noriega, M., Álvarez-Romero, J. G., Anderson, K. D., Baird, A. H., Babcock, R. C., Beger, M., Bellwood, D. R., Berkelmans, R., et al. 2017. Global warming and recurrent mass bleaching of corals. Nature, 543:373-377.

Hughes, T. P., Anderson, K. D., Connolly, S. R., Heron, S. F., Kerry, J. T., Lough, J. M., Baird, A. H., Baum, J. K., Berumen, M.L., Bridge, T. C., et al. 2018. Spatial and temporal patterns of mass bleaching of corals in the Anthropocene. Science. 359(6371):80-83.

Hume, B. C. C., D'Angelo, C., Smith, E. G., Stevens, J. R., Burt, J. & Wiedenmann, J. 2015. *Symbiodinium thermophilum* sp. nov., a thermotolerant symbiotic alga

prevalent in corals of the world's hottest sea, the Persian/Arabian Gulf. Scientific reports, 5: 8562.

Hunter, R. L., LaJeunesse, T. C. & Santos, S. R. 2007. Structure and evolution of the rDNA internal transcribed spacer (ITS) region 2 in the symbiotic dinoflagellates (*Symbiodinium*, Dinophyta). J. Phycol., 43:120-128.

Ishikura, M., Hagiwara, K., Takishita, K., Haga, M., Iwai, K. & Maruyama, T. 2004. Isolation of new *Symbiodinium* strains from Tridacnid giant clam (*Tridacna crocea*) and sea slug (*Pteraeolidia ianthina*) using culture medium containing giant clam tissue homogenate. Mar. Biotechnol., 6:378-385.

Jeong, H. J., Du Yoo, Y., Kang, N. S., Lim, A. S., Seong, K. A., Lee, S. Y., Lee, M. J., Lee, K. H., Kim, H. S. & Shin, W. 2012. Heterotrophic feeding as a newly identified survival strategy of the dinoflagellate *Symbiodinium*. Proc. Natl. Acad. Sci., 109:12604-12609.

Jeong, H. J., Lee, S. Y., Kang, N. S., Yoo, Y. D., Lim, A. S., Lee, M. J., Kim, H. S., Yih, W., Yamashita, H. & LaJeunesse, T. C. 2014. Genetics and morphology characterize the dinoflagellate *Symbiodinium voratum*, n. sp.,(Dinophyceae) as the sole representative of *Symbiodinium* clade E. J. Eukaryot. Microbiol., 61:75-94.

Jimenez, I. M., Larkum, A. W. D., Ralph, P. J. & Kühl, M. 2012. In situ thermal dynamics of shallow water corals is affected by tidal patterns and irradiance. Mar. Biol., 159:1773-1782.

Jones, A. & Berkelmans, R. 2010. Potential costs of acclimatization to a warmer climate: growth of a reef coral with heat tolerant vs. sensitive symbiont types. PLoS One, 5:e10437.

Jones, A. M. & Berkelmans, R. 2011. Tradeoffs to thermal acclimation: energetics and

reproduction of a reef coral with heat tolerant *Symbiodinium* type-D. J. Mar. Biol., 185890.

Jones, R. J. & Yellowlees, D. 1997. Regulation and control of intracellular algae (= zooxanthellae) in hard corals. Philos. Trans. R. Soc., B, 352:457-468.

Jones, A. M., Berkelmans, R., van Oppen, M. J., Mieog, J. C. & Sinclair, W. 2008. A community change in the algal endosymbionts of a scleractinian coral following a natural bleaching event: field evidence of acclimatization. Proc. R. Soc. Lond., B, Biol. Sci., 275:1359-1365.

Kahlke, T. 2018a. Basta 1.2 - Basic Sequence Taxonomy Annotation (Version 1.2). Zenodo. https://doi.org/10.5281/zenodo.1137870.

Kahlke, T. 2018b. Ampli-Tools (Version 1.0). Zenodo. https://doi.org/10.5281/zenodo.1137872.

Kahlke, T., & Fujise, L. 2017. *Symbiodinium* ITS2 Amplicon Analysis. Open Science Framework. https://doi.org/10.17605/osf.io/hcsp4.

Kaniewska, P., Alon, S., Karako-Lampert, S., Hoegh-Guldberg, O. & Levy, O. 2015. Signaling cascades and the importance of moonlight in coral broadcast mass spawning. eLife, 4:e09991.

Katoh, K. & Standley, D. M. 2013. MAFFT multiple sequence alignment software version 7: improvements in performance and usability. Mol. Biol. Evol., 30:772-780.

Kawaguti, S. 1944. On the physiology of reef corals. VII. The zooxanthella of the reef corals is *Gymnodinium* sp. dinoflagellata its culture in vitro. Palao Trop. Biol. Stn. Stud., 2:675-679.

Kevin, M. J., Hall, W. T., McLaughlin, J. J. & Zahl, P. A. 1969. *Symbiodinium microadriaticum* Freudenthal, a revised taxonomic description, ultrastructure. J.

Phycol., 5:341-350.

Khailov, K. M. & Burlakova, Z. P. 1969. Release of dissolved organic matter by marine seaweeds and distribution of their total organic production to inshore communities. Limnol. Oceanogr., 14:521-527.

Kim, H. S., Yih, W., Kim, J. H., Myung, G. & Jeong, H. J. 2011. Abundance of epiphytic dinoflagellates from coastal waters off Jeju Island, Korea during Autumn 2009. Ocean Sci. J., 46:205-209.

Kinzie III, R. A., Takayama, M., Santos, S. R. & Coffroth, M. A. 2001. The adaptive bleaching hypothesis: experimental tests of critical assumptions. Biol. Bull., 200:51-58.

Kirk, N. L. & Weis, V. M. 2016. Animal–*Symbiodinium* Symbioses: Foundations of Coral Reef Ecosystems. The Mechanistic Benefits of Microbial Symbionts. Springer.269-294.

Knowlton, N., Brainard, R. E., Fisher, R., Moews, M., Plaisance, L. & Caley, M. J. 2010. Coral reef biodiversity. Life in the World's Oceans: Diversity Distribution and Abundance:65-74.

Kohli, G. S., Murray, S. A., Neilan, B. A., Rhodes, L. L., Harwood, D. T., Smith, K. F., Meyer, L., Capper, A., Brett, S. & Hallegraeff, G. M. 2014a. High abundance of the potentially maitotoxic dinoflagellate *Gambierdiscus carpenteri* in temperate waters of New South Wales, Australia. Harmful Algae, 39:134-145.

Kohli, G. S., Neilan, B. A., Brown, M. V., Hoppenrath, M. & Murray, S. A. 2014b. *Cob* gene pyrosequencing enables characterization of benthic dinoflagellate diversity and biogeography. Environ. Microbiol., 16:467-485.

Koike, K., Jimbo, M., Sakai, R., Kaeriyama, M., Muramoto, K., Ogata, T., Maruyama, T. & Kamiya, H. 2004. Octocoral chemical signaling selects and controls

dinoflagellate symbionts. Biol. Bull., 207:80-86.

Koike, K., Yamashita, H., Oh-Uchi, A., Tamaki, M., Hayashibara, T. 2007. A quantitative real-time PCR method for monitoring *Symbiodinium* in the water column. Galaxea, 9:1-12.

Kopp, C., Pernice, M., Domart-Coulon, I., Djediat, C., Spangenberg, J. E., Alexander, D. T. L., Hignette, M, Meziane, T. & Meibom, A. 2013. Highly dynamic cellular-level response of symbiotic coral to a sudden increase in environmental nitrogen. MBio, 4:e00052-13.

Kuffner, I. B., Walters, L. J., Becerro, M. A., Paul, V. J., Ritson-Williams, R. & Beach, K. S. 2006. Inhibition of coral recruitment by macroalgae and cyanobacteria. Mar. Ecol. Prog. Ser., 323:107-117.

Kühl, N. M. & Rensing, L. 2000. Heat shock effects on cell cycle progression. Cell. Mol. Life Sci., 57:450-463.

LaJeunesse, T. C. 2001. Investigating the biodiversity, ecology, and phylogeny of endosymbiotic dinoflagellates in the genus *Symbiodinium* using the ITS region: in search of a "species" level marker. J. Phycol., 37:866-880.

LaJeunesse, T. C. 2002. Diversity and community structure of symbiotic dinoflagellates from Caribbean coral reefs. Mar. Biol., 141:387-400.

LaJeunesse, T. C. 2004. "Species" radiations of symbiotic dinoflagellates in the Atlantic and Indo-Pacific since the Miocene-Pliocene transition. Mol. Biol. Evol., 22:570-581.

LaJeunesse, T. C. 2017. Validation and description of *Symbiodinium microadriaticum* the type species of *Symbiodinium* (Dinophyta). J. Phycol., 53:1109-1114.

LaJeunesse, T. C. & Trench, R. K. 2000. Biogeography of two species of *Symbiodinium* (Freudenthal) inhabiting the intertidal sea anemone *Anthopleura*

elegantissima (Brandt). Biol. Bull., 199:126-134.

LaJeunesse, T. C. & Thornhill, D. J. 2011. Improved resolution of reef-coral endosymbiont (*Symbiodinium*) species diversity, ecology, and evolution through *psbA* non-coding region genotyping. PLoS One, 6:e29013.

LaJeunesse, T. C., Loh, W. K., Van Woesik, R., Hoegh-Guldberg, O., Schmidt, G. W. & Fitt, W. K. 2003. Low symbiont diversity in southern Great Barrier Reef corals, relative to those of the Caribbean. Limnol. Oceanogr., 48:2046-2054.

LaJeunesse, T. C., Bhagooli, R., Hidaka, M., deVantier, L., Done, T., Schmidt, G. W., Fitt, W. K. & Hoegh-Guldberg, O. 2004. Closely related *Symbiodinium* spp. differ in relative dominance in coral reef host communities across environmental, latitudinal and biogeographic gradients. Mar. Ecol. Prog. Ser., 284:147-161.

LaJeunesse, T. C., Lambert, G., Andersen, R. A., Coffroth, M. A. & Galbraith, D. W. 2005. *Symbiodinium* (Pyrrhophyta) genome sizes (DNA content) are smallest among dinoflagellates. J. Phycol., 41:880-886.

LaJeunesse, T. C., Smith, R. T., Finney, J. & Oxenford, H. 2009. Outbreak and persistence of opportunistic symbiotic dinoflagellates during the 2005 Caribbean mass coral 'bleaching'event. Proc. R. Soc. Lond. B., 276:4139-4148.

LaJeunesse, T. C., Smith, R., Walther, M., Pinzón, J., Pettay, D. T., McGinley, M., Aschaffenburg, M., Medina-Rosas, P., Cupul-Magaña, A. L. & Pérez, A. L. 2010a. Host–symbiont recombination versus natural selection in the response of coral–dinoflagellate symbioses to environmental disturbance. Proc. R. Soc. Lond. B., 277:2925-2934.

LaJeunesse, T. C., Pettay, D. T., Sampayo, E. M., Phongsuwan, N., Brown, B., Obura, D. O., Hoegh-Guldberg, O. & Fitt, W. K. 2010b. Long-standing environmental conditions, geographic isolation and host–symbiont specificity influence the

relative ecological dominance and genetic diversification of coral endosymbionts in the genus Symbiodinium. J. Biogeogr., 37:785-800.

LaJeunesse, T. C., Parkinson, J. E. & Reimer, J. D. 2012a. A genetics-based description of *Symbiodinium minutum* sp. nov. and *S. psygmophilum* sp. nov. (Dinophyceae), two dinoflagellates symbiotic with cnidaria. J. Phycol., 48:1380-1391.

LaJeunesse, T. C., Parkinson, J. E. & Trench, R. K. 2012b. *Symbiodinium*. Version 04 July 2012. http://tolweb.org/Symbiodinium/126705/2012.07.04 in The Tree of Life Web Project, http://tolweb.org/

LaJeunesse, T. C., Wham, D. C., Pettay, D. T., Parkinson, J. E., Keshavmurthy, S. & Chen, C. A. 2014. Ecologically differentiated stress-tolerant endosymbionts in the dinoflagellate genus *Symbiodinium* (Dinophyceae) Clade D are different species. Phycologia, 53:305-319.

LaJeunesse, T. C., Lee, S. Y., Gil-Agudelo, D. L., Knowlton, N. & Jeong, H. J. 2015. *Symbiodinium necroappetens* sp. nov. (Dinophyceae): an opportunist 'zooxanthella' found in bleached and diseased tissues of Caribbean reef corals. Eur. J. Phycol., 50:223-238.

Leal, M. C., Hoadley, K., Pettay, D. T., Grajales, A., Calado, R. & Warner, M. E. 2015. Symbiont type influences trophic plasticity of a model cnidarian–dinoflagellate symbiosis. J. Exp. Biol., 218:858-863.

Lee, Z. P., Du, K. P. & Arnone, R. 2005. A model for the diffuse attenuation coefficient of downwelling irradiance. J. Geophys. Res., 110:C02016.

Lee, S. Y., Jeong, H. J., Kang, N. S., Jang, T. Y., Jang, S. H. & LaJeunesse, T. C. 2015. *Symbiodinium tridacnidorum* sp. nov., a dinoflagellate common to Indo-Pacific giant clams, and a revised morphological description of *Symbiodinium microadriaticum* Freudenthal, emended Trench & Blank. Eur. J. Phycol., 50:155-

172.

Lesser, M. P. 2011. Coral bleaching: causes and mechanisms. Coral reefs: an ecosystem in transition. Springer. 405-419.

Lesser, M. P. & Farrell, J. H. 2004. Exposure to solar radiation increases damage to both host tissues and algal symbionts of corals during thermal stress. Coral Reefs, 23:367-377.

Lesser, M. P., Stat, M. & Gates, R. D. 2013. The endosymbiotic dinoflagellates (*Symbiodinium* sp.) of corals are parasites and mutualists. Coral Reefs, 32:603-611.

Leujak, W. & Ormond, R. F. G. 2007. Comparative accuracy and efficiency of six coral community survey methods. J. Exp. Mar. Biol. Ecol., 351:168-187.

Li, M., Li, L., Shi, X., Lin, L. & Lin, S. 2015. Effects of phosphorus deficiency and adenosine 5′-triphosphate (ATP) on growth and cell cycle of the dinoflagellate *Prorocentrum donghaiense*. Harmful Algae, 47:35-41.

Lien, Y.-T., Fukami, H. & Yamashita, Y. 2012. *Symbiodinium* clade C dominates zooxanthellate corals (Scleractinia) in the temperate region of Japan. Zool. Sci., 29:173-180.

Lin, S., Zhang, H., Hou, Y., Zhuang, Y. & Miranda, L. 2009. High-level diversity of dinoflagellates in the natural environment, revealed by assessment of mitochondrial *cox1* and *cob* genes for dinoflagellate DNA barcoding. Appl. Environ. Microbiol., 75:1279-1290.

Lin, Z., Chen, M. & Chen, J. 2017. Development of a protocol for specific detection and quantification of free-living and endosymbiotic *Symbiodinium* communities in coral reefs. Aquat. Microb. Ecol., 80:1-13.

Lirman, D. 2001. Competition between macroalgae and corals: effects of herbivore

exclusion and increased algal biomass on coral survivorship and growth. Coral Reefs, 19:392-399.

Littman, R. A., van Oppen, M. J. H. & Willis, B. L. 2008. Methods for sampling free-living *Symbiodinium* (zooxanthellae) and their distribution and abundance at Lizard Island (Great Barrier Reef). J. Exp. Mar. Biol. Ecol., 364:48-53.

Loeblich, A. R. & Sherley, J. L. 1979. Observations on the theca of the motile phase of free-living and symbiotic isolates of *Zooxanthella microadriatica* (Freudenthal) comb. nov. J. Mar. Biol. Assoc. U.K., 59:195-205.

Loh, W., Carter, D. & Hoegh-Guldberg, O. 1998. Diversity of zooxanthellae from scleractinian corals of One Tree Island (the Great Barrier Reef). Proceedings of the Australian Coral Reef Society 75th Anniversary Conference, Heron Island. University of Queensland, Brisbane, Australia.

Loram, J. E., Boonham, N., O'Toole, P., Trapido-Rosenthal, H. G. & Douglas, A. E. 2007. Molecular quantification of symbiotic dinoflagellate algae of the genus *Symbiodinium*. Biol. Bull., 212:259-268.

Lucas, M. Q., Stat, M., Smith, M. C., Weil, E. & Schizas, N. V. 2016. *Symbiodinium* (internal transcribed spacer 2) diversity in the coral host *Agaricia lamarcki* (Cnidaria: Scleractinia) between shallow and mesophotic reefs in the Northern Caribbean (20–70 m). Mar. Ecol., 37:1079-1087.

Madin, J. S., Anderson, K. D., Andreasen, M. H., Bridge, T. C., Cairns, S. D., Connolly, S. R., Darling, E. S., Diaz, M., Falster, D. S. & Franklin, E. C. 2016. The Coral Trait Database, a curated database of trait information for coral species from the global oceans. Scientific Data, 3:160017.

Madsen, A., Madin, J. S., Tan, C.-H. & Baird, A. H. 2014. The reproductive biology of the scleractinian coral *Plesiastrea versipora* in Sydney Harbour, Australia.

Sex. Early Dev. Aquat. Org., 1:25-33.

Madshus, I. H. 1988. Regulation of intracellular pH in eukaryotic cells. Biochem. J., 250:1-8.

Magoč, T. & Salzberg, S. L. 2011. FLASH: fast length adjustment of short reads to improve genome assemblies. Bioinformatics, 27:2957-2963.

Manning, M. M. & Gates, R. D. 2008. Diversity in populations of free-living *Symbiodinium* from a Caribbean and Pacific reef. Limnol. Oceanogr., 53:1853-1861.

Matthews, J. L., Crowder, C. M., Oakley, C. A., Lutz, A., Roessner, U., Meyer, E., Grossman, A. R., Weis, V. M. & Davy, S. K. 2017. Optimal nutrient exchange and immune responses operate in partner specificity in the cnidarian-dinoflagellate symbiosis. Proc. Natl. Acad. Sci., 114:13194-13199.

McBride, B. B., Muller-Parker, G. & Jakobsen, H. H. 2009. Low thermal limit of growth rate of *Symbiodinium californium* (Dinophyta) in culture may restrict the symbiont to southern populations of its host anemones (*Anthopleura* spp.; Anthozoa, Cnidaria). J. Phycol., 45:855-863.

McCloskey, L. R., Muscatine, L. & Wilkerson, F. P. 1994. Daily photosynthesis, respiration, and carbon budgets in a tropical marine jellyfish (*Mastigias* sp.). Mar. Biol., 119:13-22.

McCloskey, L. R., Cove, T. G. & Verde, E. A. 1996. Symbiont expulsion from the anemone *Anthopleura elegantissima* (Brandt) (Cnidaria; Anthozoa). J. Exp. Mar. Biol. Ecol., 195:173-186.

McCook, L. J., Jompa, J. & Diaz-Pulido, G. 2001. Competition between corals and algae on coral reefs: a review of evidence and mechanisms. Coral Reefs, 19:400-417.

Mercado, J. M., Gordillo, F. J. L., Figueroa, F. L. & Niell, F. X. 1998. External carbonic anhydrase and affinity for inorganic carbon in intertidal macroalgae. J. Exp. Mar. Biol. Ecol., 221:209-220.

Merget, B., Koetschan, C., Hackl, T., Förster, F., Dandekar, T., Müller, T., Schultz, J. & Wolf, M. 2012. The ITS2 database. J. Vis. Exp., 61:e3806.

Morgan, K. M., Perry, C. T., Smithers, S. G., Johnson, J. A. & Daniell, J. J. 2016. Evidence of extensive reef development and high coral cover in nearshore environments: implications for understanding coral adaptation in turbid settings. Scientific reports, 6:29616.

Morgan, K. M., Perry, C. T., Johnson, J. A. & Smithers, S. G. 2017. Nearshore turbid-zone corals exhibit high bleaching tolerance on the Great Barrier Reef following the 2016 ocean warming event. Front. Mar. Sci., 4:224.

Morton, S. L. & Faust, M. A. 1997. Survey of toxic epiphytic dinoflagellates from the Belizean barrier reef ecosystem. Bull. Mar. Sci., 61:899-906.

Muller-Parker, G., McCloskey, L. R., Hoegh-Guldberg, O. & McAuley, P. J. 1994. Effect of ammonium enrichment on animal and algal biomass of the coral *Pocillopora damicornis*. Pac. Sci. 48:273-283.

Muscatine, L. 1967. Glycerol excretion by symbiotic algae from corals and Tridacna and its control by the host. Science, 156:516-519.

Muscatine, L. & Cernichiari, E. 1969. Assimilation of photosynthetic products of zooxanthellae by a reef coral. Biol. Bull., 137:506-523.

Muscatine, L., McCloskey, L. R. & Marian, R. E. 1981. Estimating the daily contribution of carbon from zooxanthellae to coral animal respiration. Limnol. Oceanogr., 26:601-611.

Muscatine, L., Falkowski, P. G., Porter, J. W. & Dubinsky, Z. 1984. Fate of

photosynthetic fixed carbon in light-and shade-adapted colonies of the symbiotic coral *Stylophora pistillata*. Proc. R. Soc. Lond., B, 222:181-202.

Muscatine, L., McCloskey, L. R. & Loya, Y. 1985. A comparison of the growth rates of zooxanthellae and animal tissue in the Red Sea coral Stylophora pistillata. Proc. 5th Int. Coral Reef Symp.

Muscatine, L., Falkowski, P. G., Dubinsky, Z., Cook, P. A. & McCloskey, L. R. 1989. The effect of external nutrient resources on the population dynamics of zooxanthellae in a reef coral. Proc. R. Soc. Lond., B, 236:311-324.

Muscatine, L., Ferrier-Pages, C., Blackburn, A., Gates, R. D., Baghdasarian, G. & Allemand, D. 1998. Cell-specific density of symbiotic dinoflagellates in tropical anthozoans. Coral Reefs, 17:329-337.

Nakamura, Y., Feary, D. A., Kanda, M. & Yamaoka, K. 2013. Tropical fishes dominate temperate reef fish communities within western Japan. PLoS One, 8:e81107.

Nitschke, M. R., Davy, S. K., Cribb, T. H. & Ward, S. 2015. The effect of elevated temperature and substrate on free-living *Symbiodinium* cultures. Coral Reefs, 34:161-171.

Nitschke, M. R., Davy, S. K. & Ward, S. 2016. Horizontal transmission of *Symbiodinium* cells between adult and juvenile corals is aided by benthic sediment. Coral Reefs, 35:335-344.

Nitschke, M. R., Gardner, S. G., Goyen, S., Fujise, L., Camp, E. F., Ralph, P. J. & Suggett, D. J. 2018. Utility of photochemical traits as diagnostics of thermal tolerance amongst Great Barrier Reef corals. Front. Mar. Sci.,5:45.

Nitta, M., Okamura, H., Aizawa, S. & Yamaizumi, M. 1997. Heat shock induces transient p53-dependent cell cycle arrest at G1/S. Oncogene, 15:561-568.

Noisette, F. & Hurd, C. 2018. Abiotic and biotic interactions in the diffusive boundary

layer of kelp blades create a potential refuge from ocean acidification. Funct. Ecol., 32:1329-1342.

Núñez-Pons, L., Bertocci, I. & Baghdasarian, G. 2017. Symbiont dynamics during thermal acclimation using cnidarian-dinoflagellate model holobionts. Mar. Environ. Res., 130:303-314.

Odum, H. T. & Odum, E. P. 1955. Trophic structure and productivity of a windward coral reef community on Eniwetok Atoll. Ecol. Monogr., 25:291-320.

Oliver, E. C. J. & Holbrook, N. J. 2014. Extending our understanding of South Pacific gyre "spin-up": Modeling the East Australian Current in a future climate. J. Geophys. Res. Oceans, 119:2788-2805.

Park, H. G., Han, S. I., Oh, S. Y. & Kang, H. S. 2005. Cellular responses to mild heat stress. Cell. Mol. Life Sci., 62:10-23.

Parkinson, J. E., Coffroth, M. A. & LaJeunesse, T. C. 2015. New species of Clade B *Symbiodinium* (Dinophyceae) from the greater Caribbean belong to different functional guilds: *S. aenigmaticum* sp. nov., *S. antillogorgium* sp. nov., *S. endomadracis* sp. nov., and *S. pseudominutum* sp. nov. J. Phycol., 51:850-858.

Parsons, M. L. & Preskitt, L. B. 2007. A survey of epiphytic dinoflagellates from the coastal waters of the island of Hawai'i. Harmful Algae, 6:658-669.

Pauls, S. U., Nowak, C., Bálint, M. & Pfenninger, M. 2013. The impact of global climate change on genetic diversity within populations and species. Mol. Ecol., 22:925-946.

Pernice, M., Meibom, A., Van Den Heuvel, A., Kopp, C., Domart-Coulon, I., Hoegh-Guldberg, O. & Dove, S. 2012. A single-cell view of ammonium assimilation in coral–dinoflagellate symbiosis. ISME J, 6:1314-1324.

Perry, C. T. & Larcombe, P. (2003) Marginal and non-reef-building coral environments.

Coral Reefs, 22:427-432.

Pettay, D. T. & LaJeunesse, T. C. 2007. Microsatellites from clade B *Symbiodinium* spp. specialized for Caribbean corals in the genus *Madracis*. Mol. Ecol. Resour. 7:1271-1274.

Pettay, D. T., Wham, D. C., Pinzón, J. H. & LaJeunesse, T. C. 2011. Genotypic diversity and spatial–temporal distribution of *Symbiodinium* clones in an abundant reef coral. Mol. Ecol., 20:5197-5212.

Pinzón, J. H., Devlin-Durante, M. K., Weber, M. X., Baums, I. B. & LaJeunesse, T. C. 2011. Microsatellite loci for *Symbiodinium A3* (*S. fitti*) a common algal symbiont among Caribbean *Acropora* (stony corals) and Indo-Pacific giant clams (*Tridacna*). Conserv. Genet. Resour., 3:45-47.

Pochon, X. & Gates, R. D. 2010. A new *Symbiodinium* clade (Dinophyceae) from soritid foraminifera in Hawai'i. Mol. Phylogen. Evol., 56:492-497.

Pochon, X., Pawlowski, J., Zaninetti, L. & Rowan, R. 2001. High genetic diversity and relative specificity among *Symbiodinium*-like endosymbiotic dinoflagellates in soritid foraminiferans. Mar. Biol., 139:1069-1078.

Pochon, X., LaJeunesse, T. C. & Pawlowski, J. 2004. Biogeographic partitioning and host specialization among foraminiferan dinoflagellate symbionts (*Symbiodinium*; Dinophyta). Mar. Biol., 146:17-27.

Pochon, X., Montoya-Burgos, J. I., Stadelmann, B. & Pawlowski, J. 2006. Molecular phylogeny, evolutionary rates, and divergence timing of the symbiotic dinoflagellate genus *Symbiodinium*. Mol. Phylogen. Evol., 38:20-30.

Pochon, X., Garcia-Cuetos, L., Baker, A. C., Castella, E. & Pawlowski, J. 2007. One-year survey of a single Micronesian reef reveals extraordinarily rich diversity of *Symbiodinium* types in soritid foraminifera. Coral Reefs, 26:867-882.

Pochon, X., Stat, M., Takabayashi, M., Chasqui, L., Chauka, L. J., Logan, D. D. & Gates, R. D. 2010. Comparison of endosymbiotic and free-living *Symbiodinium* (Dinophyceae) diversity in a Hawaiian reef environment. J. Phycol., 46:53-65.

Pochon, X., Putnam, H. M. & Gates, R. D. 2014. Multi-gene analysis of *Symbiodinium* dinoflagellates: a perspective on rarity, symbiosis, and evolution. PeerJ, 2:e394.

Pootakham, W., Mhuantong, W., Putchim, L., Yoocha, T., Sonthirod, C., Kongkachana, W., Sangsrakru, D., Naktang, C., Jomchai, N., Thongtham, N & Tangphatsornuang, S. 2018. Dynamics of coral-associated microbiomes during a thermal bleaching event. Microbiology Open:e604.

Porter, S. N. & Schleyer, M. H. 2017. Long-term dynamics of a high-latitude coral reef community at Sodwana Bay, South Africa. Coral Reefs, 36:369-382.

Porto, I., Granados, C., Restrepo, J. C. & Sanchez, J. A. 2008. Macroalgal-associated dinoflagellates belonging to the genus *Symbiodinium* in Caribbean reefs. PLoS One, 3:e2160.

Precht, W. F. & Aronson, R. B. 2004. Climate flickers and range shifts of reef corals. Front. Ecol. Environ., 2:307-314.

Putnam, H. M. & Gates, R. D. 2015. Preconditioning in the reef-building coral *Pocillopora damicornis* and the potential for trans-generational acclimatization in coral larvae under future climate change conditions. J. Exp. Biol., 218:2365-2372.

Quigley, K. M., Bay, L. K. & Willis, B. L. 2017. Temperature and water quality-related patterns in sediment-associated *Symbiodinium* communities impact symbiont uptake and fitness of juvenile in the genus *Acropora*. Front. Mar. Sci., 4:401.

Ragni, M., Airs, R. L., Hennige, S. J., Suggett, D. J., Warner, M. E. & Geider, R. J. 2010. PSII photoinhibition and photorepair in *Symbiodinium* (Pyrrhophyta)

differs between thermally tolerant and sensitive phylotypes. Mar. Ecol. Prog. Ser., 406:57-70.

Reaka-Kudla, M. L. 1997. The global biodiversity of coral reefs: a comparison with rain forests . In:Biodiversity II: Understanding and Protecting Our Biological Resources (eds. M.L. Reaka - Kudla , D.E. Wilson & E.O. Wilson):83-108. Washington, DC:Joseph Henry Press.

Reaka-Kudla, M. L. 2005. Biodiversity of Caribbean coral reefs. Caribbean Marine Biodiversity: The Known and the Unknown:259-276. Lancaster, Pennsylvania: DEStech Publications .

Reimer, J. D., Takishita, K., Ono, S., Maruyama, T. & Tsukahara, J. 2006. Latitudinal and intracolony ITS-rDNA sequence variation in the symbiotic dinoflagellate genus *Symbiodinium* (Dinophyceae) in *Zoanthus sansibaricus* (Anthozoa: Hexacorallia). Phycol. Res., 54:122-132.

Reimer, J. D., Shah, M. M. R., Sinniger, F., Yanagi, K. & Suda, S. 2010. Preliminary analyses of cultured *Symbiodinium* isolated from sand in the oceanic Ogasawara Islands, Japan. Mar. Biodiv., 40:237-247.

Reynolds, J. M., Bruns, B. U., Fitt, W. K. & Schmidt, G. W. 2008. Enhanced photoprotection pathways in symbiotic dinoflagellates of shallow-water corals and other cnidarians. Proc. Natl. Acad. Sci., 105:13674-13678.

Ridgway, K. R. & Godfrey, J. S. 1997. Seasonal cycle of the East Australian current. J. Geophys. Res. Oceans, 102:22921-22936.

Ridgway, K. R. & Dunn, J. R. 2003. Mesoscale structure of the mean East Australian Current System and its relationship with topography. Prog. Oceanogr., 56:189-222.

Ridgway, K. & Hill, K. 2009. The East Australian Current. A marine climate change

impacts and adaptation report card for Australia, 5.

Robinson, C., Suggett, D. J., Cherukuru, N., Ralph, P. J. & Doblin, M. A. 2014. Performance of Fast Repetition Rate fluorometry based estimates of primary productivity in coastal waters. J. Mar. Syst., 139:299-310.

Robison, J. D. & Warner, M. E. 2006. Differential impacts of photoacclimation and thermal stress on the photobiology of four different phylotypes of *Symbiodinium* (Pyrrhophyta). J. Phycol., 42:568-579.

Rodriguez-Lanetty, M. & Hoegh-Guldberg, O. 2002. The phylogeography and connectivity of the latitudinally widespread scleractinian coral *Plesiastrea versipora* in the Western Pacific. Mol. Ecol., 11:1177-1189.

Rodriguez-Lanetty, M., Loh, W., Carter, D. & Hoegh-Guldberg, O. 2001. Latitudinal variability in symbiont specificity within the widespread scleractinian coral *Plesiastrea versipora*. Mar. Biol., 138:1175.

Rodriguez-Lanetty, M., Cha, H. R. & Song, J. I. 2002. Genetic diversity of symbiotic dinoflagellates associated with anthozoans from Korean waters. Proceedings of the 9th International Coral Reef Symposium, 1:163-171.

Rodriguez-Lanetty, M., Chang, S.-J. & Song, J.-I. 2003. Specificity of two temperate dinoflagellate–anthozoan associations from the north-western Pacific Ocean. Mar. Biol., 143:1193-1199.

Rodríguez-Román, A. & Iglesias-Prieto, R. 2005. Regulation of photochemical activity in cultured symbiotic dinoflagellates under nitrate limitation and deprivation. Mar. Biol., 146:1063-1073.

Rognes, T., Flouri, T., Nichols, B., Quince, C. & Mahé, F. 2016. VSEARCH: a versatile open source tool for metagenomics. PeerJ, 4:e2584.

Roth, M. S. 2014. The engine of the reef: photobiology of the coral–algal symbiosis.

Front. Microbiol., 5:422.

Rowan, R. 1998. Diversity and ecology of zooxanthellae on coral reefs. J. Phycol., 34:407-417.

Rowan, R. & Powers, D. A. 1991. A molecular genetic classification of zooxanthellae and the evolution of animal-algal symbioses. Science, 251:1348-1351.

Rowan, R. & Knowlton, N. 1995. Intraspecific diversity and ecological zonation in coral-algal symbiosis. Proc. Natl. Acad. Sci., 92:2850-2853.

Rowan, R., Knowlton, N., Baker, A. & Jara, J. 1997. Landscape ecology of algal symbionts creates variation in episodes of coral bleaching. Nature, 388:265-269.

Sampayo, E. M., Franceschinis, L., Hoegh-Guldberg, O. & Dove, S. 2007. Niche partitioning of closely related symbiotic dinoflagellates. Mol. Ecol., 16:3721-3733.

Sampayo, E. M., Dove, S. & LaJeunesse, T. C. 2009. Cohesive molecular genetic data delineate species diversity in the dinoflagellate genus *Symbiodinium*. Mol. Ecol., 18:500-519.

Santos, S. R. & Coffroth, M. A. 2003. Molecular genetic evidence that dinoflagellates belonging to the genus *Symbiodinium* Freudenthal are haploid. Biol. Bull., 204:10-20.

Santos, S. R., Taylor, D. J. & Coffroth, M. A. 2001. Genetic comparisons of freshly isolated versus cultured symbiotic dinoflagellates: implications for extrapolating to the intact symbiosis. J. Phycol., 37:900-912.

Santos, S. R., Taylor, D. J., Kinzie Iii, R. A., Hidaka, M., Sakai, K. & Coffroth, M. A. 2002. Molecular phylogeny of symbiotic dinoflagellates inferred from partial chloroplast large subunit (23S)-rDNA sequences. Mol. Phylogen. Evol., 23:97-111.

Santos, S. R., Gutierrez-Rodriguez, C., Lasker, H. R. & Coffroth, M. A. 2003a. *Symbiodinium* sp. associations in the gorgonian *Pseudopterogorgia elisabethae* in the Bahamas: high levels of genetic variability and population structure in symbiotic dinoflagellates. Mar. Biol., 143:111-120.

Santos, S. R., Gutierrez-Rodriguez, C. & Coffroth, M. A. 2003b. Phylogenetic identification of symbiotic dinoflagellates via length heteroplasmy in domain V of chloroplast large subunit (cp23S)-ribosomal DNA sequences. Mar. Biotechnol., 5:130-140.

Savage, A. M., Goodson, M. S., Visram, S., Trapido-Rosenthal, H., Wiedenmann, J. & Douglas, A. E. 2002. Molecular diversity of symbiotic algae at the latitudinal margins of their distribution: dinoflagellates of the genus *Symbiodinium* in corals and sea anemones. Mar. Ecol. Prog. Ser., 244:17-26.

Schleyer, M. H. & Celliers, L. 2003. Biodiversity on the marginal coral reefs of South Africa: What does the future hold? Zool. Verhandel., 345:387-400.

Schloss, P. D., Westcott, S. L., Ryabin, T., Hall, J. R., Hartmann, M., Hollister, E. B., Lesniewski, R. A., Oakley, B. B., Parks, D. H. & Robinson, C. J. 2009. Introducing mothur: open-source, platform-independent, community-supported software for describing and comparing microbial communities. Appl. Environ. Microbiol., 75:7537-7541.

Schoenberg, D. A. & Trench, R. K. 1980. Genetic variation in *Symbiodinium* (= *Gymnodinium*) *microadriaticum* Freudenthal, and specificity in its symbiosis with marine invertebrates. I. Isoenzyme and soluble protein patterns of axenic cultures of Symbiodinium microadriaticum. Proc. R. Soc. Lond. B, 207:405-427.

Schoenberg, C. H. & Loh, W. K. W. 2005. Molecular identity of the unique symbiotic dinoflagellates found in the bioeroding demosponge *Cliona orientalis*. Mar. Ecol.

Prog. Ser., 299:157-166.

Schoenberg, C. H. L., Suwa, R., Hidaka, M. & Loh, W. K. W. 2008. Sponge and coral zooxanthellae in heat and light: preliminary results of photochemical efficiency monitored with pulse amplitude modulated fluorometry. Mar. Ecol., 29:247-258.

Schwarz, J. A., Krupp, D. A. & Weis, V. M. 1999. Late larval development and onset of symbiosis in the scleractinian coral *Fungia scutaria*. Biol. Bull., 196:70-79.

Silverstein, R. N., Correa, A. M. S., LaJeunesse, T. C. & Baker, A. C. 2011. Novel algal symbiont (*Symbiodinium* spp.) diversity in reef corals of Western Australia. Mar. Ecol. Prog. Ser., 422:63-75.

Silverstein, R. N., Cunning, R. & Baker, A. C. 2015. Change in algal symbiont communities after bleaching, not prior heat exposure, increases heat tolerance of reef corals. Glob. Chang. Biol., 21:236-249.

Smith, G. J. & Muscatine, L. 1999. Cell cycle of symbiotic dinoflagellates: variation in G_1 phase-duration with anemone nutritional status and macronutrient supply in the *Aiptasia pulchella–Symbiodinium pulchrorum* symbiosis. Mar. Biol., 134:405-418.

Smith, E. G., Vaughan, G. O., Ketchum, R. N., McParland, D. & Burt, J. A. 2017. Symbiont community stability through severe coral bleaching in a thermally extreme lagoon. Scientific Reports, 7:2428.

Sorek, M. & Levy, O. 2012. The effect of temperature compensation on the circadian rhythmicity of photosynthesis in *Symbiodinium*, coral-symbiotic alga. Sci. Rep., 2:536.

Sorek, M., Yacobi, Y. Z., Roopin, M., Berman-Frank, I. & Levy, O. 2013. Photosynthetic circadian rhythmicity patterns of *Symbiodium*, the coral endosymbiotic algae. Proc. R. Soc. B, 280:20122942.

Stanley, G. D. & Swart, P. K. 1995. Evolution of the coral-zooxanthellae symbiosis during the Triassic: a geochemical approach. Paleobiology, 21:179-199.

Stat, M. & Gates, R. D. 2011. Clade D *Symbiodinium* in scleractinian corals: a "nugget" of hope, a selfish opportunist, an ominous sign, or all of the above? J. Mar. Biol., 730715.

Stat, M., Carter, D. & Hoegh-Guldberg, O. 2006. The evolutionary history of *Symbiodinium* and scleractinian hosts—symbiosis, diversity, and the effect of climate change. Perspect. Plant Ecol. Evol. Syst., 8:23-43.

Stat, M., Morris, E. & Gates, R. D. 2008a. Functional diversity in coral–dinoflagellate symbiosis. Proc. Natl. Acad. Sci., 105:9256-9261.

Stat, M., Loh, W. K. W., Hoegh-Guldberg, O. & Carter, D. A. 2008b. Symbiont acquisition strategy drives host–symbiont associations in the southern Great Barrier Reef. Coral Reefs, 27:763-772.

Stat, M., Loh, W. K. W., LaJeunesse, T. C., Hoegh-Guldberg, O. & Carter, D. A. 2009a. Stability of coral–endosymbiont associations during and after a thermal stress event in the southern Great Barrier Reef. Coral Reefs, 28:709-713.

Stat, M., Pochon, X., Cowie, R. O. M. & Gates, R. D. 2009b. Specificity in communities of *Symbiodinium* in corals from Johnston Atoll. Mar. Ecol. Prog. Ser., 386:83-96.

Stat, M., Bird, C. E., Pochon, X., Chasqui, L., Chauka, L. J., Concepcion, G. T., Logan, D., Takabayashi, M., Toonen, R. J. & Gates, R. D. 2011. Variation in *Symbiodinium* ITS2 sequence assemblages among coral colonies. PLoS One, 6:e15854.

Stat, M., Baker, A. C., Bourne, D. G., Correa, A. M. S., Forsman, Z., Huggett, M. J., Pochon, X., Skillings, D., Toonen, R. J., van Oppen, M. J. H. & Gates, R. D.

2012. Molecular delineation of species in the coral holobiont. Adv. Mar. Biol., 63:1-65.

Stat, M., Pochon, X., Franklin, E. C., Bruno, J. F., Casey, K. S., Selig, E. R. & Gates, R. D. 2013. The distribution of the thermally tolerant symbiont lineage (*Symbiodinium* clade D) in corals from Hawaii: correlations with host and the history of ocean thermal stress. Ecol. Evol., 3:1317-1329.

Stat, M., Yost, D. M. & Gates, R. D. 2015. Geographic structure and host specificity shape the community composition of symbiotic dinoflagellates in corals from the Northwestern Hawaiian Islands. Coral Reefs, 34:1075-1086.

Stern, R. F., Horak, A., Andrew, R. L., Coffroth, M.-A., Andersen, R. A., Küpper, F. C., Jameson, I., Hoppenrath, M., Véron, B., Kasai, F., Brand, J., James, E. R. & Keeling, P. J. 2010. Environmental barcoding reveals massive dinoflagellate diversity in marine environments. PLoS One, 5:e13991.

Stimson, J. & Kinzie, III. R. A. 1991. The temporal pattern and rate of release of zooxanthellae from the reef coral *Pocillopora damicornis* (Linnaeus) under nitrogen-enrichment and control conditions. J. Exp. Mar. Biol. Ecol., 153:63-74.

Strychar, K. B., Sammarco, P. W. & Piva, T. J. 2004a. Apoptotic and necrotic stages of *Symbiodinium* (Dinophyceae) cell death activity: bleaching of soft and scleractinian corals. Phycologia, 43:768-777.

Strychar, K. B., Coates, M. & Sammarco, P. W. 2004b. Loss of *Symbiodinium* from bleached Australian scleractinian corals (*Acropora hyacinthus*, *Favites complanata* and *Porites solida*). Mar. Freshw. Res., 55:135-144.

Suggett, D., Kraay, G., Holligan, P., Davey, M., Aiken, J. & Geider, R. 2001. Assessment of photosynthesis in a spring cyanobacterial bloom by use of a fast repetition rate fluorometer. Limnol. Oceanogr., 46:802-810.

Suggett, D. J., Warner, M. E., Smith, D. J., Davey, P., Hennige, S. & Baker, N. R. 2008. Photosynthesis and production of hydrogen peroxide by *Symbiodinium* (Pyrrhophyta) phylotypes with different thermal tolerances. J. Phycol., 44:948-956.

Suggett, D. J., Goyen, S., Evenhuis, C., Szabó, M., Pettay, D. T., Warner, M. E. & Ralph, P. J. 2015. Functional diversity of photobiological traits within the genus *Symbiodinium* appears to be governed by the interaction of cell size with cladal designation. New Phytol., 208:370-381.

Suggett, D. J., Warner, M. E. & Leggat, W. 2017. Symbiotic dinoflagellate functional diversity mediates coral survival under ecological crisis. Trends Ecol. Evol., 32:735-745.

Suharsono & Brown, B. E. 1992. Comparative measurements of mitotic index in zooxanthellae from a symbiotic cnidarian subject to temperature increase. J. Exp. Mar. Biol. Ecol., 158:179-188.

Sunagawa, S., Coelho, L. P., Chaffron, S., Kultima, J. R., Labadie, K., Salazar, G., Djahanschiri, B., Zeller, G., Mende, D. R., Alberti, A., et al. 2015. Structure and function of the global ocean microbiome. Science, 348:1261359.

Suzuki, G., Yamashita, H., Kai, S., Hayashibara, T., Suzuki, K., Iehisa, Y., Okada, W., Ando, W. & Komori, T. 2013. Early uptake of specific symbionts enhances the post-settlement survival of *Acropora* corals. Mar. Ecol. Prog. Ser., 494:149-158.

Sweet, M. J. 2014. *Symbiodinium* diversity within *Acropora muricata* and the surrounding environment. Mar. Ecol., 35:343-353.

Takabayashi, M., Adams, L. M., Pochon, X. & Gates, R. D. 2012. Genetic diversity of free-living *Symbiodinium* in surface water and sediment of Hawai‘i and Florida. Coral Reefs, 31:157-167.

Tanner, J. E. 1995. Competition between scleractinian corals and macroalgae: an experimental investigation of coral growth, survival and reproduction. J. Exp. Mar. Biol. Ecol., 190:151-168.

Taylor, D. L. 1971. Ultrastructure of the 'zooxanthella' *Endodinium chattonii in situ*. J. Mar. Biol. Assoc. U.K., 51:227-234.

Taylor, D. L. 1973. The cellular interactions of algal-invertebrate symbiosis. Adv. Mar. Biol., 11:1-56.

Thomas, L., Kendrick, G. A., Kennington, W. J., Richards, Z. T. & Stat, M. 2014. Exploring *Symbiodinium* diversity and host specificity in *Acropora* corals from geographical extremes of Western Australia with 454 amplicon pyrosequencing. Mol. Ecol., 23:3113-3126.

Thornhill, D. J., Daniel, M. W., LaJeunesse, T. C., Schmidt, G. W. & Fitt, W. K. 2006. Natural infections of aposymbiotic *Cassiopea xamachana* scyphistomae from environmental pools of *Symbiodinium*. J. Exp. Mar. Biol. Ecol., 338:50-56.

Thornhill, D. J., LaJeunesse, T. C. & Santos, S. R. 2007. Measuring rDNA diversity in eukaryotic microbial systems: how intragenomic variation, pseudogenes, and PCR artifacts confound biodiversity estimates. Mol. Ecol., 16:5326-5340.

Thornhill, D. J., Kemp, D. W., Bruns, B. U., Fitt, W. K. & Schmidt, G. W. 2008. Correspondence between cold tolerance and temperate biogeography in a western Atlantic *Symbiodinium* (Dinophyta) lineage. J. Phycol., 44:1126-1135.

Thornhill, D. J., Xiang, Y., Fitt, W. K. & Santos, S. R. 2009. Reef endemism, host specificity and temporal stability in populations of symbiotic dinoflagellates from two ecologically dominant Caribbean corals. PLoS One, 4:e6262.

Thornhill, D. J., Lewis, A. M., Wham, D. C. & LaJeunesse, T. C. 2014. Host-specialist lineages dominate the adaptive radiation of reef coral endosymbionts. Evolution,

68:352-367.

Thornhill, D. J., Howells, E. J., Wham, D. C., Steury, T. D. & Santos, S. R. 2017. Population genetics of reef coral endosymbionts (*Symbiodinium*, Dinophyceae). Mol. Ecol., 26:2640-2659.

Tonk, L., Sampayo, E. M., Chai, A., Schrameyer, V. & Hoegh-Guldberg, O. 2017. *Symbiodinium* (Dinophyceae) community patterns in invertebrate hosts from inshore marginal reefs of the southern Great Barrier Reef, Australia. J. Phycol., 53:589-600.

Towanda, T. & Thuesen, E. V. 2012. Prolonged exposure to elevated CO_2 promotes growth of the algal symbiont *Symbiodinium muscatinei* in the intertidal sea anemone *Anthopleura elegantissima*. Biol. Open, 1: 615-621.

Trench, R. K. 1979. The cell biology of plant-animal symbiosis. Ann. Rev. Plant Physiol., 30:485-531.

Trench, R. K. 1987. Dinoflagellates in non parasitic symbioses. The biology of dinoflagellates. F.J.R Taylor (Ed.), Biology of Dinoflagellates, Blackwell, Oxford.

Trench, R. K. 1993. Microalgal-invertebrate symbioses: A review. Endocytobiosis Cell Res., 9:135-175.

Trench, R. K. 1997. Diversity of symbiotic dinoflagellates and the evolution of microalgal-invertebrate symbioses. Proc. 8th Int. Coral Reef Sym., 2:1275–86.

Trench, R. K. 2000. Validation of some currently used invalid names of dinoflagellates. J. Phycol., 36:972.

Trench, R. K. & Blank, R. J. 1987. *Symbiodinium microadriaticum* Freudenthal, *S. goreauii* sp. nov., *S. kawagutii* sp. nov. and *S. pilosum* sp. nov.: gymnodinioid dinoflagellate symbionts of marine invertebrates. J. Phycol., 23:469-481.

Trench, R. K. & Thinh, L. V. 1995. *Gymnodinium linucheae* sp. nov.: the dinoflagellate symbiont of the jellyfish *Linuche unguiculata*. Eur. J. Phycol., 30:149-154.

Tuckett, C. A., de Bettignies, T., Fromont, J. & Wernberg, T. 2017. Expansion of corals on temperate reefs: direct and indirect effects of marine heatwaves. Coral Reefs, 36:947-956.

Van Bleijswijk, J. D. L & Veldhuis, M. J. W. 1995. *In situ* gross growth rates of *Emiliania huxleyi* in enclosures with different phosphate loadings revealed by diel changes in DNA content. Mar. Ecol. Prog. Ser., 121:271-277.

van de Leemput, I. A., Hughes, T. P., van Nes, E. H. & Scheffer, M. 2016. Multiple feedbacks and the prevalence of alternate stable states on coral reefs. Coral Reefs, 35:857-865.

Van Dolah, F. M. & Leighfield, T. A. 1999. Diel phasing of the cell-cycle in the Florida red tide dinoflagellate, *Gymnodinium breve*. J. Phycol., 35:1404-1411.

Van Dolah, F. M., Leighfield, T. A., Kamykowski, D. & Kirkpatrick, G. J. 2008. Cell cycle behavior of laboratory and field populations of the Florida red tide dinoflagellate, *Karenia brevis*. Cont. Shelf Res., 28:11-23.

van Oppen, M. J. H., Palstra, F. P., Piquet, A. M.-T. & Miller, D. J. 2001. Patterns of coral–dinoflagellate associations in *Acropora*: significance of local availability and physiology of *Symbiodinium* strains and host–symbiont selectivity. Proc. R. Soc. Lond. B, 268:1759-1767.

van Oppen, M. J. H., Mieog, J. C., Sanchez, C. A. & Fabricius, K. E. 2005. Diversity of algal endosymbionts (zooxanthellae) in octocorals: the roles of geography and host relationships. Mol. Ecol., 14:2403-2417.

Vaulot, D. 1995. The cell cycle of phytoplankton: coupling cell growth to population growth. Mol. Ecol. Aquat. Microbes, 38:303-322.

Venera-Ponton, D. E., Diaz-Pulido, G., Rodriguez-Lanetty, M. & Hoegh-Guldberg, O. 2010. Presence of *Symbiodinium* spp. in macroalgal microhabitats from the southern Great Barrier Reef. Coral Reefs, 29:1049-1060.

Vergés, A., Steinberg, P. D., Hay, M. E., Poore, A. G. B., Campbell, A. H., Ballesteros, E., Heck, K. L. Jr., Booth, D. J., Coleman, M. A., Feary, D. A., et al. 2014. The tropicalization of temperate marine ecosystems: climate-mediated changes in herbivory and community phase shifts. Proc. R. Soc. B, 281: 20140846.

Veron, J. E. N. 1986. Corals of Australia and the Indo-pacific. Angus and Robertson Publishers, Sydney.

Veron, J. E. N. 1993. A biogeographic database of hermatypic corals: species of the central Indo-Pacific, genera of the world. Australian Inst. Mar. Sci., Monogr. Ser., 10: 1-433.

Veron, J. E. N. 2000. Corals of the World. Australian Inst. Mar. Sci., Townsville.

Wada, S., Aoki, M. N., Tsuchiya, Y., Sato, T., Shinagawa, H. & Hama, T. 2007. Quantitative and qualitative analyses of dissolved organic matter released from *Ecklonia cava* Kjellman, in Oura Bay, Shimoda, Izu Peninsula, Japan. J. Exp. Mar. Biol. Ecol., 349:344-358.

Wagner, D., Pochon, X., Irwin, L., Toonen, R. J. & Gates, R. D. 2011. Azooxanthellate? Most Hawaiian black corals contain *Symbiodinium*. Proc. R. Soc. Lond. B, 278:1323-1328.

Wahl, M., Saderne, V. & Sawall, Y. 2016. How good are we at assessing the impact of ocean acidification in coastal systems? Limitations, omissions and strengths of commonly used experimental approaches with special emphasis on the neglected role of fluctuations. Mar. Fresh. Res., 67:25-36.

Wakefield, T. S., Farmer, M. A. & Kempf, S. C. 2000. Revised description of the fine

structure of *in situ* “zooxanthellae” genus *Symbiodinium*. Biol. Bull., 199:76-84.

Wallace, C. C., Fellegara, I., Muir, P. R. & Harrison, P. L. 2009. The scleractinian corals of Moreton Bay, eastern Australia: high latitude, marginal assemblages with increasing species richness. Mem. Queensl. Mus., 54:1-118.

Wang, L.-H., Liu, Y.-H., Ju, Y.-M., Hsiao, Y.-Y., Fang, L.-S. & Chen, C.-S. 2008. Cell cycle propagation is driven by light–dark stimulation in a cultured symbiotic dinoflagellate isolated from corals. Coral Reefs, 27:823-835.

Wang, D.-Z., Zhang, Y.-J., Zhang, S.-F., Lin, L. & Hong, H.-S. 2013a. Quantitative proteomic analysis of cell cycle of the dinoflagellate *Prorocentrum donghaiense* (Dinophyceae). PLoS One, 8:e63659.

Wang, L.-H., Lee, H.-H., Fang, L.-S., Mayfield, A. B. & Chen, C.-S. 2013b. Fatty acid and phospholipid syntheses are prerequisites for the cell cycle of *Symbiodinium* and their endosymbiosis within sea anemones. PLoS One, 8:e72486.

Wangpraseurt, D., Larkum, A. W. D., Ralph, P. J. & Kühl, M. 2012. Light gradients and optical microniches in coral tissues. Front. Microbiol., 3:316.

Warner, M. E. & Suggett, D. J. 2016. The Photobiology of *Symbiodinium* spp.: Linking physiological diversity to the implications of stress and resilience. The Cnidaria, Past, Present and Future. Springer. 489-509.

Warner, M. E., Fitt, W. K. & Schmidt, G. W. 1996. The effects of elevated temperature on the photosynthetic efficiency of zooxanthellae *in hospite* from four different species of reef coral: a novel approach. Plant, Cell Environ., 19:291-299.

Warner, M. E., Fitt, W. K. & Schmidt, G. W. 1999. Damage to photosystem II in symbiotic dinoflagellates: a determinant of coral bleaching. Proc. Natl. Acad. Sci., 96:8007-8012.

Warnes, G. R., Bolker, B., Bonebakker, L., Gentleman, R., Liaw, W. H. A., Lumley, T.,

Maechler, M., Magnusson, A., Moeller, S. & Schwartz, M. 2015. gplots: various R programming tools for plotting data. R package version 2.17. Available online at: http://CRAN. R-project. org/package= gplots.

Wham, D. C., Ning, G. & LaJeunesse, T. C. 2017. *Symbiodinium glynnii* sp. nov., a species of stress-tolerant symbiotic dinoflagellates from pocilloporid and montiporid corals in the Pacific Ocean. Phycologia, 56:396-409.

Wicks, L. C., Sampayo, E., Gardner, J. P. A. & Davy, S. K. 2010. Local endemicity and high diversity characterise high-latitude coral–*Symbiodinium* partnerships. Coral Reefs, 29:989-1003.

Wilkerson, F. P., Muller-Parker, G. & Muscatine, L. 1983. Temporal patterns of cell division in natural populations of endosymbiotic algae. Limnol. Oceanogr., 28:1009-1014.

Wilkerson, F. P., Kobayashi, D. & Muscatine, L. 1988. Mitotic index and size of symbiotic algae in Caribbean reef corals. Coral Reefs, 7:29-36.

Wilkinson, C. 2008. Status of coral reefs of the world: 2008. Global Coral Reef Monitoring Network and Reef and Rainforest Research Centre, Townsville.

Winkler, N. S., Pandolfi, J. M. & Sampayo, E. M. 2015. *Symbiodinium* identity alters the temperature-dependent settlement behaviour of *Acropora millepora* coral larvae before the onset of symbiosis. Proc. R. Soc. Lond. B, 282:20142260.

Wood-Charlson, E. M., Hollingsworth, L. L., Krupp, D. A. & Weis, V. M. 2006. Lectin/glycan interactions play a role in recognition in a coral/dinoflagellate symbiosis. Cell. Microbiol., 8:1985-1993.

Wu, L., Cai, W., Zhang, L., Nakamura, H., Timmermann, A., Joyce, T., McPhaden, M. J., Alexander, M., Qiu, B., Visbeck, M., Chang, P. & Giese, B. 2012. Enhanced warming over the global subtropical western boundary currents. Nat. Clim.

Change, 2:161-166.

Yamano, H., Sugihara, K. & Nomura, K. 2011. Rapid poleward range expansion of tropical reef corals in response to rising sea surface temperatures. Geophys. Res. Lett., 38:L04601.

Yamashita, H. & Koike, K. 2013. Genetic identity of free-living *Symbiodinium* obtained over a broad latitudinal range in the Japanese coast. Phycol. Res., 61:68-80.

Yamashita, H., Kobiyama, A. & Koike, K. 2009. Do uric acid deposits in zooxanthellae function as eye-spots? PLoS One, 4:e6303.

Yamashita, H., Suzuki, G., Hayashibara, T. & Koike, K. 2011. Do corals select zooxanthellae by alternative discharge? Mar. Biol., 158:87-100.

Yamashita, H., Suzuki, G., Hayashibara, T. & Koike, K. 2013. *Acropora* recruits harbor "rare" *Symbiodinium* in the environmental pool. Coral Reefs, 32:355-366.

Yamashita, H., Suzuki, G., Kai, S., Hayashibara, T. & Koike, K. 2014. Establishment of coral–algal symbiosis requires attraction and selection. PLoS One, 9:e97003.

Yellowlees, D., Rees, T. A. V. & Leggat, W. 2008. Metabolic interactions between algal symbionts and invertebrate hosts. Plant, Cell Environ., 31:679-694.

Zann, L. P. 2000. The eastern Australian region: a dynamic tropical/temperate biotone. Mar. Pollut. Bull., 41:188-203.

Zhang, C., Lin, S., Huang, L., Lu, W., Li, M. & Liu, S. 2014. Suppression subtraction hybridization analysis revealed regulation of some cell cycle and toxin genes in *Alexandrium catenella* by phosphate limitation. Harmful Algae, 39:26-39.

Zhou, G., Huang, H., Yu, Z., Dong, Z. & Li, Y. 2012. Genetic diversity of potentially free-living *Symbiodinium* in the Xisha Islands, South China Sea: Implications for the resilience of coral reefs. Aquat. Ecosyst. Health Manage., 15:152-160.

Ziegler, M., Arif, C., Burt, J. A., Dobretsov, S., Roder, C., LaJeunesse, T. C. & Voolstra, C. R. 2017. Biogeography and molecular diversity of coral symbionts in the genus *Symbiodinium* around the Arabian Peninsula. J. Biogeogr., 44:674-686.

Ziegler, M., Eguíluz, V. M., Duarte, C. M. & Voolstra, C. R. 2018. Rare symbionts may contribute to the resilience of coral–algal assemblages. ISME J, 12:161-172.